Pacific Northwest
NATIONAL LABORATORY

X-Ray Photoelectron Spectroscopy (XPS)

Part 1: Basic Principles

June 12, 2023

Vaithiyalingam Shutthanandan

Ajay Karakoti

Theva Thevuthasan

U.S. DEPARTMENT OF ENERGY BATTELLE

PNNL is operated by Battelle for the U.S. Department of Energy

Where are we from……

Pacific Northwest NATIONAL LABORATORY

We are from Pacific Northwest National Lab……..

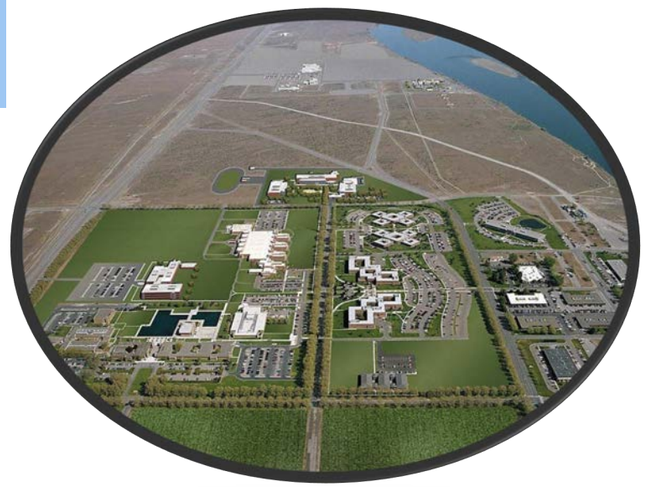

Pacific Northwest
NATIONAL LABORATORY

Introduction

Introduction

This is a four-part series of seminars

- Seminar 1 : Basic Principles of XPS
- Seminar 2 : Instrumentation
- Seminar 3 : Data Analysis
- Seminar 4 : Application of XPS in battery, nano and solar cell materials research

Why do we need Surface Sensitive Techniques ?

- Surface plays a major role in controlling materials properties and processes

Properties

- Optical Properties
- Tribological Properties
- Wettability
- Solderability
- Transistor Gate Dielectric
- Work Function

Processes

- Oxidation
- Catalysis
- Corrosion
- Diffusion
- Electrochemical
- Passivation and Surface treatment

To understand these properties and processes we need a surface sensitive technique that can give quantitative information about chemical composition, reactivity and bonding at the surface and interfaces

How to Study Surfaces ?

Signal Beam (out)

Probe Beam (in)

Photons (hν)
Electrons
Ions

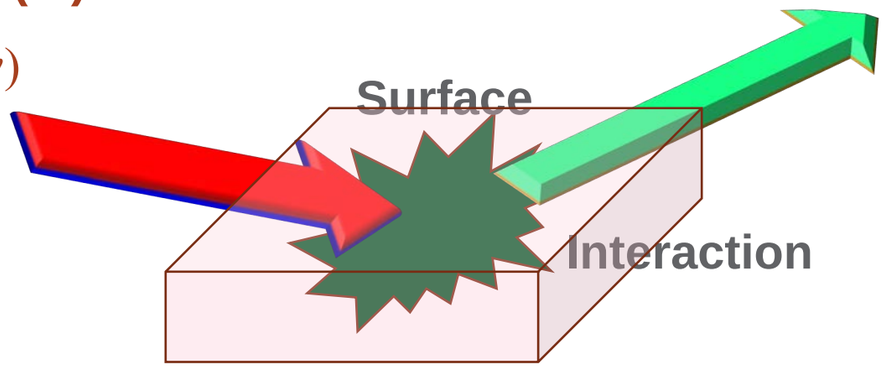

Photons (hν)
Electrons
Ions

Analyzed by Spectrometer

Probe beams can have different penetration depth depending on their incident energy

At 1000 eV

Photons (hν)	~ 1000 nm
Electrons	~ 2 nm
Ions	~ 1 nm

Major Surface Analysis Methods

- X-Ray Photoelectron Spectroscopy (XPS): Photons **In** and electrons **out**
- Auger Electron Spectroscopy (AES): Electrons **in** and electrons **out**
- Ion Scattering Spectrometry: Ions **in** and Ions **out**
- Secondary Ion Mass Spectrometry (SIMS): Ions **in** and secondary ions **out**

What Information can be Obtained from X-ray Photoelectron Spectroscopy (XPS)?

- Over the past 20 years, the use of XPS in materials research have grown phenomenally

  ➡ It can provide unique insights to surface chemistry

- XPS is mainly used for……
  - **Product development**
  - **Identification of failure mechanisms**
  - **Test hypotheses**
  - **Provide information to support conclusion**

……..In industries, national labs and universities

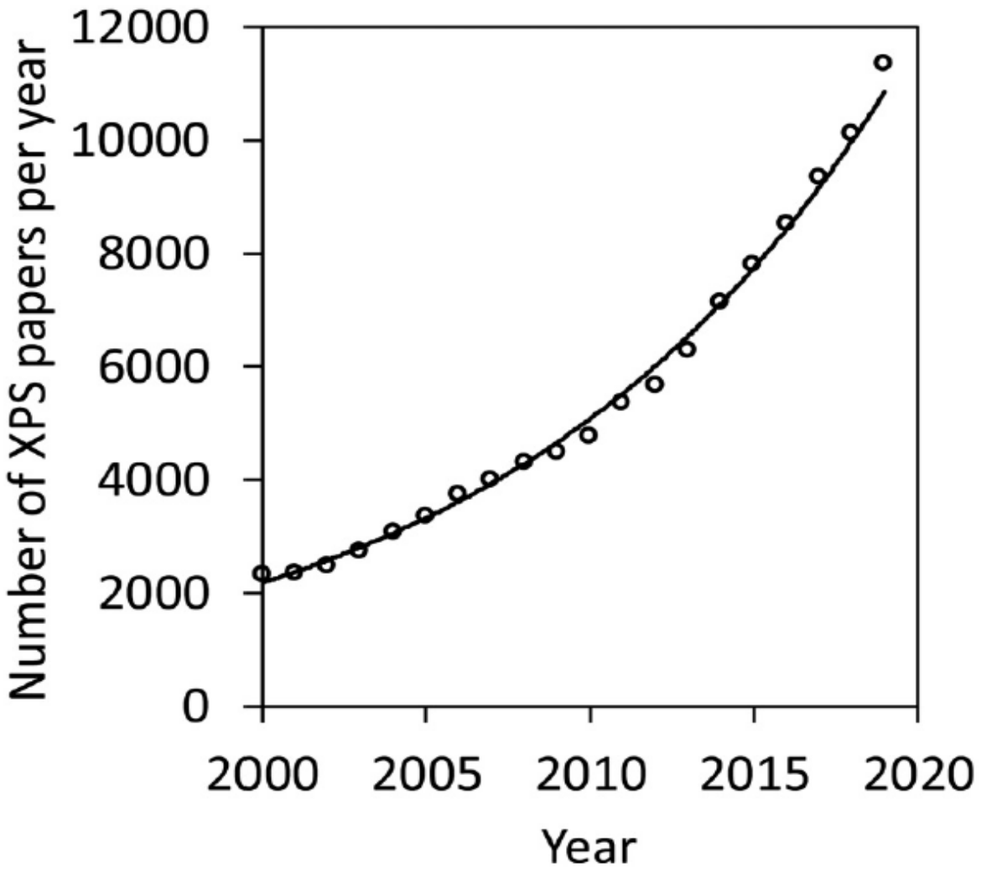

Number of papers published with “XPS” in the title, abstract, or keywords in past two decades

Don Baer and et.al, https://doi.org/10.1116/6.0000873

What Information can be Obtained from X-ray Photoelectron Spectroscopy (XPS)?

- Elements identification: can detect **Li to U**
- Quantitative (Compositional analysis)
- Chemical state identification
- Valence band electronic structure
- Conducting and insulating materials can be analyzed
- Analysis depth (up to **10 nm**)
- Detection limit approximately **0.1** atom percent
- Surface composition mapping (x, y) **< 3 μm** resolution
- Chemical state distributions with **< 3 μm** resolution
- Depth analysis (z)
  - Sputter depth profiling (Destructive)
    - Inert gas ions
    - C_{60} ions
    - Ar cluster ions
  - Angle dependent depth profiling: Angle resolved XPS (Non-destructive)

Pacific Northwest
NATIONAL LABORATORY

Basic Principle of XPS

The Photoelectric Process: X-Ray Photoelectron Emission

XPS is widely used because of its relatively simple operation and data interpretation

An incoming photon causes the ejection of the photoelectron

Ejected Photoelectron (Kinetic Energy = E_k)

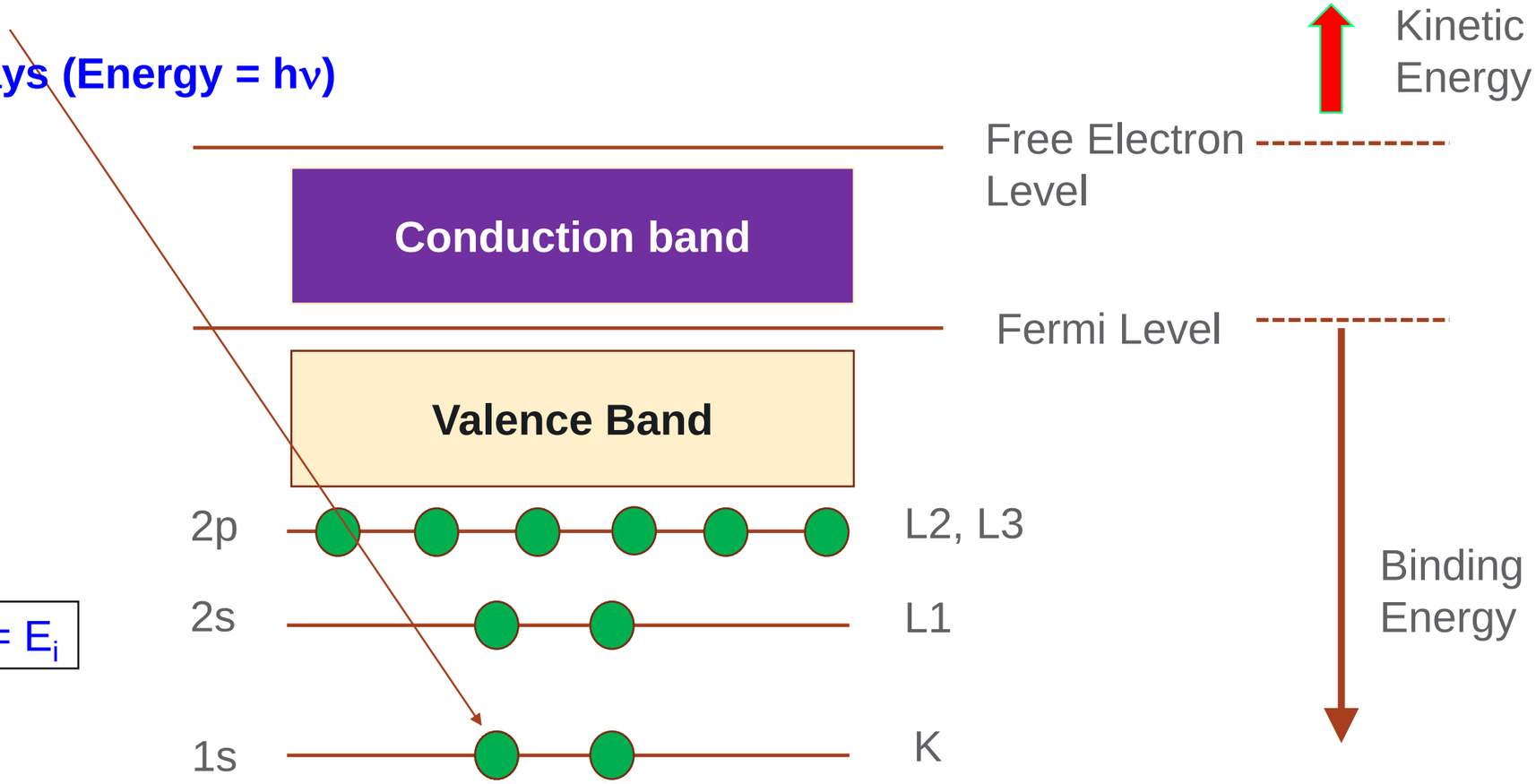

Initial Energy (atom)= E_i

The Photoelectric Process: X-Ray Photoelectron Emission

XPS is widely used because of its relatively simple operation and data interpretation

An incoming photon causes the ejection of the photoelectron

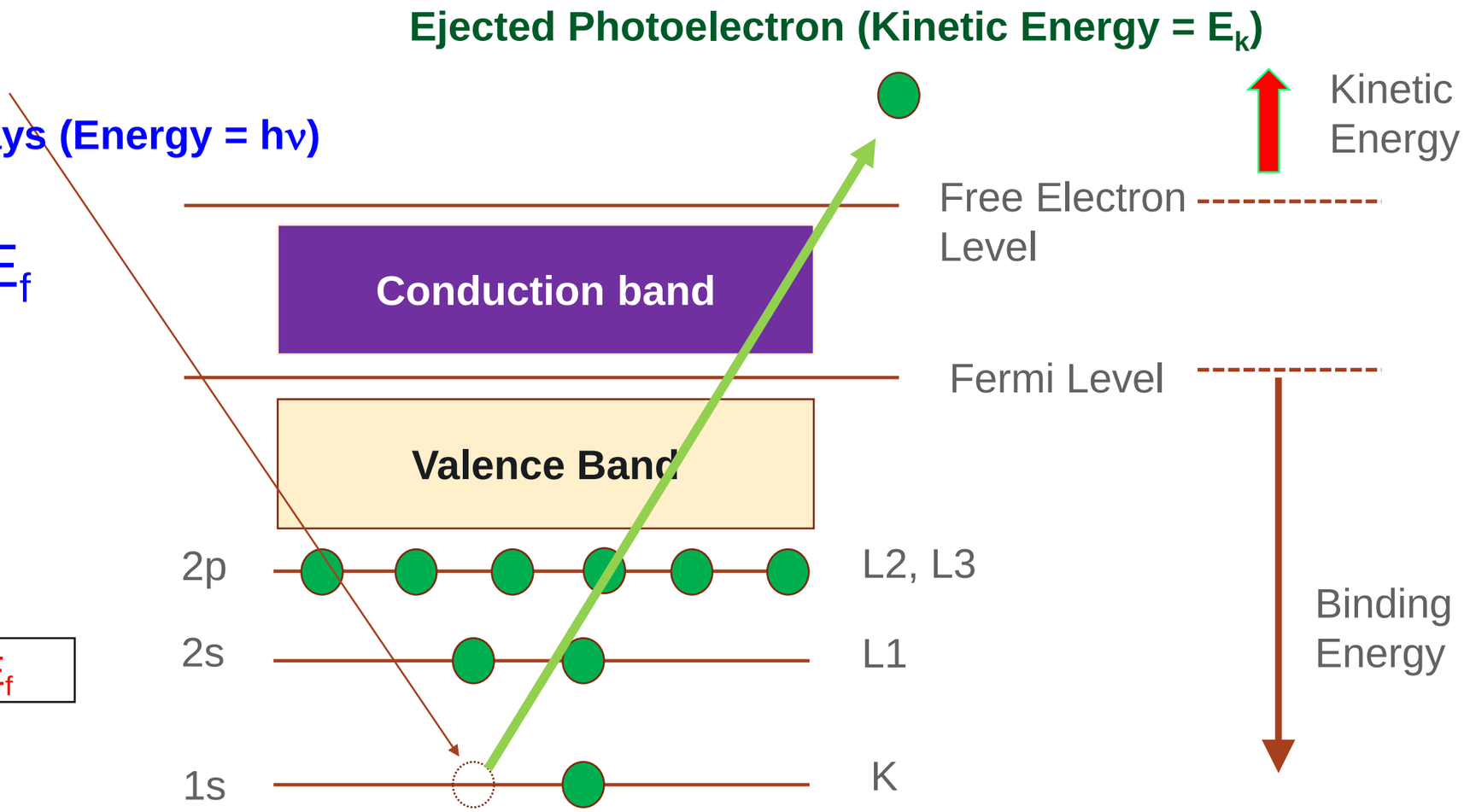

$h\nu + E_i = E_k + E_f$

$h\nu - E_k = E_f - E_i$

$h\nu - E_k = E_b$

Final Energy (ion)= E_f

The Photoelectric Process: X-Rays Induced Auger Electron Emission

Pacific Northwest NATIONAL LABORATORY

Emitted Auger Electron

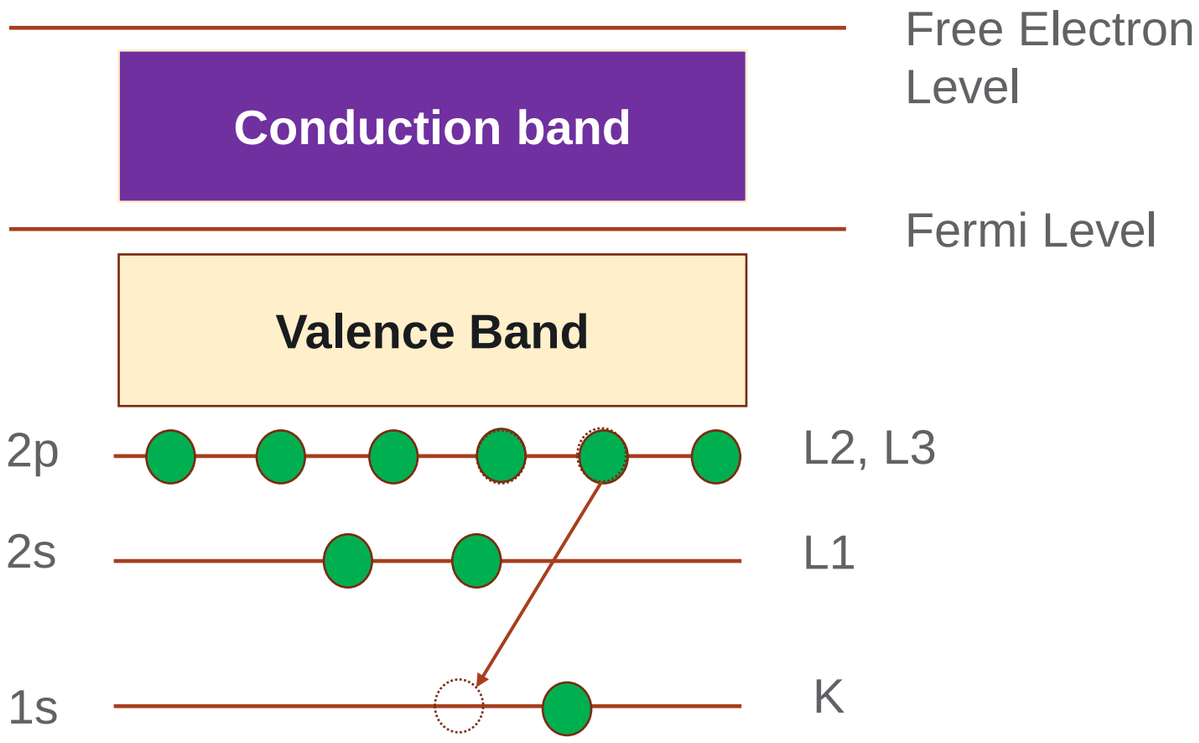

Atom

- L electron Falls to fill core level vacancy to reduce the energy
- KLL Auger electron emitted to conserve energy released in the first step

The Photoelectric Process: X-Rays Induced Auger Electron Emission

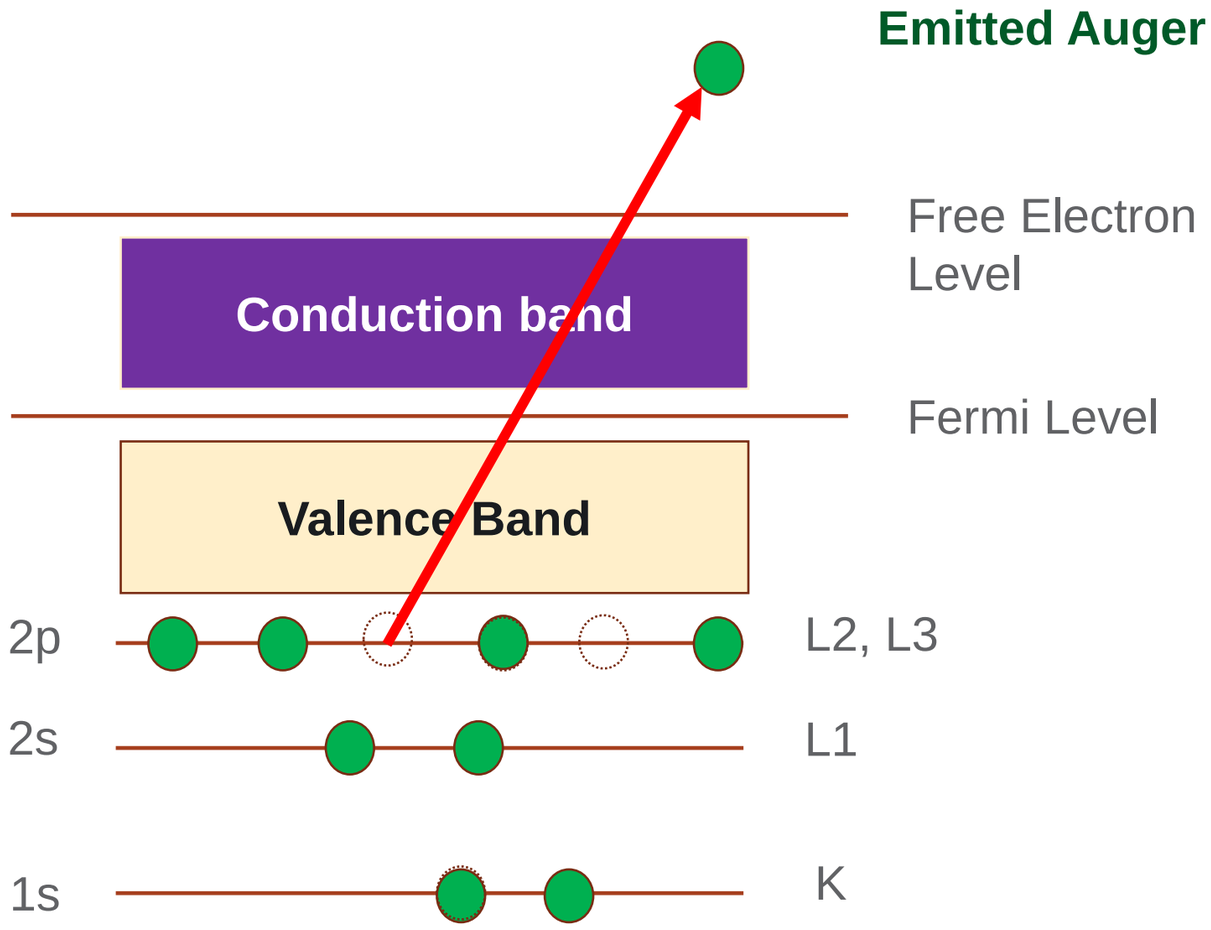

- L electron Falls to fill core level vacancy to reduce the energy
- KLL Auger electron emitted to conserve energy released in the first step

Energy Level Diagram in X-ray Photoelectron Process

For Conducting Sample

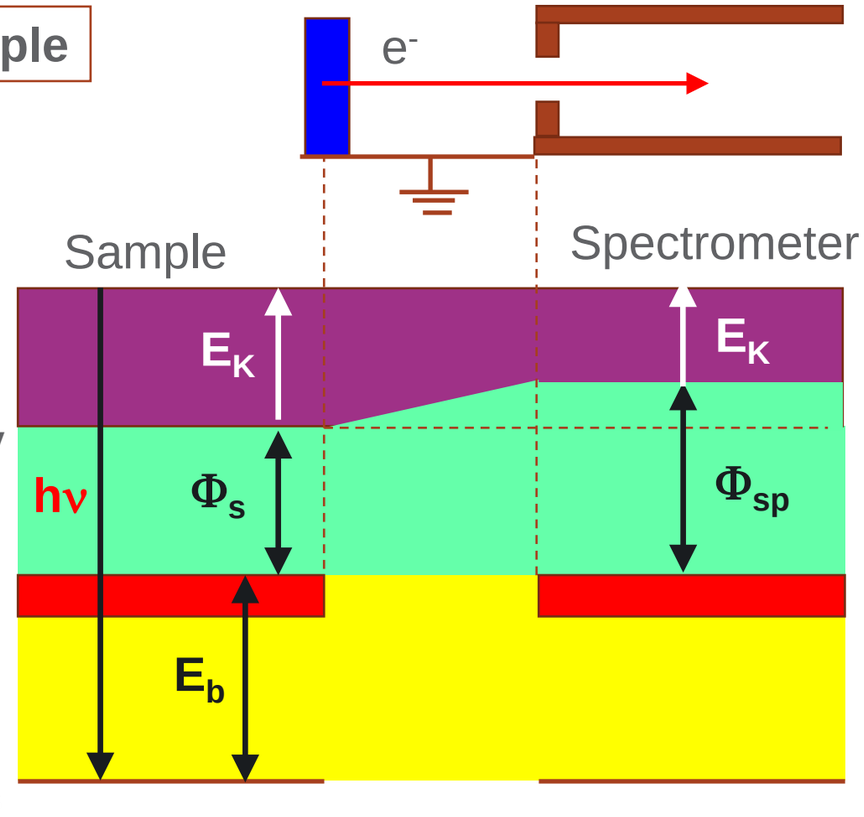

$$h\nu = E_b + \Phi_{sp} + E_\kappa$$

$$E_b = h\nu - E_\kappa - \Phi_{sp}$$

E_b depends on chemical Environment:

- Element
- Valence state
- Coordination (types of ligands, number, tetrahedral, octahedral, etc)

- Because the Fermi levels of the sample and the spectrometer are aligned, we only need to know the spectrometer's work function, Φ_{sp} ,to calculate E_b
- *Every* element has an *unique* electronic structure, hence the electrons are emitted with specific kinetic energies

Energy Level Diagram in X-ray Photoelectron Process

For Conducting Sample

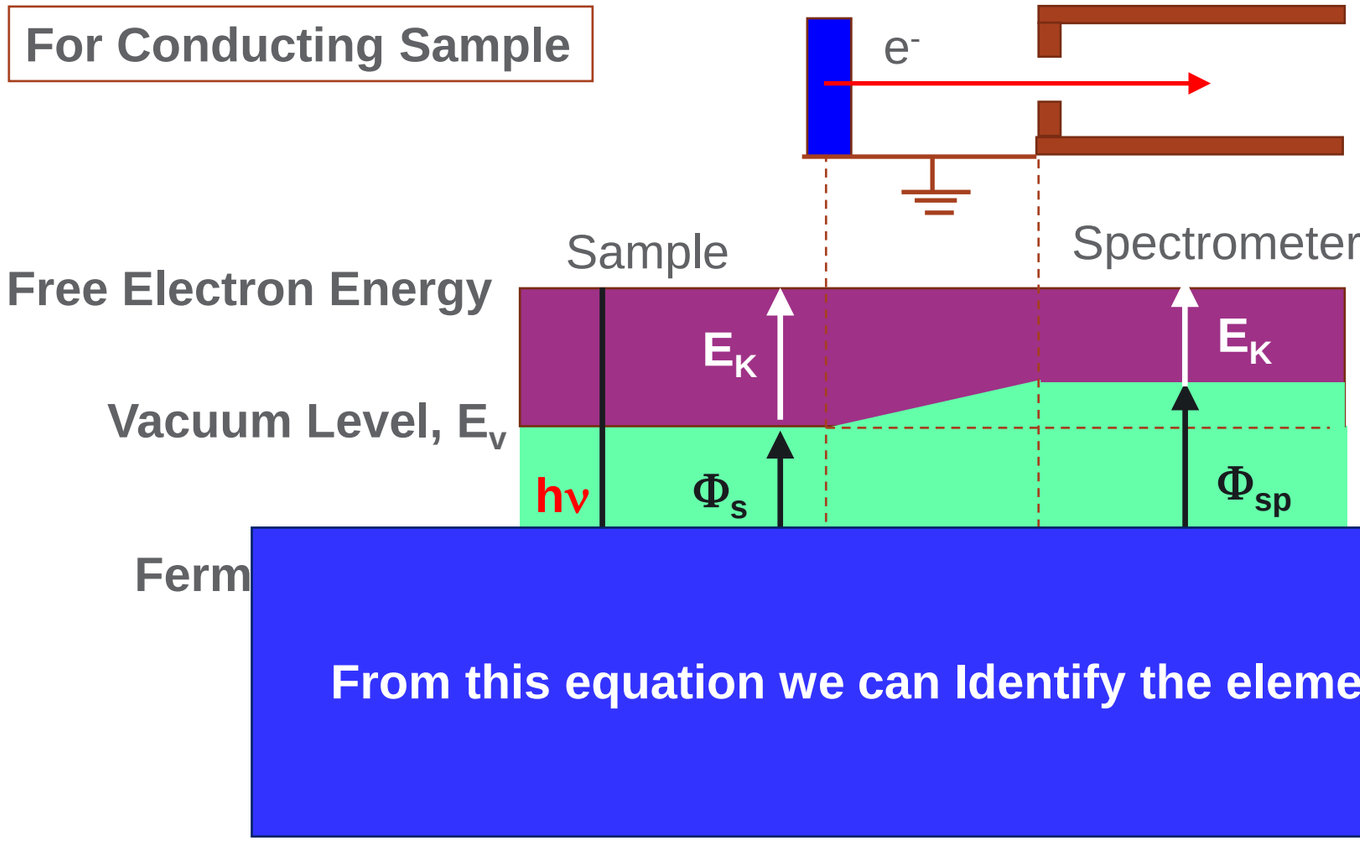

$$h\nu = E_b + \Phi_{sp} + E_\kappa$$

$$E_b = h\nu - E_\kappa - \Phi_{sp}$$

E_b depends on chemical Environment:

- Element

f ligands,
octahedral, etc)

From this equation we can Identify the elements present in any samples!

- Because the Fermi levels of the sample and the spectrometer are aligned, we only need to know the spectrometer's work function, Φ_{sp} ,to calculate E_b
- *Every* element has an *unique* electronic structure, hence the electrons are emitted with specific kinetic energies

Interpretation of XPS Spectra: Survey Scan

XPS spectrum: Intensities of photoelectrons versus Binding energy (E_b) or Kinetic Energy (E_k)

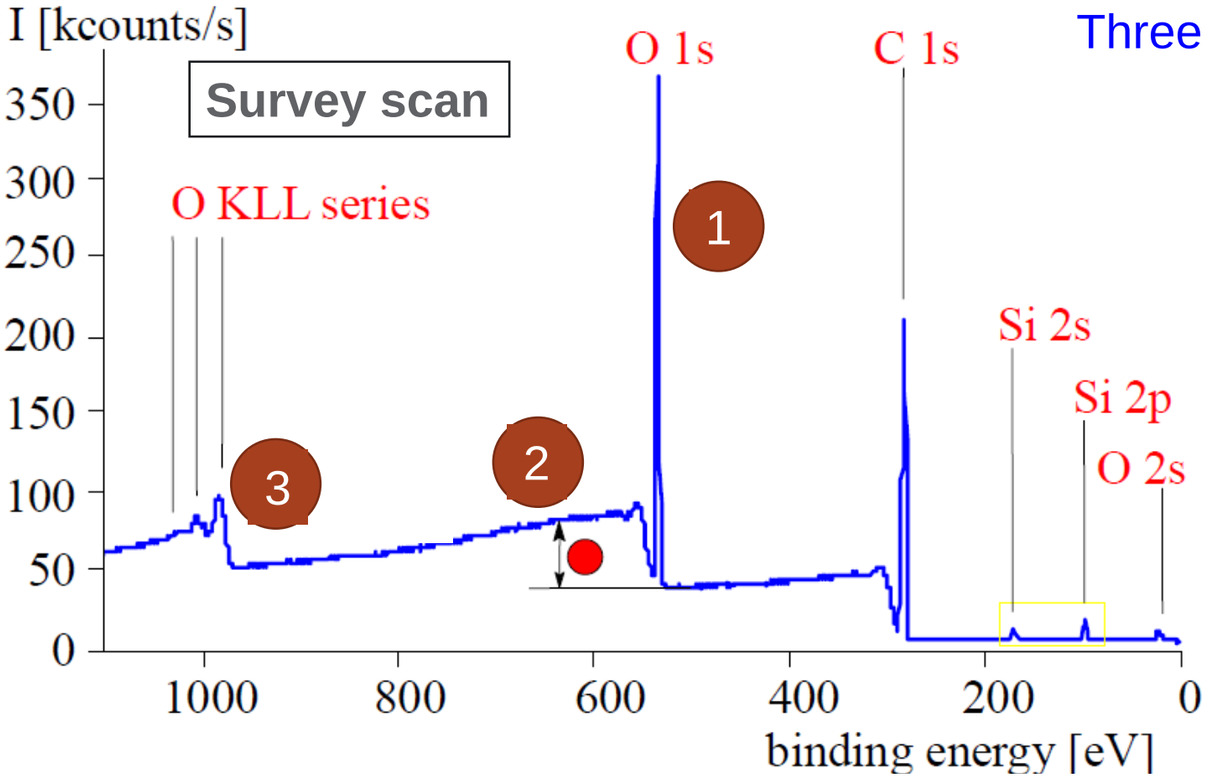

Three main features are identified in each spectrum:

1. Element peak (photoelectrons **without** energy loss)
2. Background (photoelectrons **with** energy loss)
3. Relaxation phenomena (Auger peaks)

Photoelectrons contributes to the main peak

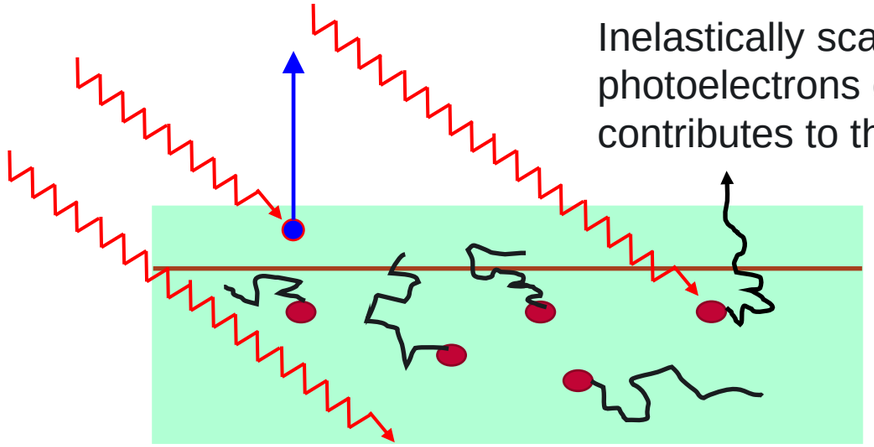

- Identification of the elements can be made directly from the kinetic energies of the ejected photoelectrons.

$$E_b = h\nu - E_\kappa - \Phi_{sp}$$

- The relative concentrations of elements can be determined from the photoelectron intensities and using the appropriate cross-sections.

Interpretation of XPS Spectra: Survey Scan

XPS spectrum: Intensities of photoelectrons versus Binding energy (E_b) or Kinetic Energy (E_k)

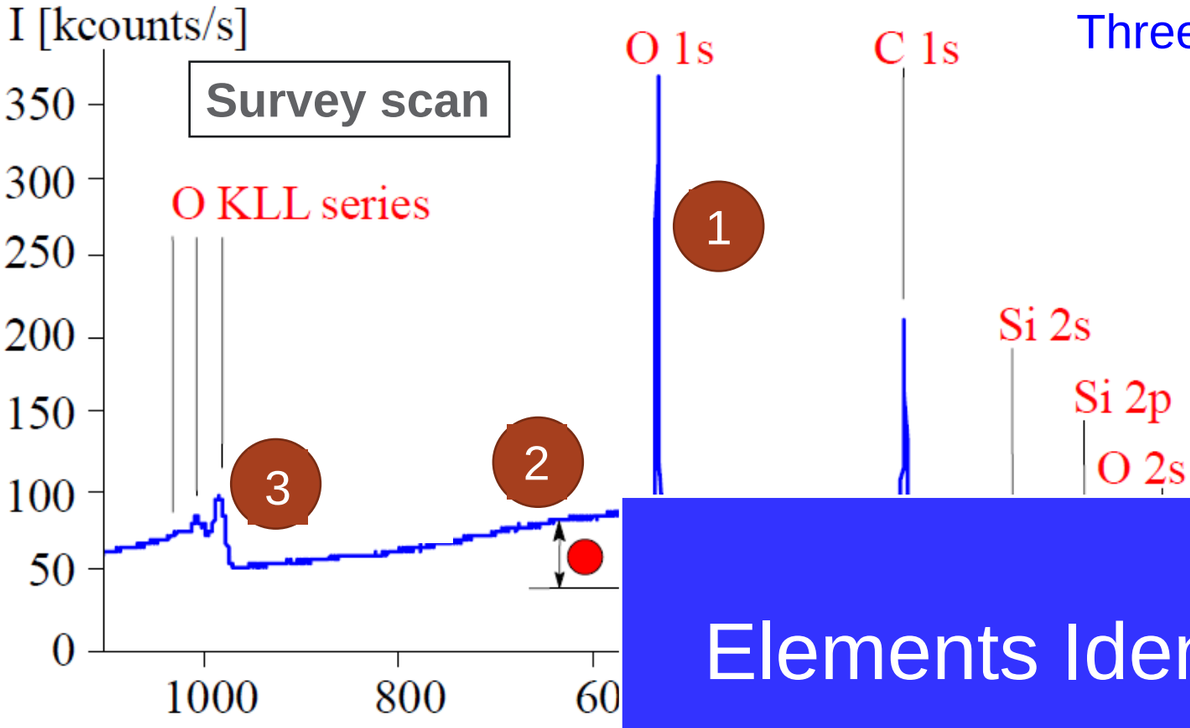

Three main features are identified in each spectrum:

1. Element peak (photoelectrons **without** energy loss)
2. Background (photoelectrons **with** energy loss)
3. Relaxation phenomena (Auger peaks)

Elements Identification

ontributes to the main peak

Inelastically scattered photoelectrons only contributes to the background

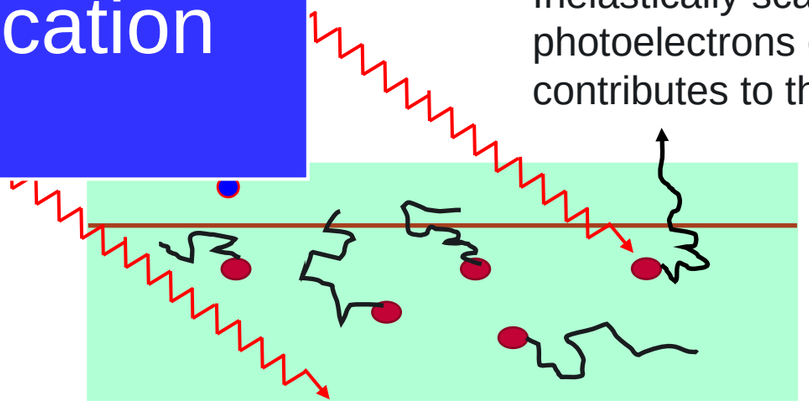

- Identification of the elements can be made directly from the kinetic energies of the ejected photoelectrons.

$$E_b = h\nu - E_\kappa - \Phi_{sp}$$

- The relative concentrations of elements can be determined from the photoelectron intensities and using the appropriate cross-sections.

Interpretation of XPS Spectra: Peak Identifications

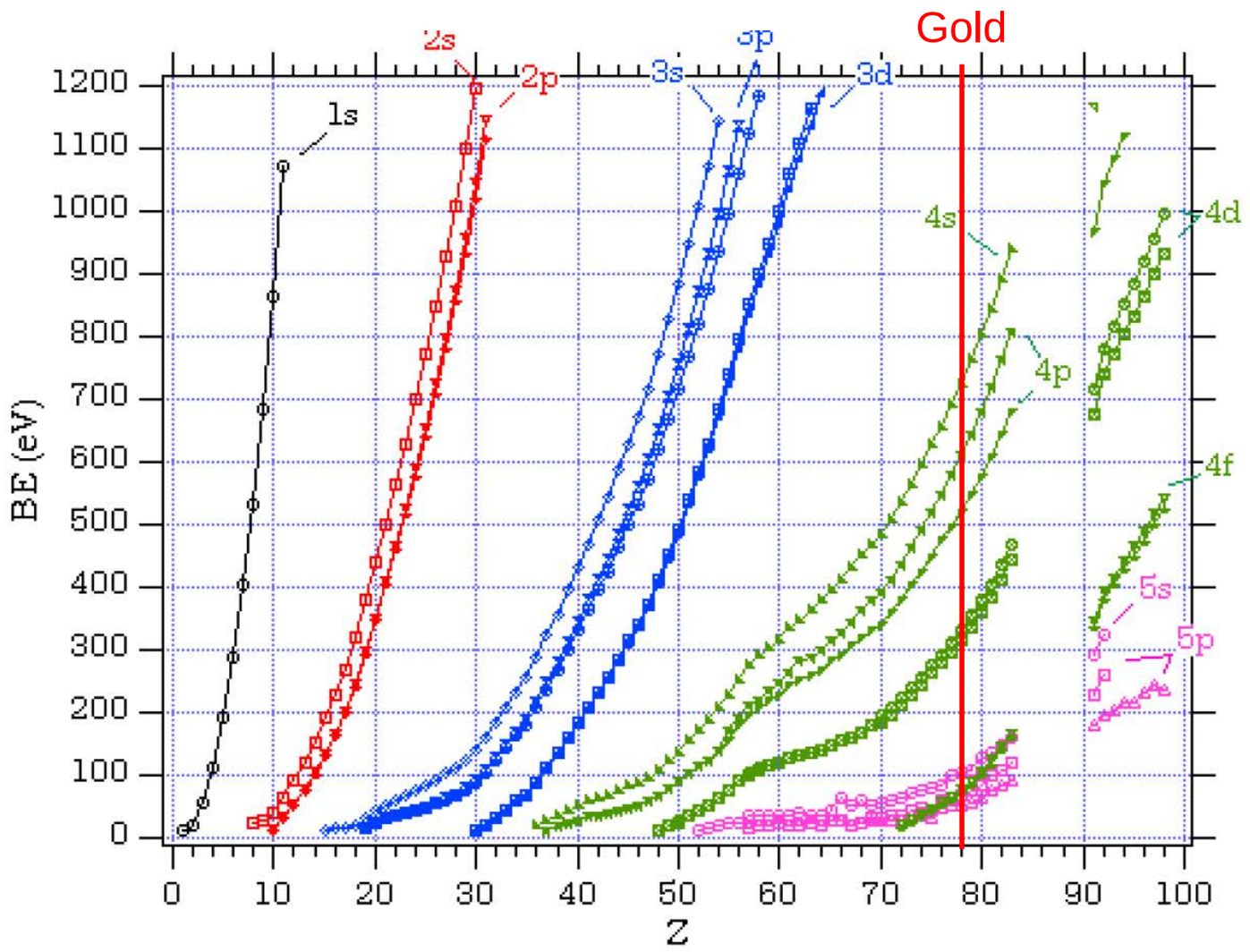

http://www.lasurface.com/database/elementxps.php
http://srdata.nist.gov/xps/Default.aspx
Data from C.D. Wagner, W.M. Riggs, L.E. Davis, J.F. Moulder and G.E. Muilenberg, Eds.,
"Handbook of X-ray Photoelectron Spectroscopy, Perkin-Elmer Corp., Flying Cloud, MN, 1979.

Interpretation of XPS Spectra: Typical Spectrum

Gold XPS wide scan spectrum

Monochromated Al Kα

Photoelectron Peaks	4s	$4p_{1/2}$	$4p_{3/2}$	$4d_{3/2}$	$4d_{5/2}$	5s	$4f_{5/2}$	$4f_{7/2}$	$5f_{1/2}$	$5p_{3/2}$
Binding energies	763	643	547	353	335	110	88	84	74	57

Auger Peaks	$N_{67}O_{45}O_{45}$	$N_5N_6N_{67}$	$N_4N_6N_{67}$	$N_5N_{67}V$
Binding Energies	1416	1342	1324	1247

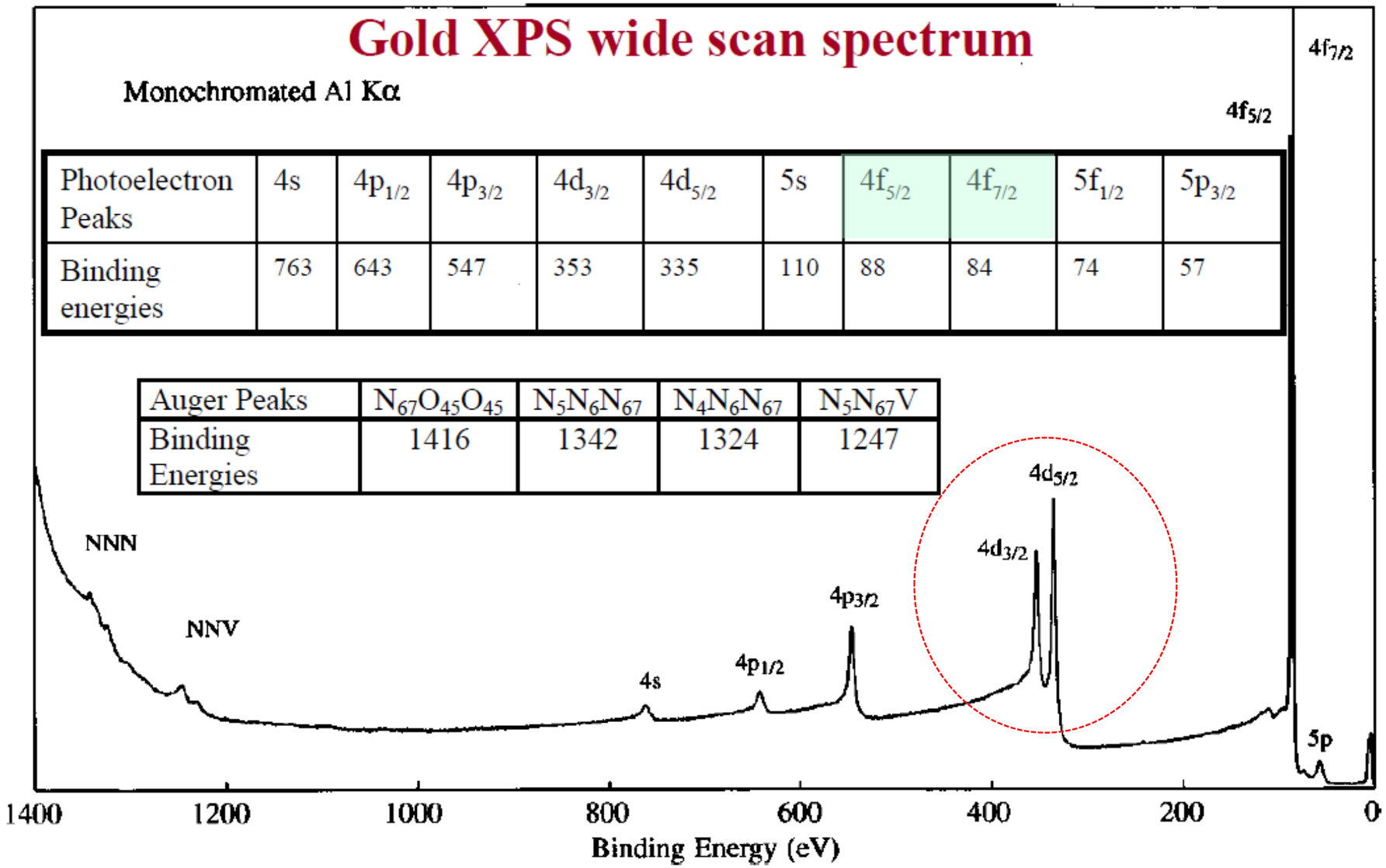

https://xps-database.com/

Interpretation of XPS Spectra: Designation of the Peaks

- XPS peak is originated from the photoelectrons in the core leaves and valence band
- Coupling of **orbital quantum number (l)** and **electron spin (s):** $|j| = l + s$ will split the energy levels

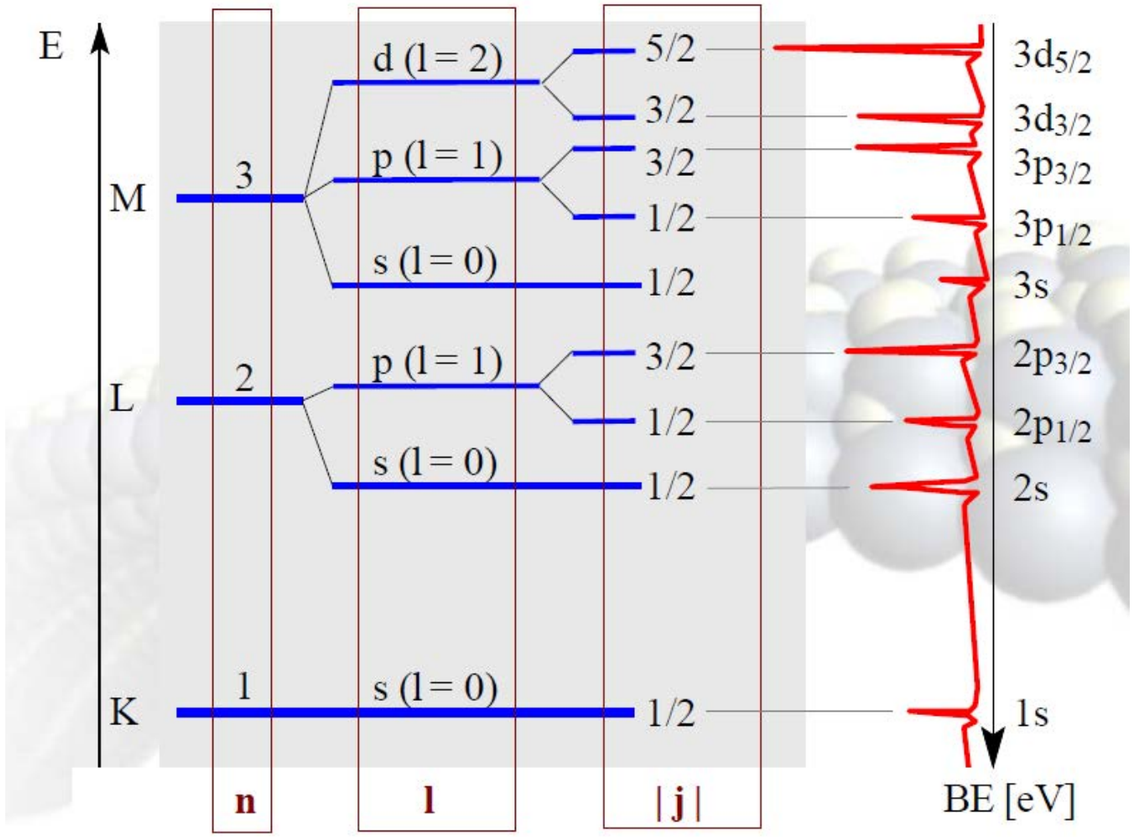

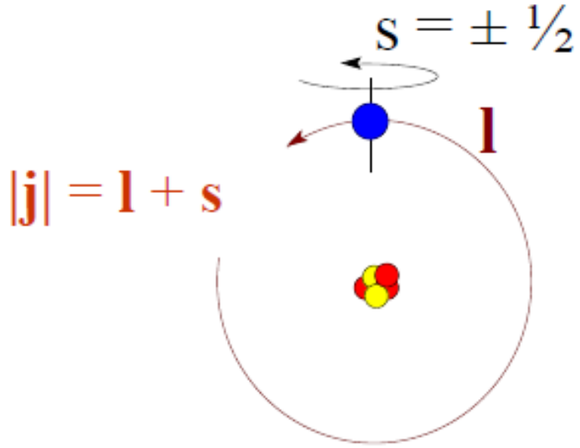

Interpretation of XPS Spectra: Designation of the Peaks

The **area** ratios are determined by the ratio of the degeneracy of each electronic level (2j + 1)

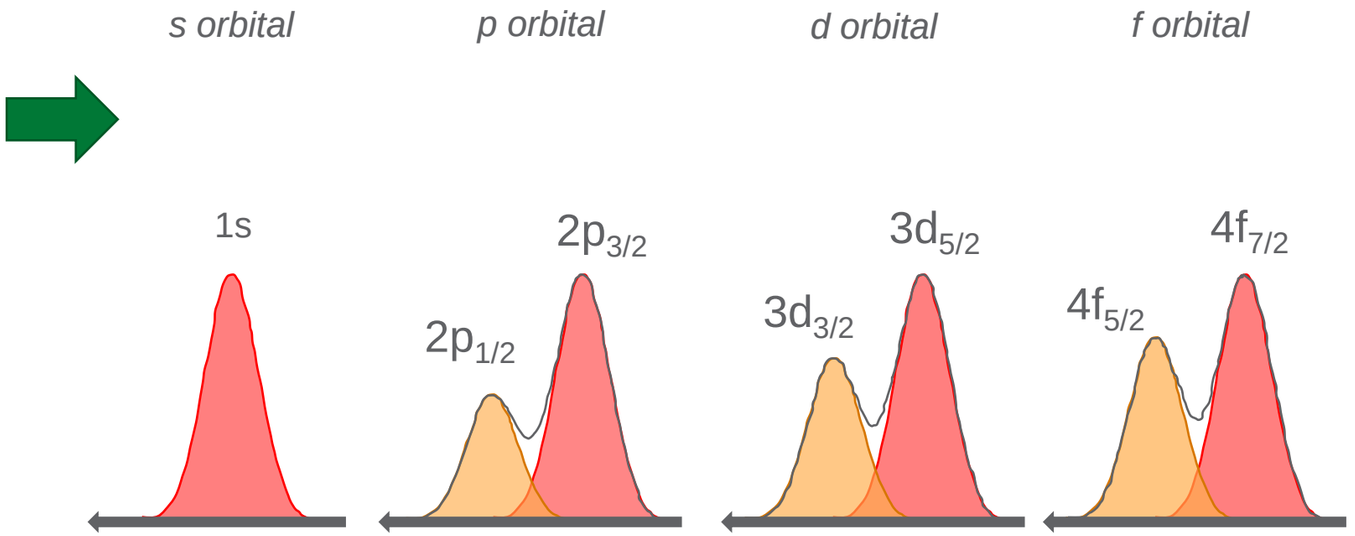

Cu 2p

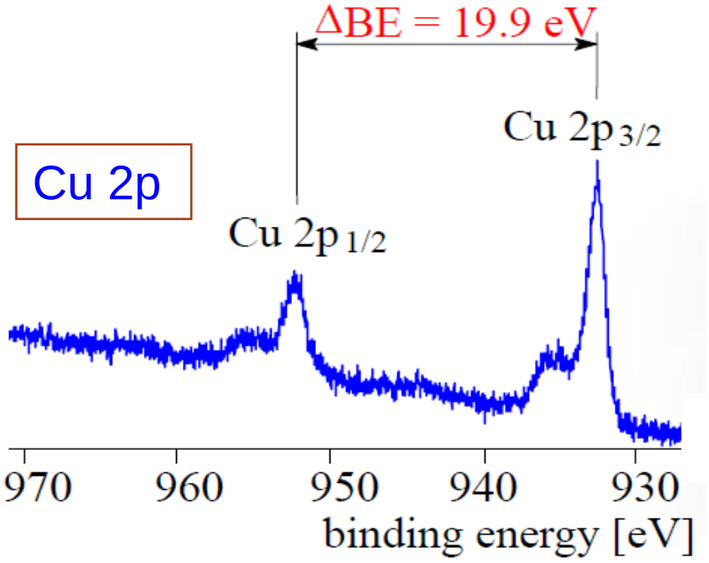

S 2p

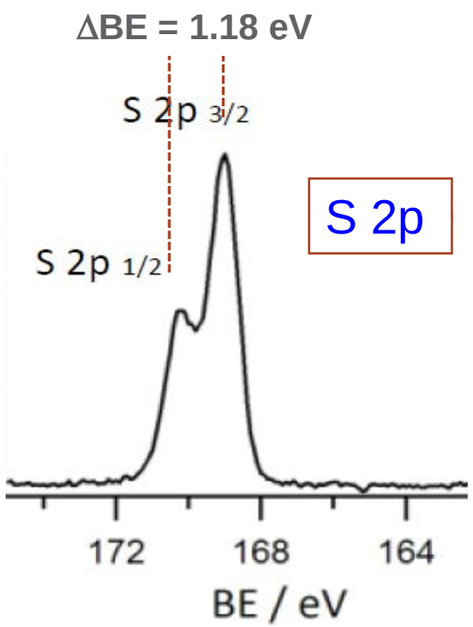

Cu 2p3/2

- Total orbit quantum number **j**
- Orbit quantum number **l**
- Main quantum number **n**
- Chemical Symbol

Interpretation of XPS Spectra: Peak Shapes and Widths

- Peak shapes can be different for different materials
- Peaks shapes are the combination of
  - (1) Physics involved with the ionization process and
  - (2) Distortion due to measurement process
- Observed peak in most of the compounds is a convolution of Gaussian (measurement process) and Lorentzian (Ionization process)
- Many non-conducting and semiconducting materials have symmetrical line shape
- Metals have some asymmetry in their peaks in the higher binding side due to energy loss of photoelectrons due to their interactions with valence electrons

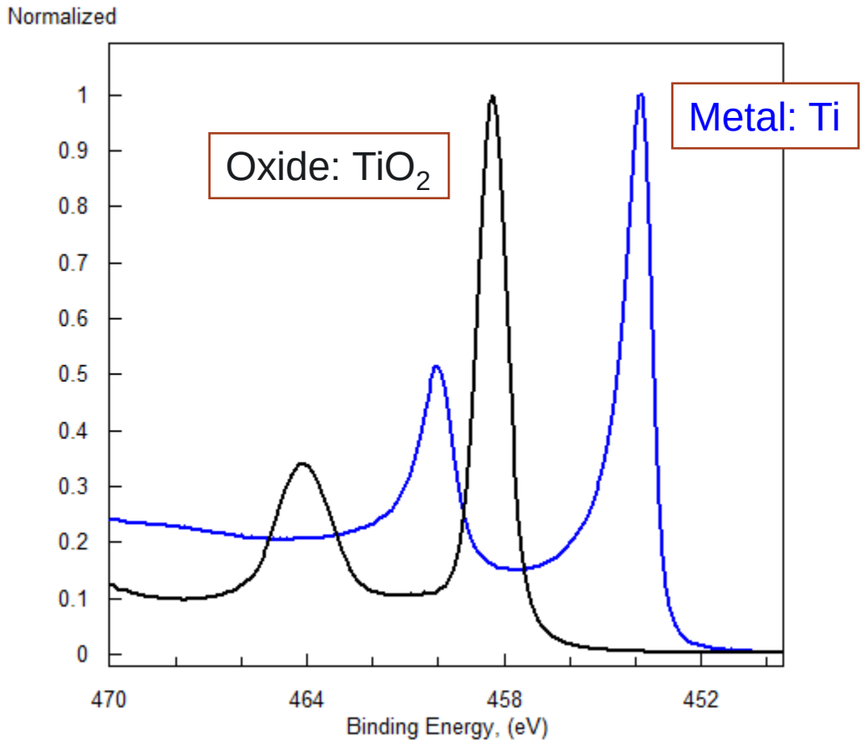

https://xps-database.com/titanium-spectra-ti-metal/

Pacific Northwest
NATIONAL LABORATORY

Surface Sensitive Technique

Why XPS is the Surface Sensitive Technique?

- X-rays penetrate deep into the sample (~microns in depth), but only the photoelectrons which escape the sample without energy loss will reach the detector
- Only electrons from 1st few layers can escape without inelastic collisions
- Electrons originates from deeper in the sample (lose most of its energy) will end up in the background spectrum

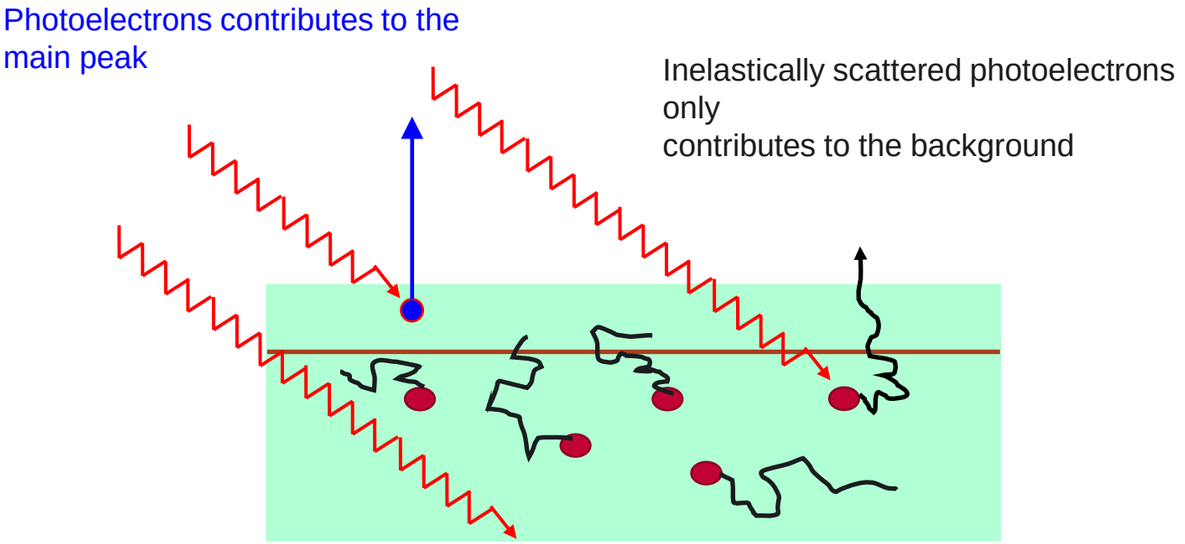

Why XPS is the Surface Sensitive Technique?

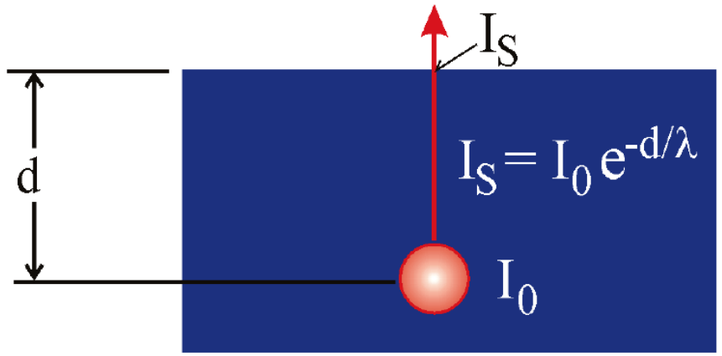

For an electron of intensity I_o emitted at depth **d** below the surface, the intensity is attenuated according to the Beer-Lambert low.

The intensity I_s of the same electron as it reaches the surface is

$$I_s = I_o \, e^{-d/\lambda}$$

where λ is the **inelastic mean free path (IMFP)** of an electron in a solid = is the average distance an electron travel before it undergoes an inelastic collision, losing energy

Inelastic Mean Free Path (IMFP): Universal Curve

- λ depends on (1) kinetic energy of the electron and (2) the specific material
- Several experimental measurements yield a universal curve for IMFP

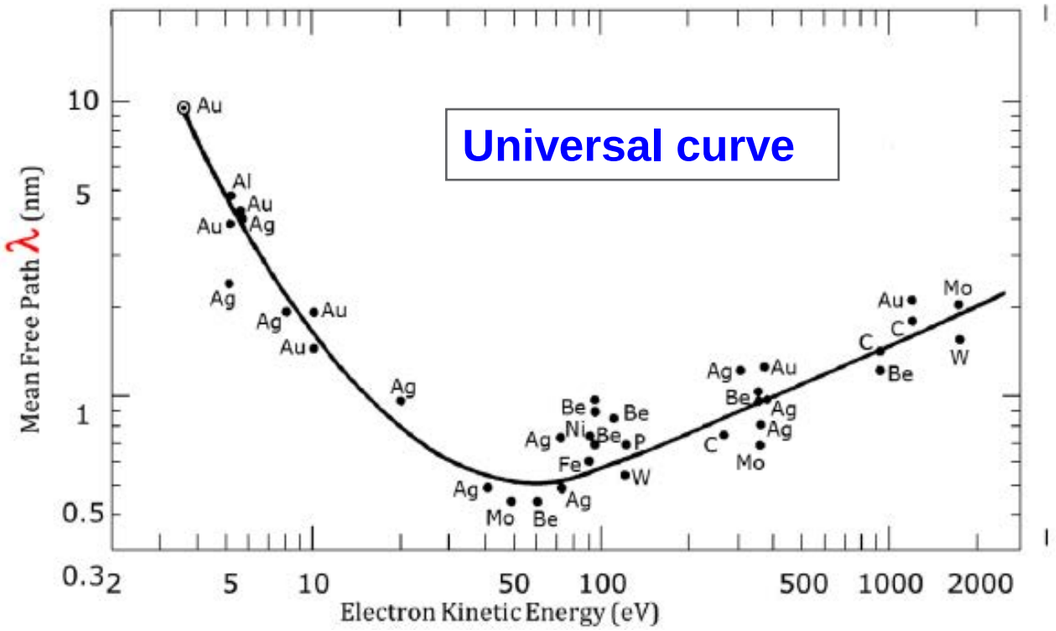

$$\lambda = \frac{(0.65 + 0.007E^{0.93})}{Z^{0.38}}$$

Recently, from many experimental measurements and theoretical calculations scientists have developed a semiempirical equation to calculate IMFP for the XPS measurement range (~500 eV to 1500 eV) :

SURFACE and INTERFACE ANALYSIS

Research Article | Full Access

Simple universal curve for the energy-dependent electron attenuation length for all materials

M. P. Seah*

XPS Sampling Depth

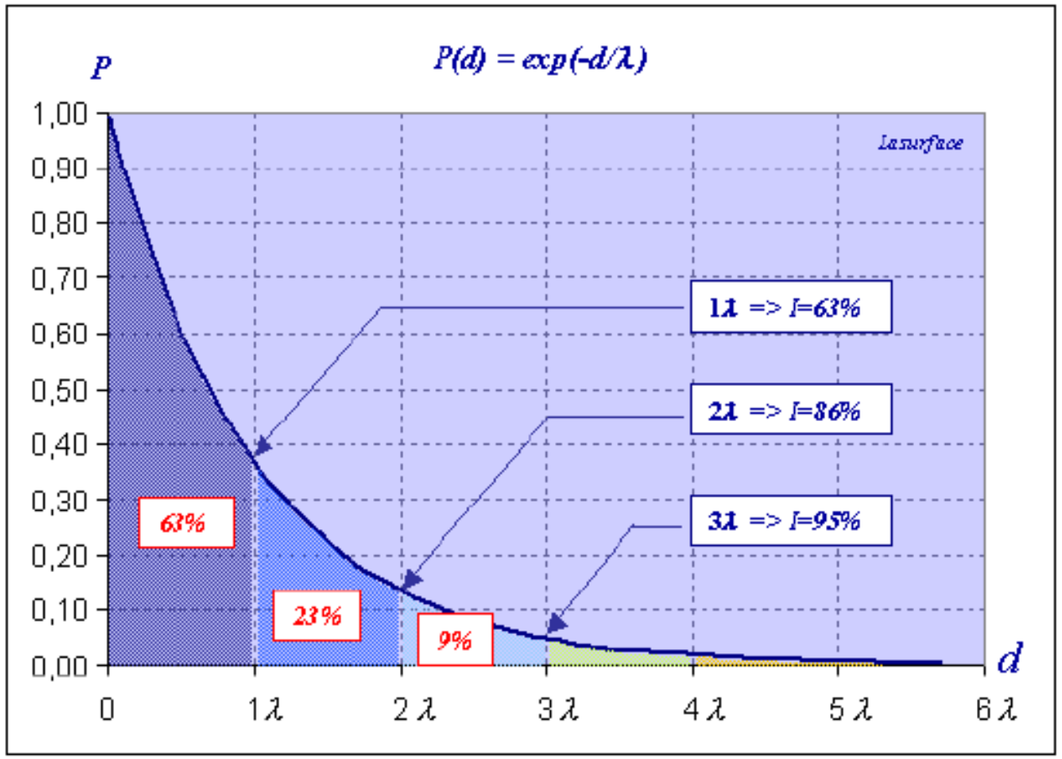

$$I_s = I_o\, e^{-d/\lambda}$$

The probability of a scattering event for any single electron passing through the surface layer is given by:

$$P = I_s/I_o = e^{-d/\lambda}$$

Intensity as a function of depth:

- 63% of signal originated with 1 λ
- 86% of signal originated with 2 λ
- 95% of signal originated with 3 λ

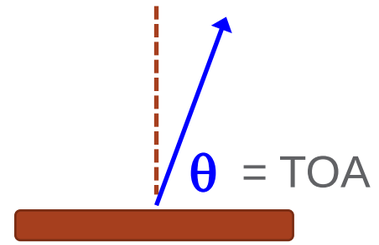

Majority of electrons come from within one λ of the surface
95% photoelectrons detected come from within 3 λ of the surface

XPS Information Depth ~ 3 λ ∗ sin θ

θ = Emission angle relative to the surface (called “Take-off angle TOA)

Courtesy of LaSurface.com

XPS Sampling Depth

$$I_s = I_o\, e^{-d/\lambda}$$

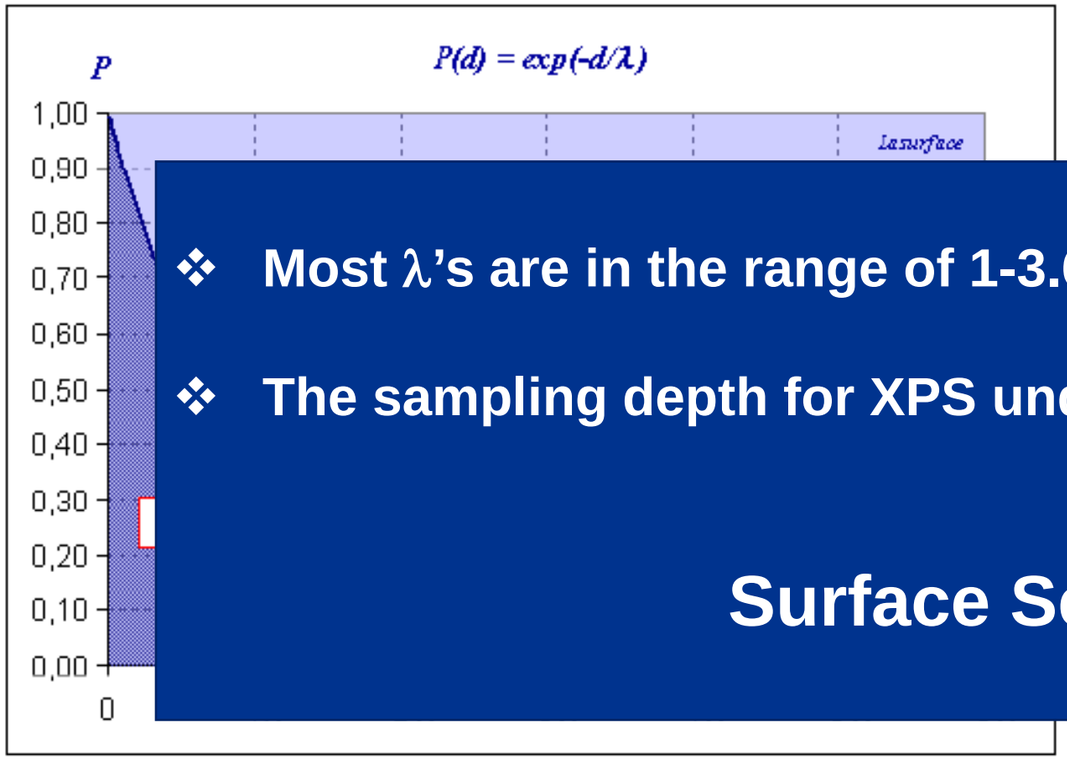

The probability of a scattering event for any single
s given by:

- Most λ's are in the range of 1-3.6 nm for Al k_α radiation
- The sampling depth for XPS under these conditions is 3 -10 nm

Surface Sensitive!

Majority of electrons come from within one λ of the surface
95% photoelectrons detected come from within 3 λ of the surface

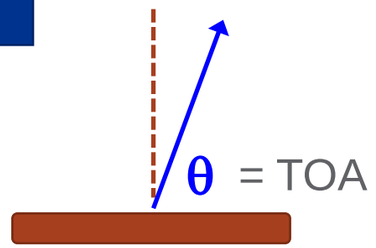

XPS Information Depth ~ 3 λ ∗ sin θ

θ = Emission angle relative to the surface (called "Take-off angle TOA)

Courtesy of LaSurface.com

Pacific Northwest
NATIONAL LABORATORY

Quantification

Background in XPS Spectrum

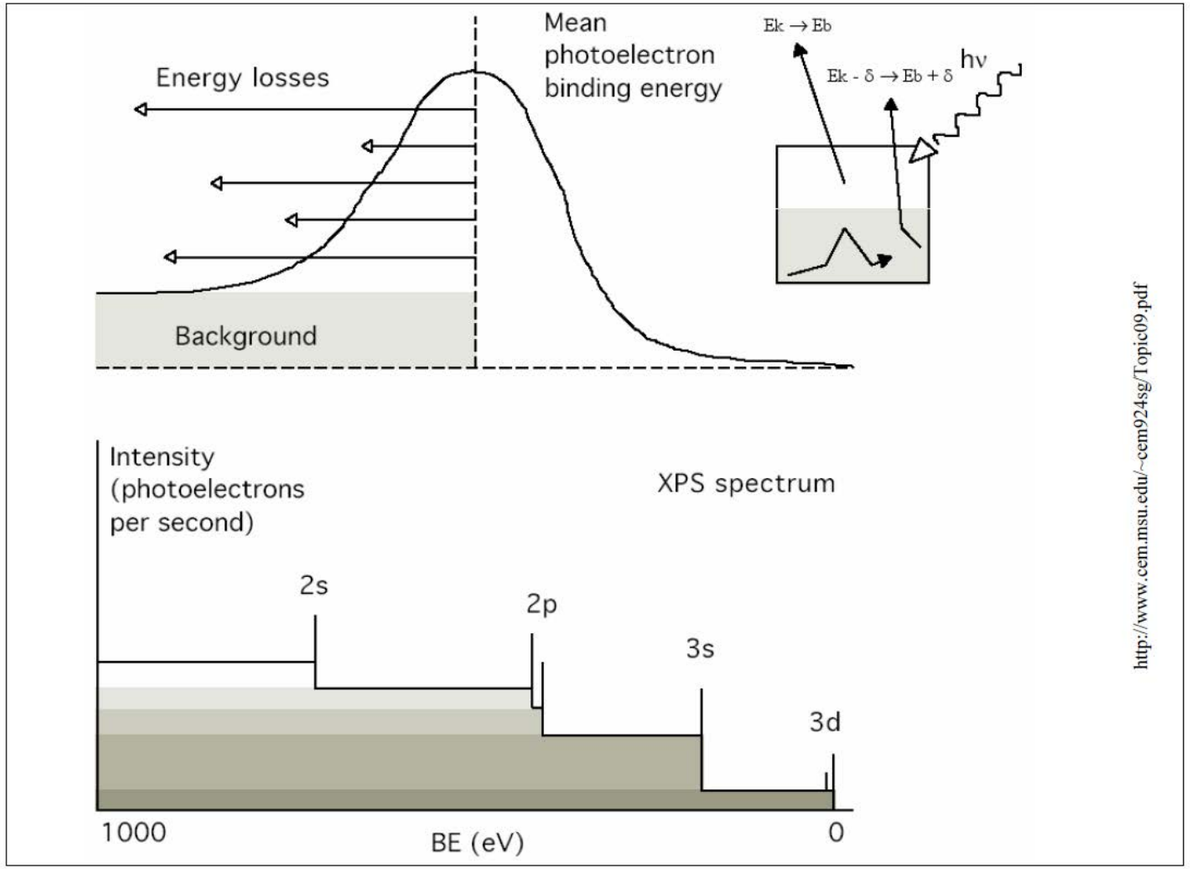

- **Background** = electrons excited by the X-ray Bremsstrahlung radiation (continuous) + photoelectrons which lost energy due to collision (inelastic scattering)
- Each successive photoelectron peak on the binding energy scale will pile additional inelastically scattered photoelectrons onto the background produced by those peaks preceding it, and the aggregate background will exhibit a step-like structure

Background in XPS Spectrum

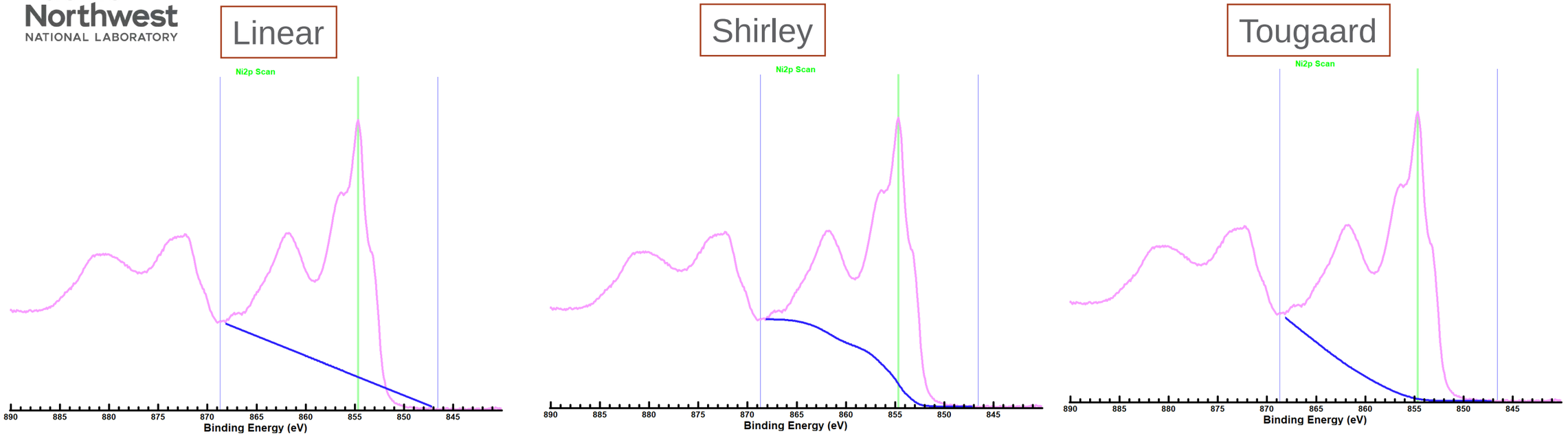

Shirley background: The background goes up in proportion to the total number of photoelectrons below its binding energy position

Tougaard background: Integrating the intensity of the background at a given binding energy from the spectral intensities to higher kinetic energies

- Each background style give slightly different peak areas
- Commonly used background is "**Shirley**" background

Quantitative Analysis by XPS

For a homogeneous sample:

Intensity of the XPS peak = $I = N\sigma DJL\,\lambda\,AT$

$$\Rightarrow \quad N = \frac{I}{\sigma DJL\,\lambda\,AT}$$

- N = Concentration, atoms/cm^3
- σ = Photoelectric cross-section, cm^2
- D = Detector efficiency
- J = X-ray flux, photon/cm^2-sec
- L = Orbital symmetry factor
- λ = Inelastic electron mean free path, cm
- A = Analysis area, cm^2
- T = Analyzer transmission efficiency

Let's define **$S = \sigma DJL\,\lambda\,AT$** = **Elemental Sensitivity Factor**

sensitivity factors (S) are usually given by the XPS instrument manufactures

$$N = \frac{I}{S}$$

Relative concentration $C_x = \dfrac{N_x}{\sum N_i} = \dfrac{\frac{I_x}{S_x}}{\sum \frac{I_i}{S_i}}$

C.S. Fadley "Basic Concepts of X-ray Photoelectron Spectroscopy" From "Electron Spectroscopy, Theory, Techniques, and Applications" C.R. Brundle and A.D. Baker, Eds., Pergamon Press, 1978, Volume 11, Chapter 1

Quantification of Elemental Concentration

For sample with unknown composition

Step 1: Acquire survey scan to identify what elements are present

Step 2: Acquire high resolution scans for each elements present

Step 3: Calculate the peak area under each peak (after background subtraction - we will come back to this later)

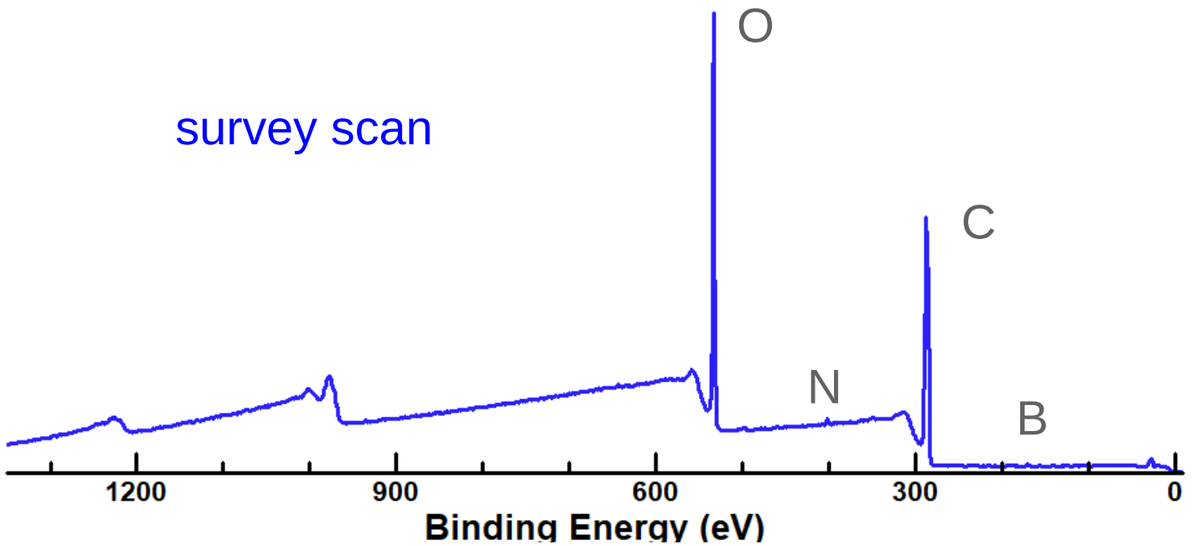

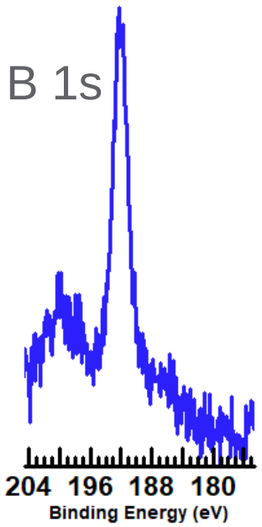

Area= 1516

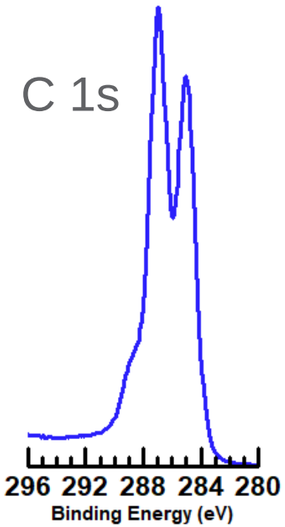

Area= 376767

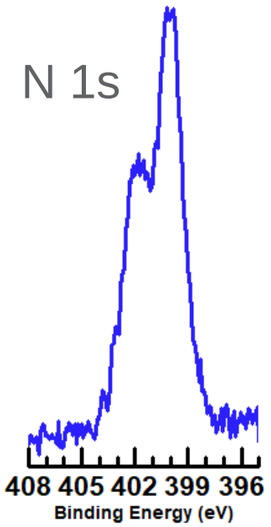

Area= 8698

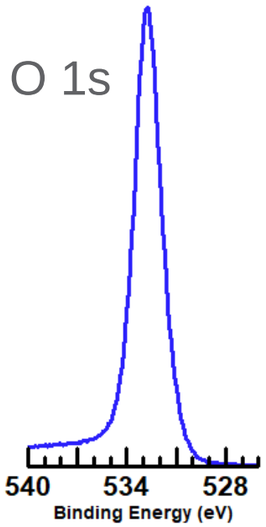

Area= 466020

Quantification of Elemental Concentration

Step 4: Calculate the concentration using the equations

Relative concentration $C_C = \frac{N_C}{\sum N_i} = \frac{\frac{I_C}{S_C}}{\frac{I_C}{S_C} + \frac{I_O}{S_O} + \frac{I_N}{S_N} + \frac{I_B}{S_B}}$

Element	Sensitivity Factor
C 1s	1
O 1s	2.93
N 1s	1.8
B 1s	0.486

$$C_C = \frac{376767/1}{376767/1 + 466020/2.93 + 8698/1.8 + 1516/0.486}$$

$C_C = 0.695$

$C_C = 69.5$ at %

Similarly, we can calculate other concentrations: C = 69.5 at % ; O = 29 at%, N = 0.9 at %, B = 0.6 at %

Detection Limits

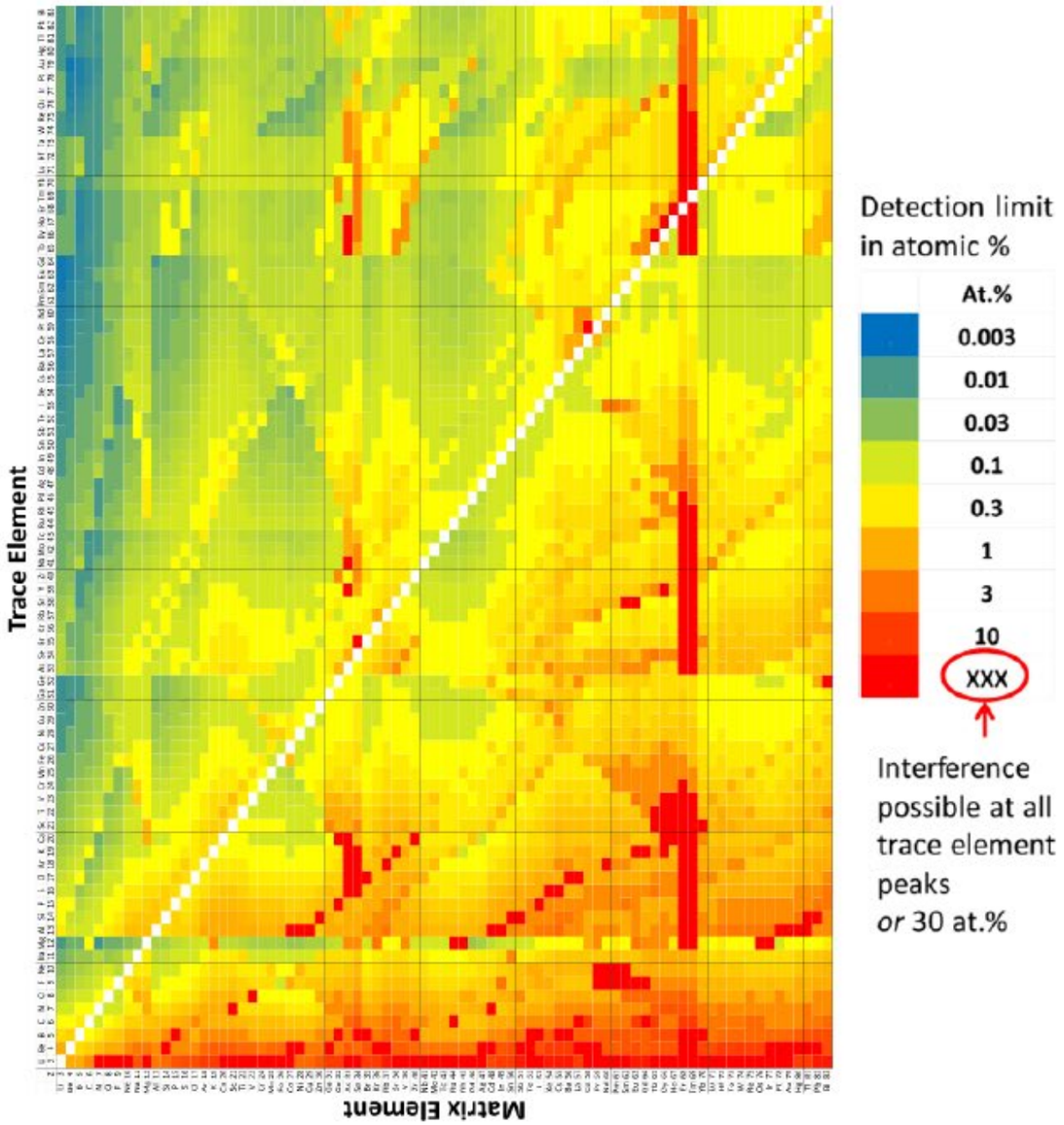

Detection limit in atomic %

At.%
0.003
0.01
0.03
0.1
0.3
1
3
10
XXX

Interference possible at all trace element peaks *or* 30 at.%

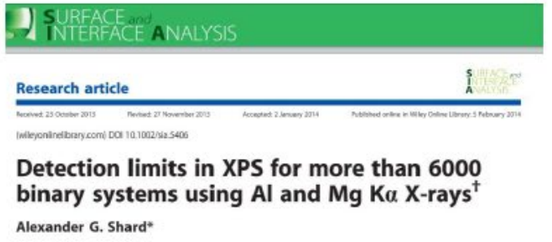

SURFACE and INTERFACE ANALYSIS

Research article

Received: 23 October 2013 Revised: 27 November 2013 Accepted: 2 January 2014 Published online in Wiley Online Library: 5 February 2014

(wileyonlinelibrary.com) DOI 10.1002/sia.5406

Detection limits in XPS for more than 6000 binary systems using Al and Mg Kα X-rays†

Alexander G. Shard*

Pacific Northwest
NATIONAL LABORATORY

Chemical Shifts

Chemical Effects (Shifts) in XPS

An important advantage of XPS is its ability to obtain information on chemical states from the variations in binding energies

- Core level binding energies are determined by **electrostatic interaction between the electron and the nucleus**
  - The shifts observed in XPS have their origin in either **initial-state** and/or **final-state** effects

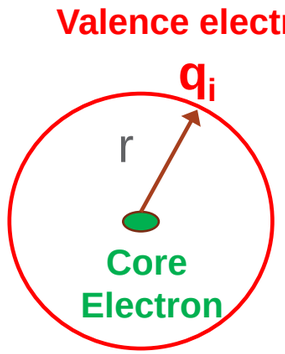

In a simplistic point-charge model, the binding energy of atom i is given by:

$$E_b = E_i^0 + kq_i/r - \sum q_i/r_{ij}$$

E_i^0 in atom i in given reference state.
It considered to Eb for the neutral atom

Weighted charge of i

Potential at i due to surrounding charges

Chemical Shift $\Delta E_b \cong \frac{\Delta q_i}{r} - \Delta R$ ⟹ Influenced by **relaxation effects** in the final state and **lattice effects**

⇓

Related to **electro-negativity** such as change in **valence charge**

Chemical Effects (Shifts) in XPS : Oxides

Withdrawals of valence electron charge ➡ **Increase the binding energy**

Addition of valence electron charge ➡ **Decrease the binding energy**

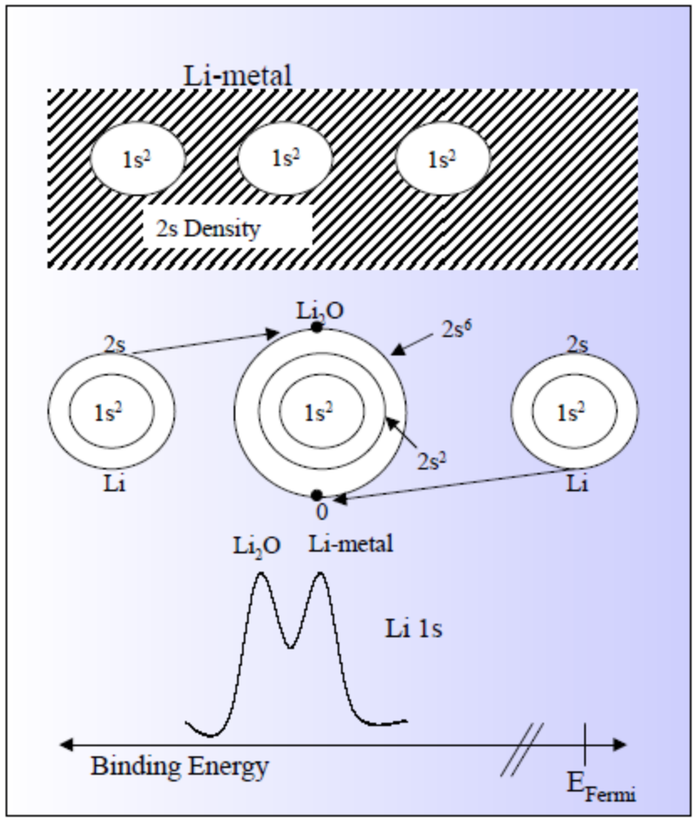

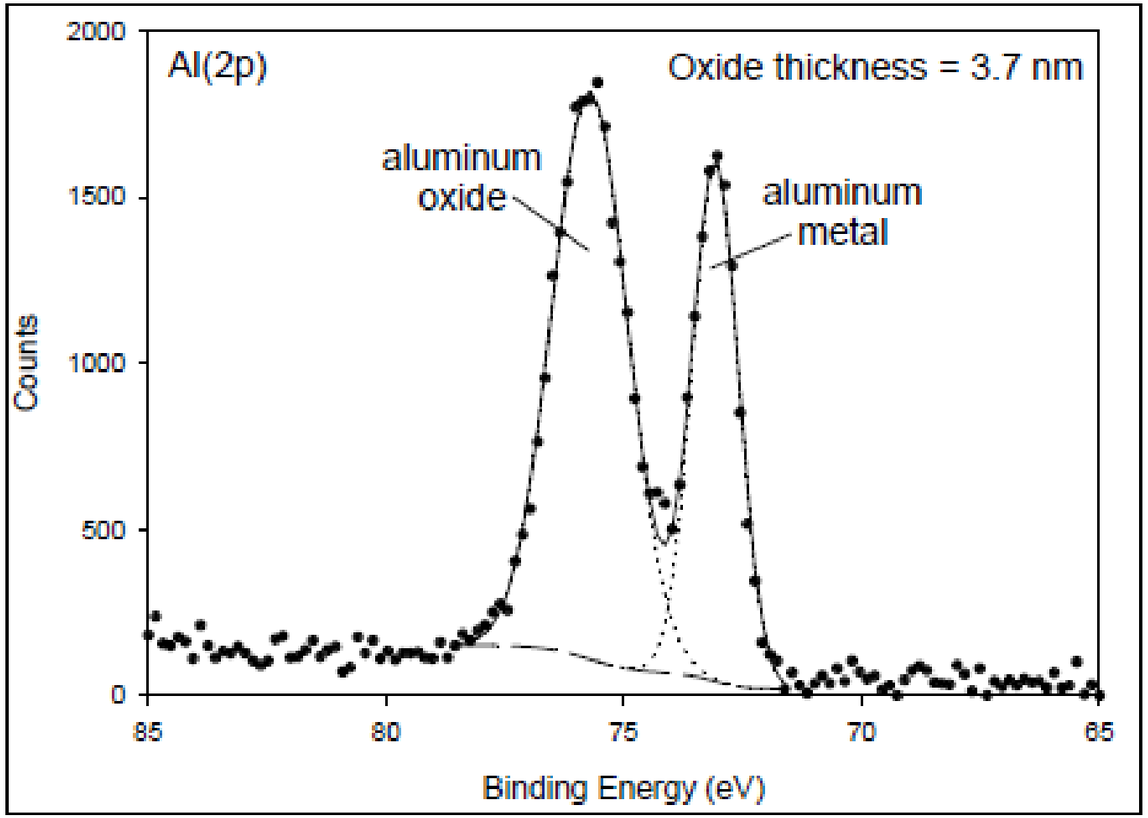

Chemical Effects (Shifts) in XPS : Oxides

- In general, the amount of chemical **shift increases as the oxidation state increases** for most of the metals

Element	Peak	Metal (0 valence)	Bivalent (2+)	Trivalent (3+)	Tetravalent (4+)
Ti	$2p_{3/2}$	454.1	455.0 (+0.9)	–	459.0 (+4.9)
Fe	$2p_{3/2}$	706.7	709.7 (+3.0)	710.9 (+4.2)	–
Ni	$2p_{3/2}$	852.7	853.8 (+1.1)	856.5 (+3.8)	–

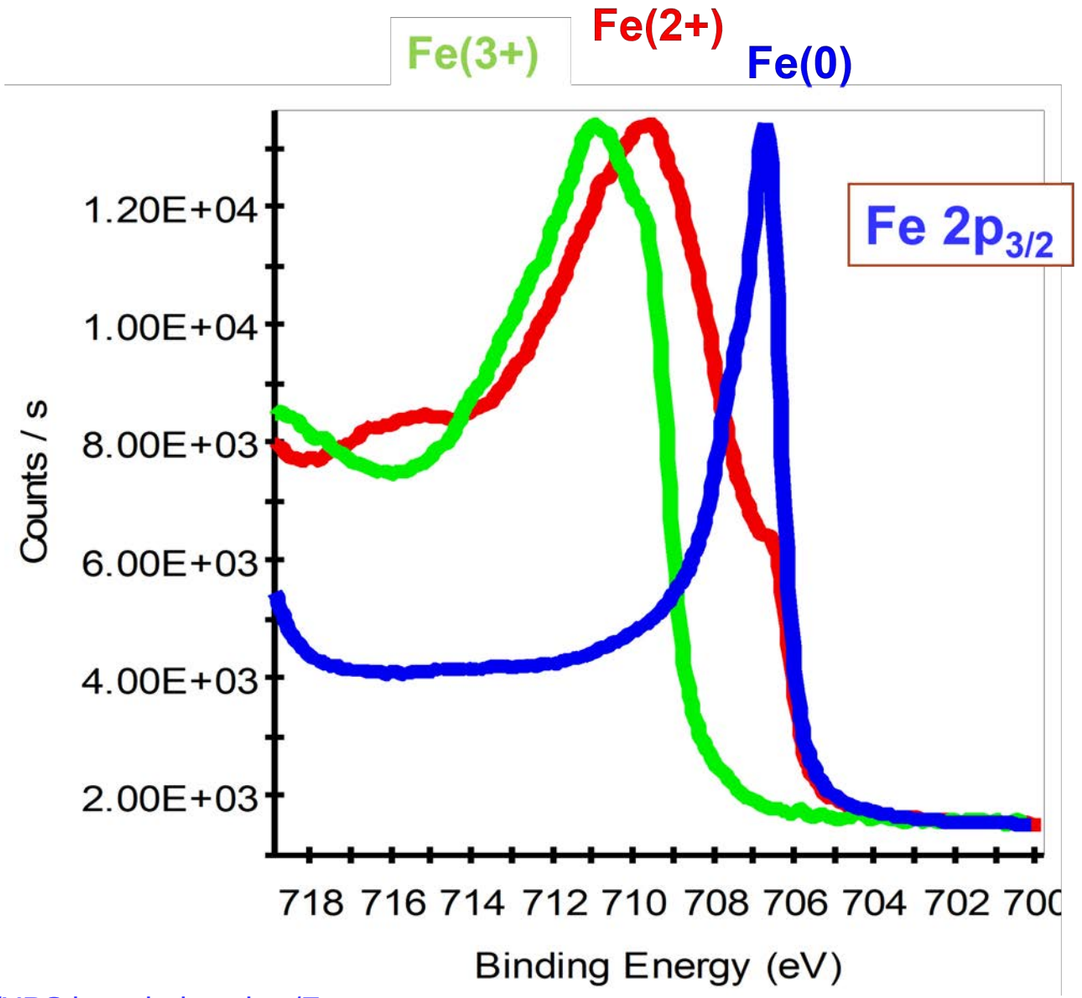

ThermoFisher/Advantage software/XPS knowledge view/Fe

Chemical Effects (Shifts) in XPS : Oxides

- The correlation between binding energy and electronegativity of neighboring elements is not always linear.
- The chemical shift in ionic solids is influenced by the **collective electronic environment within the lattice**, as well as the **relaxation effects** occurring during the photoemission process

Chemical Shift $\Delta E_b \cong \frac{\Delta q_i}{r} - \Delta R$

Element	peak	Metal (0 valence)	Monovalent (1+)	Bivalent (2+)	Trivalent (3+)	Tetravalent (4+)
Cu	$2p_{3/2}$	932.7	932.5 (-0.2)	933.6 (+0.9)	–	–
Pb	$4f_{7/2}$	136.9	–	138.8 (+1.9)	–	137.5 (+0.6)
Ag	$3d^5_{/2}$	368.2	367.62 (-0.6)	368.3 (+0.1)		

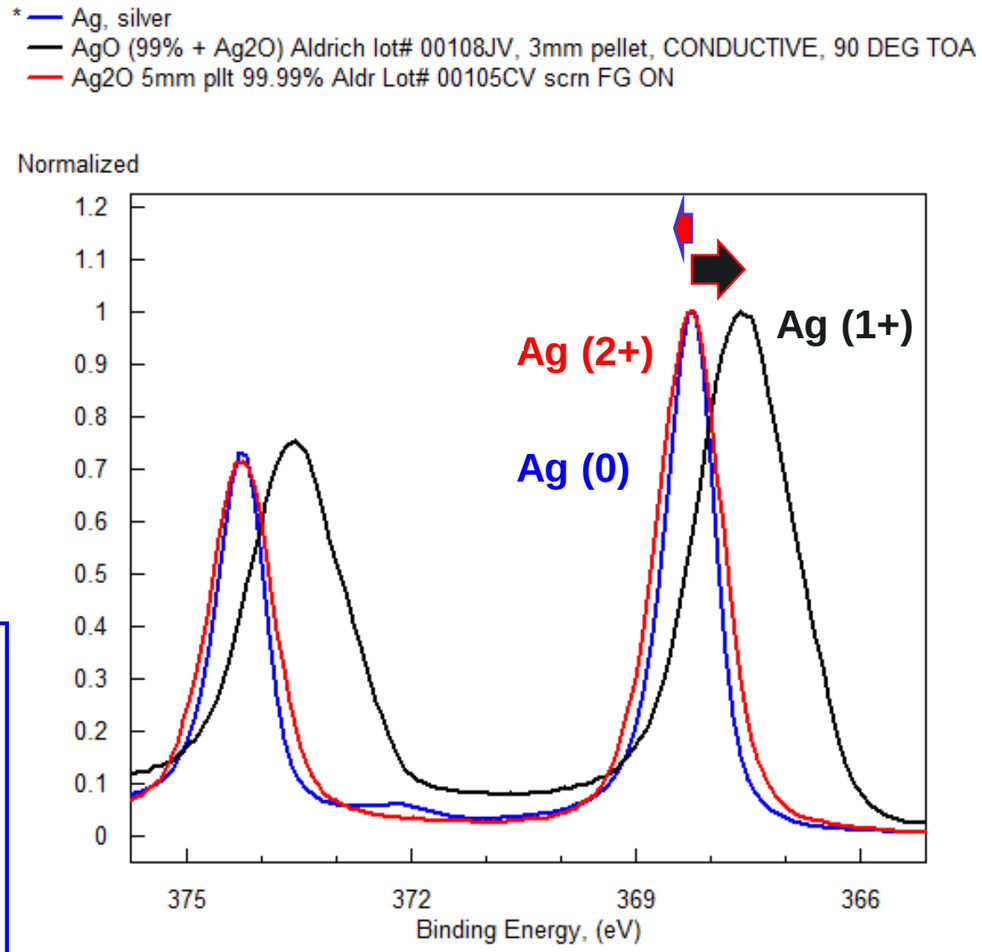

https://xps-database.com/silver-ag-z47-silver-compounds/

Chemical Effects (Shifts) in XPS : Oxides

- The amount of chemical shift is also **dependent on the electronegativity of the atoms surrounding** the metal
- For example, the chemical shifts for metal oxides are smaller than the chemical shifts for metal fluorides

Element	peak	Metal (0 valence)	Li_2O (1+)	LiF (1+)
Li	2s	54.5	55.6	57

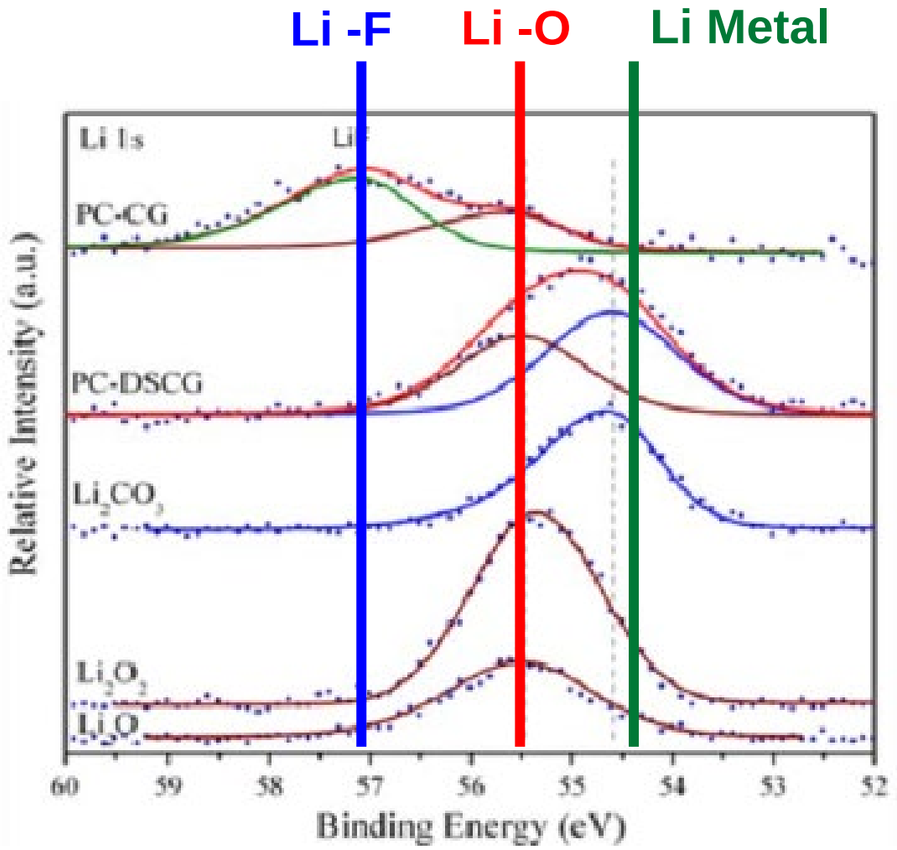

Energies **2013**, *6*, 6016-6044; doi:10.3390/en6116016

Chemical Effects (Shifts) in XPS : Organics

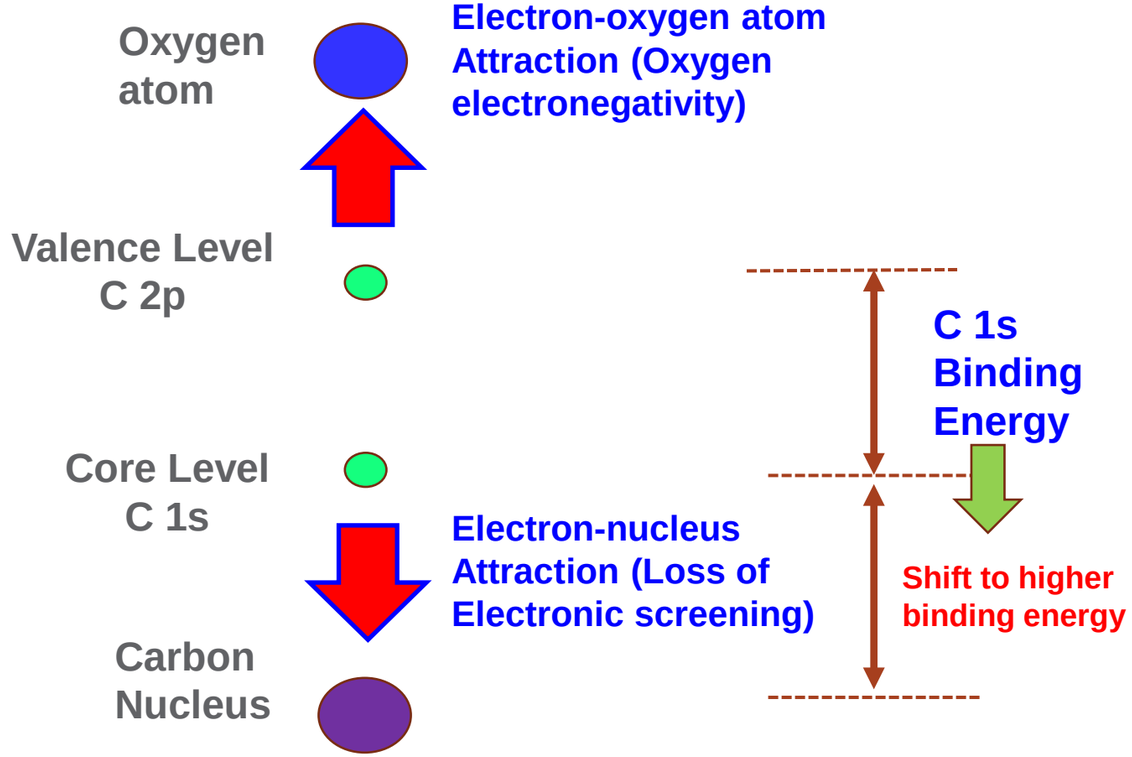

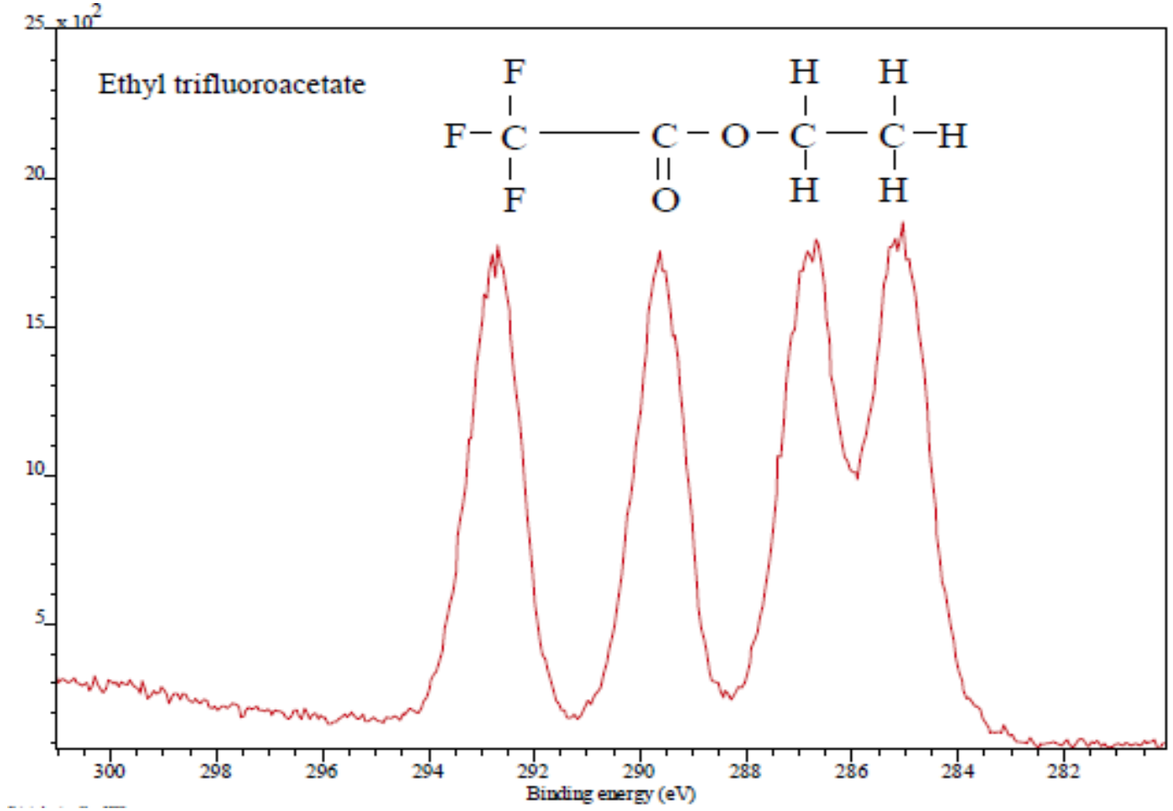

- The biggest shifts are observed when nearest neighbors have the largest electronegativity differences

BE C 1s (eV):

(C-C) <	(C-N) <	(C-O) <	(C-F)
285	*285.6*	*286.7*	*291.3*

http://srdata.nist.gov/xps/Default.aspx
High resolution XPS of organic polymers : the Scient

Chemical Effects (Shifts) in XPS : Secondary Chemical Shift

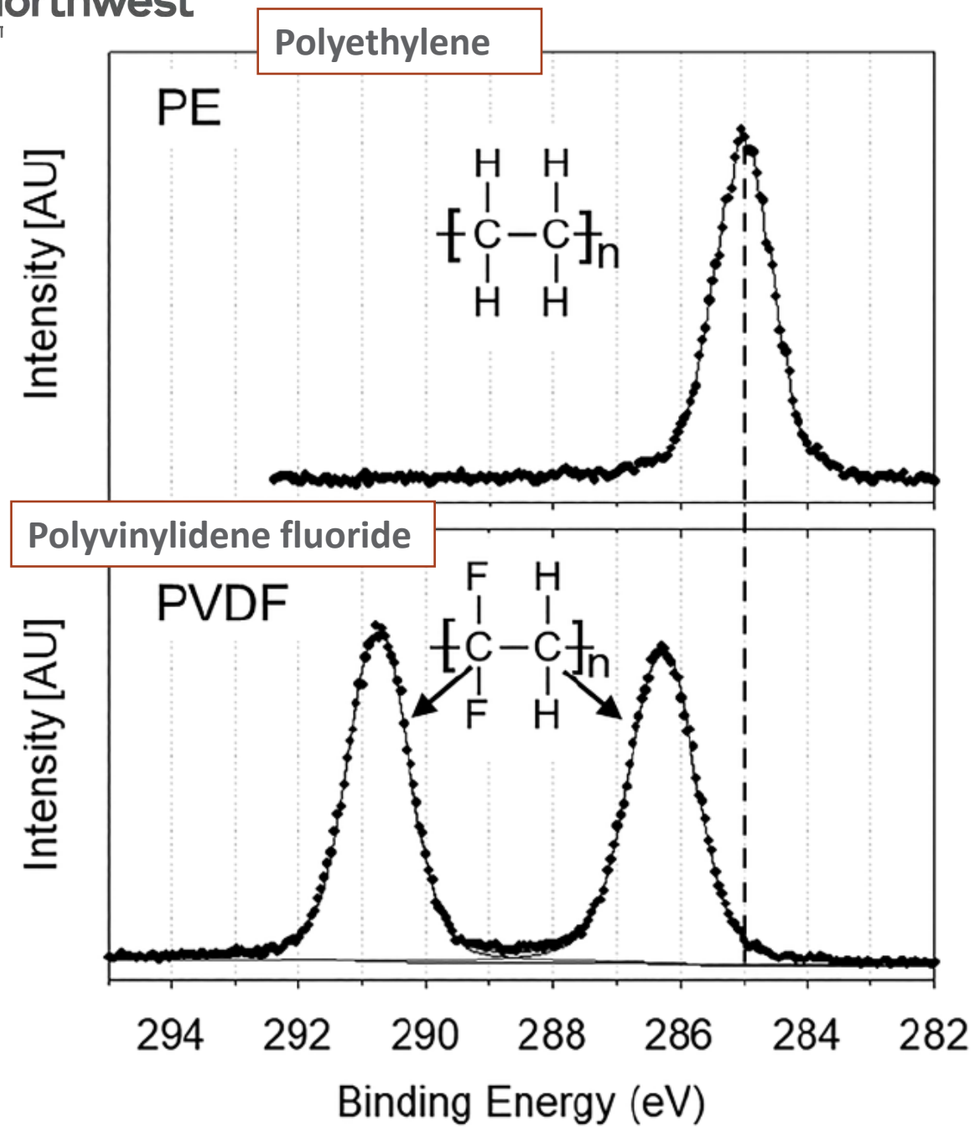

- Lower binding energy peak in the PVDF C 1s spectrum due to C atoms that are bonded to hydrogens (CH_2) is shifted with respect to the C 1s signal from PE by 1.3 eV.
- Clearly, significantly lowered valence charge density on C atoms in CF_2 units of PVDF affected the valence charge density on neighboring C atoms from CH_2 units

This shift is called **secondary chemical shift**

Journal of Applied Physics. 2022;132(1). doi:10.1063/5.0086359

Chemical Effects (Shifts) in XPS : Organics

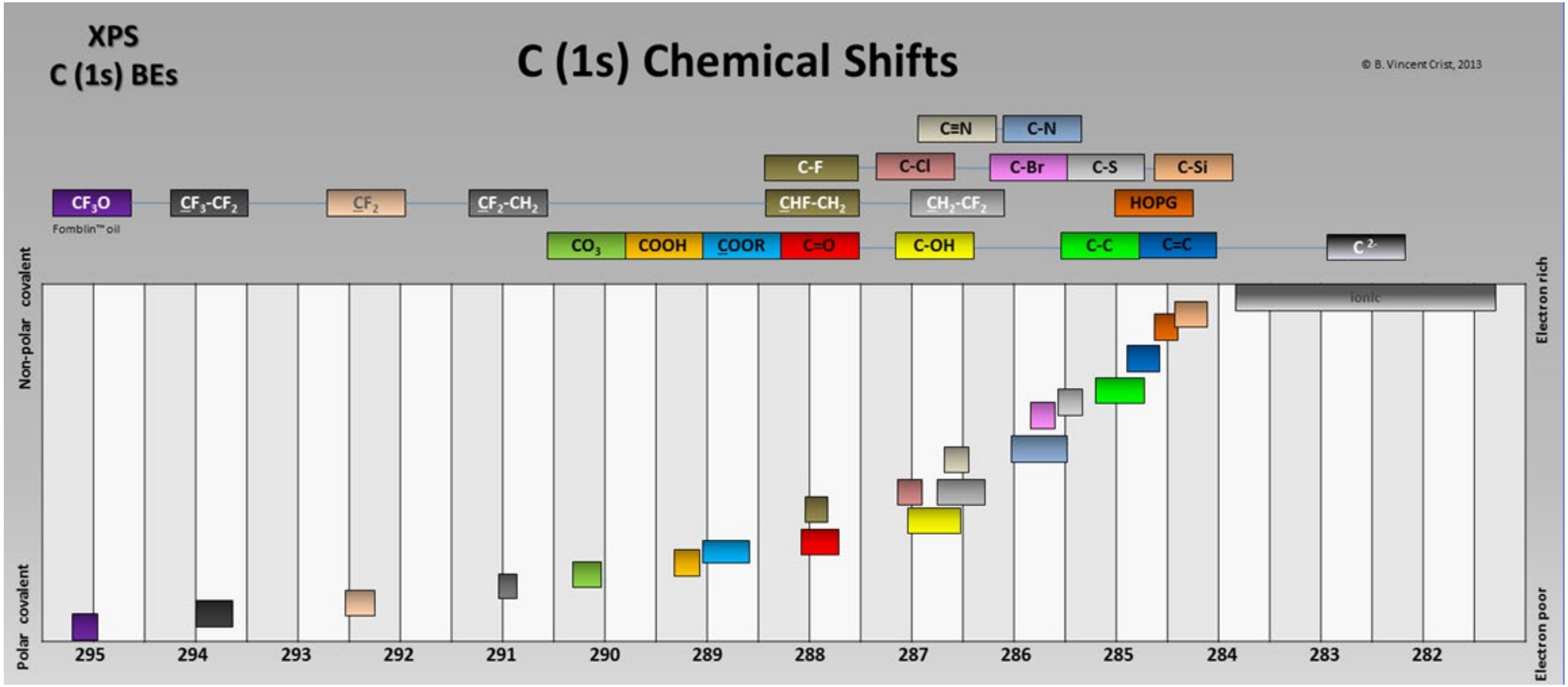

http://srdata.nist.gov/xps/Default.aspx
High resolution XPS of organic polymers : the Scienta ESCA300 database

Chemical Effects (Shifts) in XPS : Sulfates and Sulfides

Na thiosulfate ($Na_2S_2O_3$)

Na sulfate (Na_2SO_4)

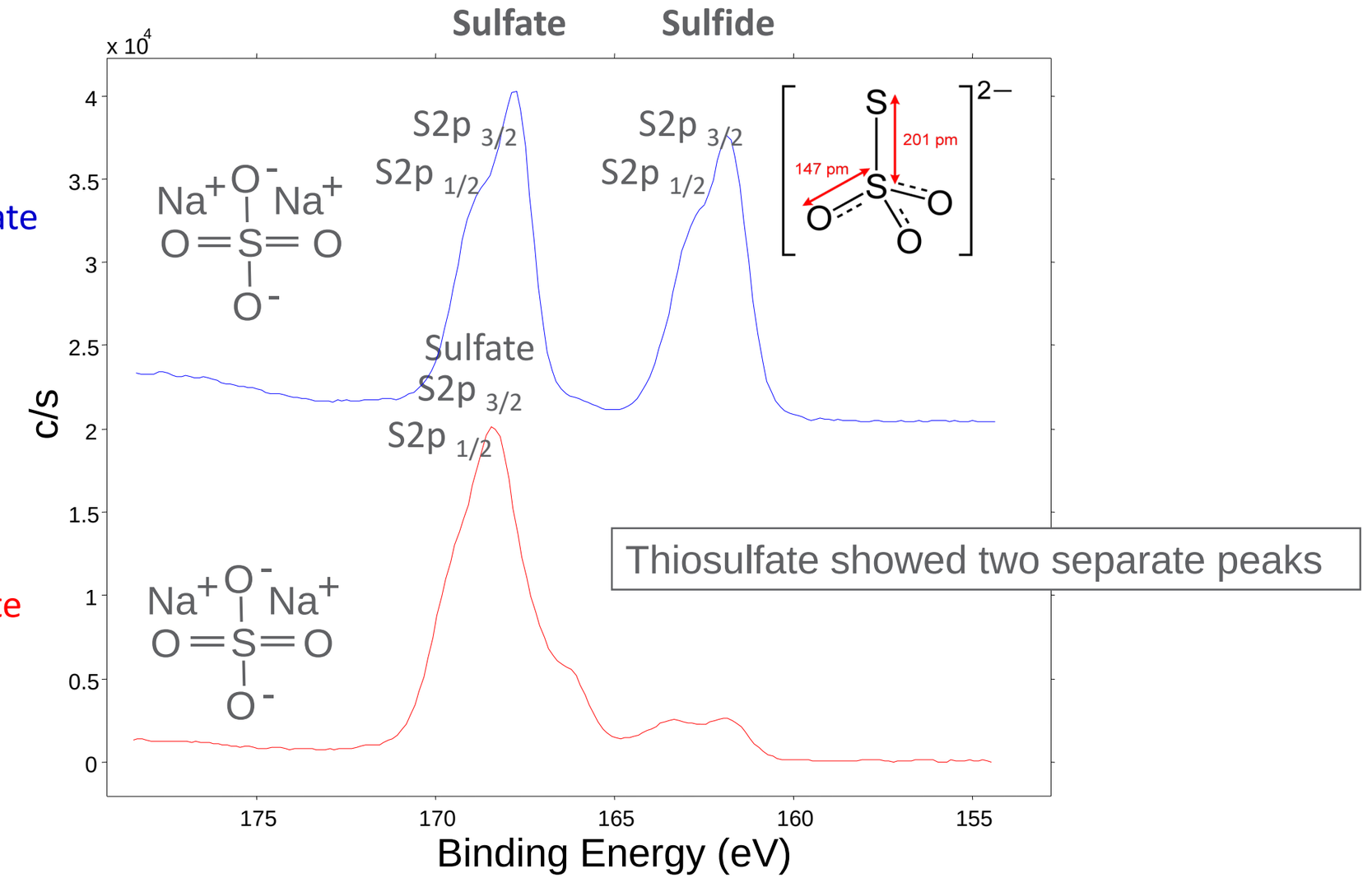

Thiosulfate showed two separate peaks

Pacific Northwest
NATIONAL LABORATORY

Other useful spectroscopic Features

Other XPS Spectroscopy Features: Shake-up and Shake-off Satellites

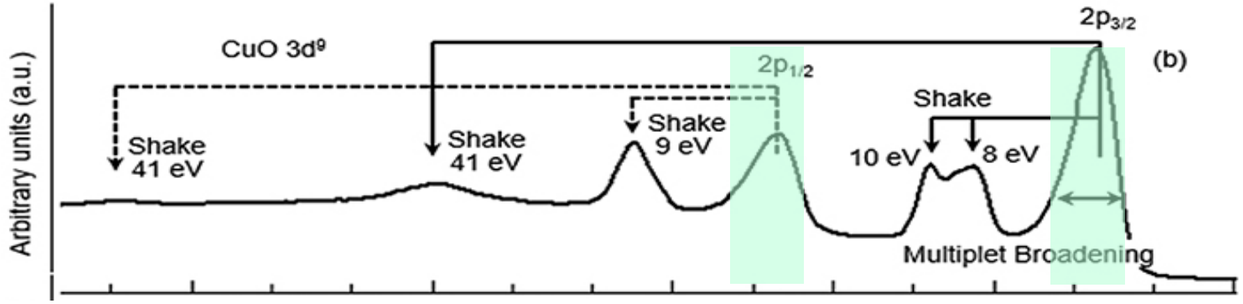

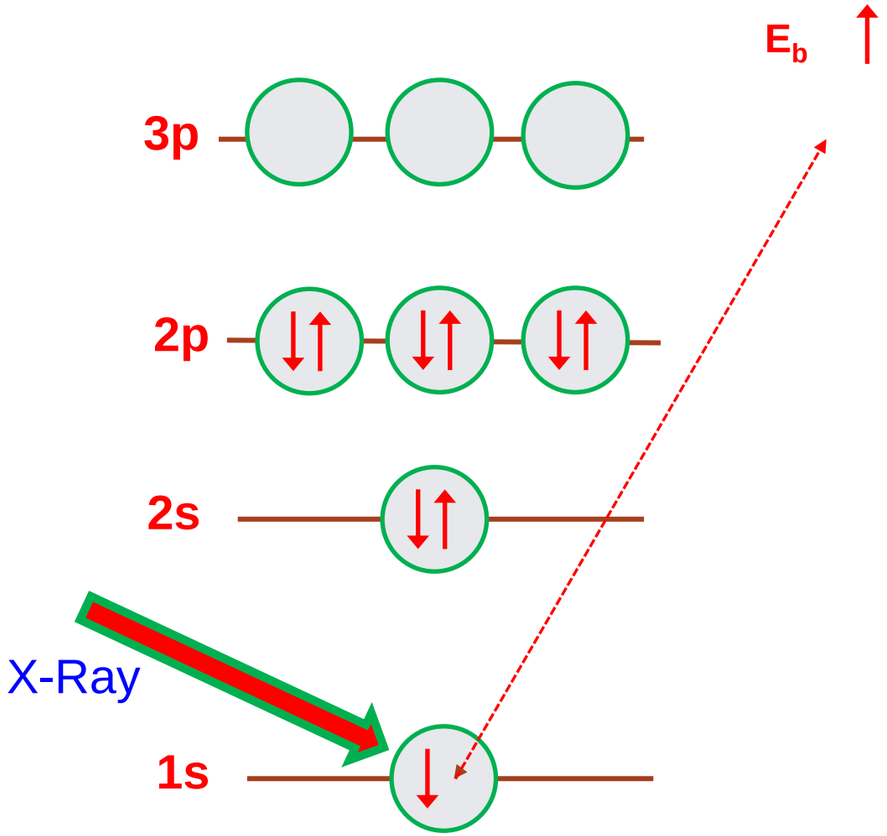

Main Photoemission Peak

Journal of Vacuum Science & Technology A. 2020;38(4). doi:10.1116/1.5143897

Other XPS Spectroscopy Features: Shake-up Satellites

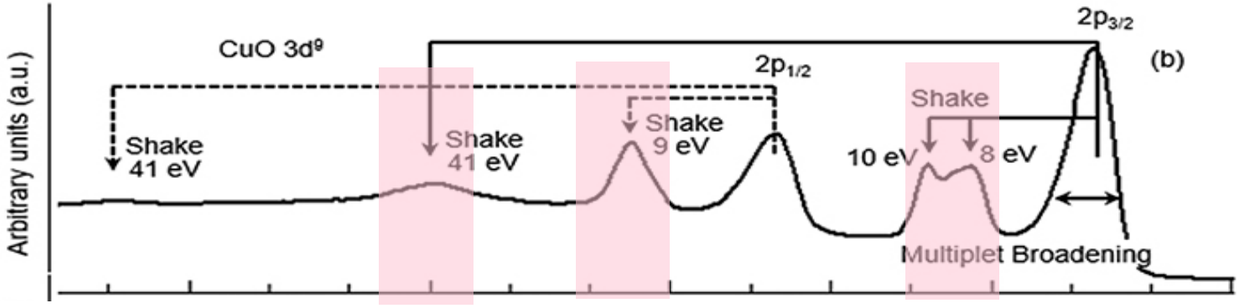

Journal of Vacuum Science & Technology A. 2020;38(4). doi:10.1116/1.5143897

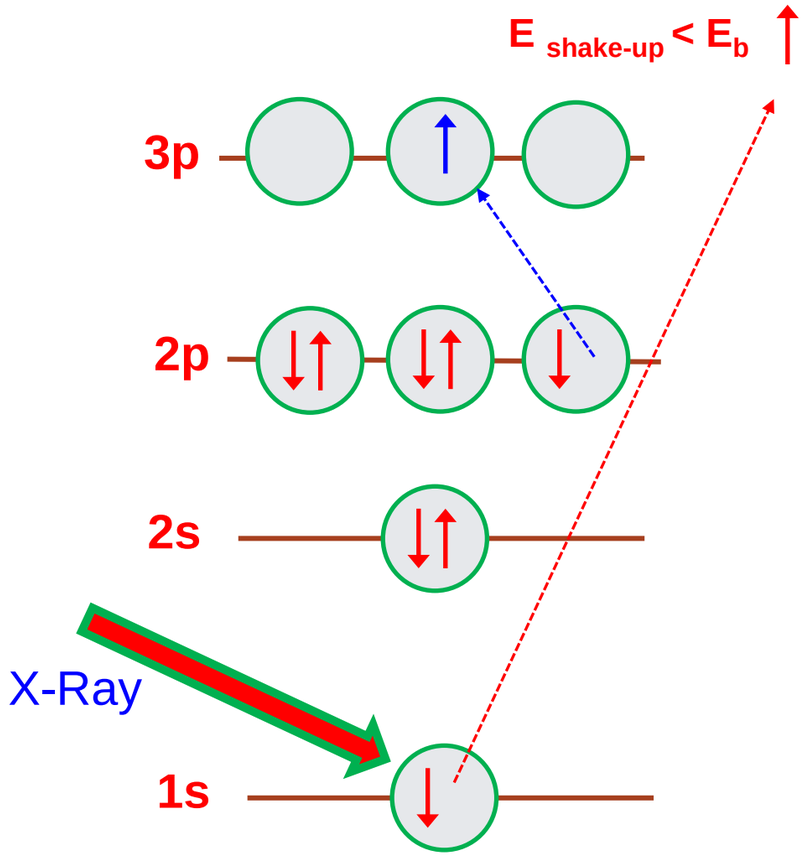

Shake-up Features

Other XPS Spectroscopy Features: Shake-off Satellites

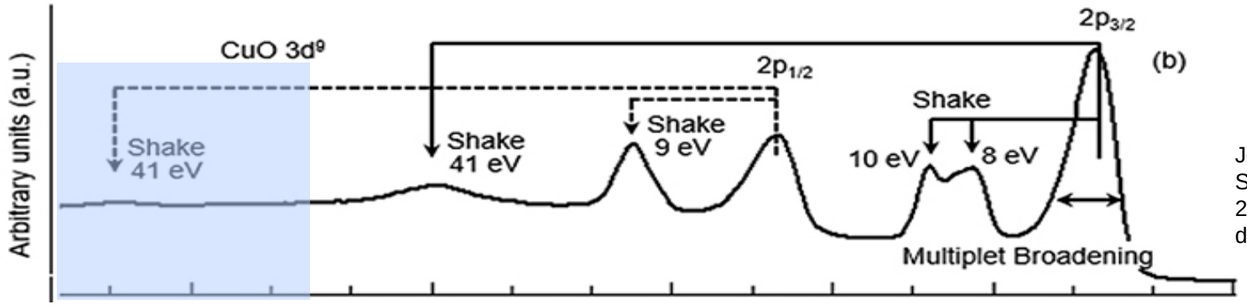

Journal of Vacuum Science & Technology A. 2020;38(4). doi:10.1116/1.5143897

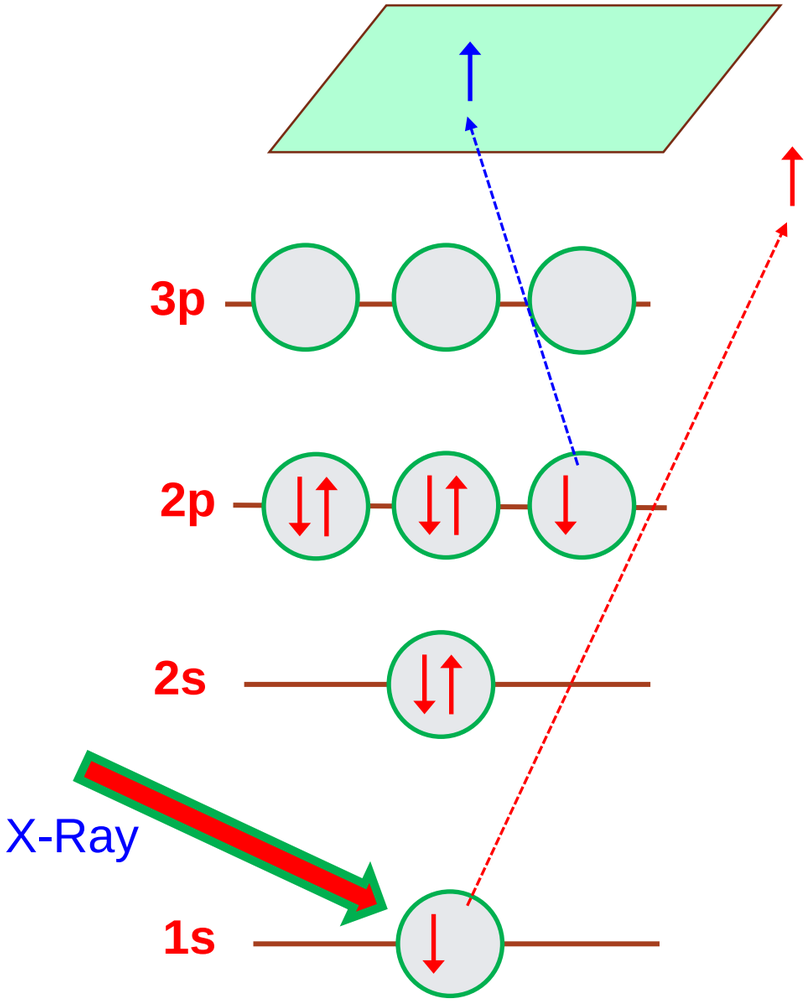

Shake-off Features

Other XPS Spectroscopy Features: Multiplet Splitting

- After photoemission, the unpaired electron may couple with other unpaired electrons in the atom

e- (3d+4s)	0	1	2	3	3	4	4	5	5	6	6	7	7	8	8	9	9	10	10	11	12
Electronic Configuration	[Ar]	[Ar] 3d1	[Ar] 3d2	[Ar] 3d3	[Ar] 3d1 4s2	[Ar] 3d4	[Ar] 3d2 4s2	[Ar] 3d5	[Ar] 3d3 4s2	[Ar] 3d6	[Ar] 3d5 4s1	[Ar] 3d7	[Ar] 3d5 4s2	[Ar] 3d8	[Ar] 3d6 4s2	[Ar] 3d9	[Ar] 3d7 4s2	[Ar] 3d10	[Ar] 3d8 4s2	[Ar] 3d10 4s1	[Ar] 3d10 4s2
Sc	Sc(III)				Sc(0)																
Ti	Ti(IV)	Ti(III)	Ti(II)				Ti(0)														
V	V(V)	V(IV)	V(III)	V(II)					V(0)												
Cr	Cr(VI)		Cr(IV)	Cr(III)		Cr(II)					Cr(0)										
Mn	Mn(VII)	Mn(VI)		Mn(V)		Mn(III)		Mn(II)					Mn(0)								
Fe								Fe(III)		Fe(II)*					Fe(0)						
Co										Co(III)		Co(II)					Co(0)				
Ni												Ni(III)		Ni(II)*					Ni(0)		
Cu																Cu(II)		Cu(I)		Cu(0)	
Zn																		Zn(II)			Zn(0)

No Mulitplet Splitting
Multiplet Splitting (Resolved in XPS)
Multiplet Splitting (Not Well-Resolved or Peak Broadening Only)

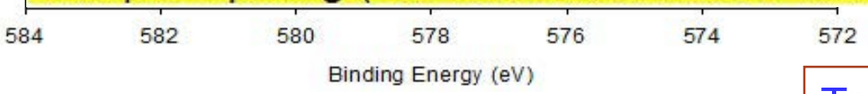

Cr 2p 3/2 peak in Cr_2O_3 exhibiting multiplet splitting.
(Taken from XPSfitting website c/o Mark Biesinger)

Initial State

Final States

Transition metals (*unfilled d orbitals*) and rare earth (*unfilled f orbitals*) show Multiplet Splitting

Other XPS Spectroscopy Features: Plasmon Loss Features

- Photoelectrons travelling through the solid can interact with other electrons
- These interactions can result in the photoelectron exciting some electronic transition

→ **Lose its energy**

$$e_{ph} + e_{solid} \longrightarrow e^{*}_{ph} + e^{**}_{solid}$$

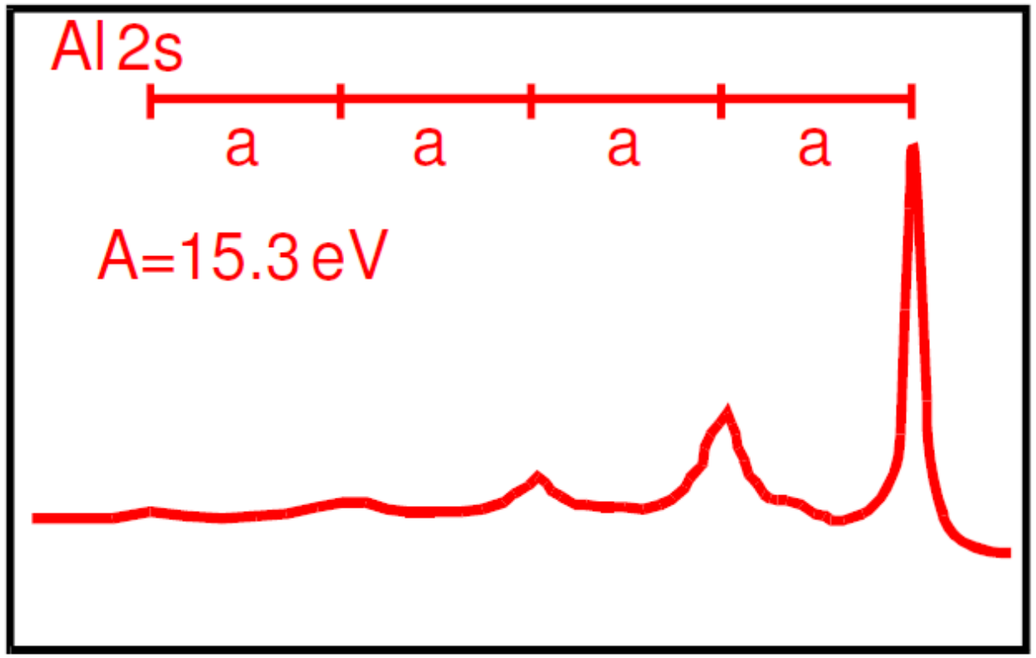

Metal

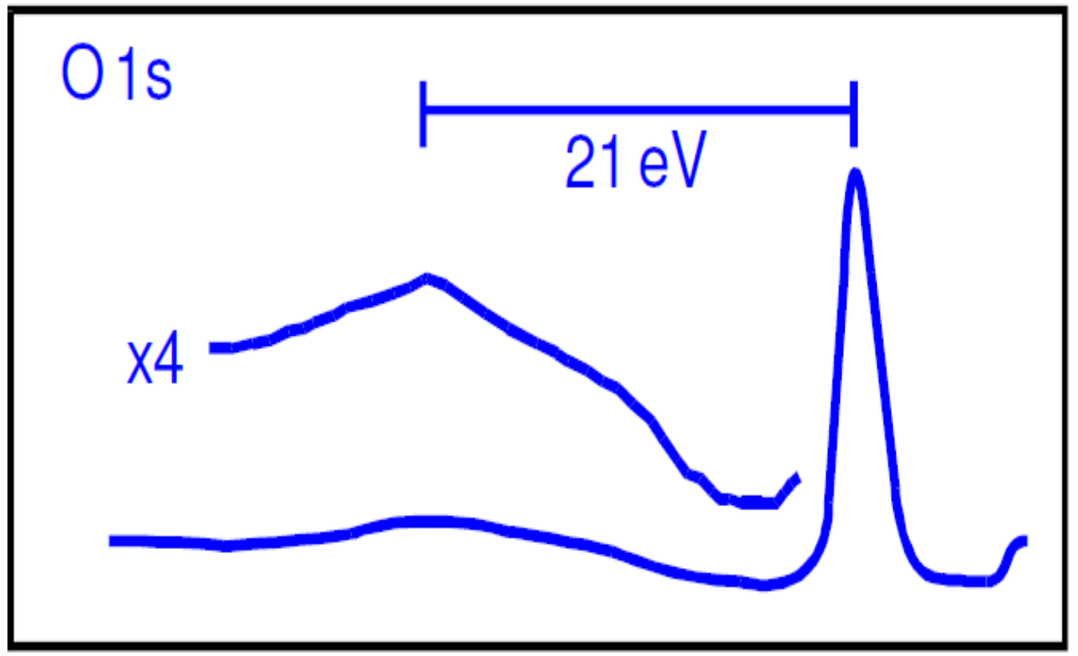

Oxides

Pacific Northwest
NATIONAL LABORATORY

Sampling Depth

Different Ways to Change Sampling Depth

(1) Use of high binding energy and low binding energy peaks from the same element

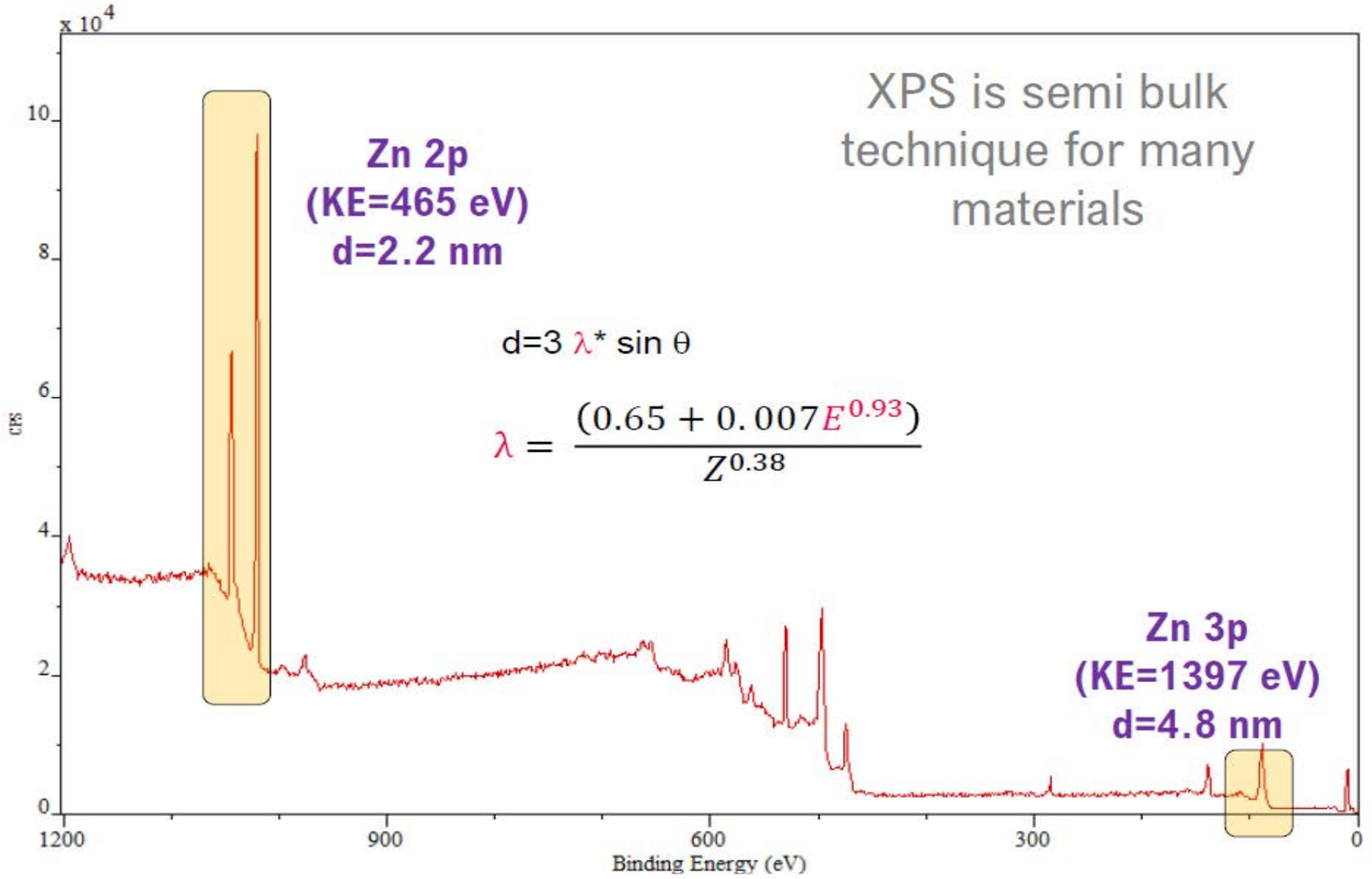

Different Ways to Change Sampling Depth

(2) Change the take-off angle (**Angle Resolved XPS**)

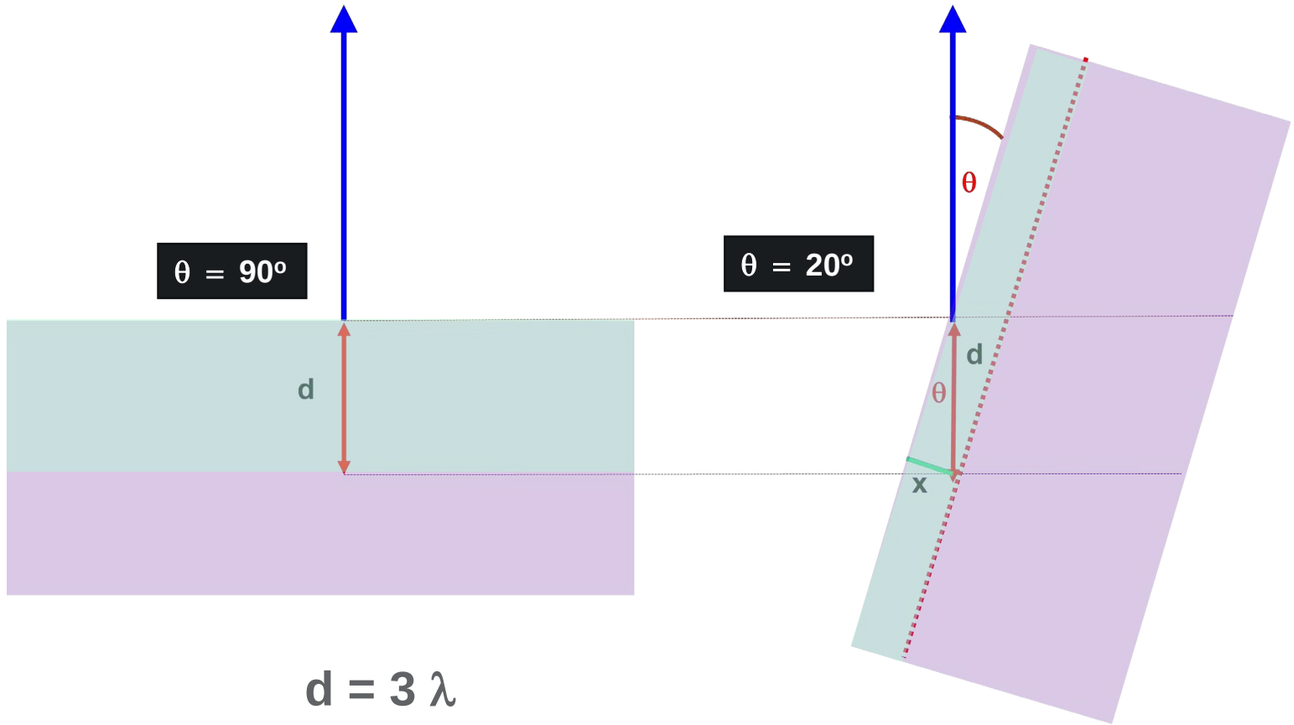

d = 3 λ

Effective depth x = d * sin(θ)

x = **3** λ * sin(θ)

For Pt 4f: **90 TOA = 4.2 nm** **20 TOA = 2.7 nm**

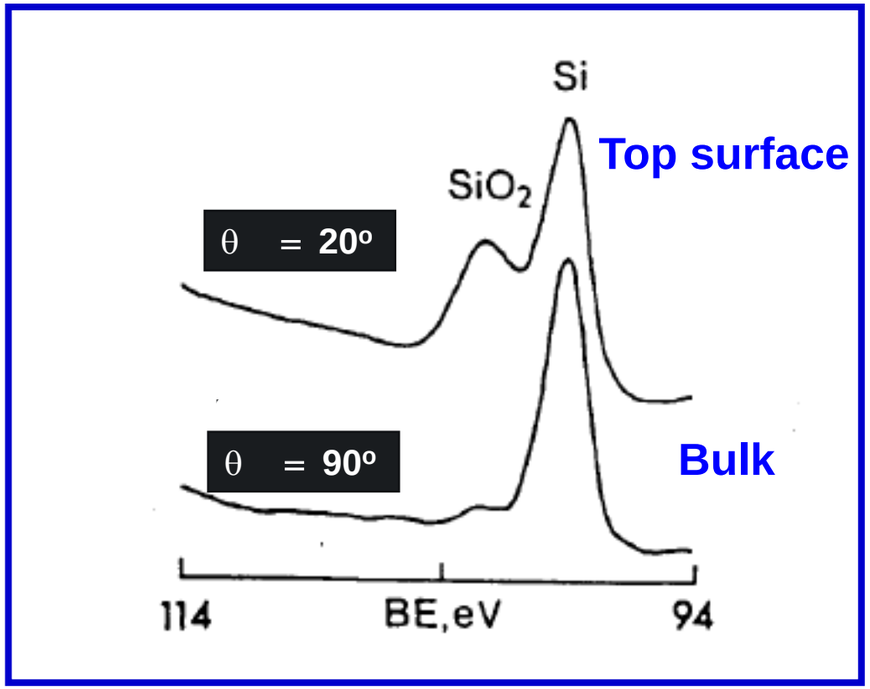

❖ Works well for flat samples and overlayers

Different Ways to Change Sampling Depth

(3) Remove layer by layer with Argon mono ions or cluster ions

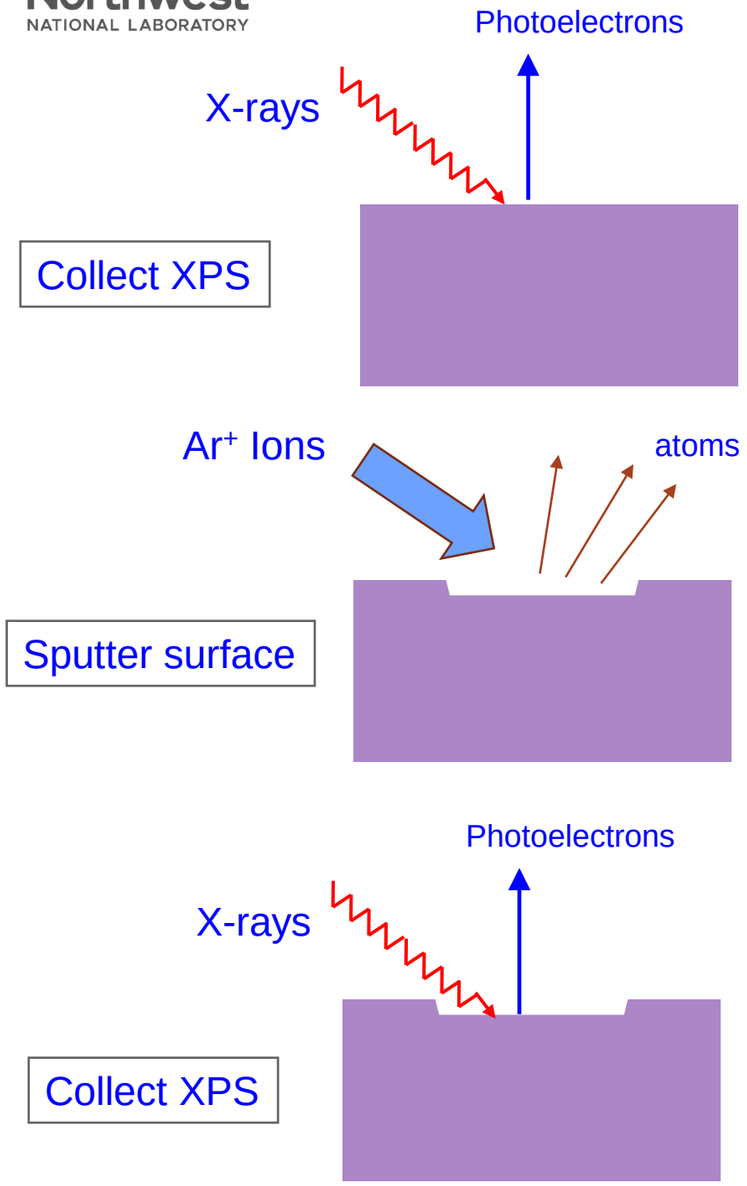

Different Ways to Change Sampling Depth

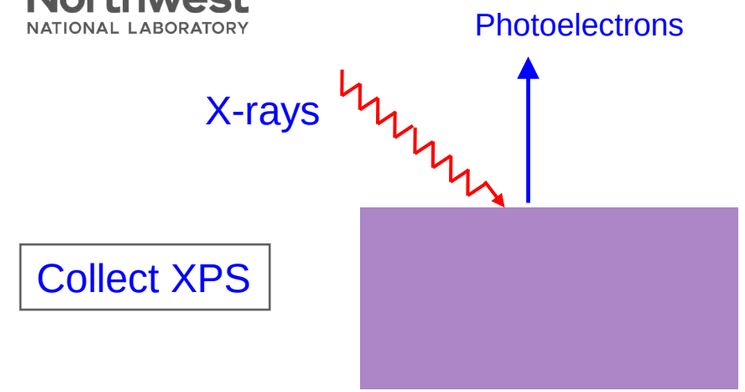

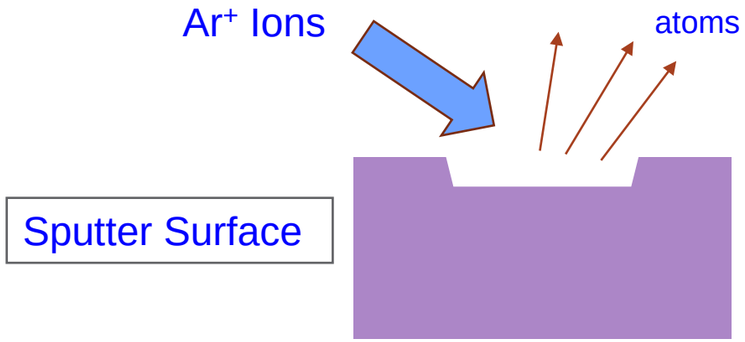

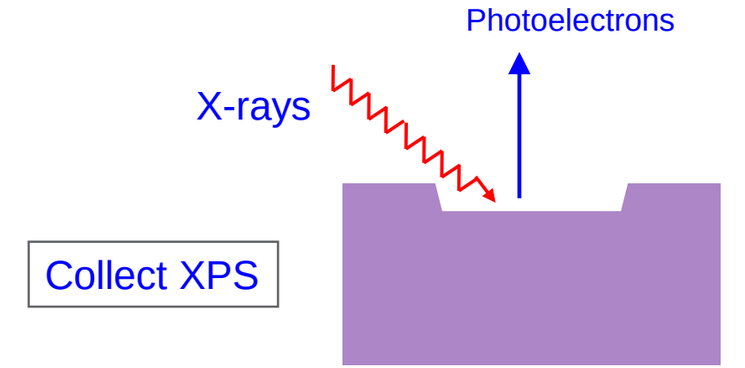

Different Ways to Change Sampling Depth

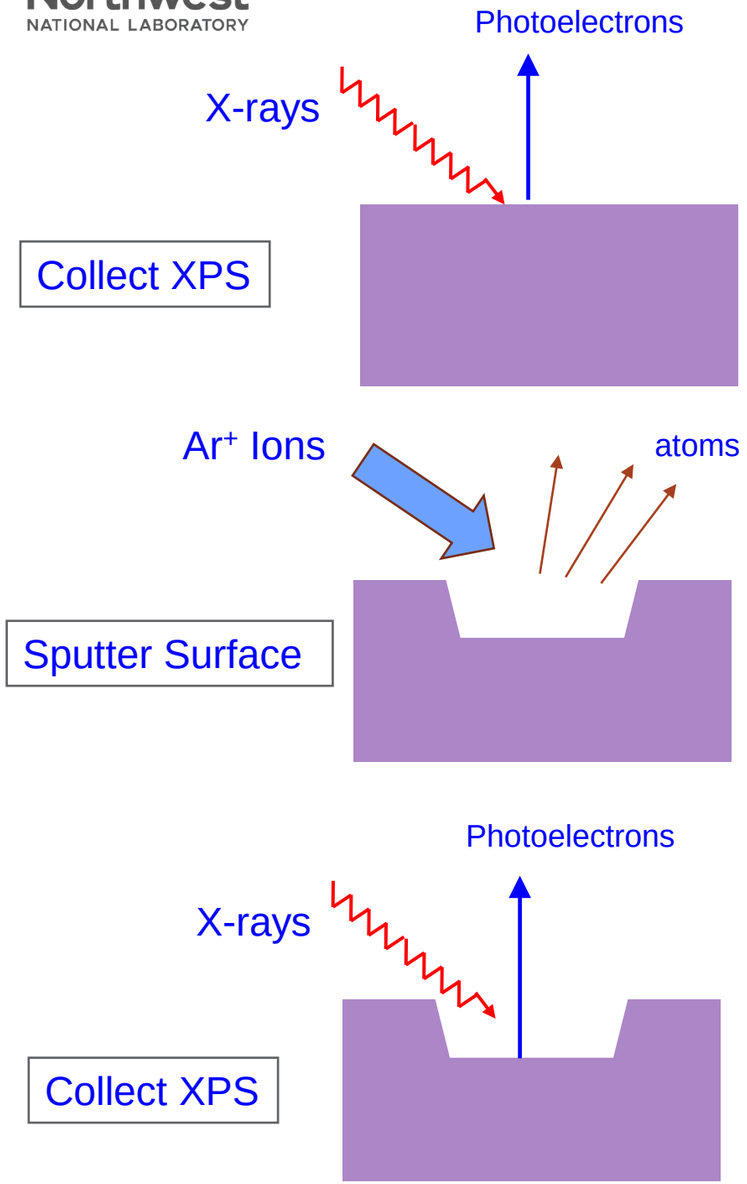

High energy resolution
Si2p spectral region

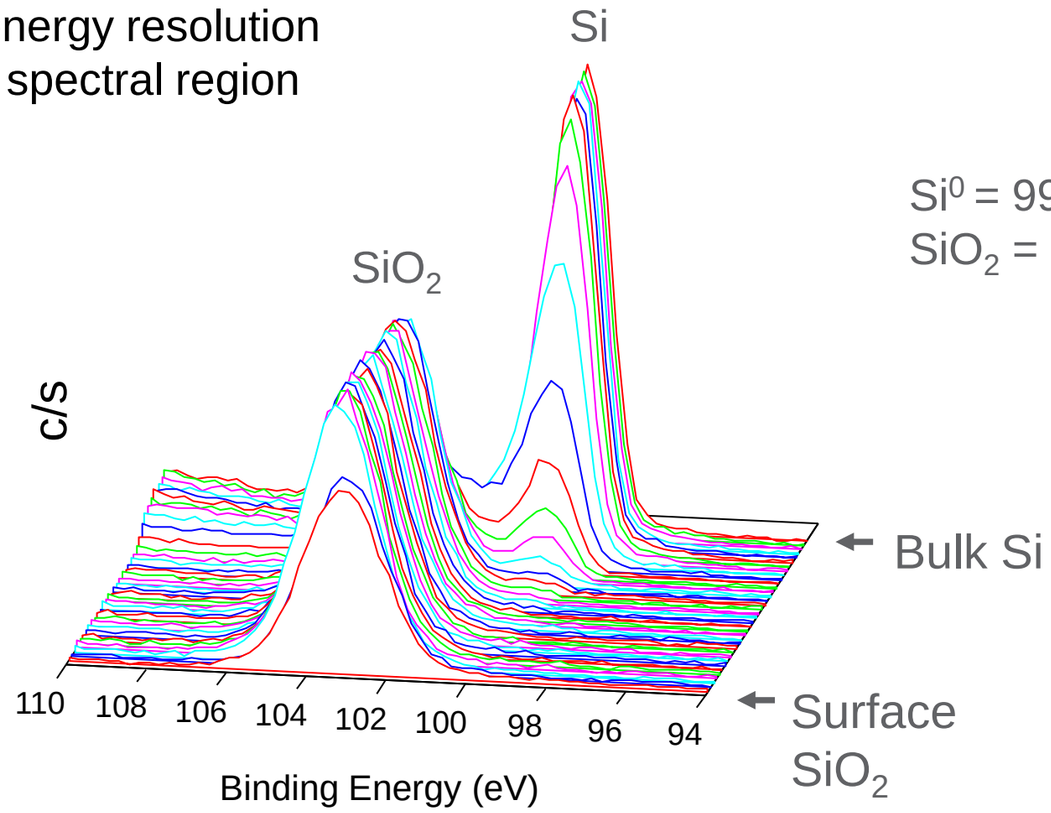

Si^0 = 99.3 eV
SiO_2 = 103.3 eV

Si 2p spectra as a function of sputter cycles

- Can obtain concentration as a function of sputter depth
- Obtaining chemical state information is difficult due to ion beam induced mixing

Pacific Northwest
NATIONAL LABORATORY

Thank you

Pacific Northwest
NATIONAL LABORATORY

X-Ray Photoelectron Spectroscopy (XPS)

Part 2: Applications

June 19, 2023

Ajay Karakoti

Vaithiyalingam Shutthanandan

Theva Thevuthasan

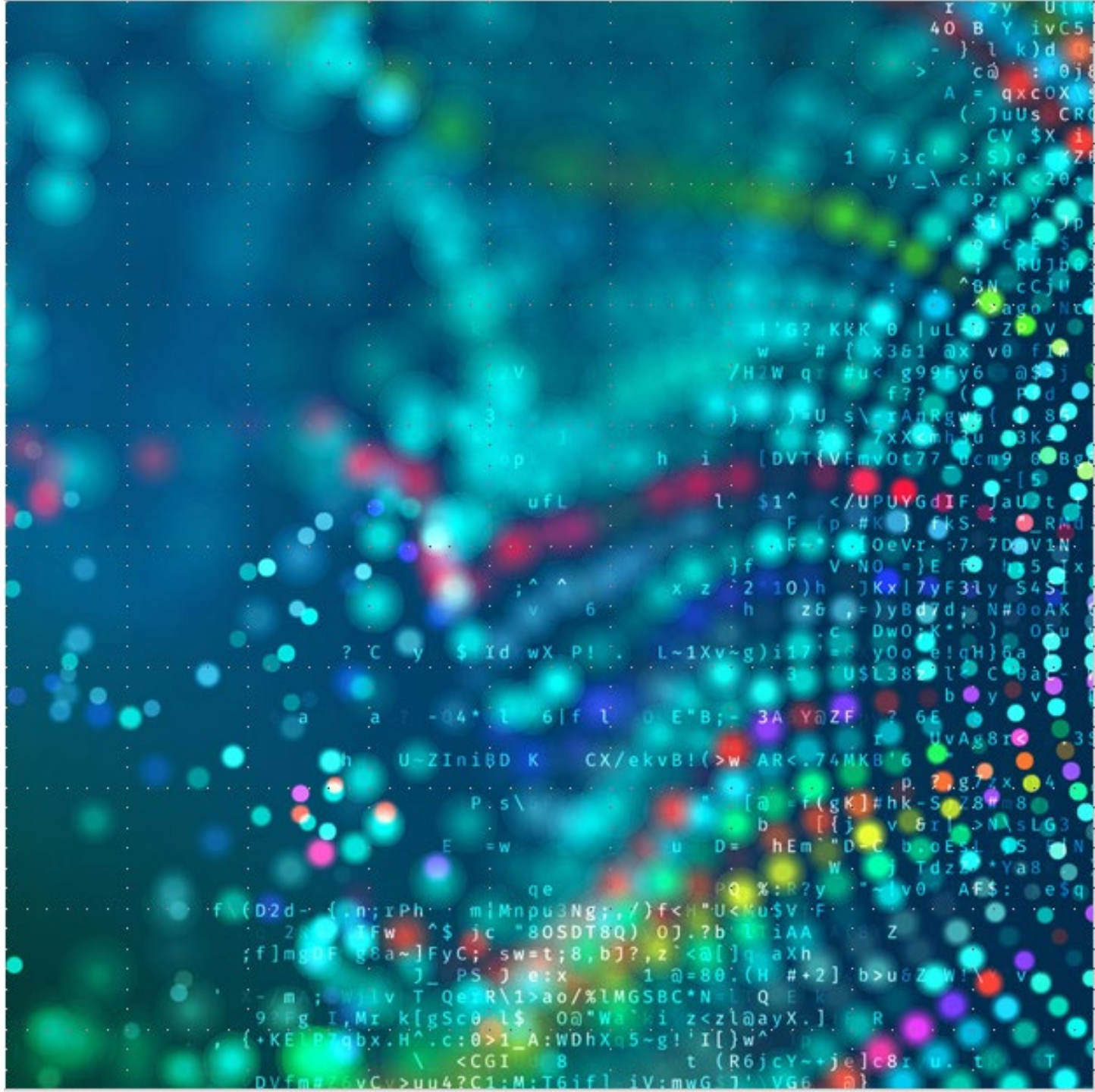

U.S. DEPARTMENT OF ENERGY BATTELLE

PNNL is operated by Battelle for the U.S. Department of Energy

Outline

- Quick recap
- Depth composition from XPS
- Examples
  - Application in Li-S batteries – polysulfide formation at SEI layer
  - Degradation and passivation of perovskite solar cells
  - Ligand interaction with cerium oxide (thin film and nanoparticles)
- Summary

Principle of X-ray Photoelectron Spectroscopy (XPS)

XPS is the most widely used surface analysis technique because of its relative simplicity in use and data interpretation

An incoming photon causes the ejection of the photoelectron

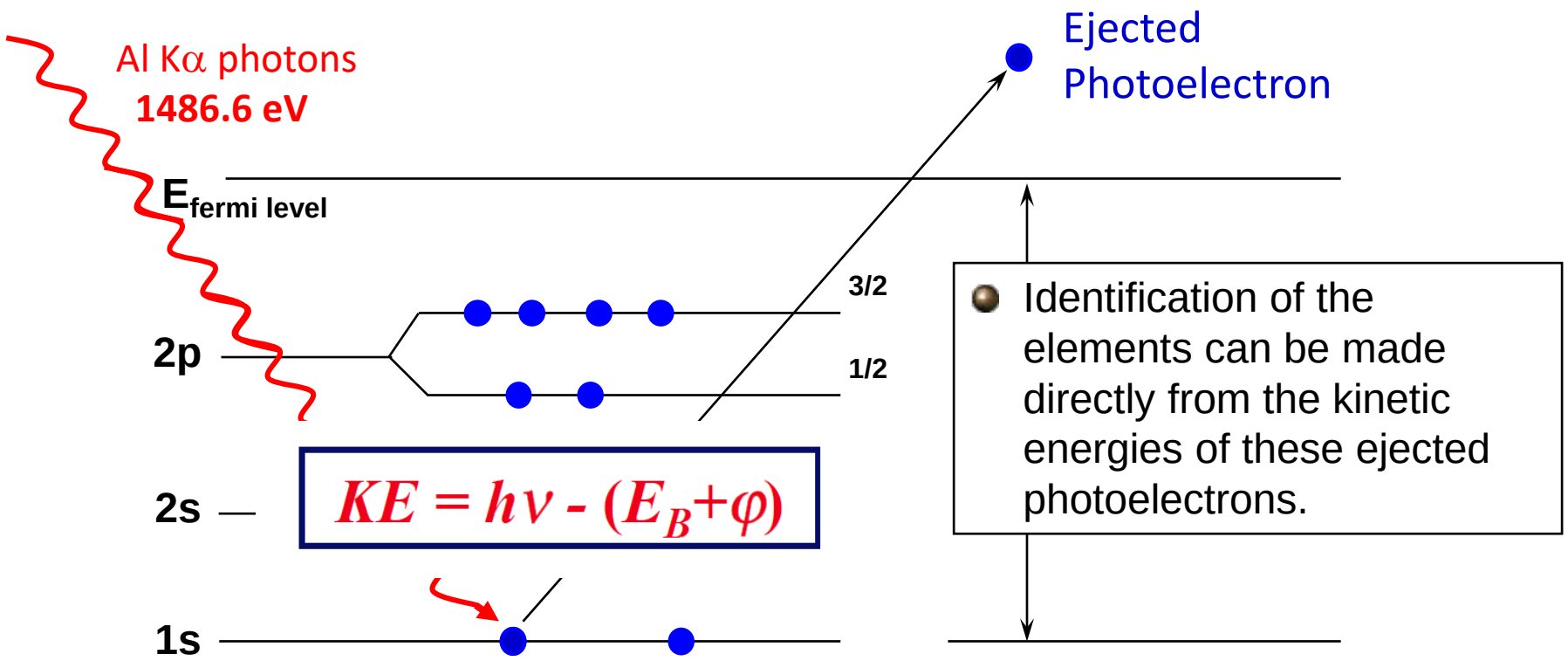

Principle of X-ray Photoelectron Spectroscopy (XPS)

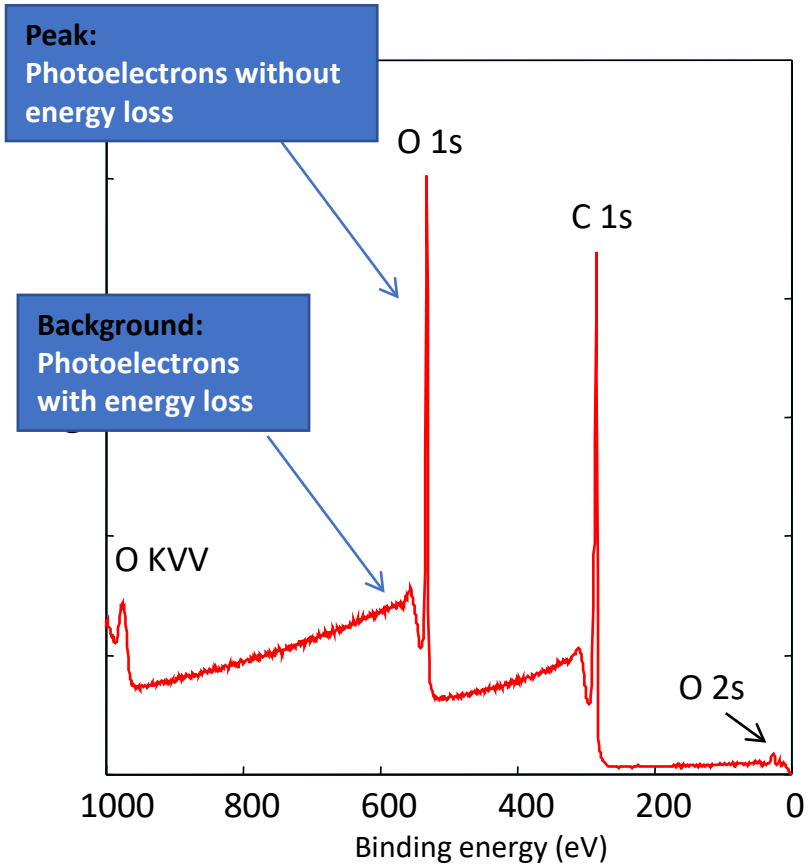

- Elemental composition of the sample can be obtained
- The relative concentrations of elements can be determined from the photoelectron intensities
- An important advantage of XPS is it's ability to obtain information on chemical states from the variations in binding energies

Chemical Effects (shifts) in XPS

Chemical shift: Change in binding energy of a core electron of an element due to change in the chemical bonding of that element

Core binding energies are determined by:

- Electrostatic interaction between the electron and the nucleus

and reduced by:

- The electrostatic shielding of the nuclear charge from all other electrons in the atom (including valence electrons)
- Removal or addition of electronic charge as a result of changes in bonding will alter the shielding

Withdrawals of valence electron charge → **Increase the binding energy**

Addition of valence electron charge → **Decrease the binding energy**

Chemical Effects (shifts) in XPS

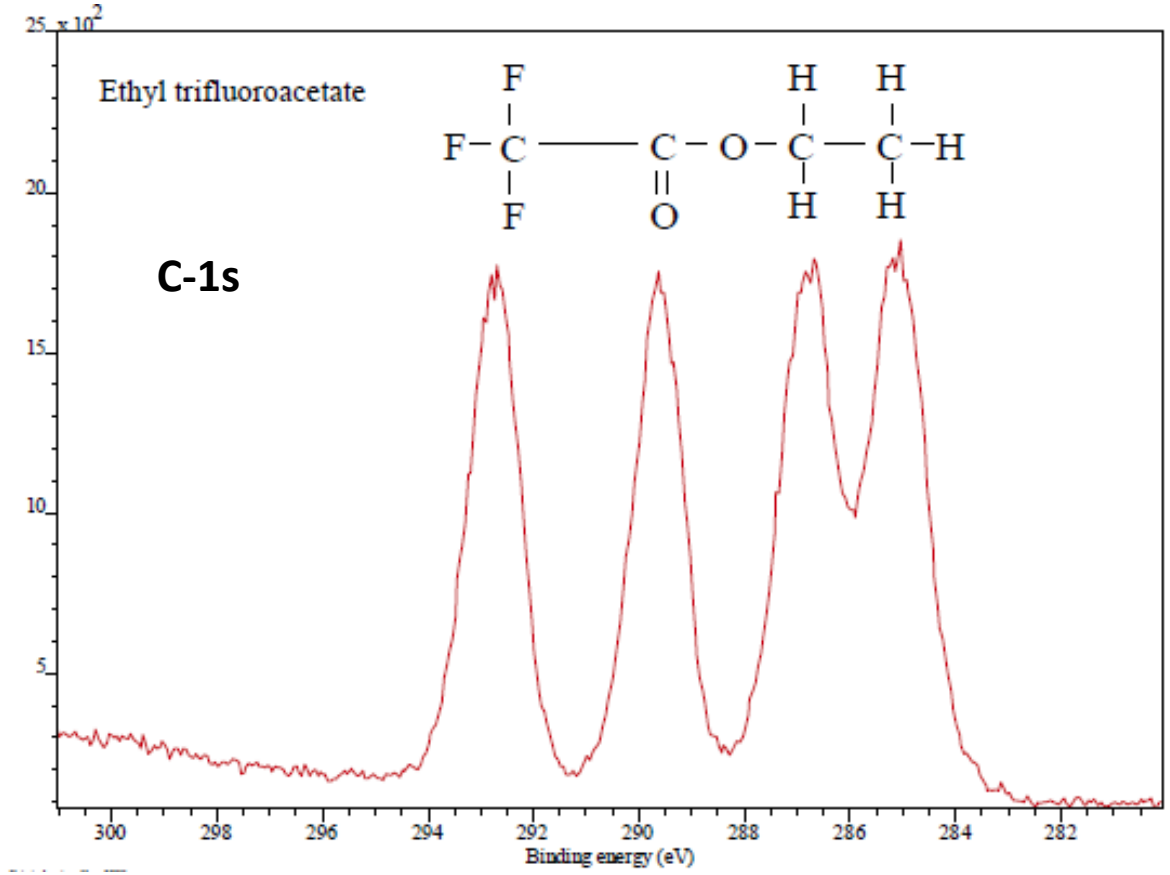

The component peak arising from the 1s orbitals of the $-CH_3$ carbon is assigned a binding energy of 285 eV by convention and the energy scale is shifted accordingly

XPS Analysis - Resolution

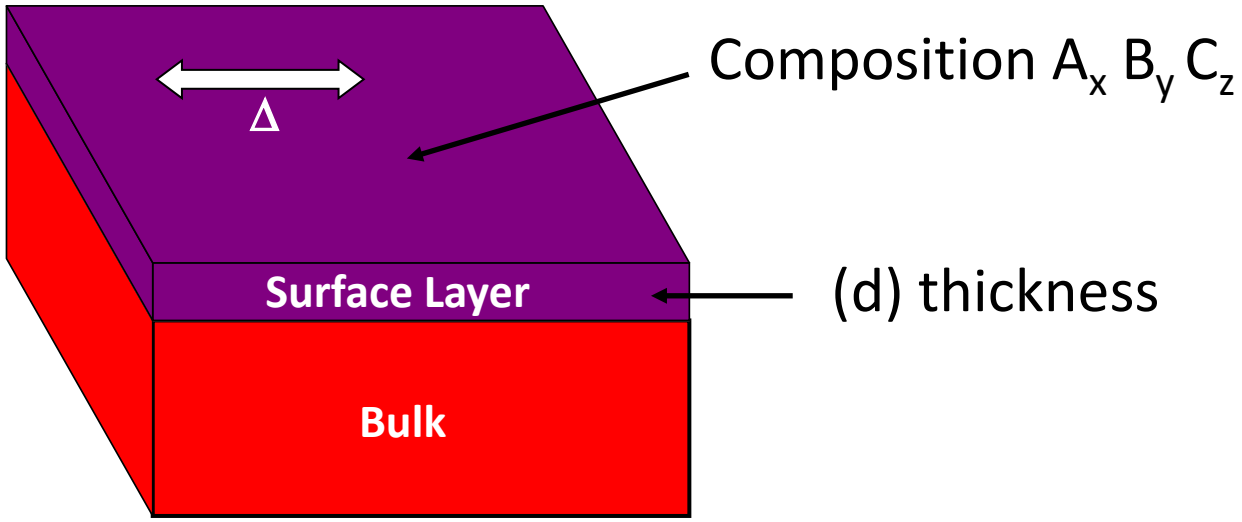

- Composition ($A_x B_y C_z$)
- (d) Thickness (depth resolution)
- Δ Lateral resolution (spatial resolution)

XPS Composition Depth Profile of SiO_2/Si

Sputter source:
2 kV Ar^+ ions

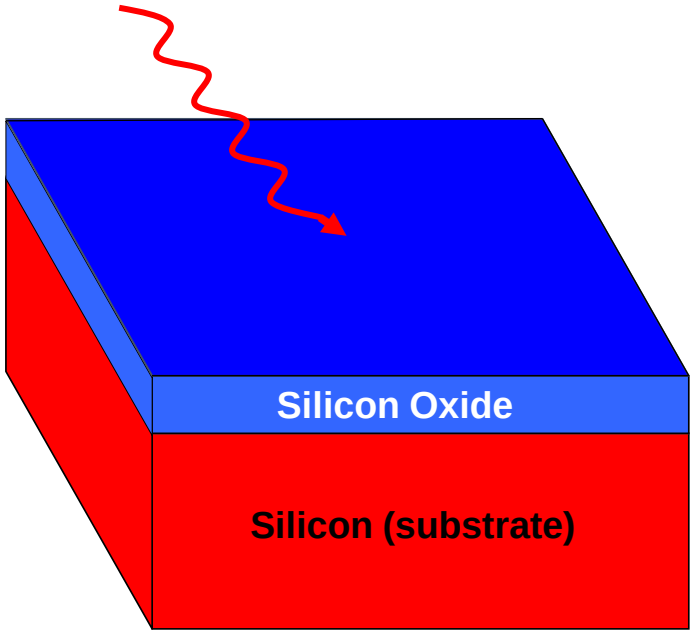

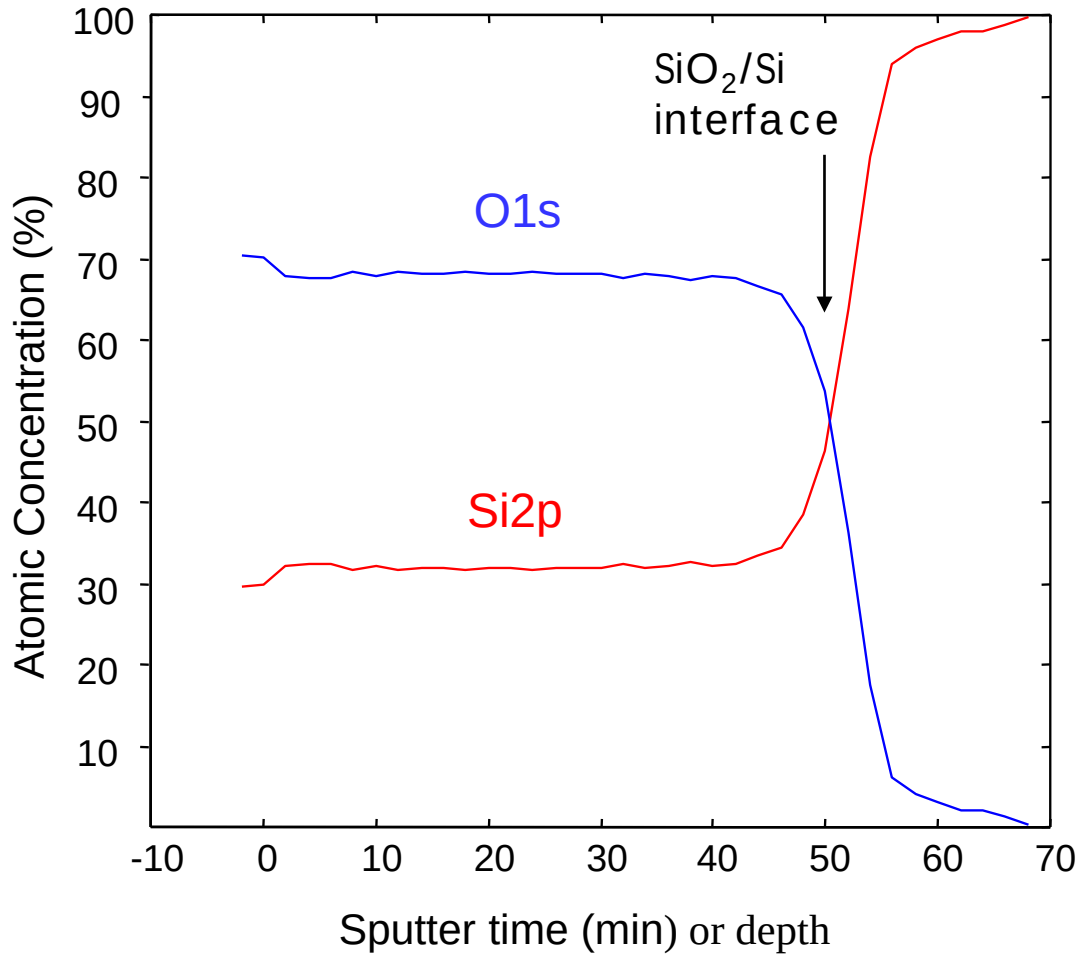

Concentration as a function of sputter depth

XPS Composition Depth Profile of SiO_2/Si

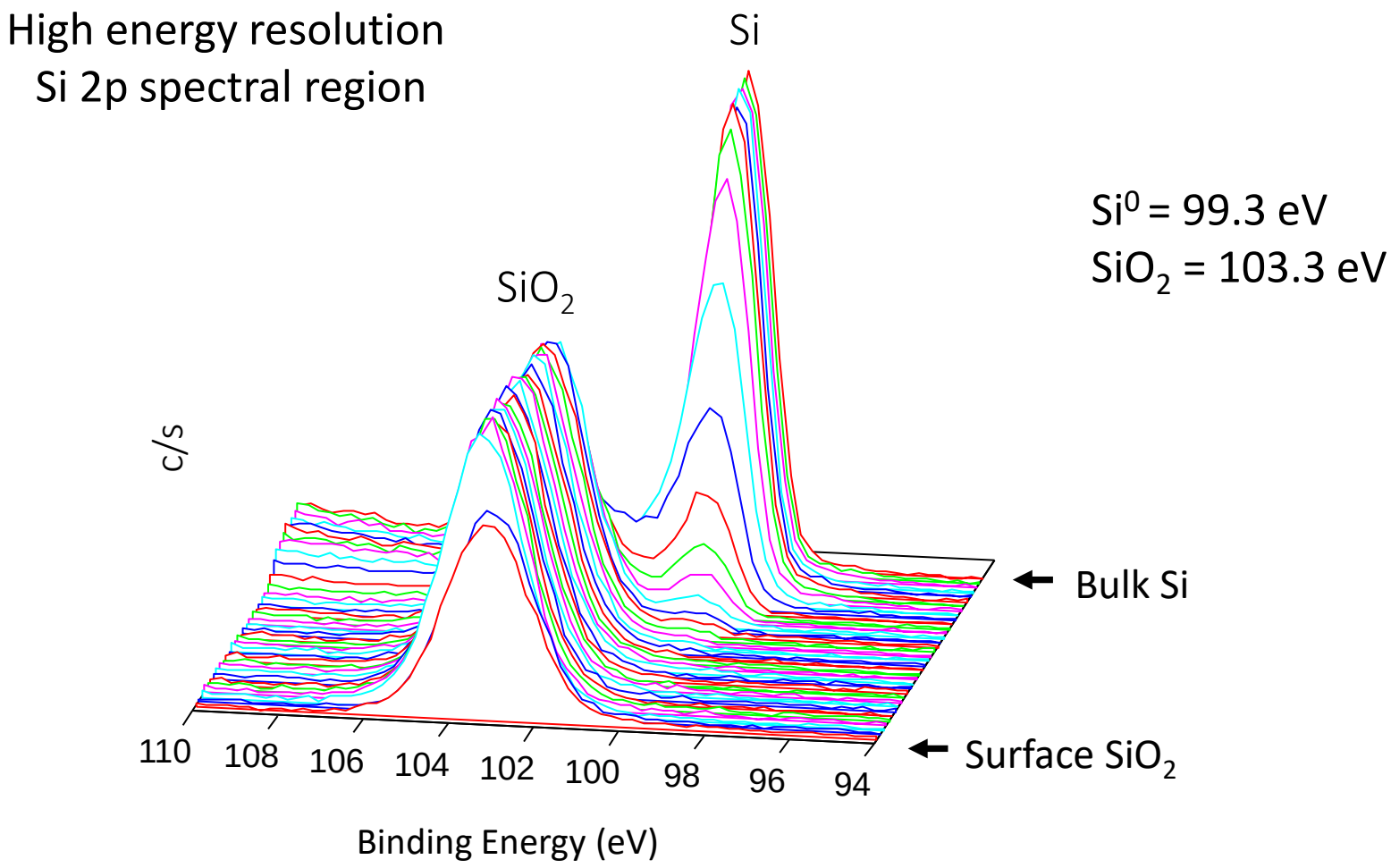

Si 2p spectra as a function of sputter cycles

Attenuation of XPS Signal Intensity with Depth

$$dI_z \approx I_0 \exp\left[-z/(\lambda\cos\theta)\right]$$

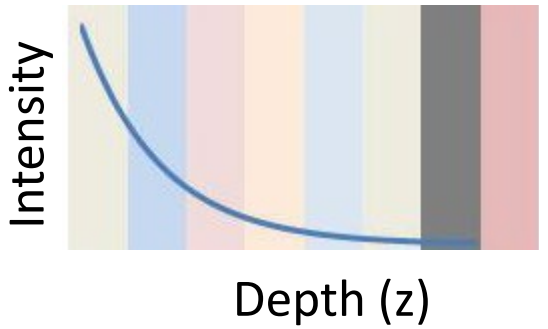

- dI_z is the intensity of the detected signal at depth z
- I_0 is the intensity that would have been produced if the layer were at z = 0 (the outer surface)
- λ is the IMFP
- θ is the angle of the detected electron relative to the surface normal

Application of XPS in Battery Technologies

- Multitude of energy storage requirement such as mobile and transportation application demands wide variety of devices such as Li-ion based batteries (LIB) and Li-Sulfur based batteries (LSB)

- Several technical challenges…….

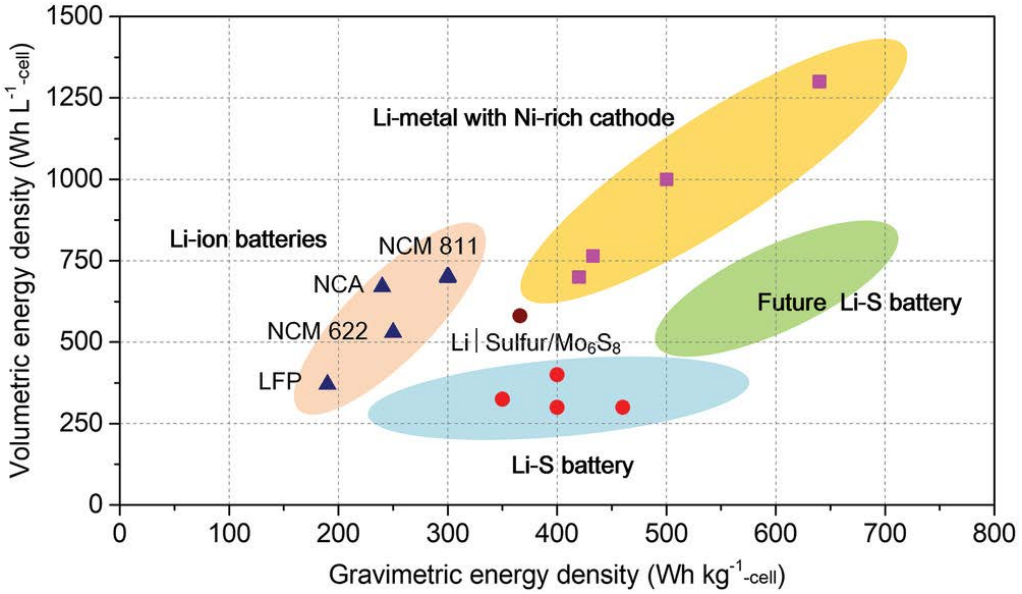

Liu et al., Advanced Materials 33 (8), 2021, 2003955

➡ Dendritic Li growth

➡ Insulating secondary electrolyte interphase (SEI) layer formation at the interfacial regime between Li-metal anode and electrolyte

……hinder the successful utilization of these batteries

Understanding and controlling the interfacial reactions between the electrode and the electrolyte is a crucial need for development of high-energy, long-life batteries

Challenges in Li-S Battery Technology

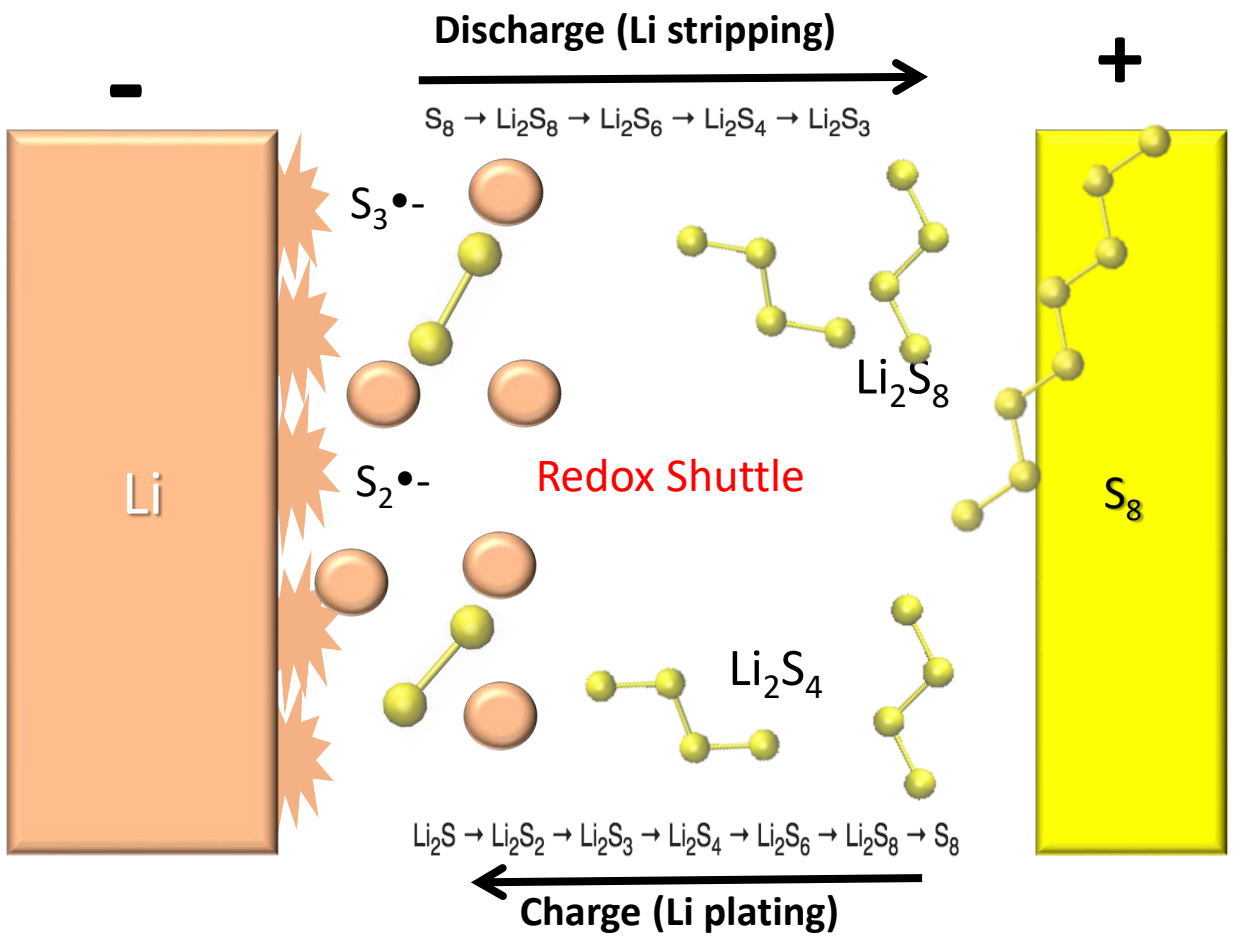

- Consume active S species
- Corrode Li anode
- Polarize Li anode once insoluble Li_2S/Li_2S_2 are deposited

Loss of charge-discharge capacity

How XPS Can Help?

Postmortem Analysis

- XPS can be effectively used to identify the poisoning components of the solid electrolyte interphase (SEI) layers formed at the lithium anodes

In situ Analysis

- In situ XPS development to study the interphase evolution during the charge/discharge cycles

In-situ Imaging XPS/Battery Cycling Set-Up

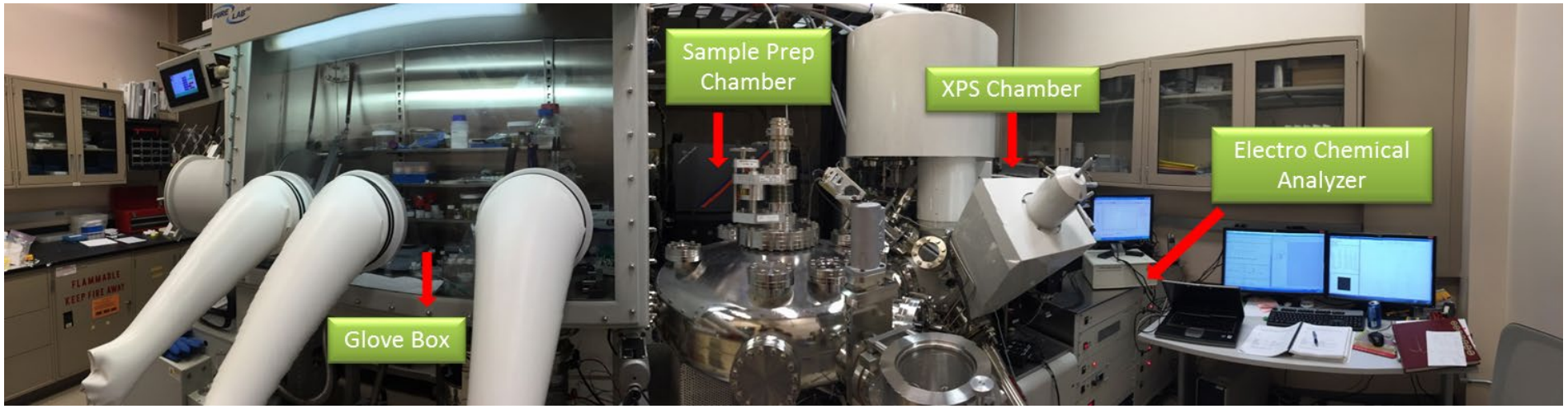

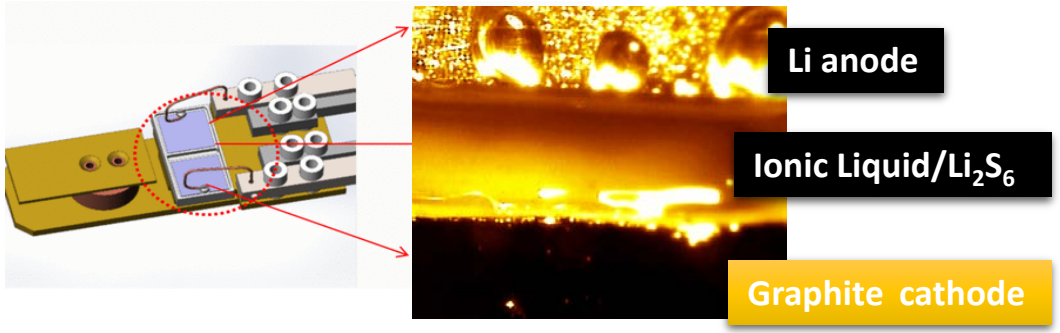

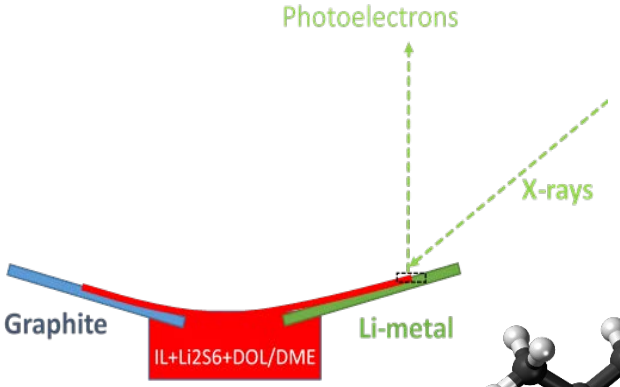

BMIM-TFSI

1-butyl-1-methylpyrrolidinium bis(trifloromethylsulfonyl)imide

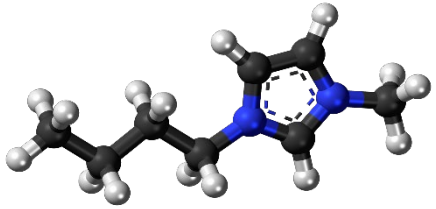

- BMIM-TFSI ionic liquid with Li_2S_6 was used as electrolyte
- XPS data were collected on the electrodes after charging and discharging cycles

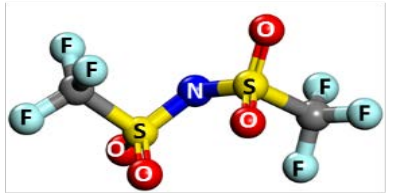

XPS Analysis of Li Anode – S 2P data

S $2p_{3/2}$ and $2p_{1/2}$

ΔE = 1.16 eV

intensity ratio = 0.511

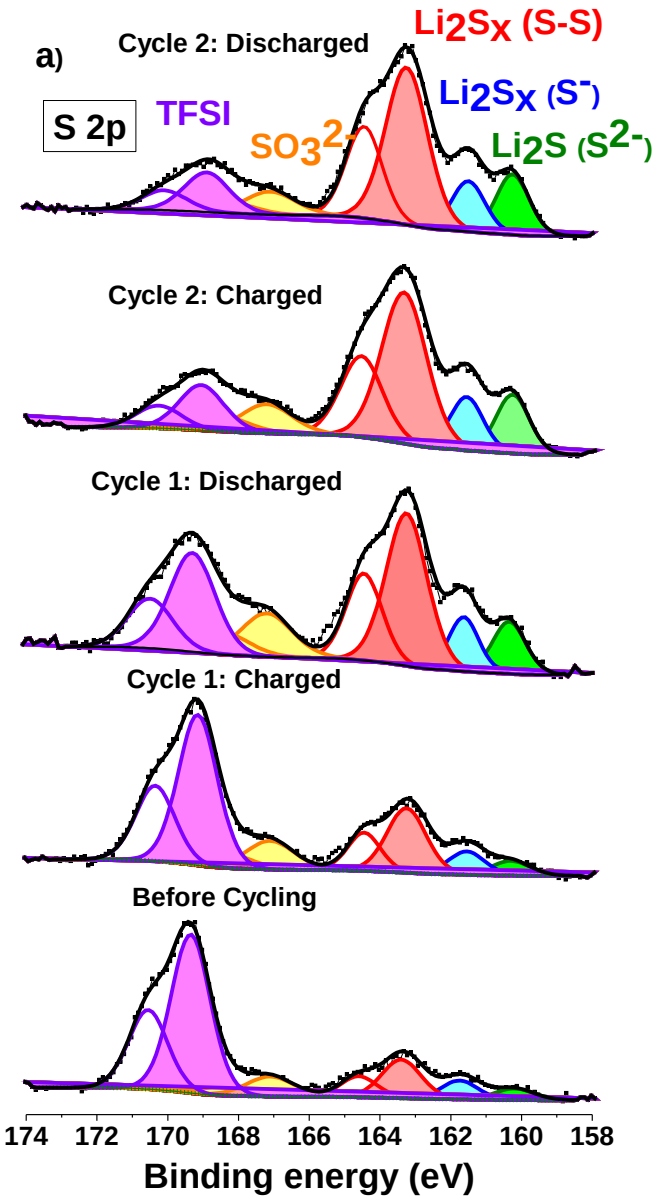

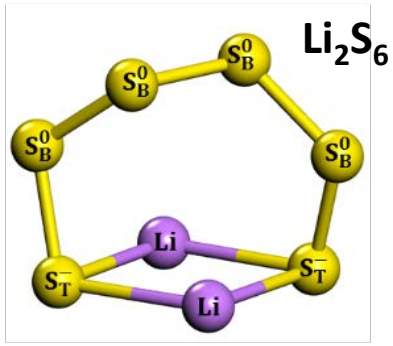

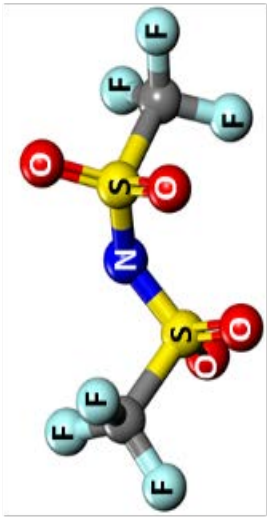

- S 2p spectroscopy clearly indicates various (Li, S) compounds formation on Li anode
- TFSI appears to be decomposing during charging and discharging
- S_T – terminal sulfur, S_B – bridging sulfur

Nandasiri et. Al. Chem. Mater. 2017, 29, 11, 4728−4737

Detailed S 2P Analysis Demonstrate New (Li,S) Compounds

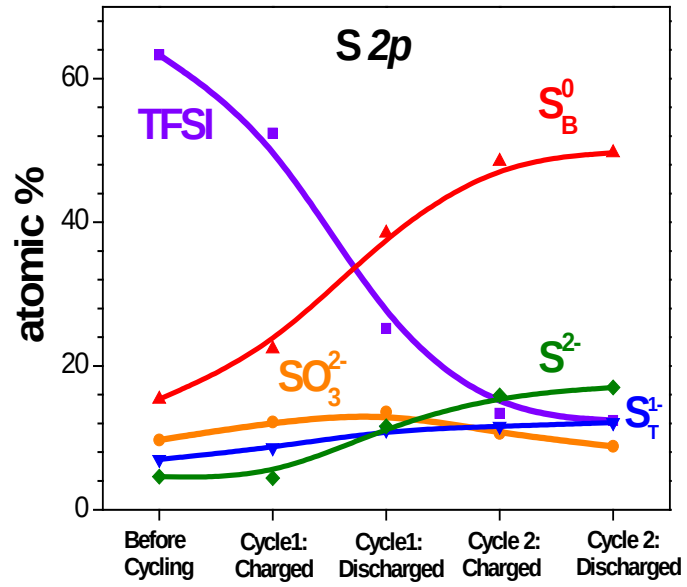

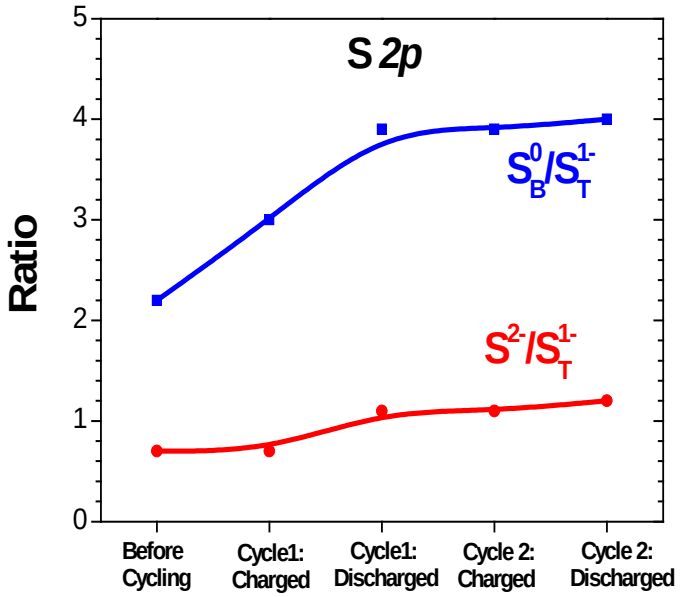

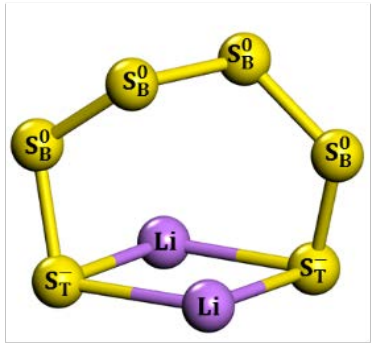

Li_2S_6

- S_B^0/S_T^{1-} ratio appears to be greater than 3 (Li_2S_8) under some conditions
- Total polysulfide content increases after 1st charge
- Insoluble Li_2S forms during discharge and becomes part of SEI layer
- Continuous loss of Li during charge/discharge

Nandasiri et. Al. Chem. Mater. 2017, 29, 11, 4728−4737

TFSI Decomposition Using F 1s Analysis

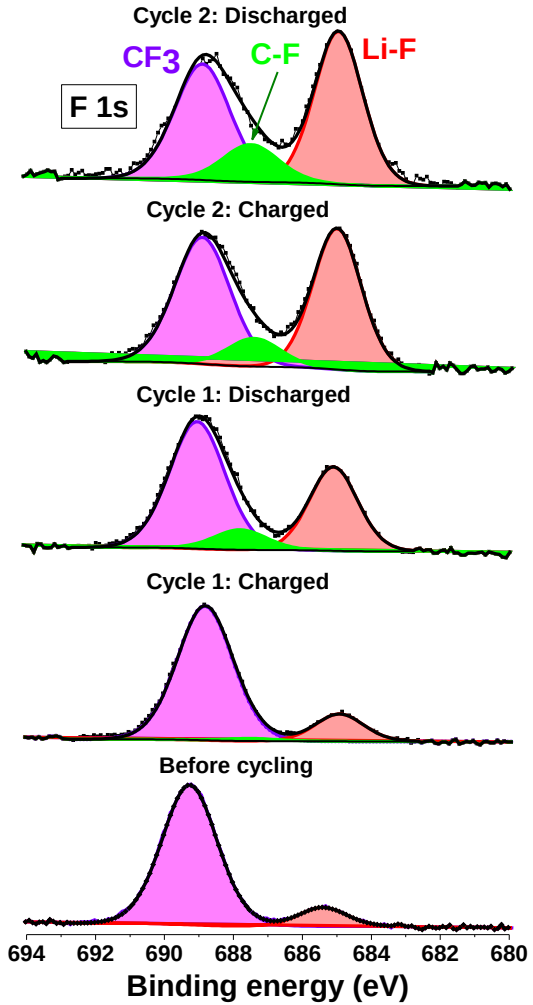

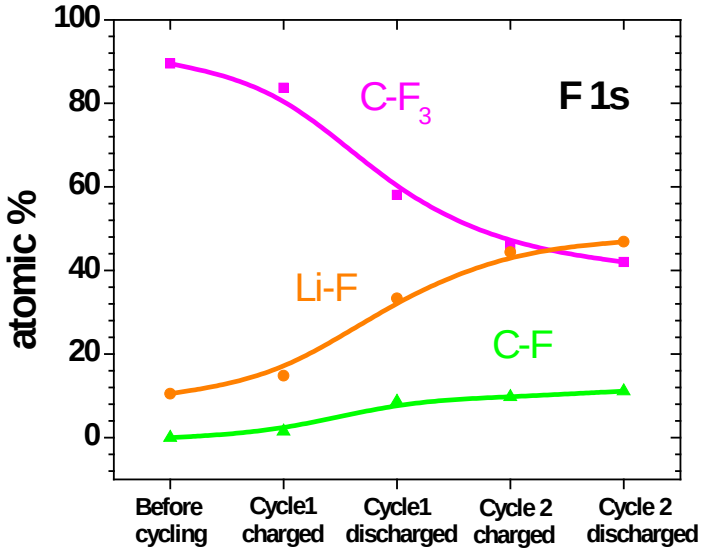

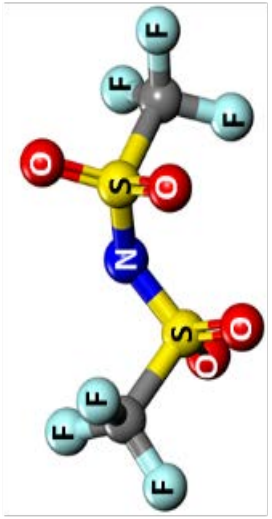

- TFSI anion decomposes leading to multiphase components such as LiF and C-F/Li-F-X within SEI layer

Nandasiri et. Al. Chem. Mater. 2017, 29, 11, 4728−4737

Summary

- An *in situ* XPS capability was developed to understand the formation of solid electrolyte interphase (SEI) layer and decomposition of liquid electrolyte on the electrode surfaces
- SEI layer is complex and it appears that the anode surface is covered by a mixture of several Li compounds after charging and discharging cycles

Applications of XPS in Development of Solar Materials

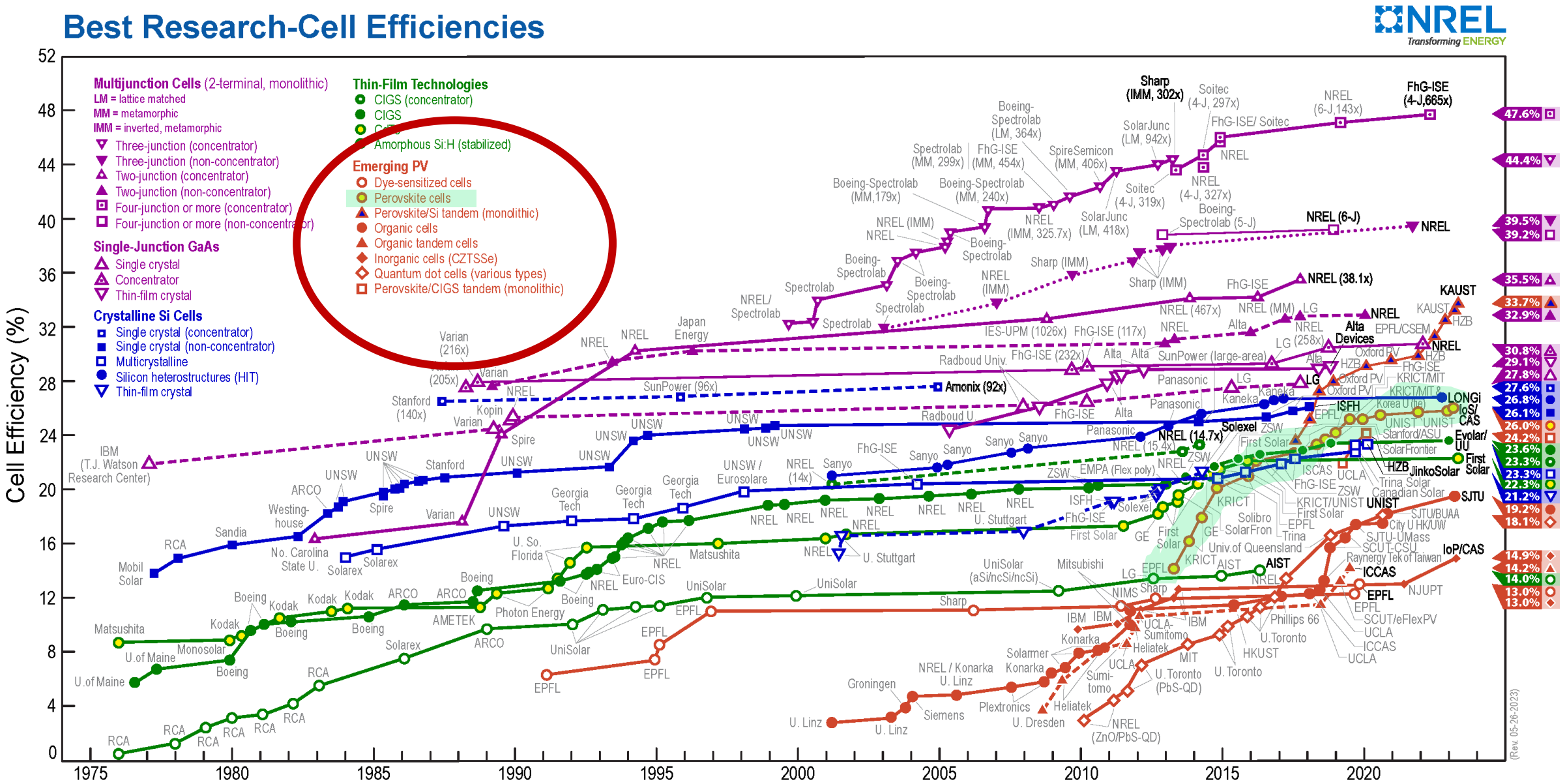

Perovskites Solar Cells – Challenges and Opportunities

- Organo-metal-halide perovskite solar cells have achieved remarkable efficiency levels, reaching beyond 24%%.
- Conversion efficiency of standard $CH_3NH_3PbI_3$ solar cells falls to < 50% within 2 days under normal operating conditions
- In the presence of oxygen, moisture and light, $CH_3NH_3PbI_3$ perovskite decomposes into CH_3NH_2, HI, PbI_2, PbO and $PbCO_3$, thus removing the organic part from the film
- Perovskite can also lose its photoelectronic activity upon the formation of metallic lead species under illumination in an oxygen-free environment
- To protect the perovskite cells from degradation, various research groups have successfully encapsulated the devices.
- Stabilization of perovskite solar cells could be enhanced by using a combination of different cations and anions, such as cesium, formamidinium, and bromide, to form the perovskite absorber layer

Phys. Chem. Chem. Phys., 2018, **20**, 17180-17187

In situ XPS study of the surface chemistry of MAPI solar cells under operating conditions in vacuum†

C. Das *, M. Wussler , T. Hellmann , T. Mayer and W. Jaegermann

- Intrinsic stability of methylammonium lead triiodide ($CH_3NH_3PbI_3$) perovskite by *in situ* X-ray photoelectron spectroscopy (XPS)
- XPS data were collected under dark conditions, at applied voltage, under illumination, at open circuit, and under operating conditions
- Charge referencing to Au
- Al X-rays, 250 um spot size, 20 scans per sample, pass energy 10 eV
- Experiments conducted in vacuum and in air

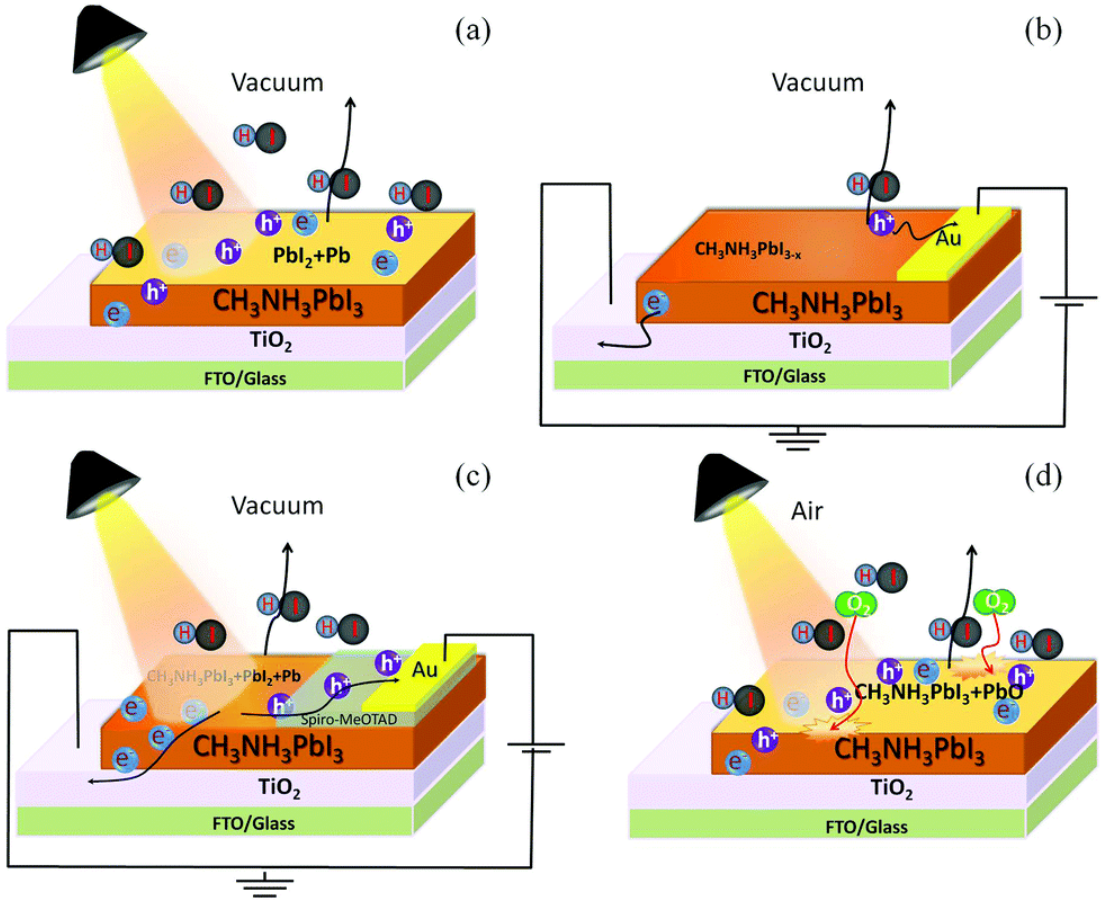

Phys. Chem. Chem. Phys., 2018, **20**, 17180-17187

In-situ XPS – Dark and Light Conditions

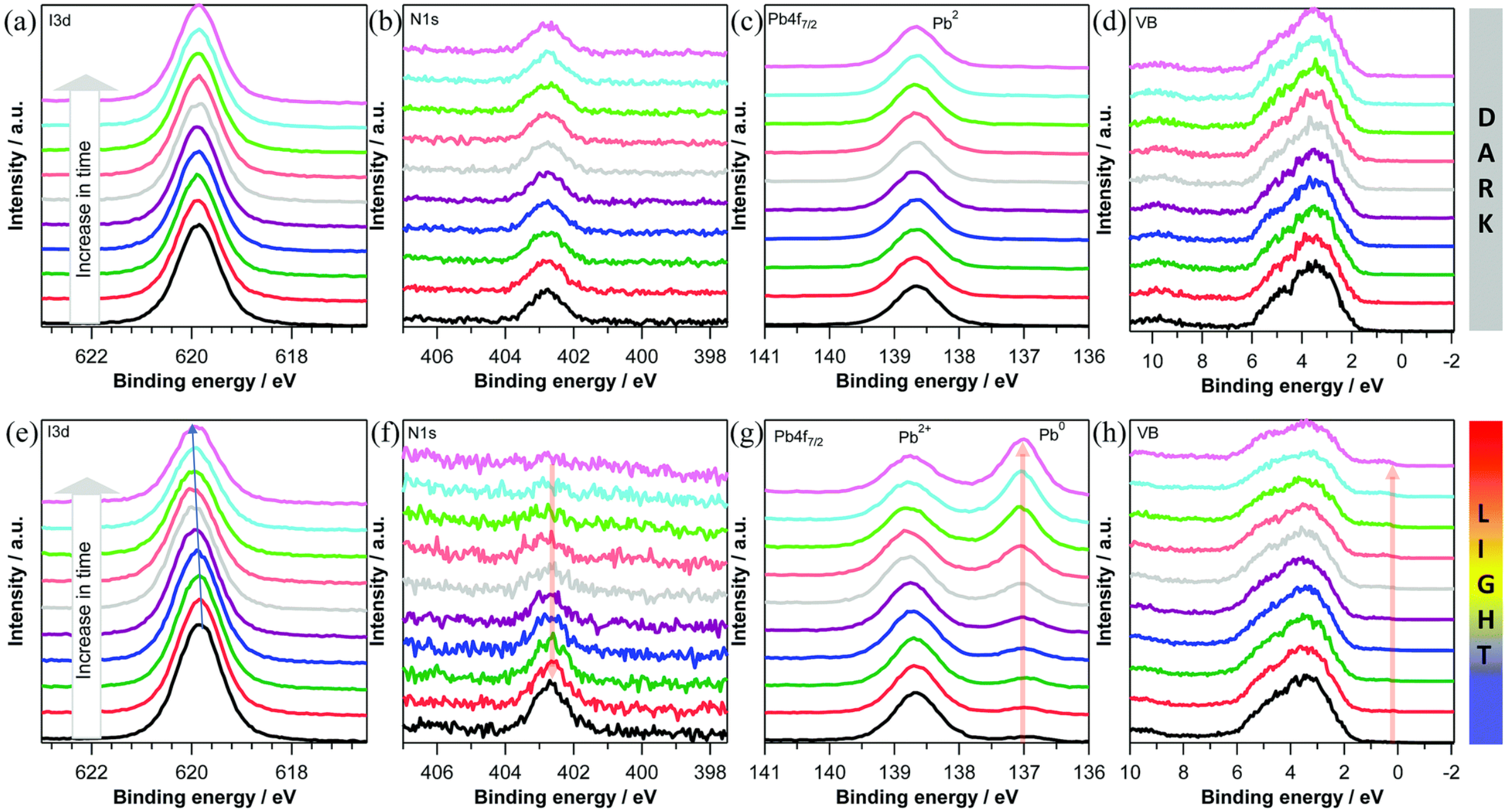

In-situ XPS – Degradation Mechanism

- In dark, 15 h
  - I:Pb – 3.3 → 3.1
  - I:N – 3.3 → 3.5
- Outgassing of gaseous products
- Under light, 15 h
  - I:Pb – 3.0 → 2.2
  - I:N – 4 → 7.4
- Light and dark measurements conducted at different spots
- Combination of vacancy formation and photogenerated charge trapping at the vacancies results in the formation of Pb^{2+} (as PbI_2), Pb^0 and $I_2\uparrow$
- Confirms dissociation of perovskite under illumination and in vacuum conditions

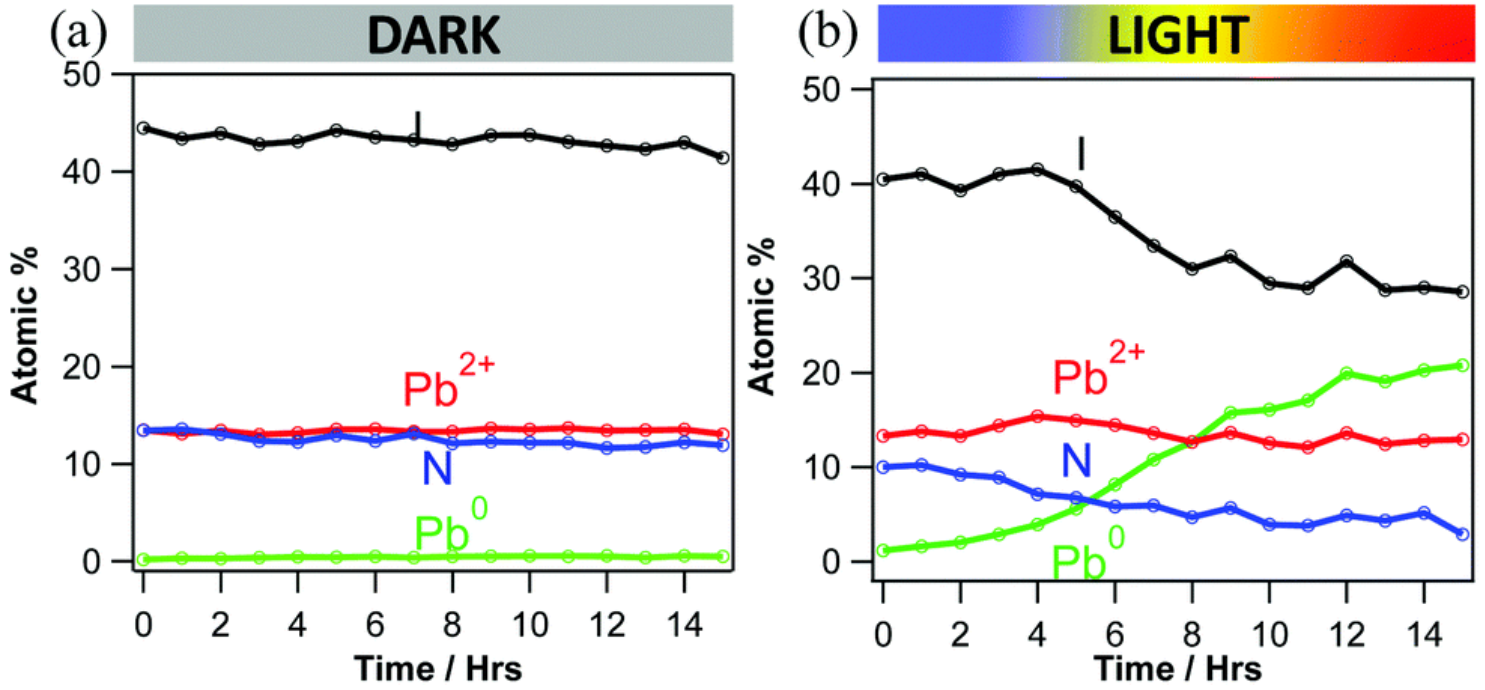

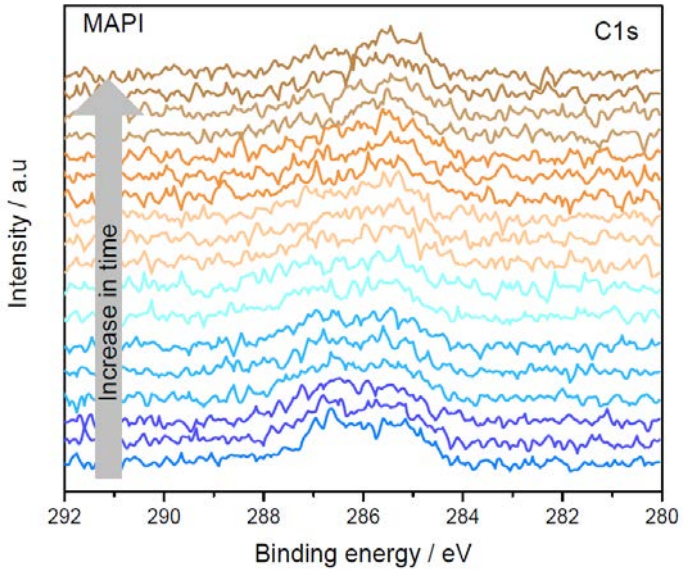

$$CH_3NH_3PbI_3 \xrightarrow{h\nu} PbI_2 + CH_3NH_2\uparrow + HI\uparrow$$

$$PbI_2 \longrightarrow Pb + I_2$$

$$(CH_3NH_3)_{1-x}PbI_{3-x} \longrightarrow Pb + I_2$$

In-situ XPS – Effect of Bias

- Potentials of +1 V (electrons are forced into MAPI) and −1 V (holes are forced into MAPI) were applied at the back gold contact in dark.
- No change was noted by external application of negative or positive bias
- Electrons and holes injected by application of external bias are unable to initiate the subsequent decomposition of perovskite
- Under illumination, application of bias reduces the decomposition due to extraction of holes

Applied voltage = 1V , dark

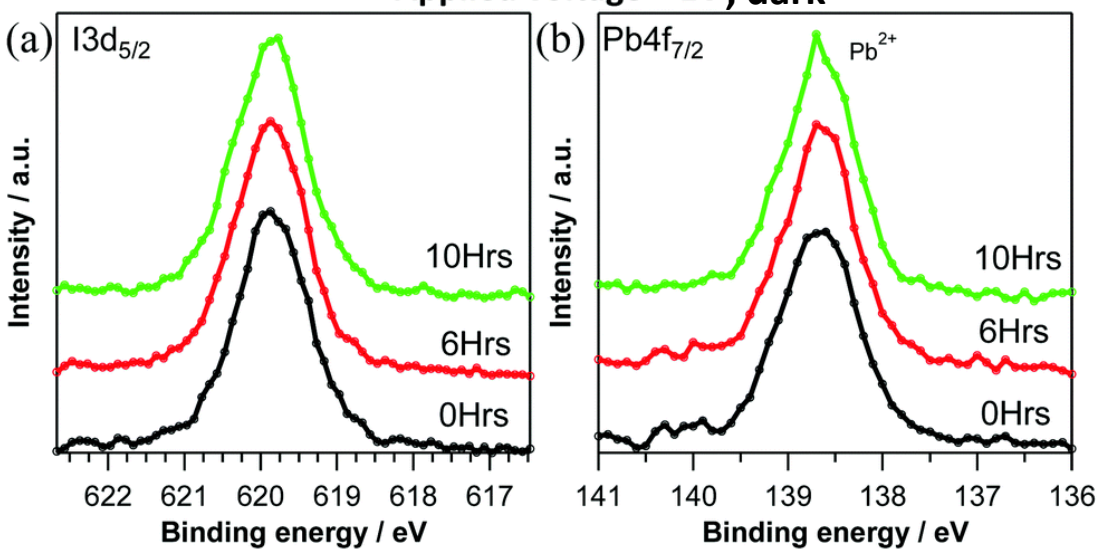

Applied voltage = -1V, dark

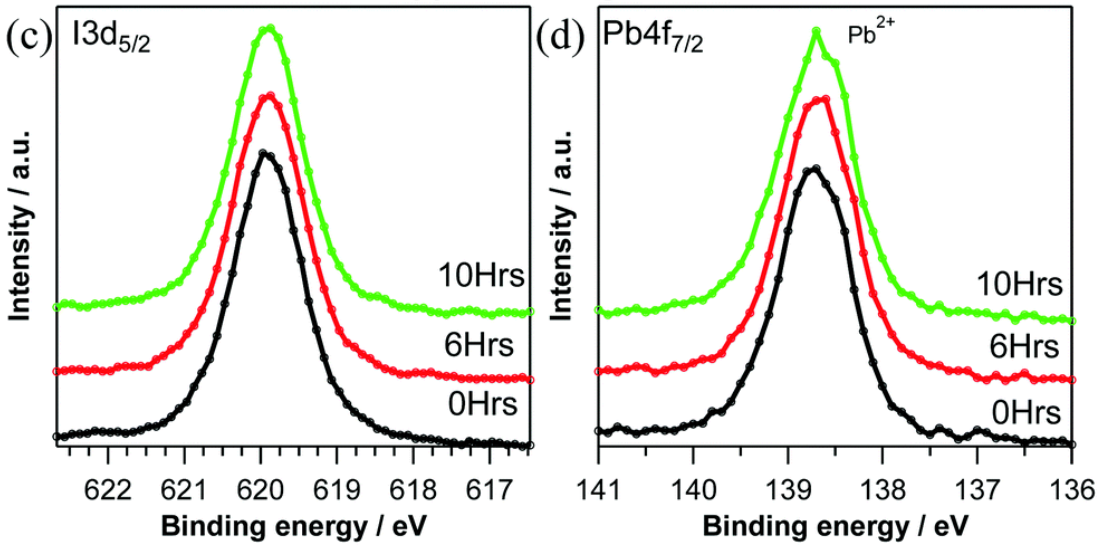

Applied voltage 1V, light

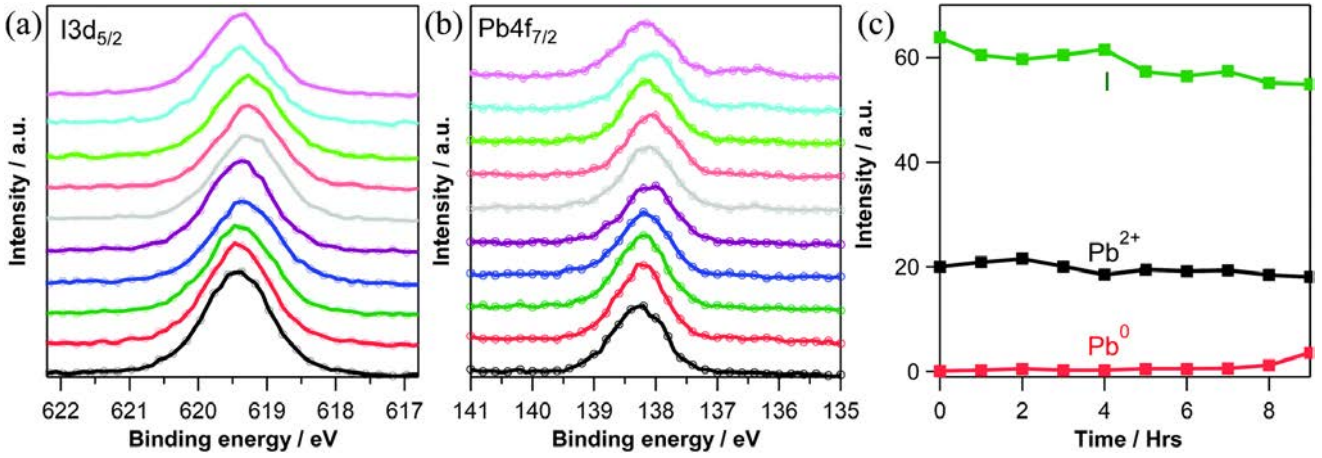

Passivating Agents to Increase the Stability of Perovskite Films

- Degradation of PSCs occurs in present of moisture, heat, oxygen, and UV light
- Methylammonium lead iodide ($MAPbI_3$), a prototypical halide perovskite, is not thermally unstable at 85 °C
- Investigation of the surface composition at an elevated temperature show significant loss of surface nitrogen at 100 °C.
- The decomposition occurs through the evaporation of MAI and production of lead iodide

$$CH_3NH_3PbI_3 \xrightarrow{\triangle} PbI_2 + CH_3NH_2 \uparrow + HI \uparrow$$

$$PbI_2 \xrightarrow{\triangle} Pb + I_2$$

Surface passivation can prevent decomposition of $MAPbI_3$

ACS Appl. Mater. Interfaces 2020, 12, 39, 43705−43713

Near Ambient Pressure XPS to Understand the Passivation of $MAPbI_3$ by DBTA

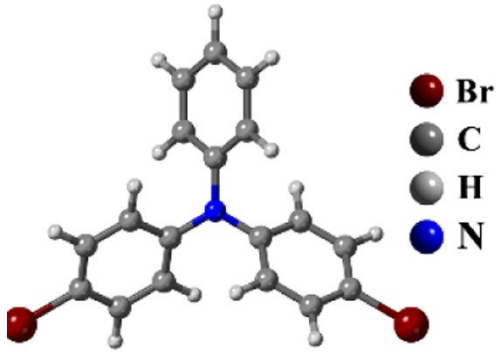

4,4'-dibromotriphenylamine (DBTPA)

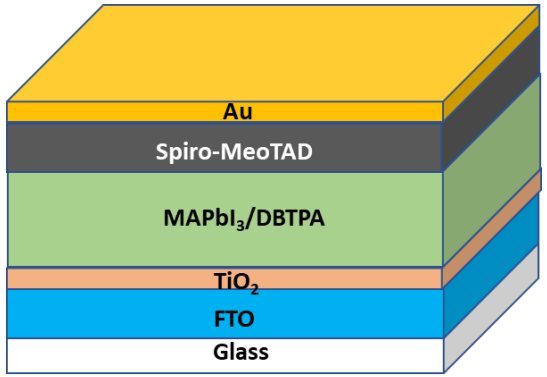

Increase humidity from 6.8 to 27 % RH in NAP-XPS

Without DBTA | With DBTA

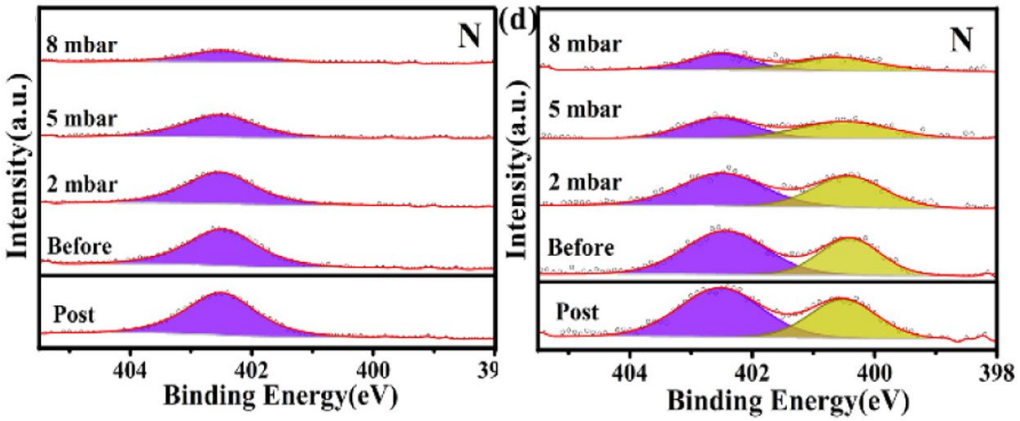

Without DBTA | With DBTA

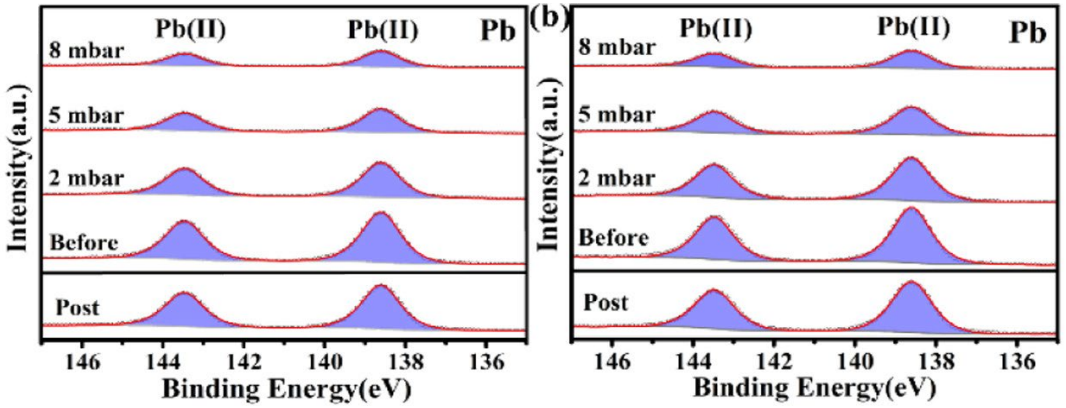

The signal attenuation occurs with increasing pressure due to inelastic scattering of the photoelectrons

NAP-XPS – Heat Induced Degradation

- Heat induced degradation is prevented by DBTPA
- Absence of metallic lead during heating up to 150 ^{o}C in DBTA coated $MAPbI_3$
- MA is stable up to ^{o}150 C and then decomposes as CH_3NH_2 (g)
- PbI_2 may form as a product of decomposition and the I:Pb ratio at 200 ^{o}C was 1.55 and 2.23 for pristine and DBTA coated films

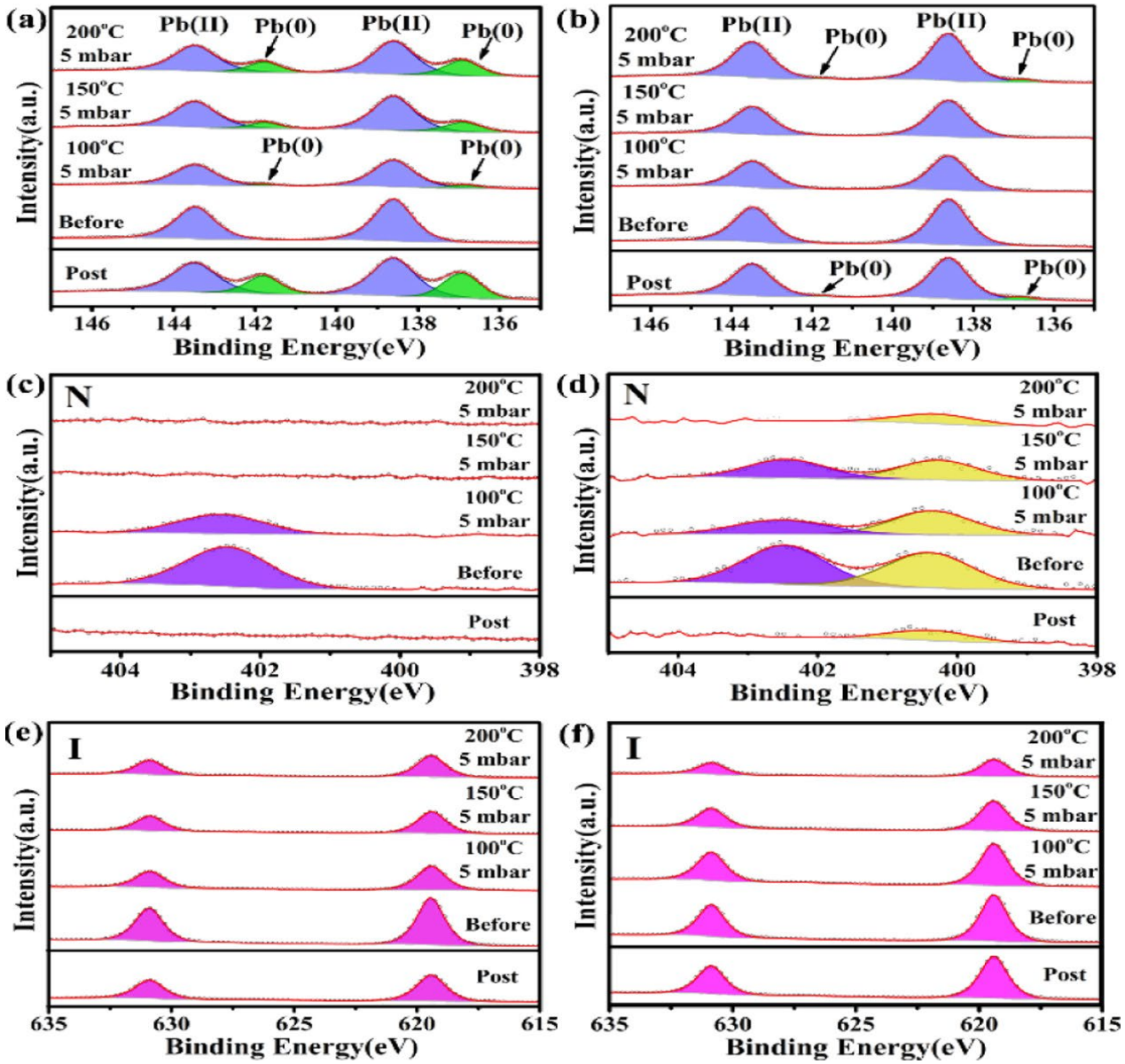

UHV-XPS – Effect of DBTA on $MAPbI_3$

- HR XPS spectra of $MAPbI_3$ films passivated with DBTPA on Si wafer
- Pb^{2+} peaks shift to lower BE suggesting Br- ions from DBTPA donate electrons to Pb or oxidizing it to Pb^{4+}
- Br ions dissociate under XPS in pure DBTA but are stabilized on $MAPbI_3$
- N peak in $MAPbI_3$ also shift to lower binding energy indicating cation–π interaction between $CH_3NH_3^+$ in $MAPbI_3$ and aryl group of DBTPA molecules

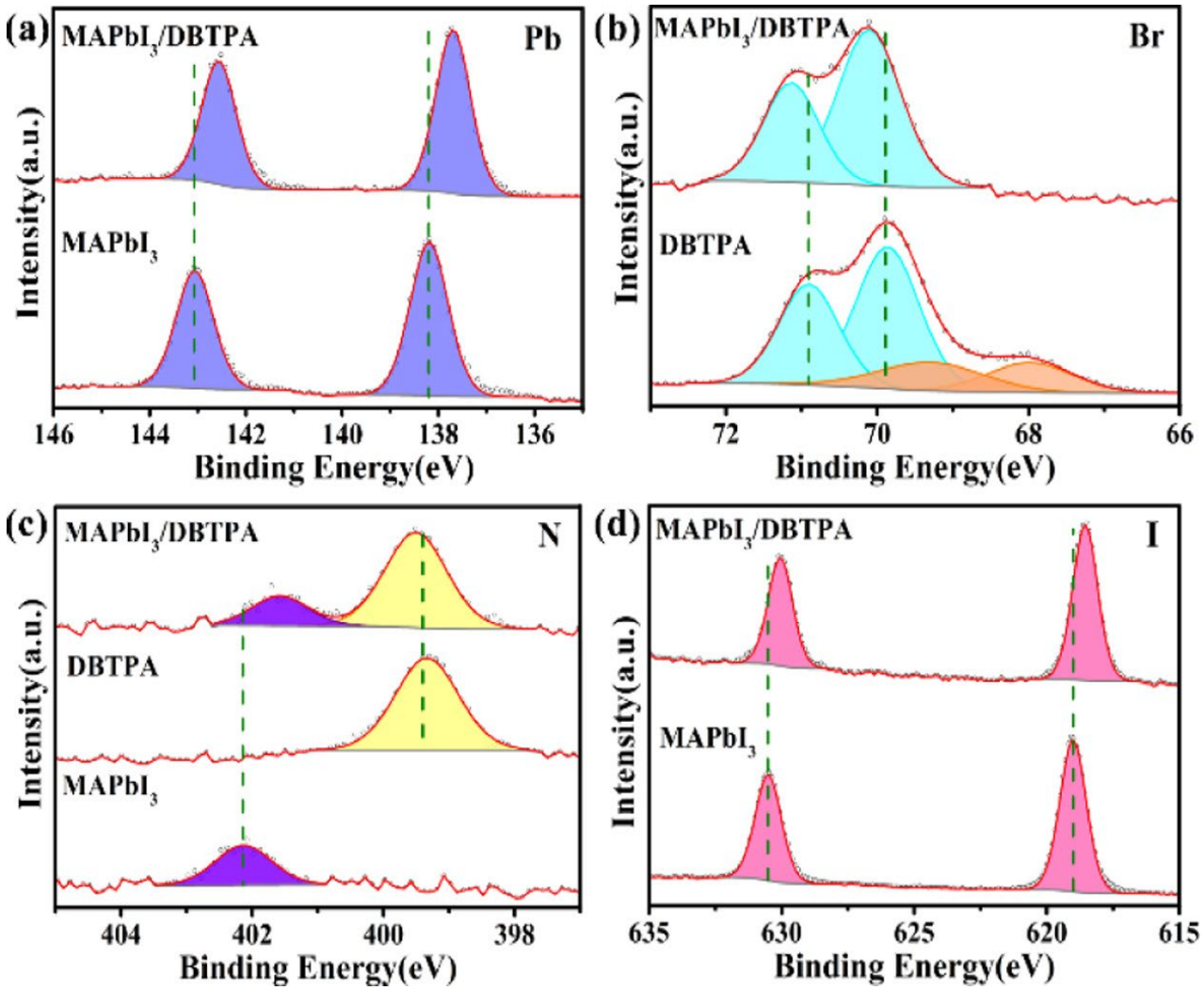

Passivation by DBTA proceeds via a strong interaction with $MAPbI_3$

Summary

- XPS can be effectively used to study the stability of perovskite solar cells
- Corresponding shifts in peaks of elements can be used to track the stability under different conditions
- Use of passivating agent or bias is a good strategy to prevent degradation of $MAPbI_3$
- Caution – XPS can also cause beam damage and must be taken into account

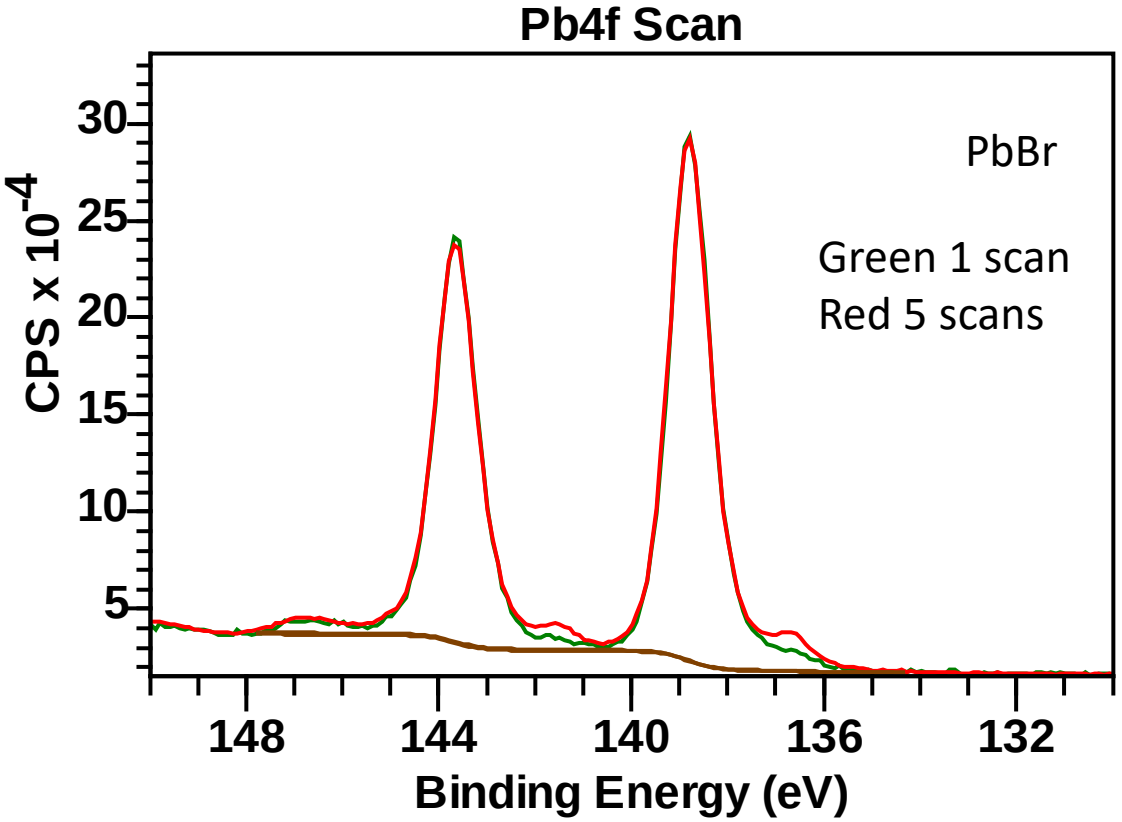

Pacific Northwest NATIONAL LABORATORY

X-Ray Photoelectron Spectroscopy (XPS)

Part 3: Applications and Instrumentation

June 19, 2023

Ajay Karakoti
Vaithiyalingam Shutthanandan

Theva Thevuthasan

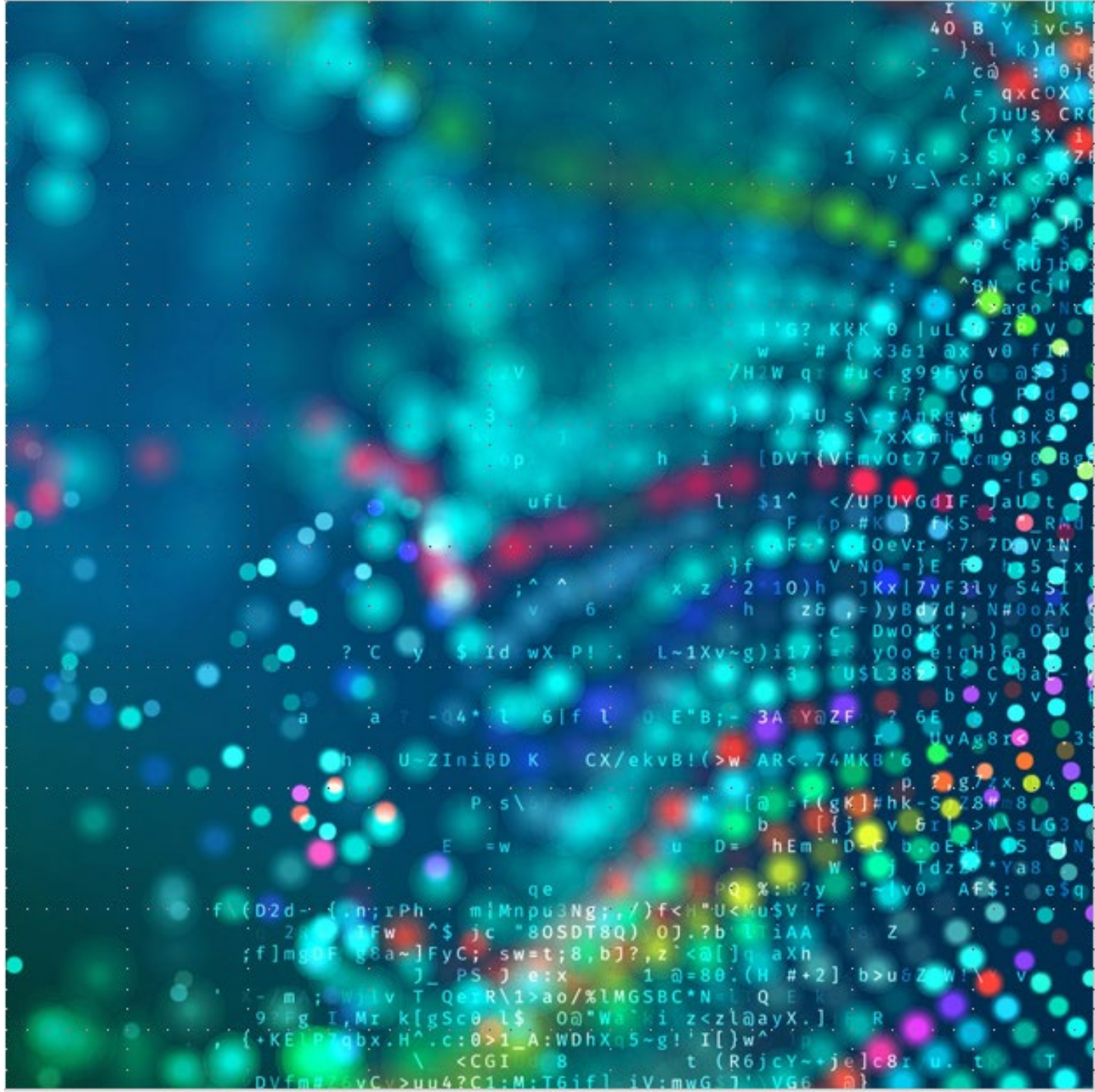

U.S. DEPARTMENT OF ENERGY BATTELLE

PNNL is operated by Battelle for the U.S. Department of Energy

Principle of X-ray Photoelectron Spectroscopy (XPS)

XPS is the most widely used surface analysis technique because of its relative simplicity in use and data interpretation

An incoming photon causes the ejection of the photoelectron

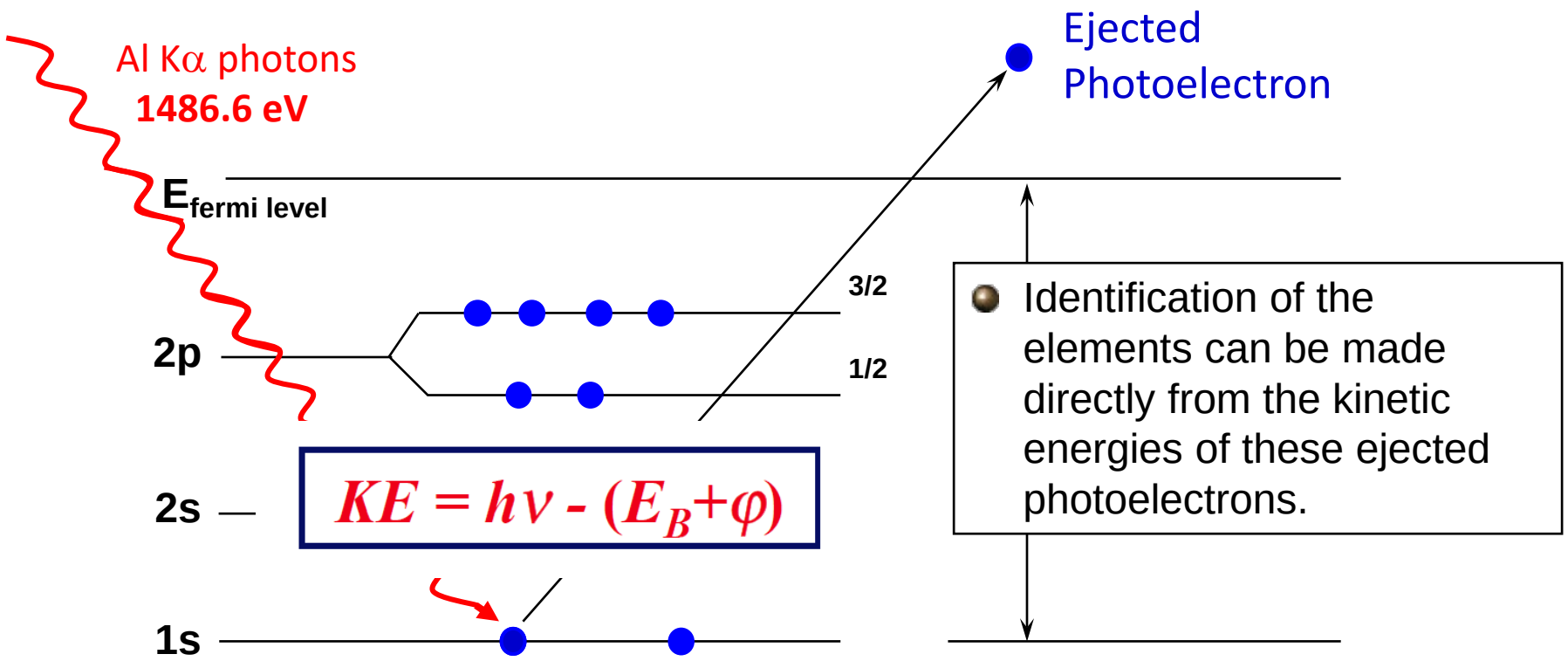

Other XPS Spectroscopy Features: Shake-up and Shake-off Satellites

Satellite peak possess following attributes

a) It involves both configurations of initial state and final state of atom and involve at least one electron “pulled up” to a given higher energy empty level
b) Its BE is higher than that of the main peak
c) Its intensity is lower than that of the main peak

Other XPS Spectroscopy Features: Multiplet Splitting

- After photoemission, the unpaired electron may couple with other unpaired electrons in the atom

e- (3d+4s)	0	1	2	3	3	4	4	5	5	6	6	7	7	8	8	9	9	10	10	11	12
Electronic Configuration	[Ar]	[Ar] 3d1	[Ar] 3d2	[Ar] 3d3	[Ar] 3d1 4s2	[Ar] 3d4	[Ar] 3d2 4s2	[Ar] 3d5	[Ar] 3d3 4s2	[Ar] 3d6	[Ar] 3d5 4s1	[Ar] 3d7	[Ar] 3d5 4s2	[Ar] 3d8	[Ar] 3d6 4s2	[Ar] 3d9	[Ar] 3d7 4s2	[Ar] 3d10	[Ar] 3d8 4s2	[Ar] 3d10 4s1	[Ar] 3d10 4s2
Sc	Sc(III)				Sc(0)																
Ti	Ti(IV)	Ti(III)	Ti(II)				Ti(0)														
V	V(V)	V(IV)	V(III)	V(II)					V(0)												
Cr	Cr(VI)		Cr(IV)	Cr(III)		Cr(II)					Cr(0)										
Mn	Mn(VII)	Mn(VI)		Mn(VI)		Mn(III)		Mn(II)					Mn(0)								
Fe								Fe(III)		Fe(II)*					Fe(0)						
Co										Co(III)		Co(II)					Co(0)				
Ni												Ni(III)		Ni(II)*					Ni(0)		
Cu																Cu(II)		Cu(I)		Cu(0)	
Zn																		Zn(II)			Zn(0)

No Mulitplet Splitting
Multiplet Splitting (Resolved in XPS)
Multiplet Splitting (Not Well-Resolved or Peak Broadening Only)

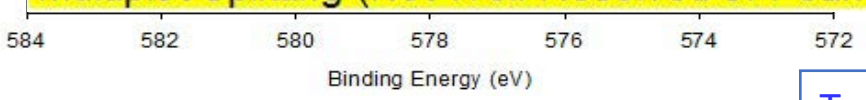

Cr 2p 3/2 peak in Cr_2O_3 exhibiting multiplet splitting.
(Taken from XPSfitting website c/o Mark Biesinger)

Initial State

Final States

Transition metals (*unfilled d orbitals*) and rare earth (*unfilled f orbitals*) show Multiplet Splitting

Ligand Interaction with Nanoceria: Bonding Information at Molecular Scale

In-situ XPS and cryo-XPS for understanding the interaction of nanoceria with carboxylic acid

Objective

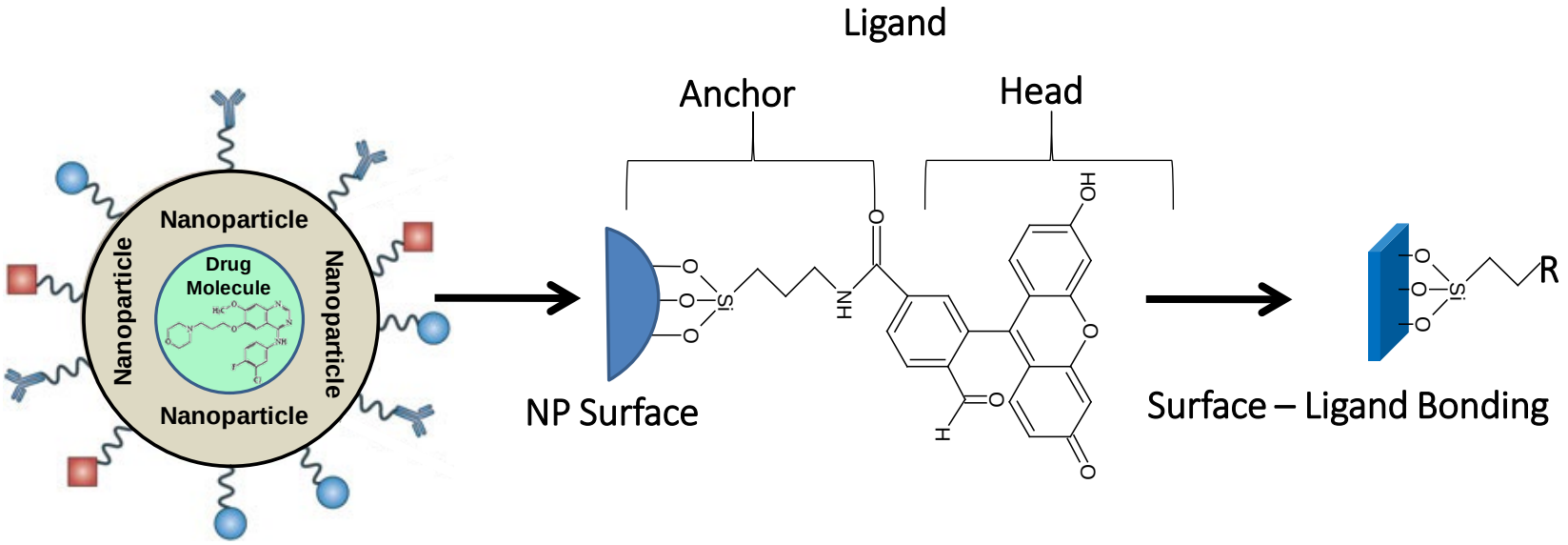

Multiple applications of nanoceria in healthy, sensing and drug delivery applications

Surface – Ligand interaction is of paramount importance!!!!

Problem Statement : Understand the surface of ceria nanoparticles and the adsorption mechanism of an anchoring ligand to the surface of ceria

Challenges and Approach

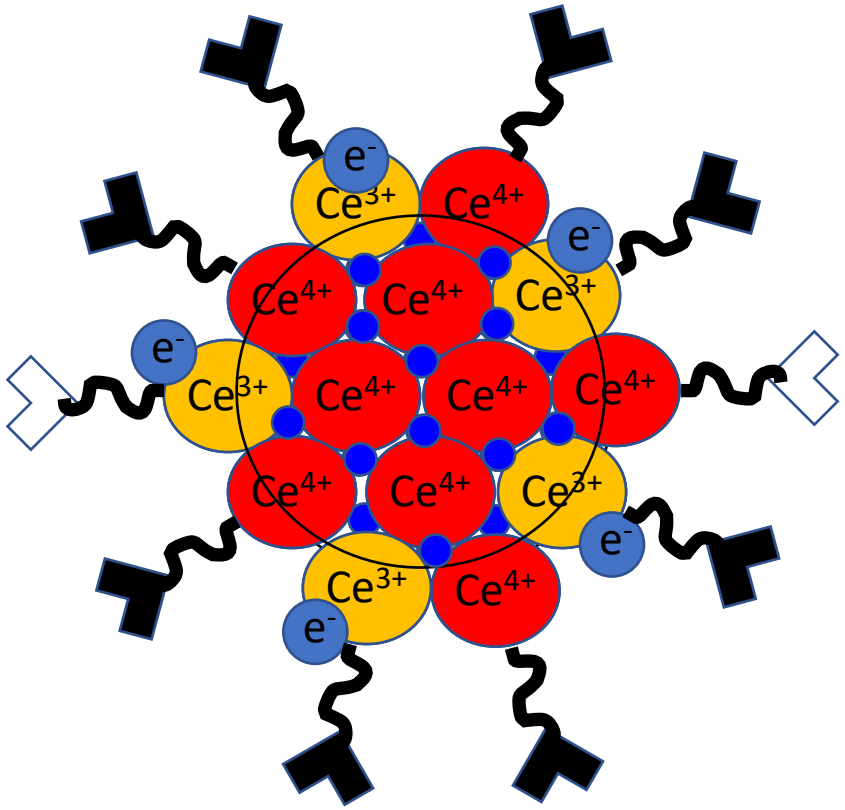

- Surface of ceria nanoparticles is reactive and has a mixed state of Ce^{4+} and Ce^{3+}

- Obtaining contamination free functionalization of ceria nanoparticles is difficult and to characterize them using conventional spectroscopic method is challenging

- Grow a CeO_2 (111) thin film on YSZ (111) to perform a model system study

- Create oxygen deficiency by vacuum annealing to produce mixed state of Ce^{4+} and Ce^{3+}

- Functionalized these surfaces with carboxylic acid molecules (trimethylacetic acid)

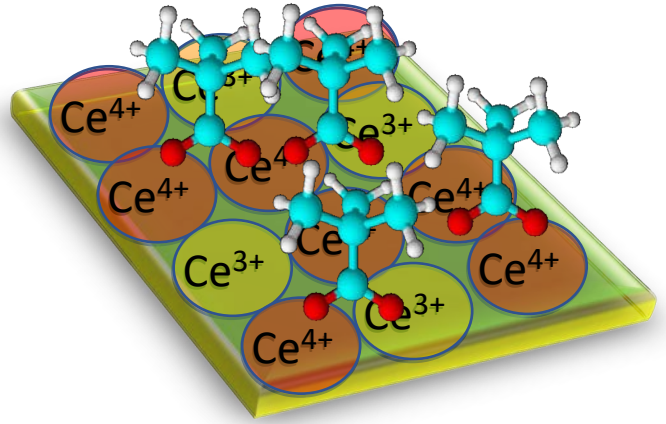

Film characterization

In – situ film characterization

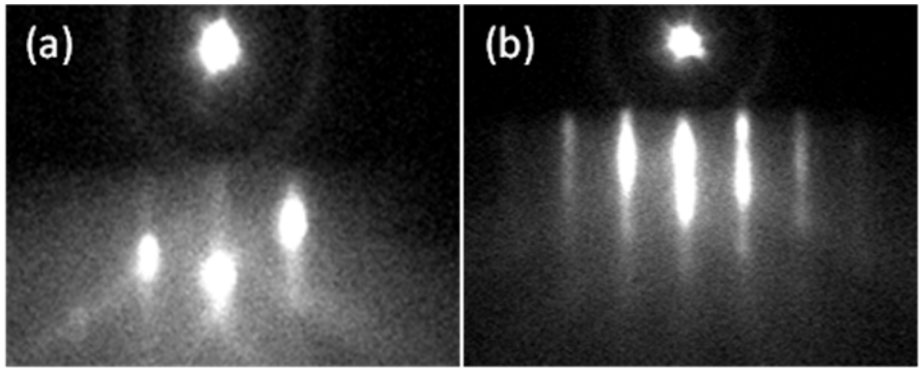

RHEED patterns of (a) YSZ(111) substrate and (b) CeO_2 thin film

Ex – situ film characterization

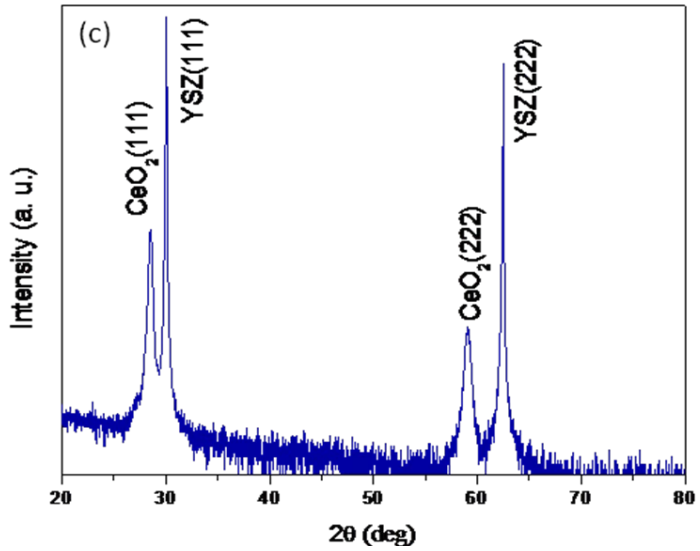

(c) HRXRD pattern of CeO_2 thin film grown on YSZ(111) substrate at ~ 650°C.

- A layer by later growth of CeO_2 (111) on YSZ (111) substrate

PHI 5000 Versa Probe XPS Capability

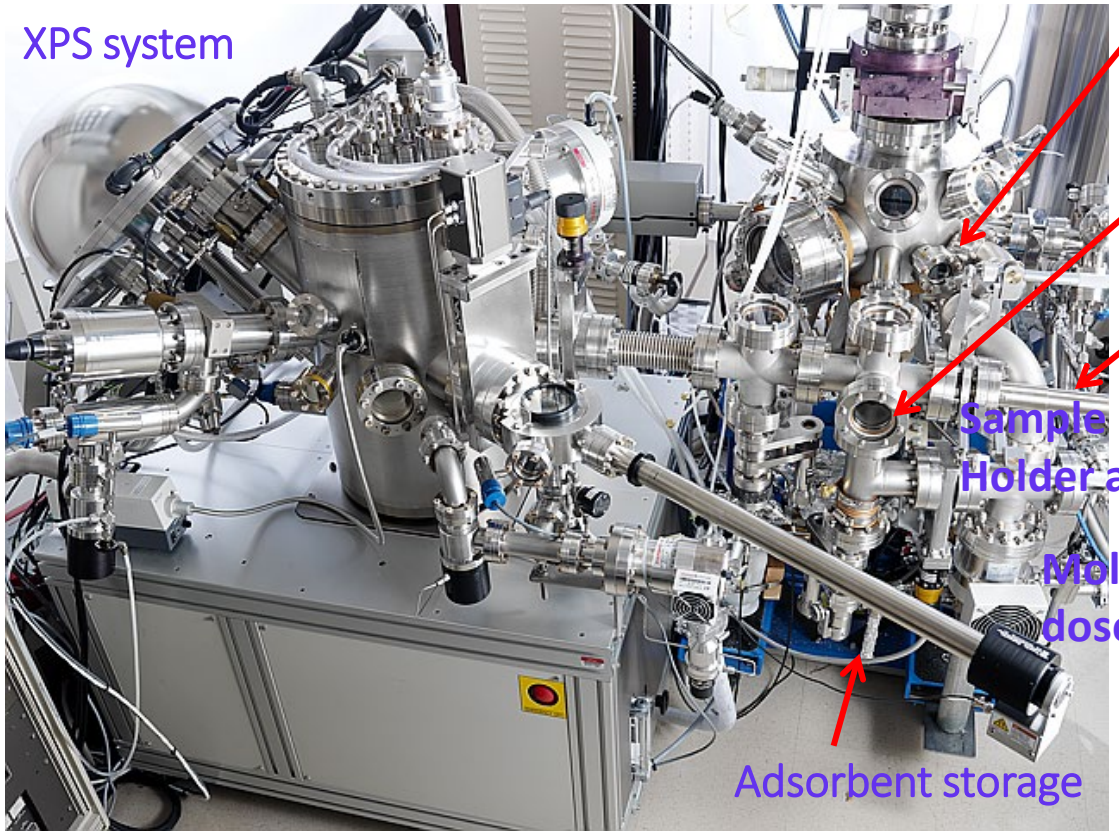

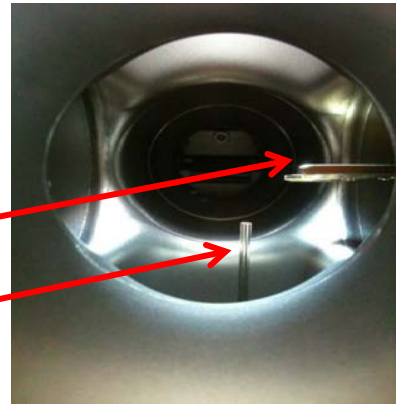

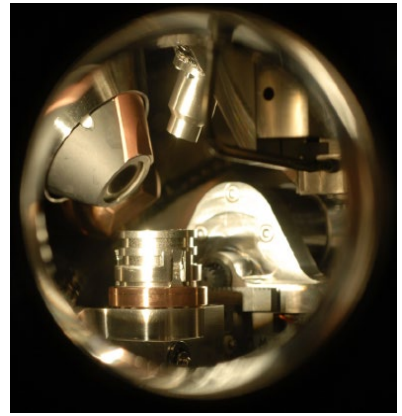

- XPS for chemical analysis before and after TMAA adsorption of oxidized (Ce^{4+}) and oxygen deficient surface (Ce^{3+})
- Vacuum annealing at 550, 650, 750 and 850°C to reduce the surface ➔ Mimic the partially reduced surface in nanoparticles

XPS from UHV annealed $CeO_2(111)$

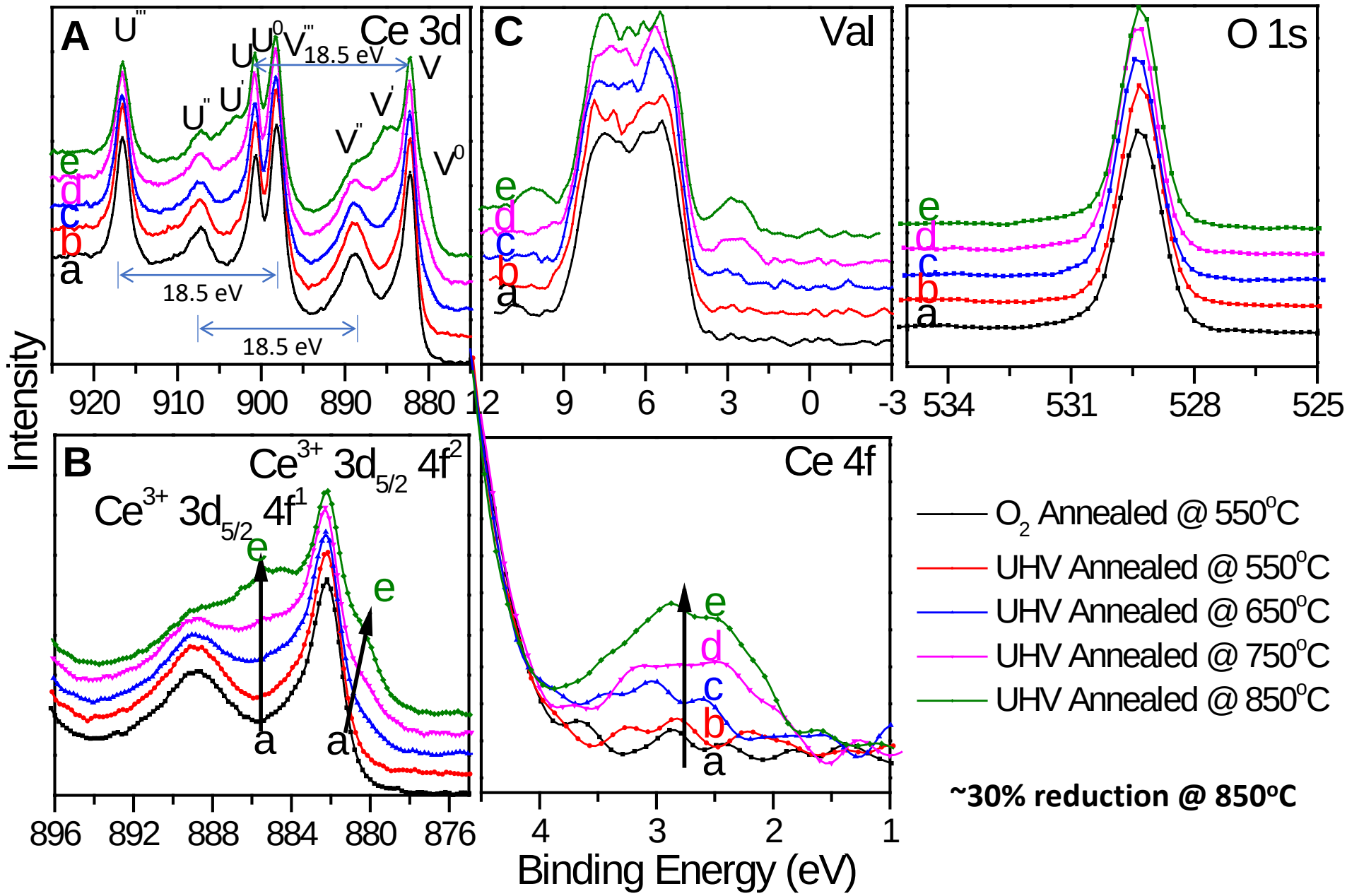

Ce^{4+}

V, V'',V''' and U, U'', U'''

Ce^{3+}

U^o, V^o, U', V'

High Resolution XPS Scans on CeO_2 (111) surfaces after O_2 and Vacuum annealing

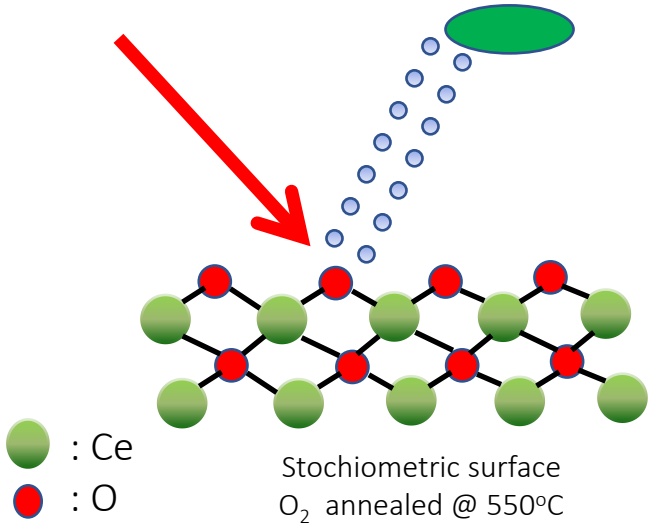

Stochiometric surface
O_2 annealed @ 550°C

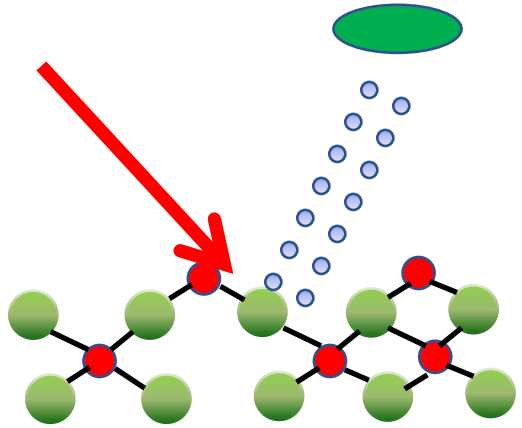

Oxygen deficient surface
Vacuum annealed @ 850°C

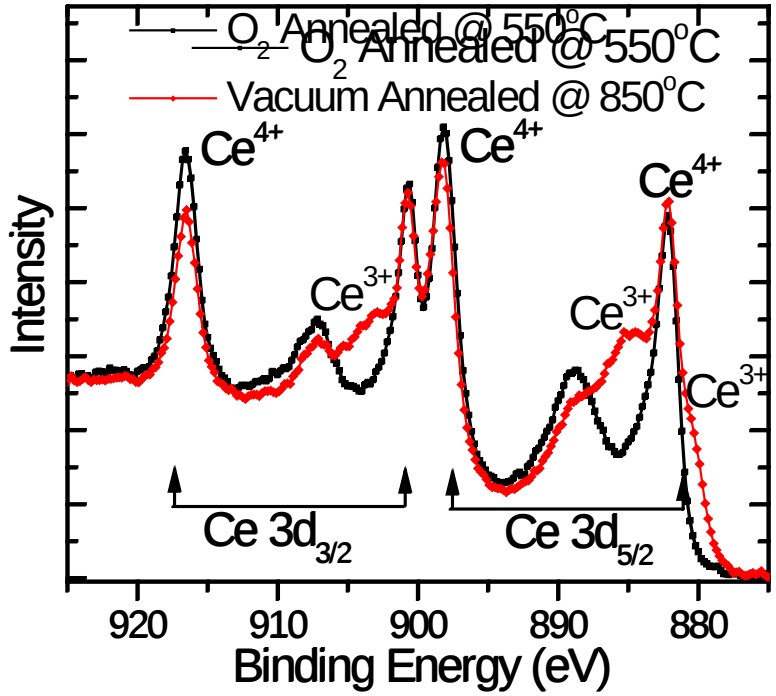

- Oxygen vacancies are formed by vacuum annealing the ceria surfaces at high temperatures
- Vacancies increase proportionally with annealing temperatures

High Resolution XPS Scans on CeO_2 (111) surfaces after O_2 and Vacuum annealing

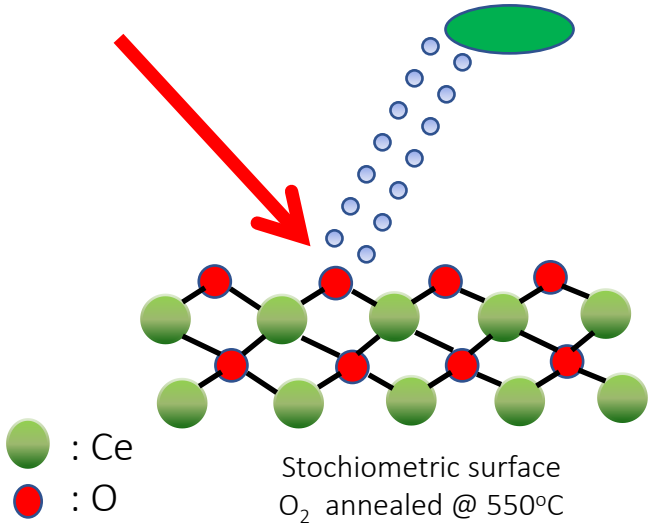

Stochiometric surface
O_2 annealed @ 550°C

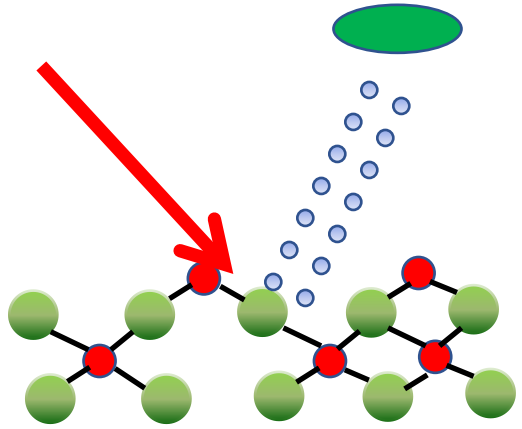

Oxygen deficient surface
Vacuum annealed @ 850°C

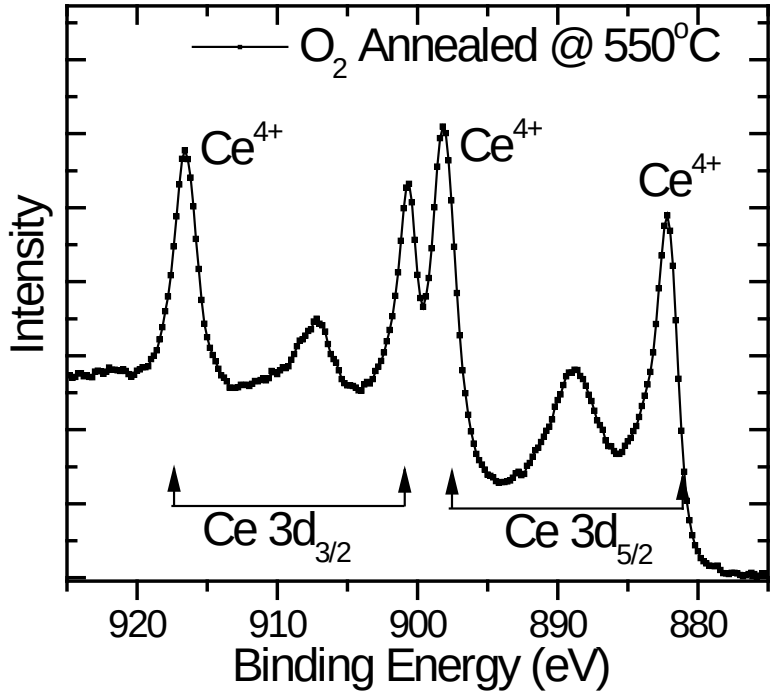

- Oxygen vacancies are formed by vacuum annealing the ceria surfaces at high temperatures
- Vacancies increase proportionally with annealing temperatures

High Resolution XPS Scans on CeO_2 (111) surfaces after TMAA($(CH_3)_3COOH$) Adsorption

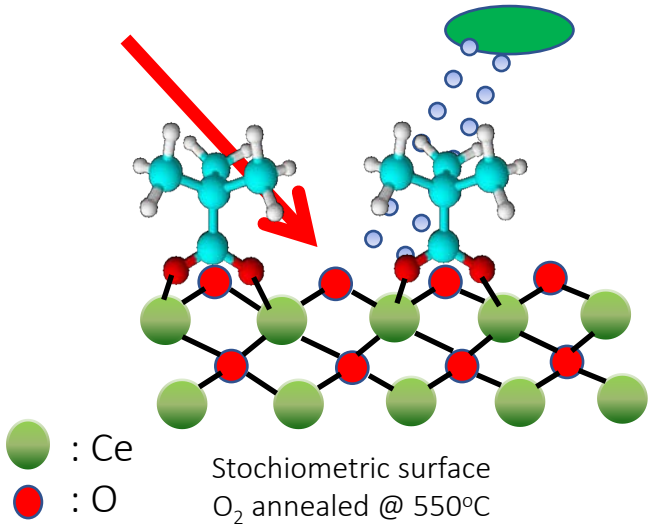

Stochiometric surface
O_2 annealed @ 550°C

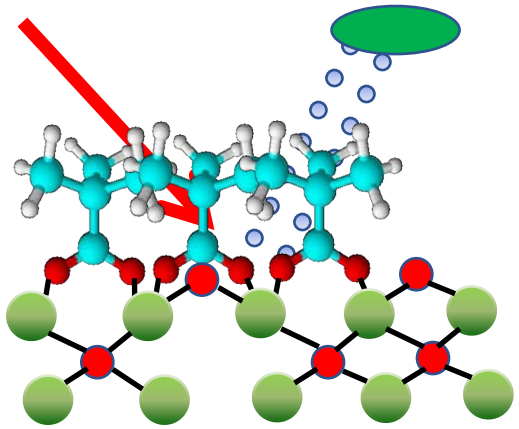

Oxygen deficient surface
Vacuum annealed @ 850°C

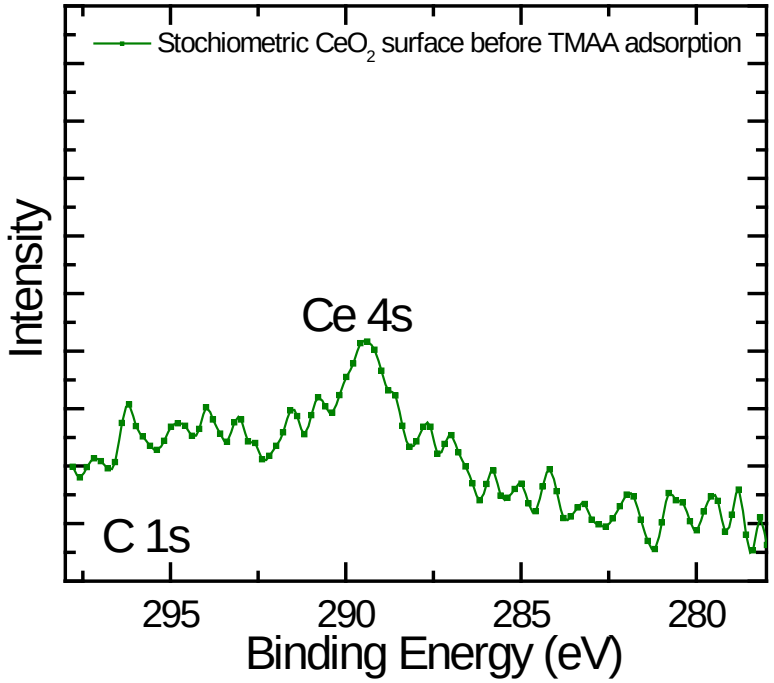

Surface	Atomic %			% Ce^{3+}
	Ce	O	C	
Oxidized	30.5	60.6	8.9	0
Reduced	29.5	58.2	12.3	33

- Oxygen vacancies leads to more adsorption of carboxylic acid molecules on CeO_2(111) surface!!!!

High Resolution XPS Scans on CeO_2 (111) surfaces after TMAA($(CH_3)_3COOH$) Adsorption

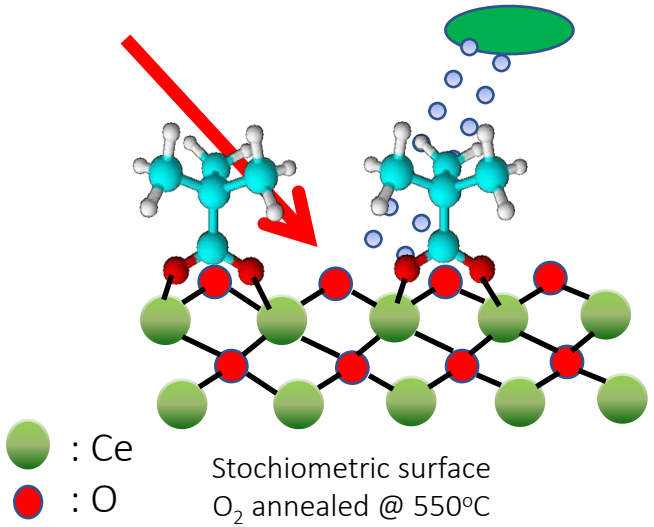

Stochiometric surface
O_2 annealed @ 550°C

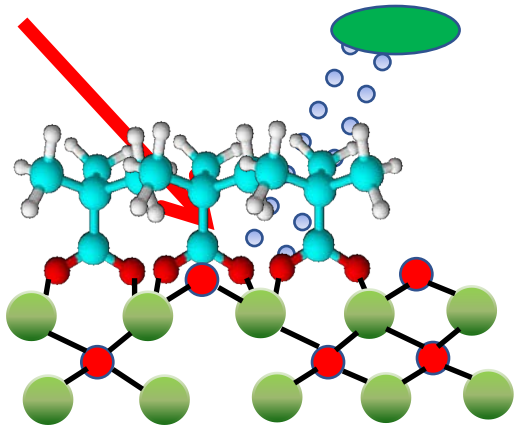

Oxygen deficient surface
Vacuum annealed @ 850°C

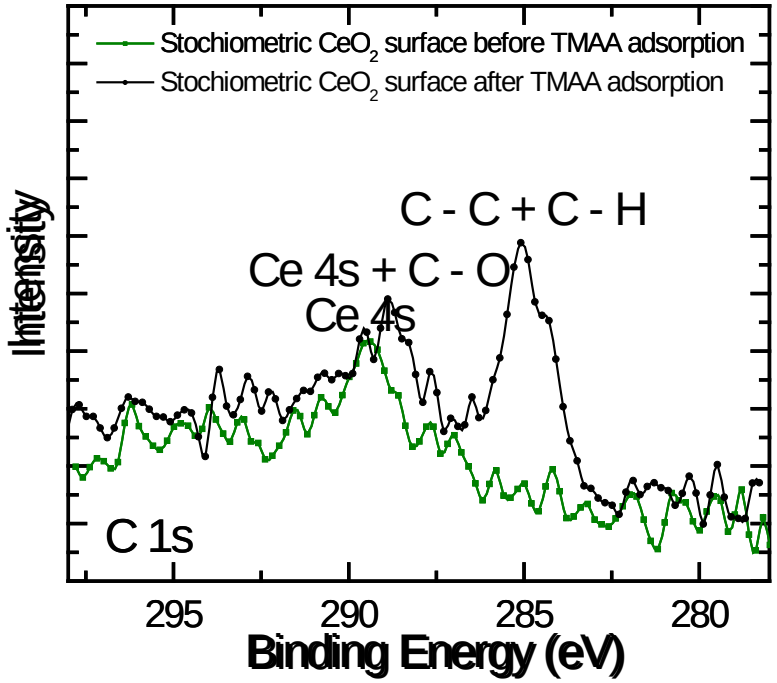

Surface	Atomic %			% Ce^{3+}
	Ce	O	C	
Oxidized	30.5	60.6	8.9	0
Reduced	29.5	58.2	12.3	33

- Oxygen vacancies leads to more adsorption of carboxylic acid molecules on CeO_2(111) surface!!!!

High Resolution XPS Scans on CeO_2 (111) surfaces after TMAA($(CH_3)_3COOH$) Adsorption

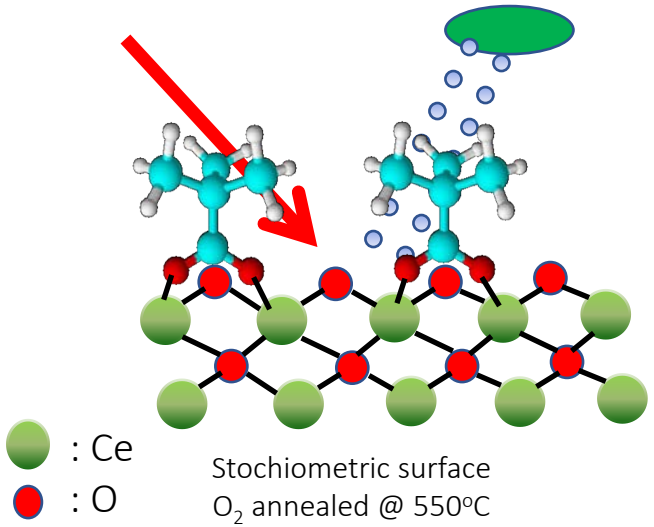

Stochiometric surface
O_2 annealed @ 550°C

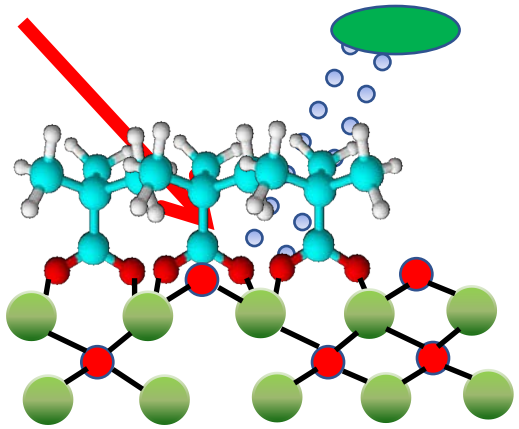

Oxygen deficient surface
Vacuum annealed @ 850°C

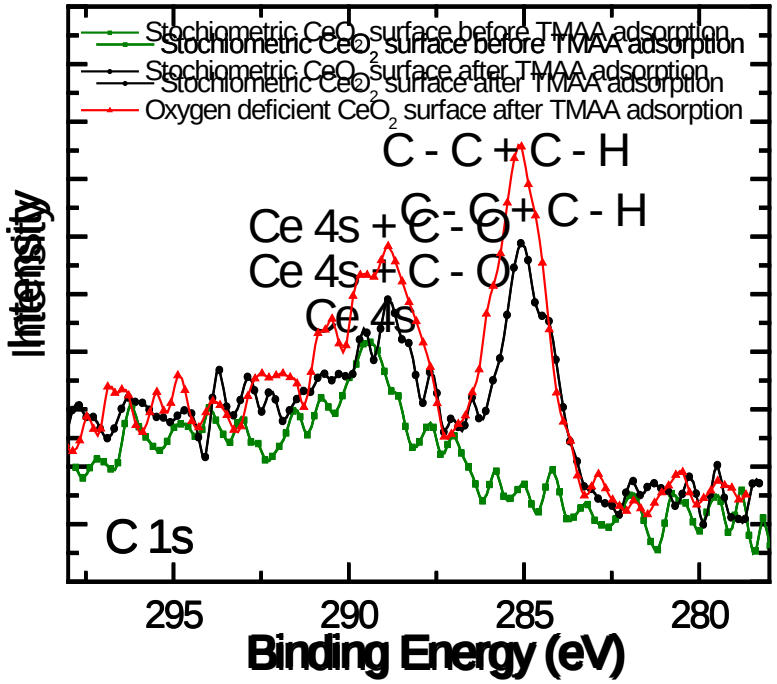

Surface	Atomic %			% Ce^{3+}
	Ce	O	C	
Oxidized	30.5	60.6	8.9	0
Reduced	29.5	58.2	12.3	33

- Oxygen vacancies leads to more adsorption of carboxylic acid molecules on CeO_2(111) surface!!!!

High Resolution XPS Scans on CeO_2 (111) surfaces

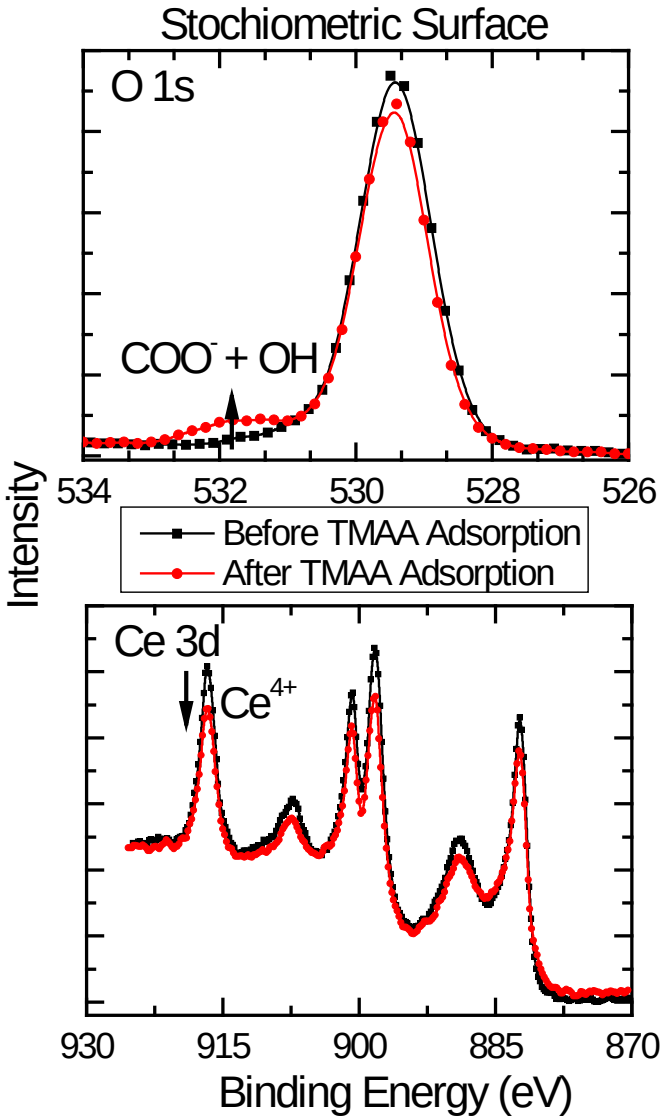

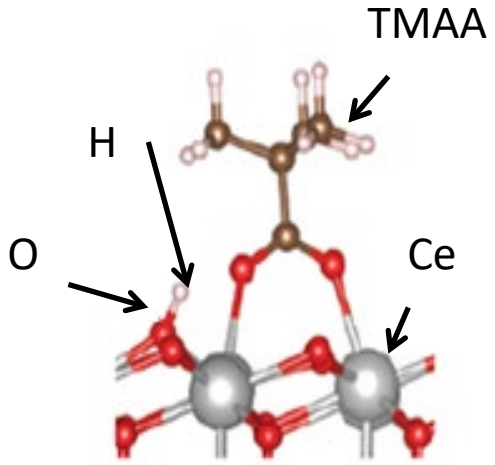

Dissociative Adsorption

- Ce^{3+}/Ce^{4+} increases after TMAA adsorption
- Indicates dissociative adsorption!!!

High Resolution XPS Scans on CeO_2 (111) surfaces

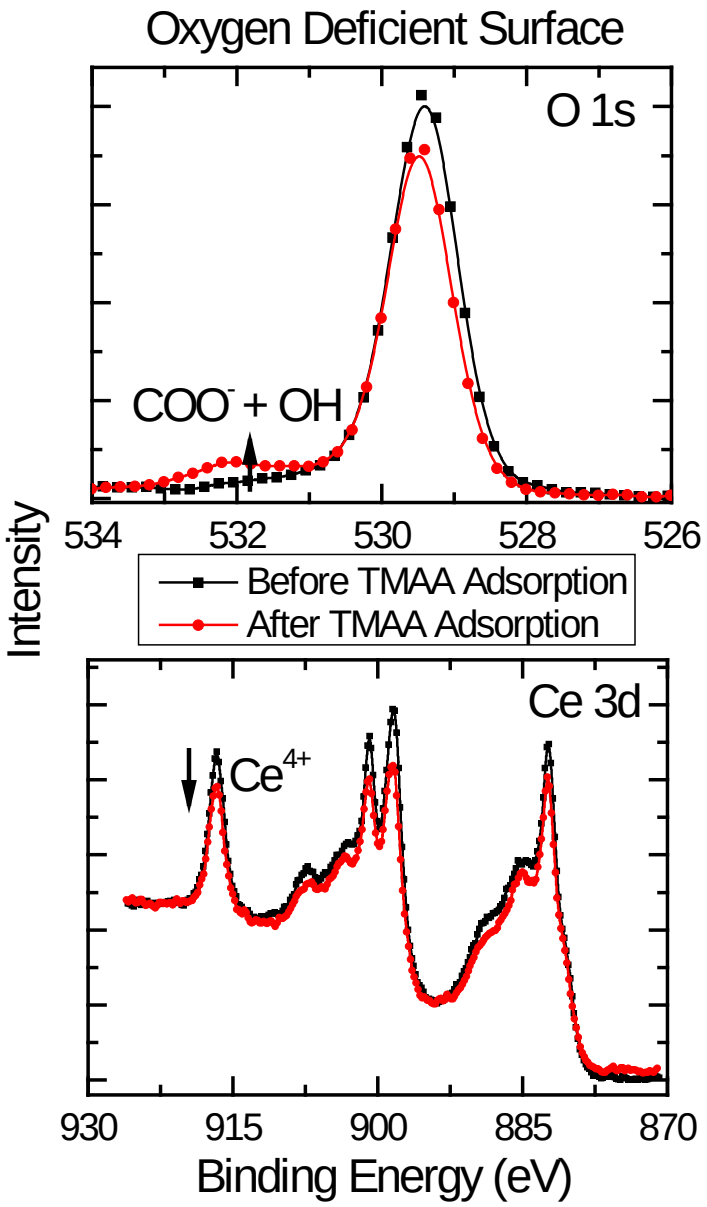

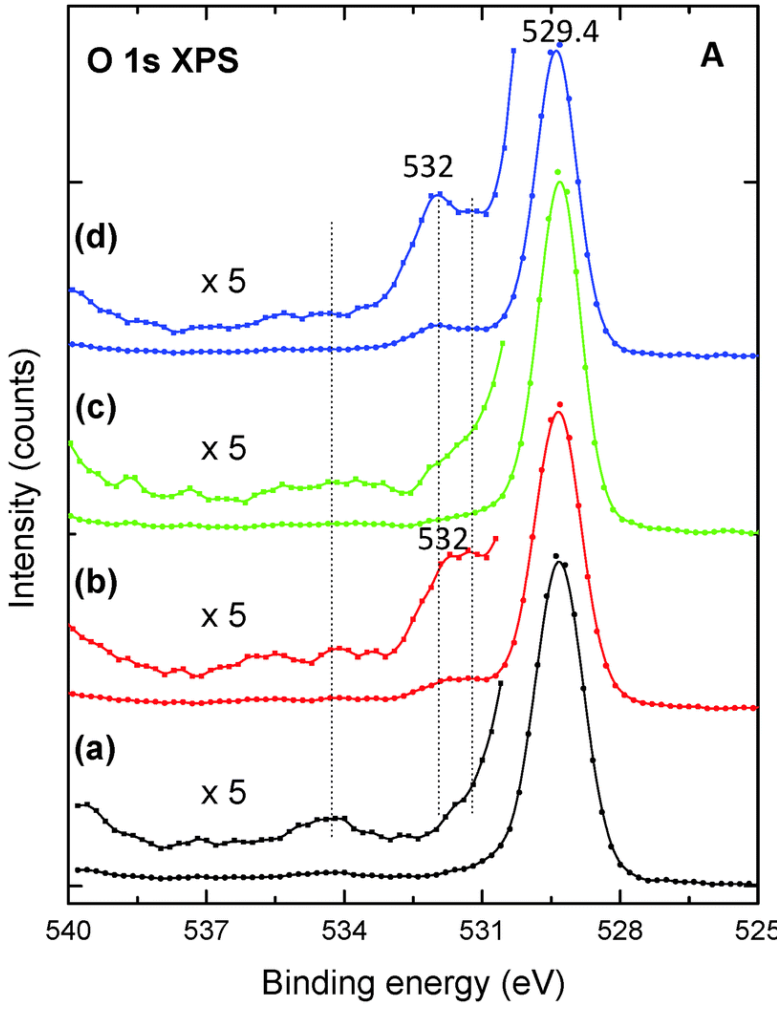

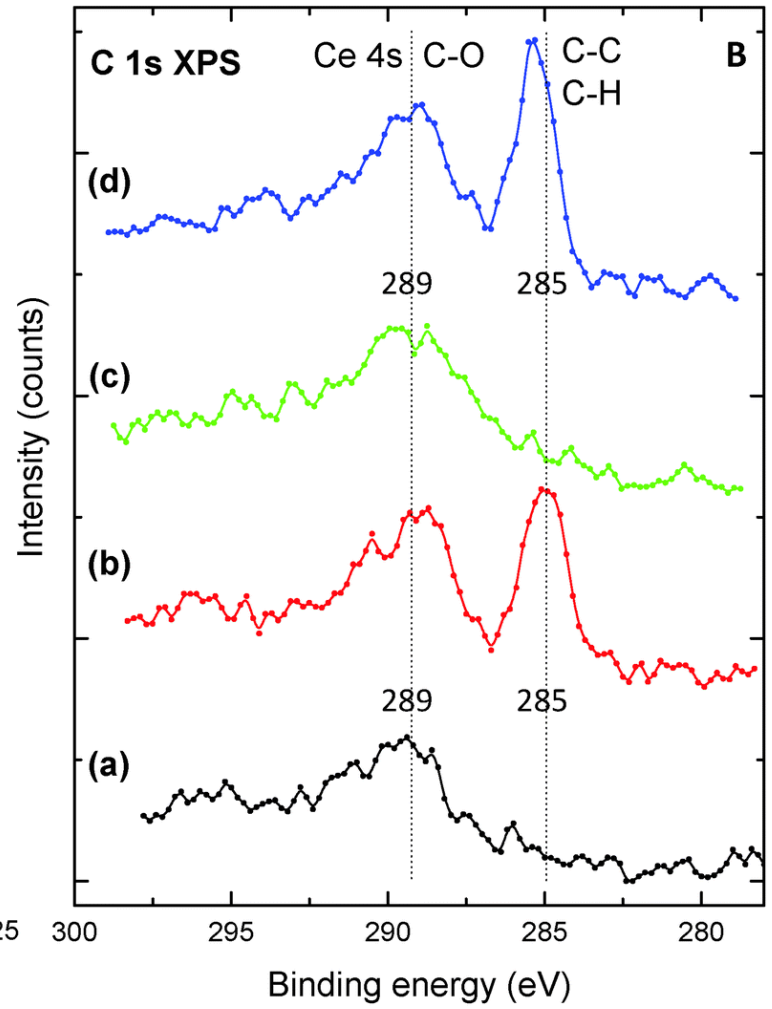

Theoretical studies – Energy calculations (Unit: kcal/mol)

Stoichiometric surface

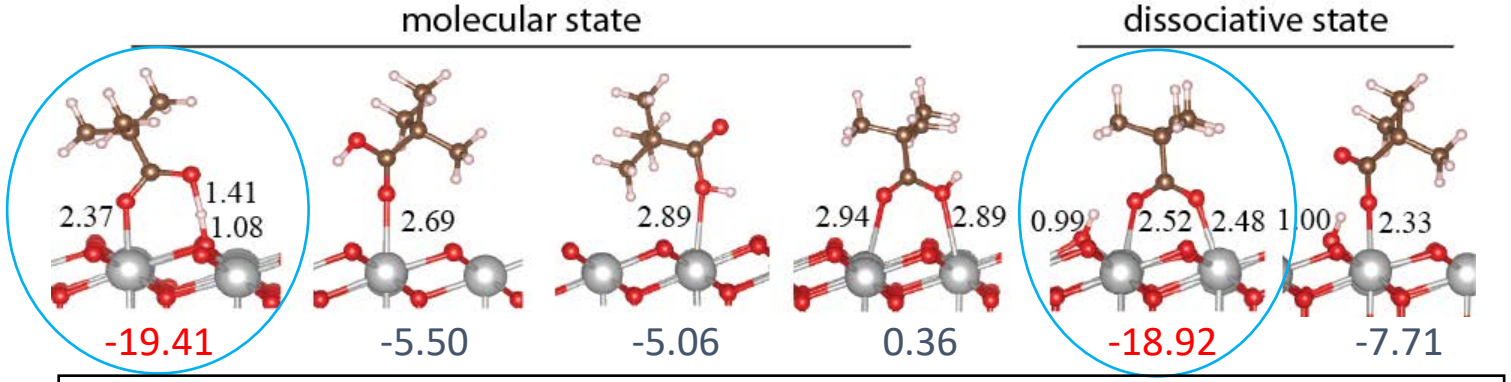

vdW	-19.41	-5.50	-5.06	0.36	-18.92	-7.71
correction	-47.12	-45.46	-35.34	-31.12	-55.52	-38.28

Oxygen deficient surface

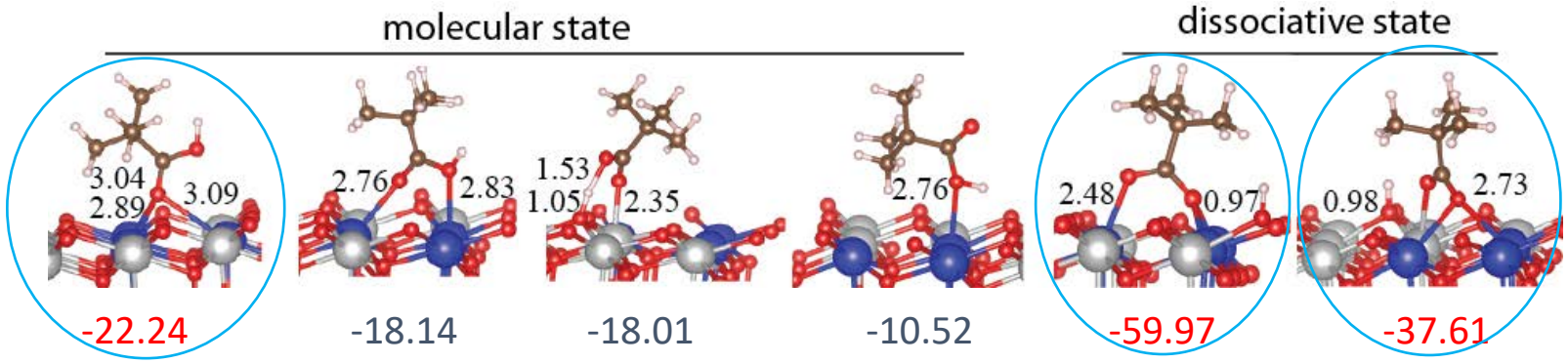

vdW	-22.24	-18.14	-18.01	-10.52	-59.97	-37.61
correction	-61.28	-57.18	-56.05	-47.00	-102.96	-78.28

- Bidendate bonding is the most stable configuration and dissociative adsorption is more favorable than molecular adsorption
- Oxygen replaces the lattice oxygen vacancies on oxygen deficient surface

But..
What about real nanoparticles??

Surface Contamination – Challenges in Surface Characterization

System - Ceria nanoparticles and acetic acid

Bare ceria nanoparticles

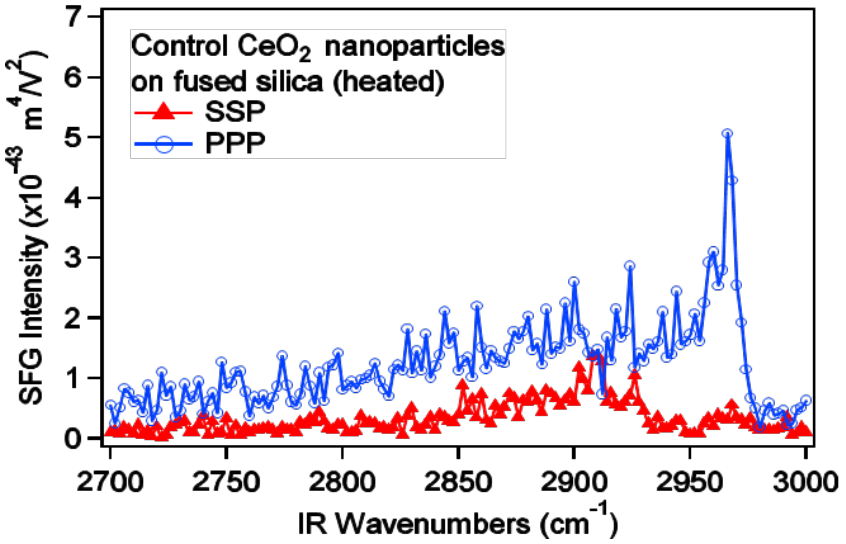

CeO_2/acetate nanoparticles

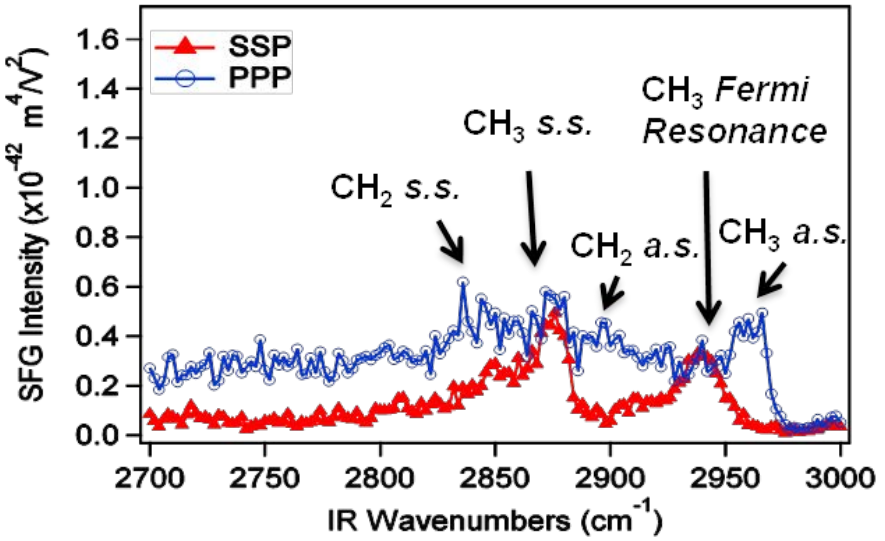

Carbon contamination in bare and functionalized nanoparticles hamper surface characterization

Preserving the Surface Chemistry and Composition of Nanoparticles – *In-situ* XPS

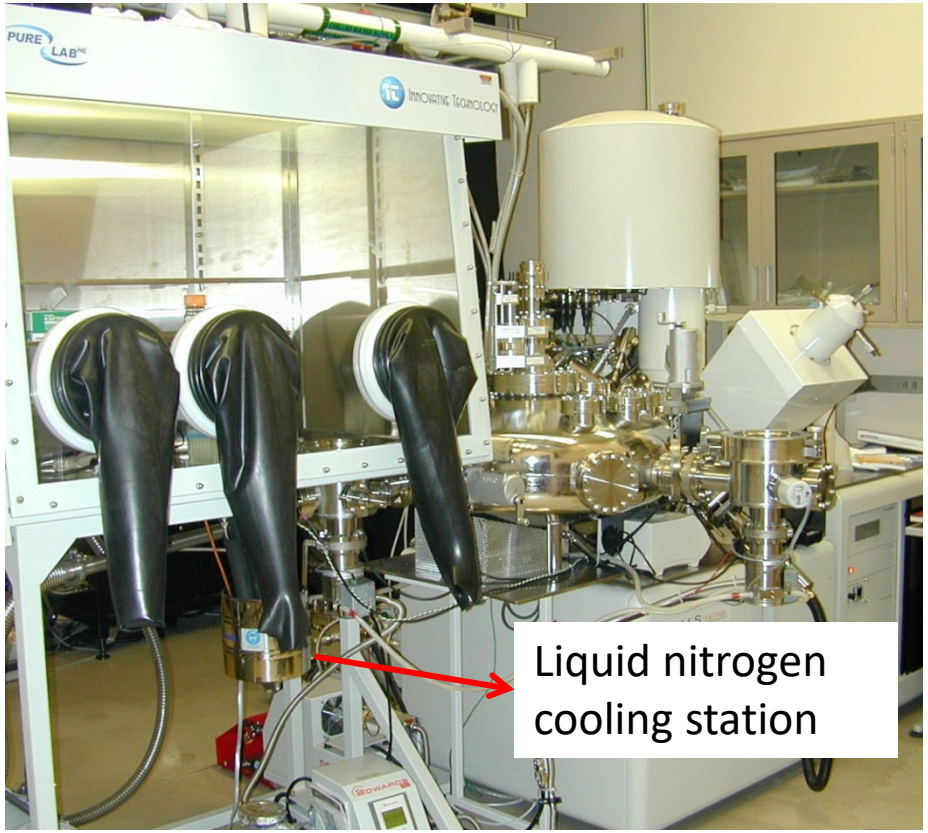

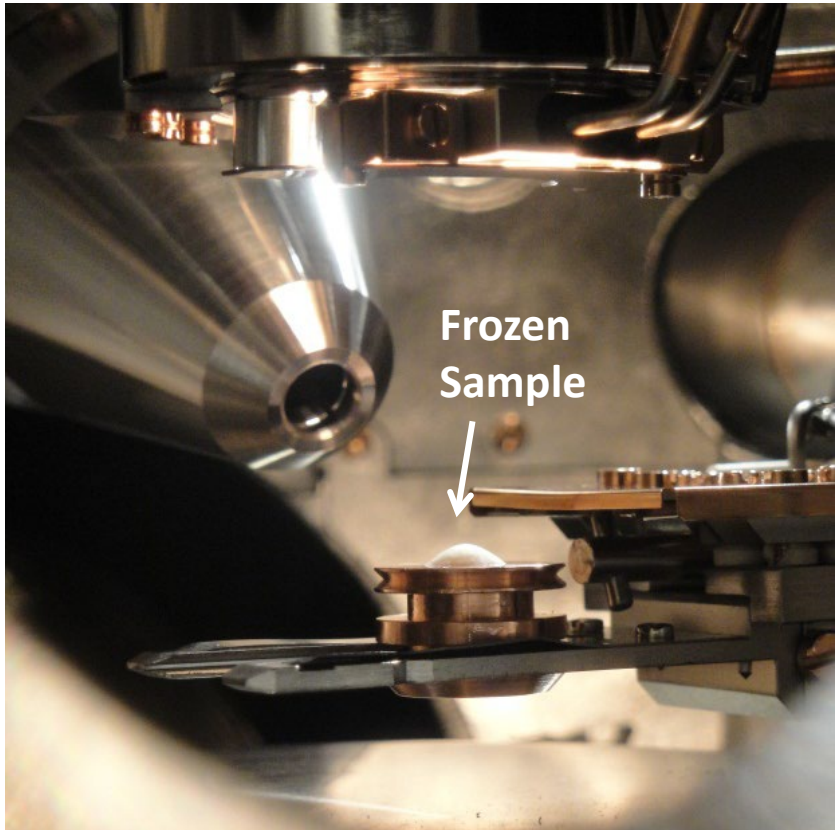

- Sample preparation in glove box
- Instantaneously frozen at liquid nitrogen temperature
- Maintained at liquid nitrogen temperature during XPS measurements

Advantages of freezing NPs solution

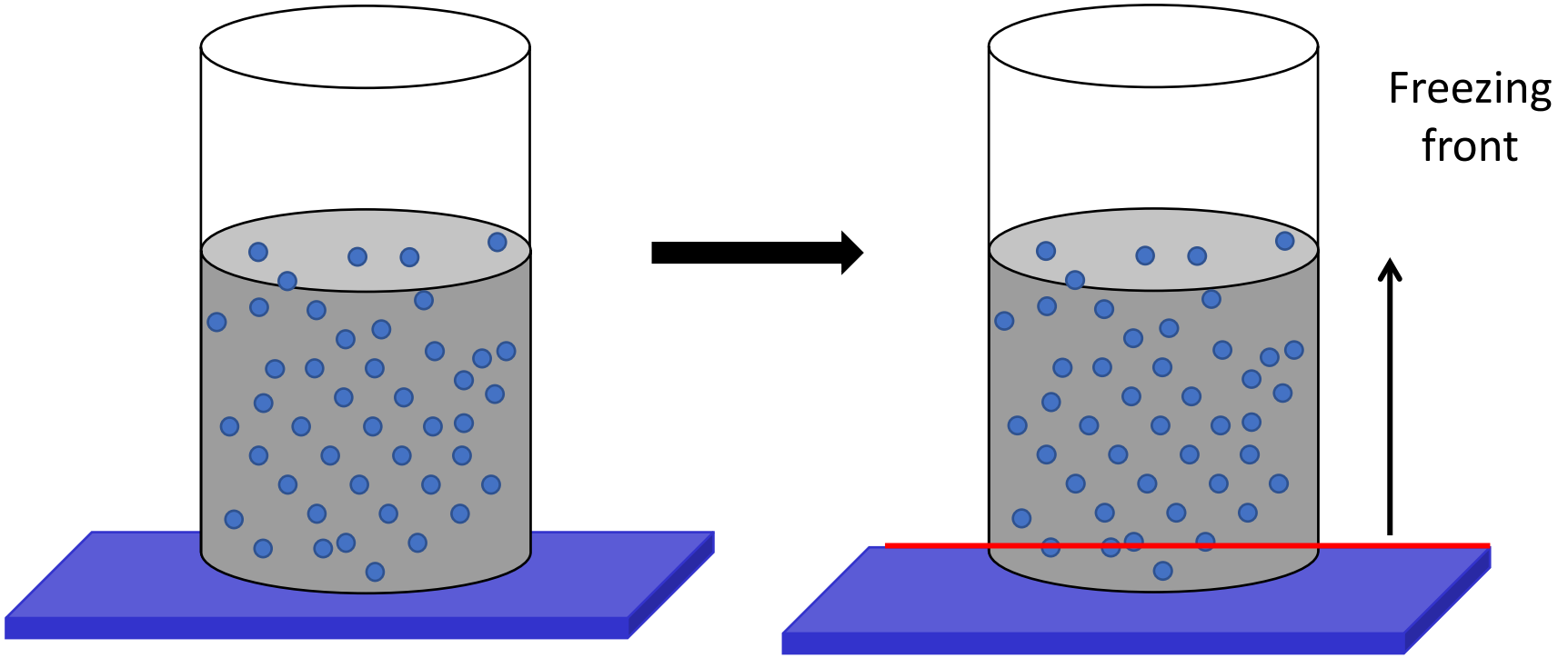

Cooling from bottom

Freezing front rejects the solute from the freezing water segregating nanoparticles at the top for analysis

Advantages of freezing NPs solution

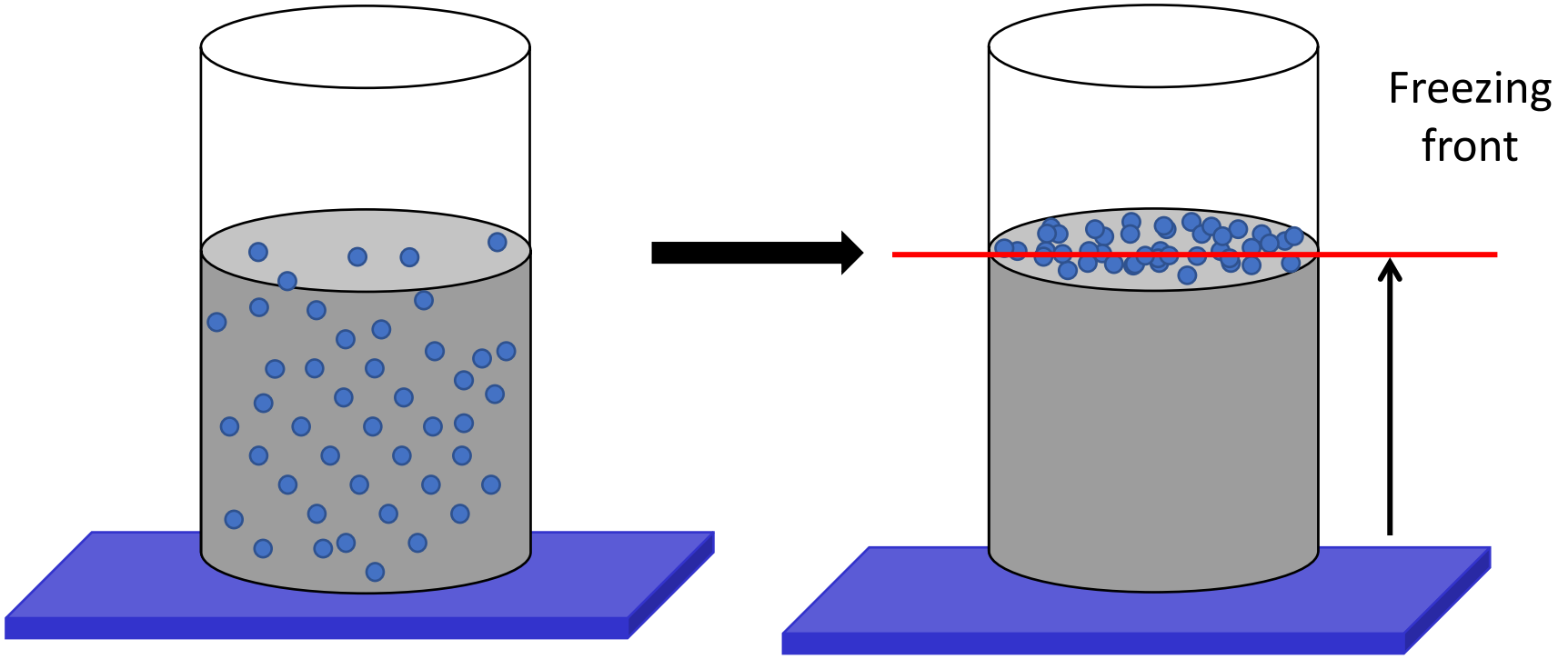

Cooling from bottom

Freezing front rejects the solute from the freezing water segregating nanoparticles at the top for analysis

Characterization of Nanoparticles

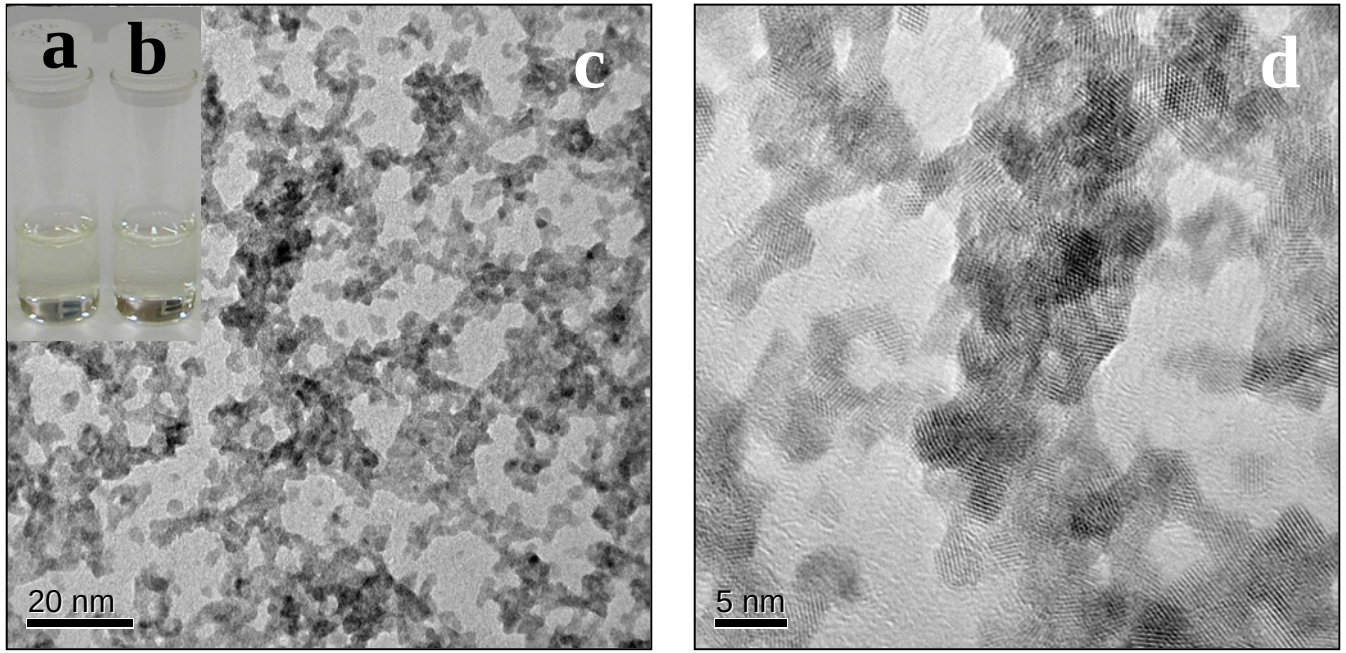

Table 1: Hydrodynamic size and zeta potential of CNPs

NPs	Particle Size (nm)		Zeta Potential (mV)	
	Before dialysis	After dialysis	Before dialysis	After dialysis
Bare	12.4	148	30.33	0.056
AcOH	12.1	30.9	22.2	0.07

Acetic acid functionalized nanoparticles - *In-situ* XPS

- 3 at % carbon in UV cleaned DI water !!!!!
- Good signal from frozen nanoparticles
- Cerium is predominantly in Ce^{4+} oxidation state
- CeO_2 – Ce:O = 1:2

  CH_3COOH – C:O = 1:1
- Acetic acid is present over cerium oxide surface
- Minimal contamination

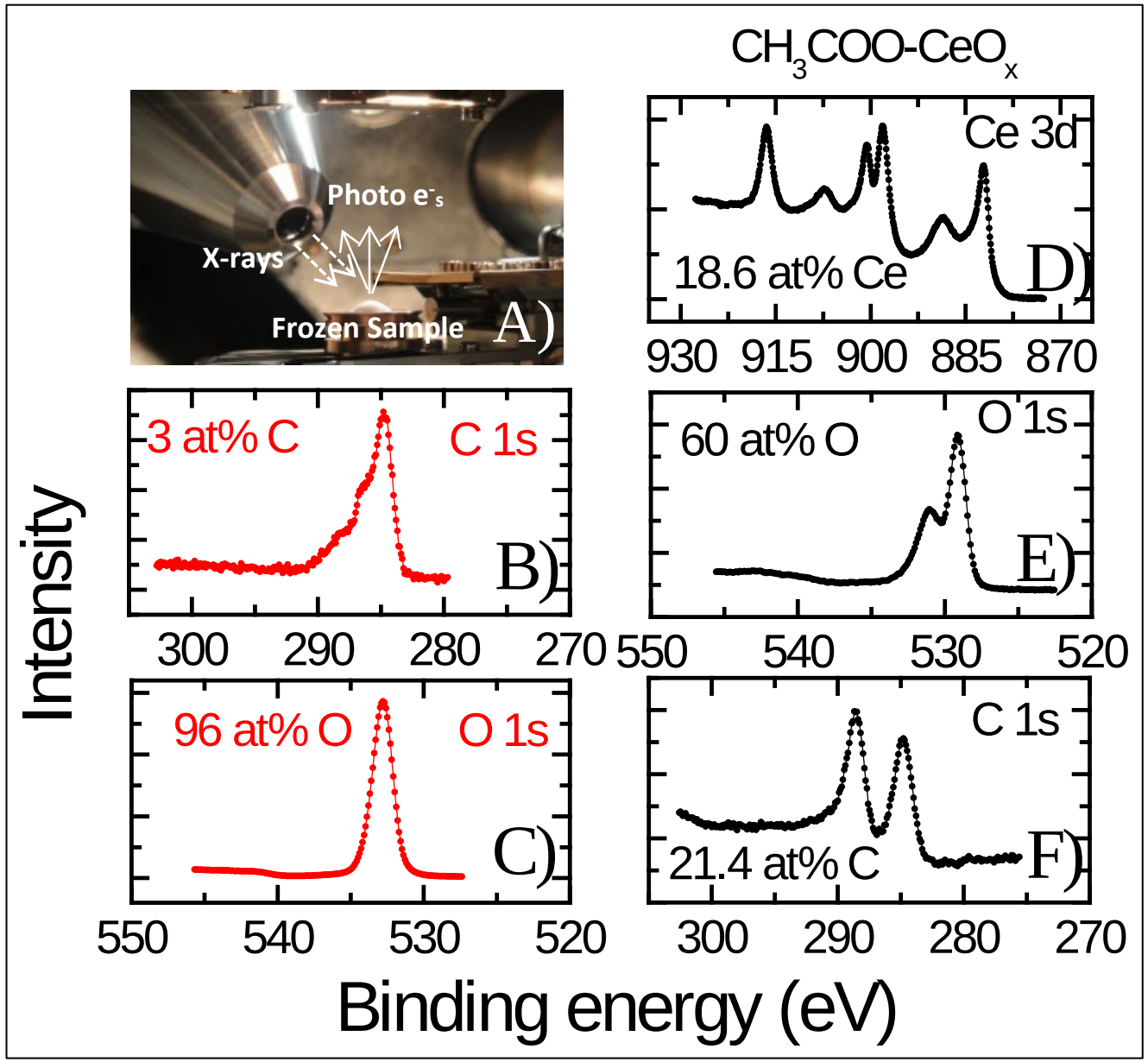

Comparison: Pure Acetic Acid Vs Ceria Surfaces

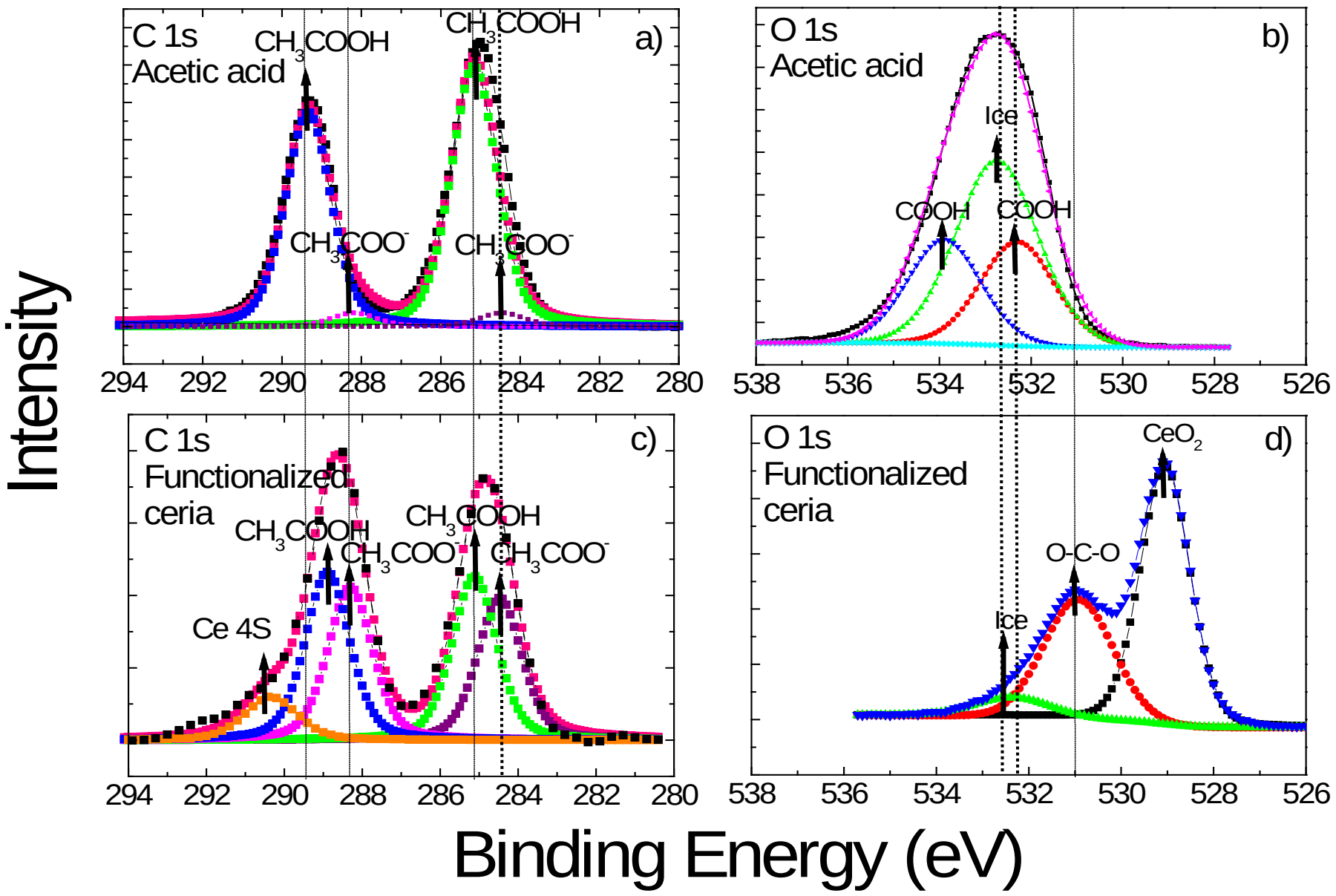

Theoretical Considerations

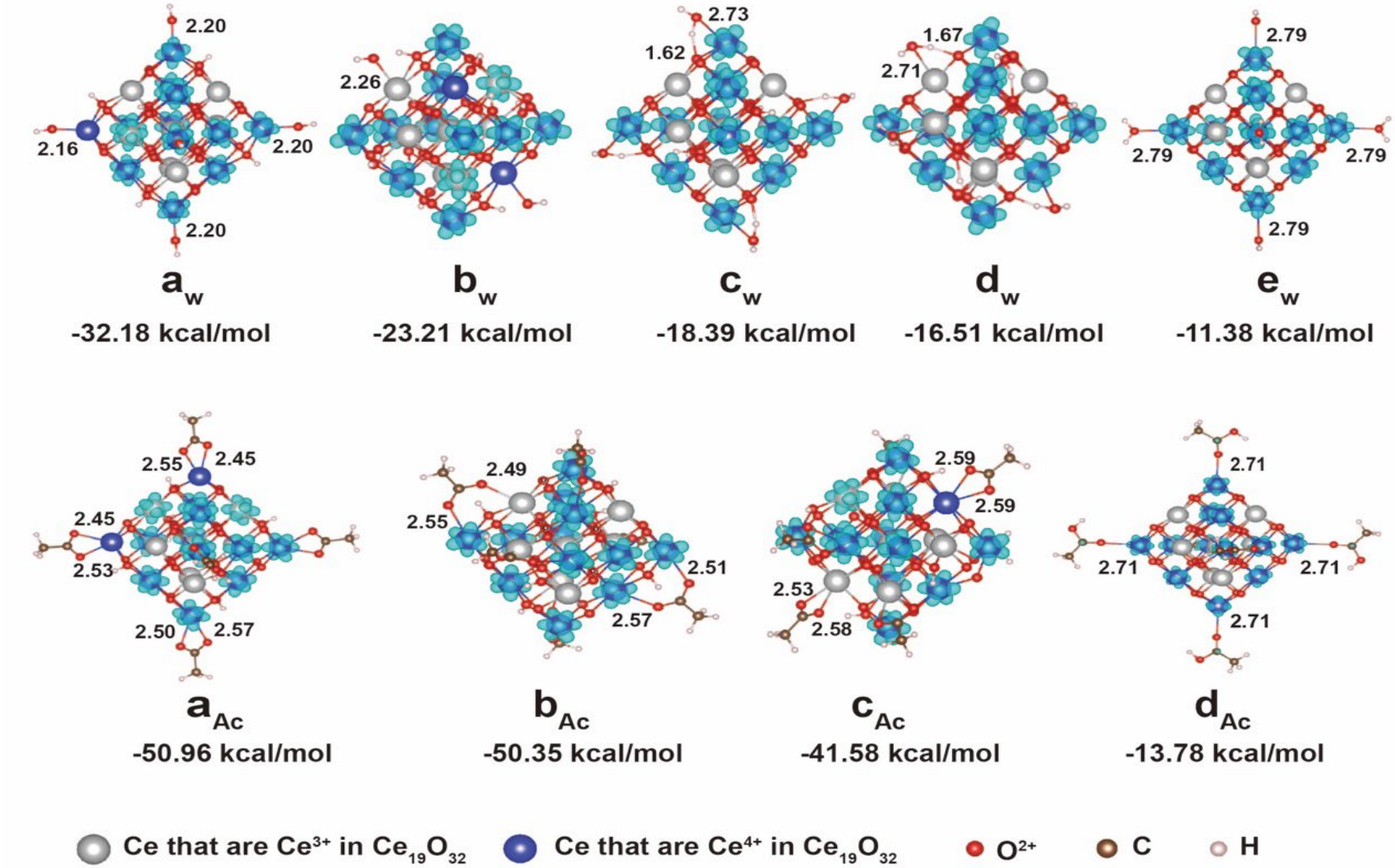

Summary

- Oxygen deficiencies were created at high vacuum annealing temperatures on ceria surfaces
- Adsorption of TMAA on cerium oxide surfaces is thermodynamically feasible and experimentally proven using XPS
- Oxygen deficiency leads to more surface coverage of TMAA on ceria surfaces
- TMAA binds dissociatively to the surface of ceria resulting in bidentate binding of oxygen atoms to cerium atoms
- On ceria nanoparticles though a mixture of dissociated and molecular bonding states were observed that is consistent with the oxidation state of cerium

Redox Catalyst

Bismuth Molybdate

Background

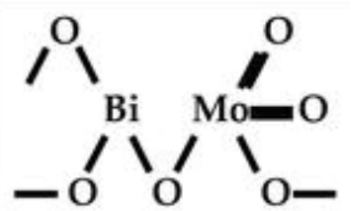

Oregon State University
College of Engineering

Bismuth Molybdenum Oxides ($Bi_xMo_yO_z$)

- General formula $xBi_2O_3.yMoO_3$
- Well-known Industrial Catalysts. Garnered attention since 1959 since the discovery of the "SOHIO" process
- Highly selective and active in partial oxidation reactions

probe Rxn's → SOHIO or (Amm)oxidation of small Hydrocarbons

- The synergy between Bi and Mo is the key to their excellent redox properties
- Exist in different crystal structures based on Bi/Mo

α Bi:Mo = 2:3

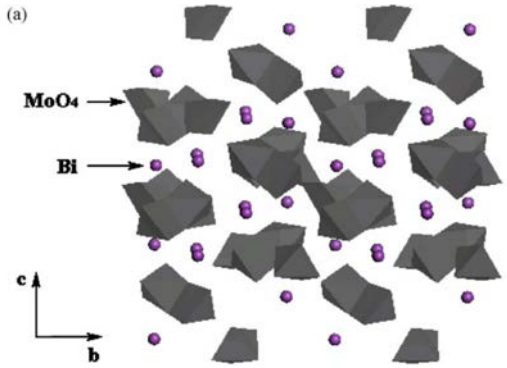

β 1:1

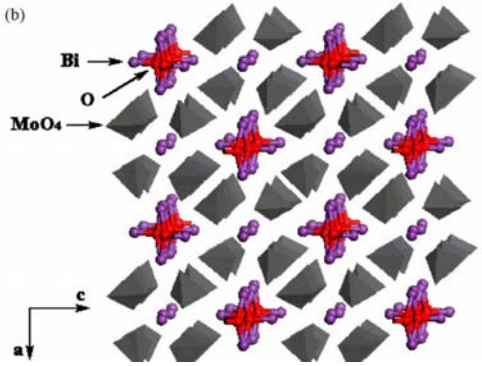

γ 2:1

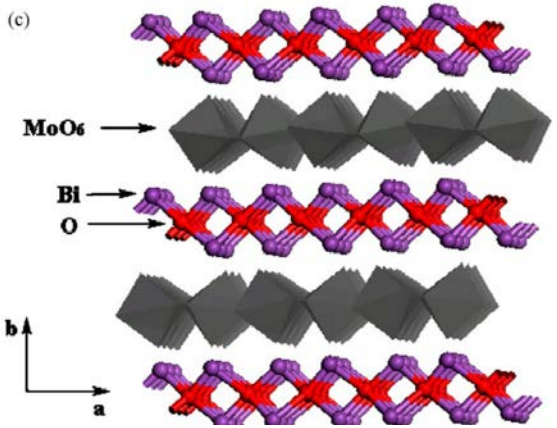

References:
https://pubs.acs.org/doi/10.1021/acscatal.7b01149

Background

Ammoxidation chemistry over α – Bismuth Molybdates

- Propylene adsorption over Mo-O
- Ammonia activation on the neighboring Bi

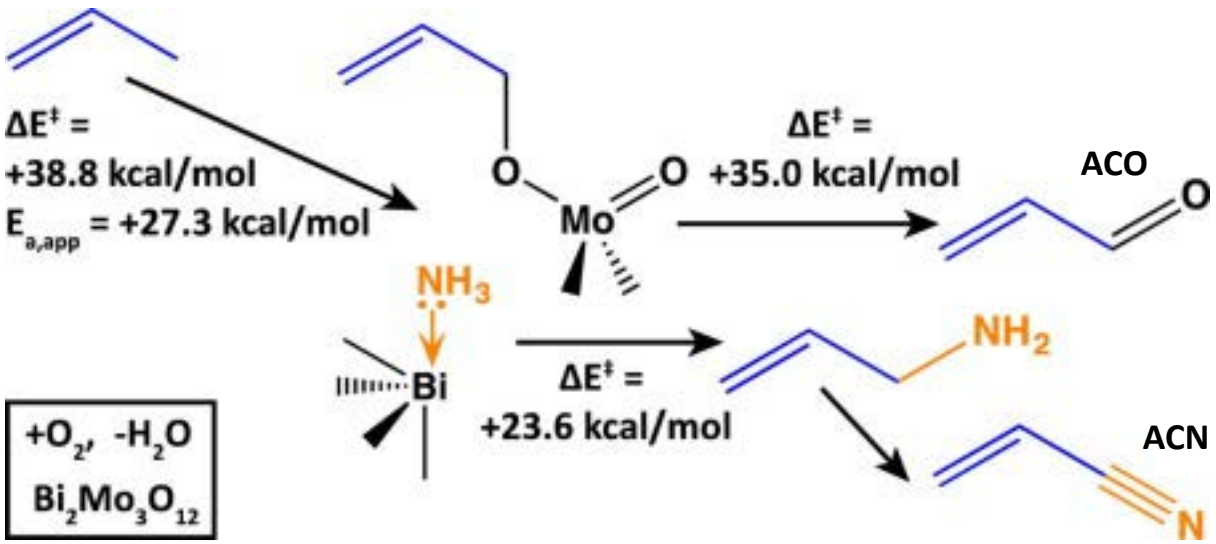

- C-N bond formation involves the reaction of allyl species with surface Mo =NH groups
- The two abstracted hydrogen atoms are released as water

References:
https://ars.els-cdn.com/content/image/1-s2.0-S0021951721001949-gr18_lrg.jpg
https://doi.org/10.1016/j.jcat.2021.05.009

Preliminary Results: Synthesis

- **Homemade BMO samples prepared via co-precipitation**

Reagents:

Ammonium Molybdate Tetrahydrate (AMT)	$(NH_4)_6Mo_7O_{24} * 4H_2O$
Bismuth (III) Nitrate Pentahydrate (BNP)	$Bi(NO_3)_3 * 5H_2O$
Silica dioxide	SiO_2
Aluminium oxide	Al_2O_3
Ammonia Hydroxide	NH_4OH
Nitric Acid	HNO_3
Distilled Water	H_2O

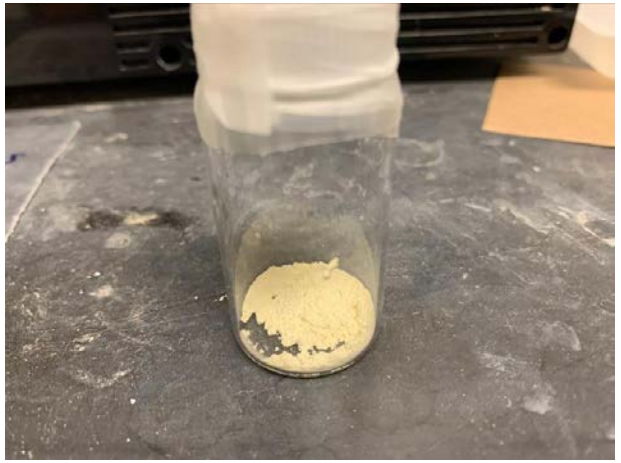

***Calcination*. 500℃ of calcination for 6 hours followed by 300℃ for 3 hours . 5℃/minute is the temperature increase and decrease rate for calcination**.**

- Promoted (NiFe-BMO/SiO_2) catalysts are acquired from collaborators

References:
DOI: 10.1016/j.jcat.2016.04.012

Preliminary Results: XPS

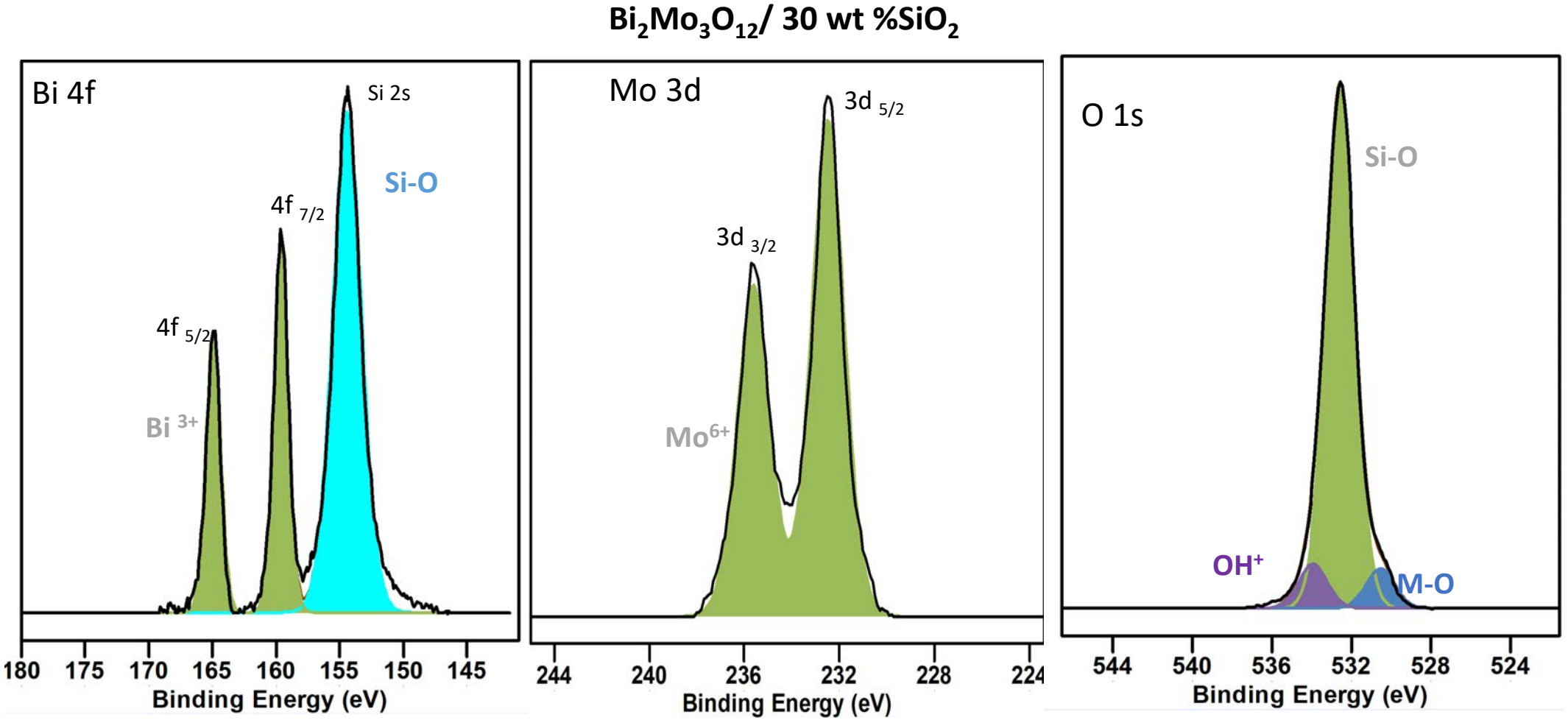

XPS: Redox cycles

- All the reduction and oxidation treatments were done in a flow reactor using gases: 10%H_2/Ar, 2%C_3H_6/N_2, 10% O_2/He , 10%CO_2/Ar
- The samples are treated at 450℃ with the gas flow rates 20 cc/min for 15 min each cycle

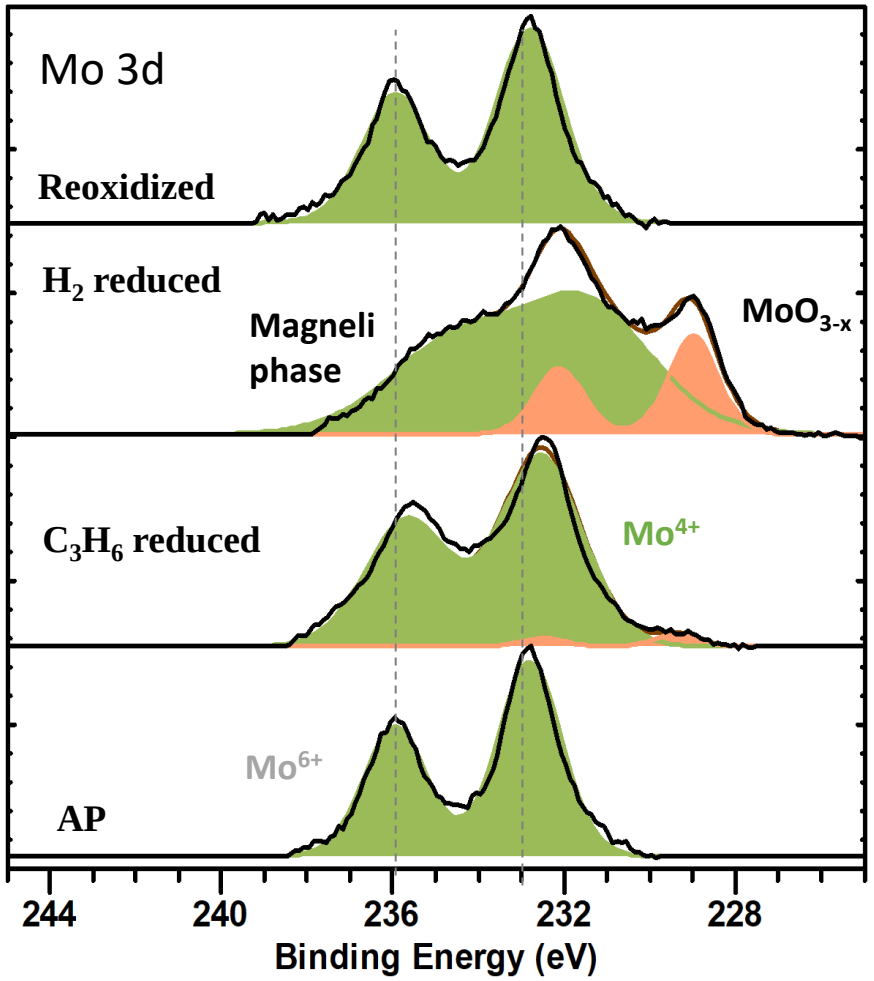

$Bi_2Mo_3O_{12}/SiO_2$

- **Mo^{6+} reduces to Mo^{4+}**
- **H_2 stronger reductant than C_3H_6**
- **Violent reduction with H_2 gives rise to Magneli phase or Mo_nO_{3n-1} consisting of metastable oxidation states**
- **Bi^{3+} remains unchanged.**

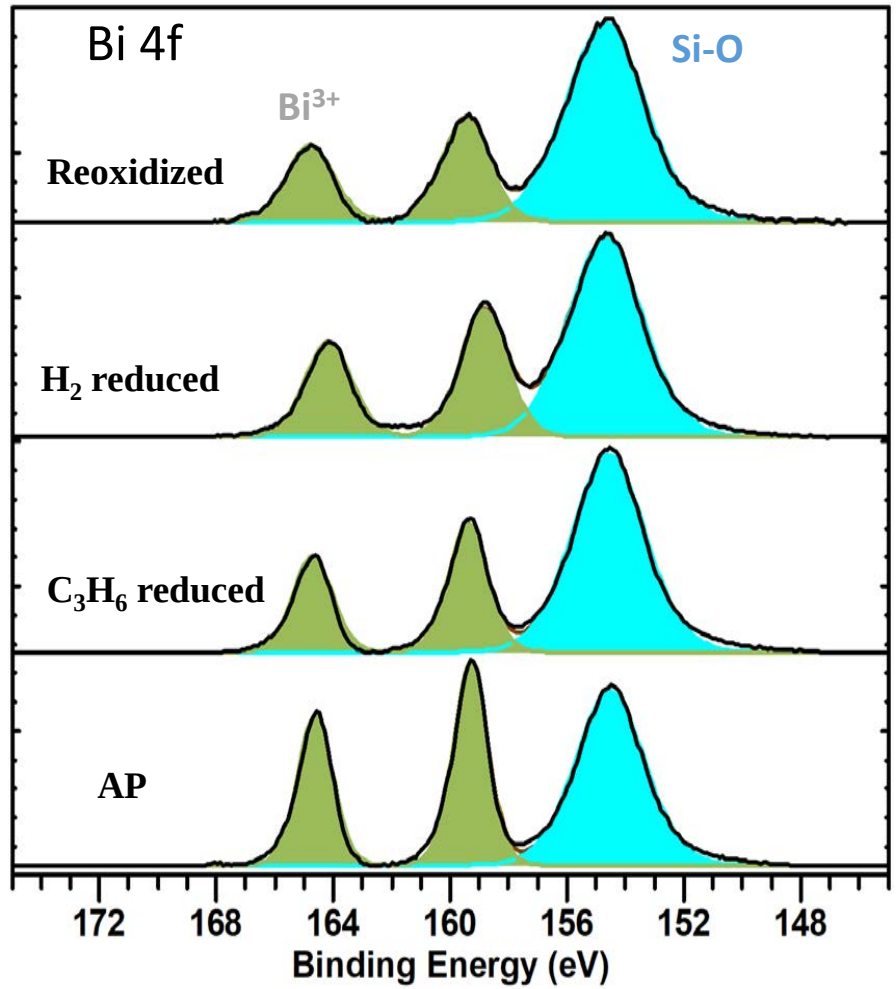

Refs:
https://doi.org/10.1016/j.apsusc.2022.153827
https://doi.org/10.1016/j.nanoen.2018.02.044

Preliminary Results:XPS

$Bi_2Mo_3O_{12}/SiO_2$

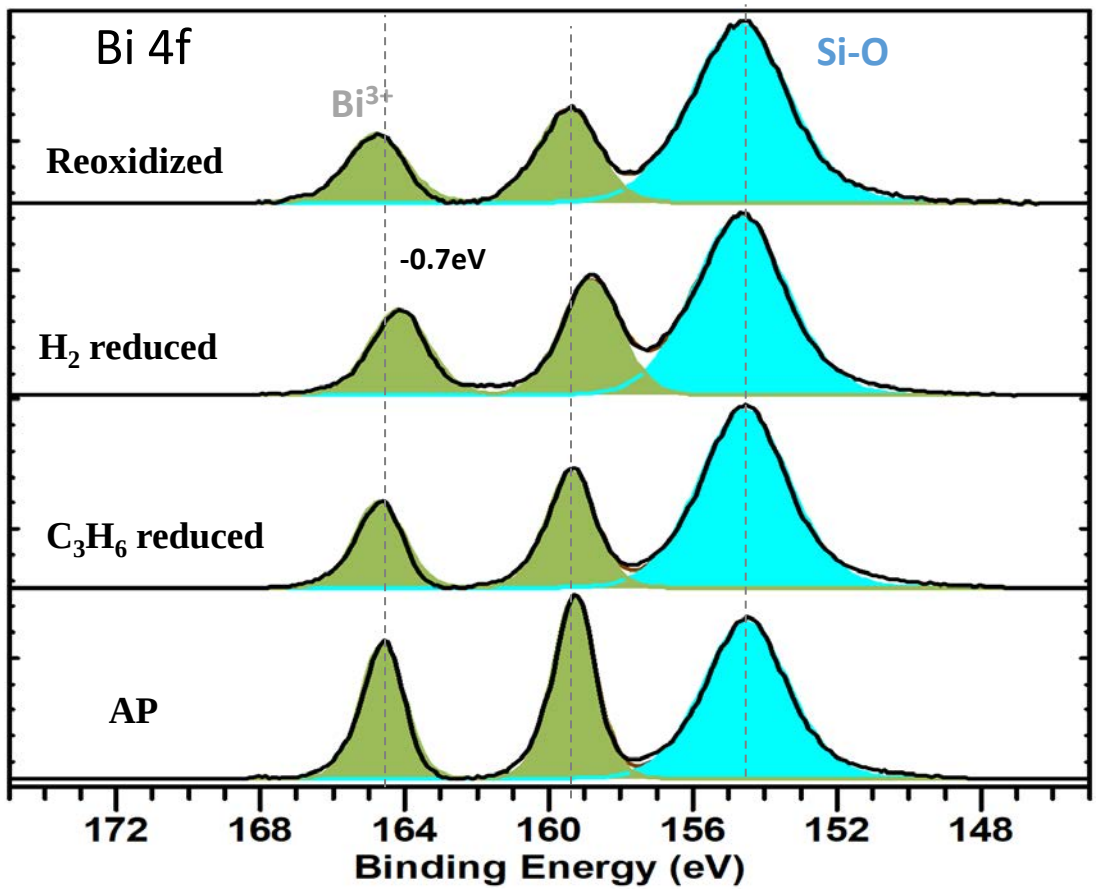

- With reduction Bi peaks shift to higher B.E as a part of electronic effects, while the Mo peaks do not show any shifts
- This B.E shift is interpreted as arising from the change in the chemical state of Bi

Refs:
https://doi.org/10.1016/j.apsusc.2022.153827
https://doi.org/10.1016/j.nanoen.2018.02.044

XPS Results: Metal support Interaction

Oregon State University
College of Engineering

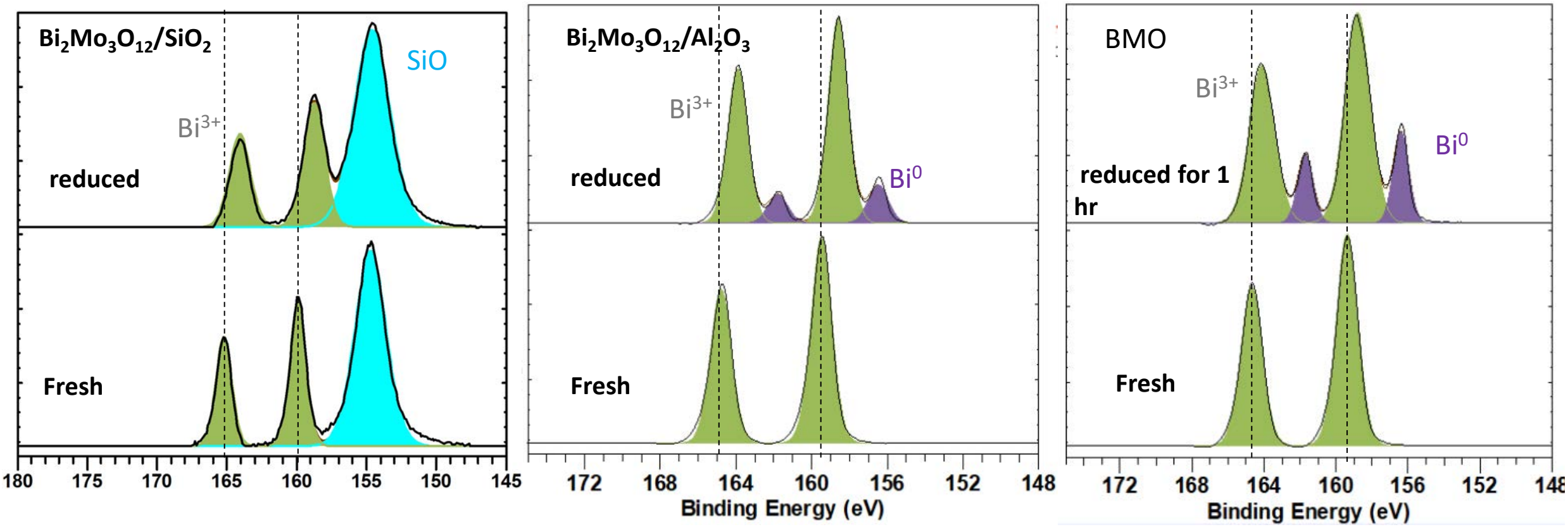

- Al_2O_3 supported samples are more reducible
- Si segregates to the surface due to its higher surface energy, partially blocking the Bi and Mo sites, therefore the catalyst is less reduced
- Unsupported samples are not easily reduced due to dispersion effects

Summary

- XPS is useful for chemical state analysis
- XPS can be quantitative
- XPS is a highly surface sensitive technique
- XPS is useful in combination with other techniques
- In-situ processing and analysis is essential for the study of advanced materials

Useful references

XPS analysis consistent with Au core Ag shell structure

XPS calculated atomic concentrations for Au/Ag nanoparticles

C1s	O1s	Na1s	Ag3d	Au4f	Atomic Ratio
40.3	29.0	4.3	26.1	0.41	0.16

A straightforward method for interpreting XPS data from core–shell nanoparticles

A. G. Shard *Journal of Physical Chemistry* C 2012, 116

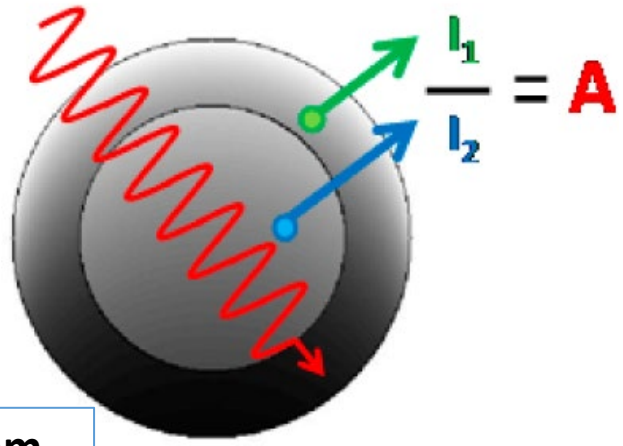

XPS Au/Ag signal ratio equivalent to 11 nm Ag shell on 8 nm Au core (ignoring some contamination)
8 nm + 11 nm = ~19 nm particle

The 20 nm particles with the Au core dissolve more quickly than pure Ag particles

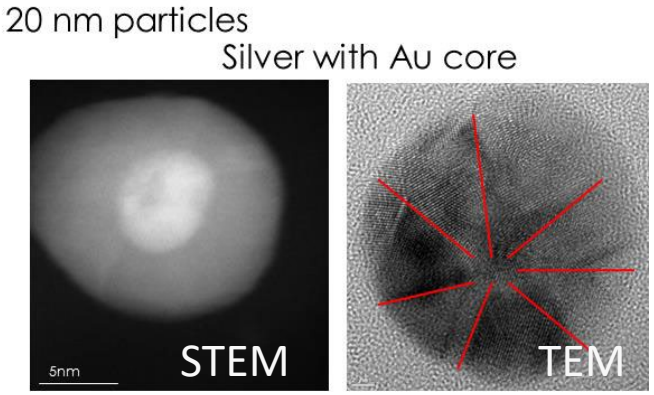

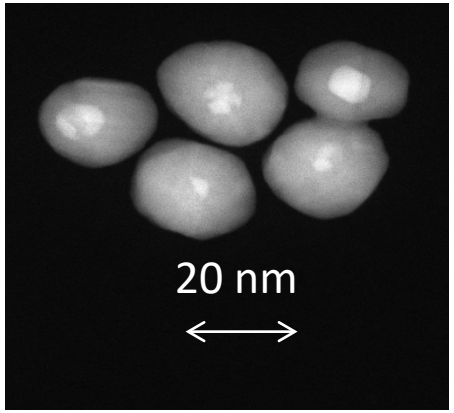

STEM dark field images

Equations used for Overlayer Calculations

Overlayer thickness:

$$d = -\lambda_{C1s,\,C} \cos\theta \ln(1-x/100)$$

x = nominal carbon concentration assuming uniform analysis

$\lambda_{C1s,\,C}$ = effective attenuation length of C1s photoelectrons in adventitious carbon (~3.5nm)

Overlayer corrected signal intensity:

$$I_{x(corr)} = I_{x(meas)} \exp(d/\lambda_{x,C} \cos\theta)$$

$\lambda_{x,C}$ = IMFP of x photoelectron in C overlayer = $0.016(E)^{0.7608}$

Overlayer corrected concentration:

$$\% x = 100 * [(I_{x(corr)}/S_x)/ \Sigma_i(I_{i(corr)}/S_i)]$$

S_x = corrected sensitivity factor element x = $RSF_x\ T(E)\ F_x$

RSFx relative sensitivity factor
T(E) Transmission function

Fx = source angle correction

G. C. Smith, *J. Electron Spectrosc. Relat. Phenom*. 2005, 148, 21.
S. Tanuma, C. J. Powell,D. R. Penn, *Surf. Interface Anal*. 1993, 21, 165.

Characterization of Nanoparticles

Measurement Processes for Nanoparticles

Micro and Nano Technologies

2020, Pages 295-347

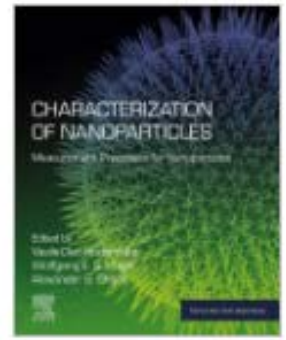

Chapter 4.2 - Preparation of nanoparticles for surface analysis

Donald R. Baer [a], David J.H. Cant [b], David G. Castner [c d], Giacomo Ceccone [e], Mark H. Engelhard [a], Ajay S. Karakoti [f g], Anja Müller [h]

Importance of sample preparation on reliable surface characterisation of nano-objects: ISO standard 20579-4

Donald R. Baer, Ajay S. Karakoti, Charles A. Clifford, Caterina Minelli, Wolfgang E. S. Unger

First published: 04 July 2018 | https://doi.org/10.1002/sia.6490 | Citations: 13

Pacific Northwest
NATIONAL LABORATORY

X-Ray Photoelectron Spectroscopy (XPS)

Part 3: Instrumentation

June 26, 2023

Vaithiyalingam Shutthanandan

Ajay Karakoti

Theva Thevuthasan

U.S. DEPARTMENT OF ENERGY BATTELLE

PNNL is operated by Battelle for the U.S. Department of Energy

Instrumentation Components

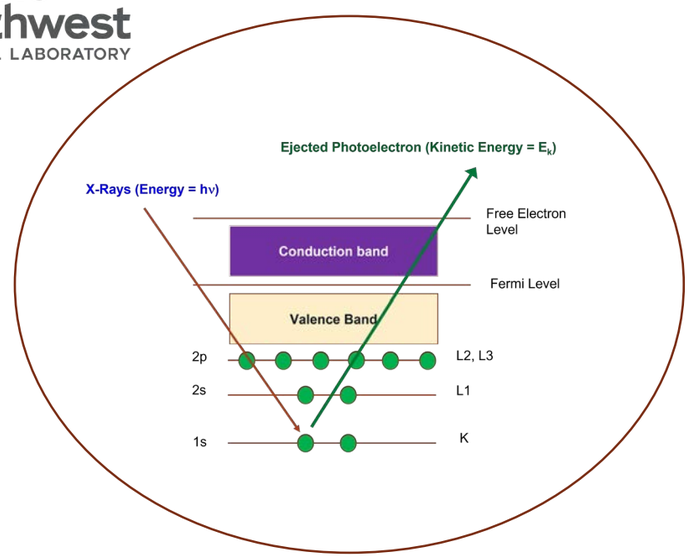

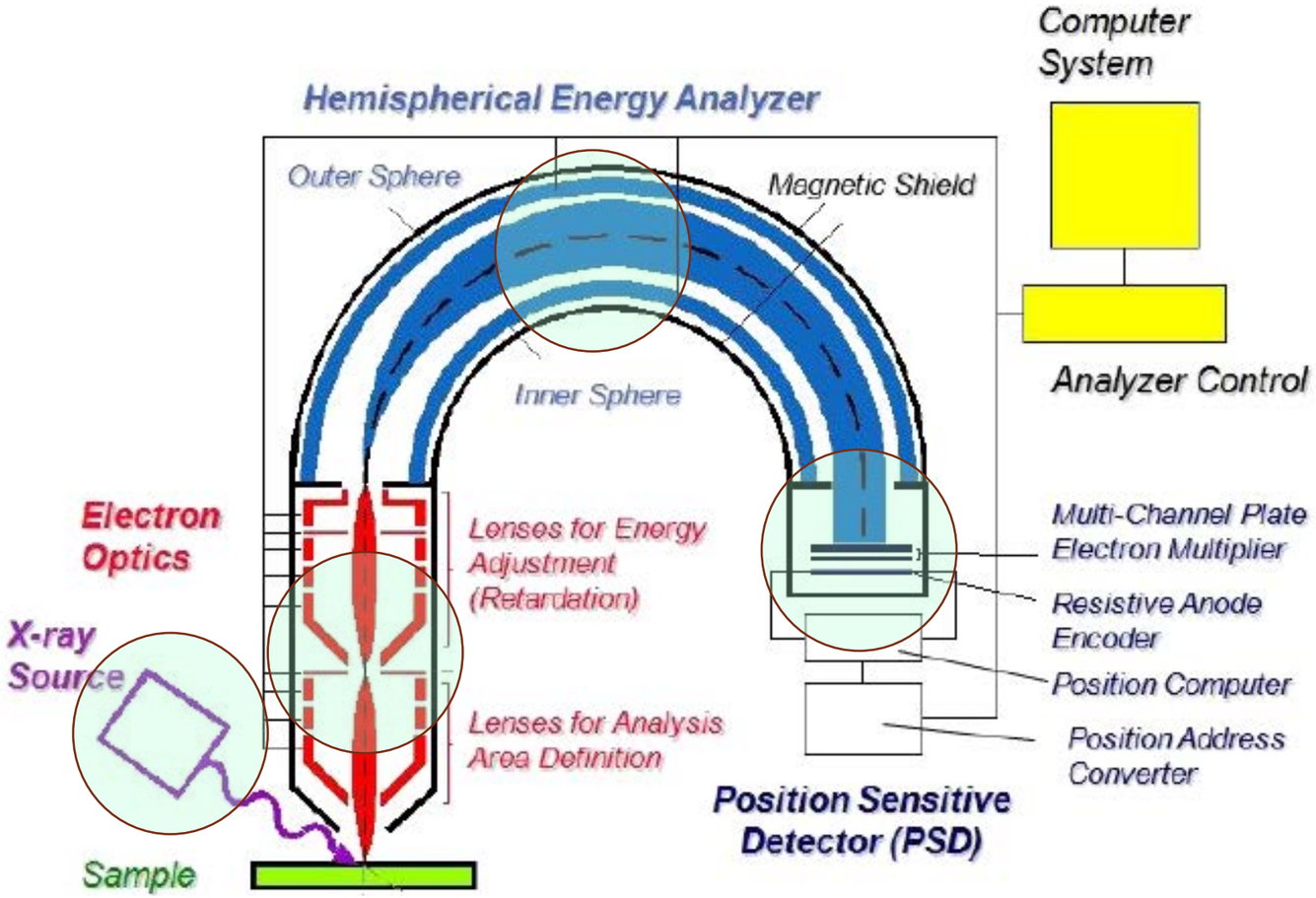

- Vacuum System
- X-Ray Gun
- Transfer of Electrons (Electron Optics)
- Energy Analyzing (Hemi Spherical analyzer)
- Electron Counting (Multi-Channel Plate)
- Computer System
- Insulating Samples (charge compensation)

Why Ultra High Vacuum (UHV) Needed?

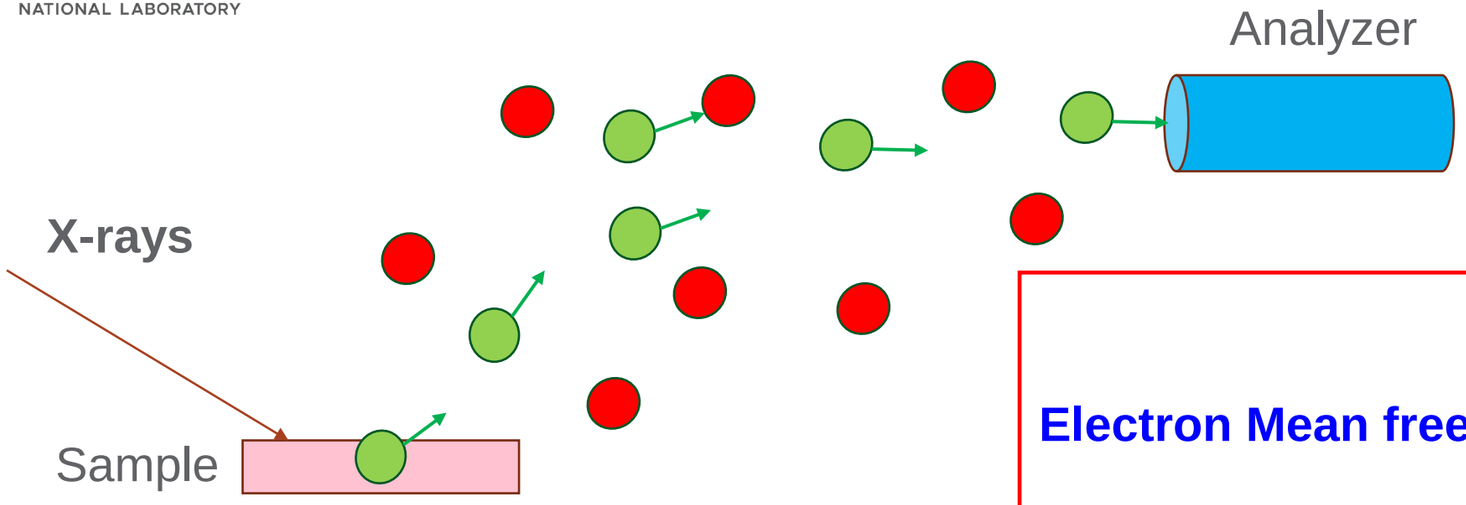

Electron Mean free path = $\lambda = \frac{kT}{\sqrt{2}\sigma p}$

atmosphere	→	0.1 μm
10^3 mbar	→	0.1 μm
100 mbar	→	0.1 mm
10^{-6} mbar	→	100 m
10^{-9} mbar	→	100 km

UHV Needed!

Need powerful Pumps!

Another advantage of UHV is ➡ Avoid Surface Contamination during the analysis

What Contribute to Peak Width of Photoelectron Peak?

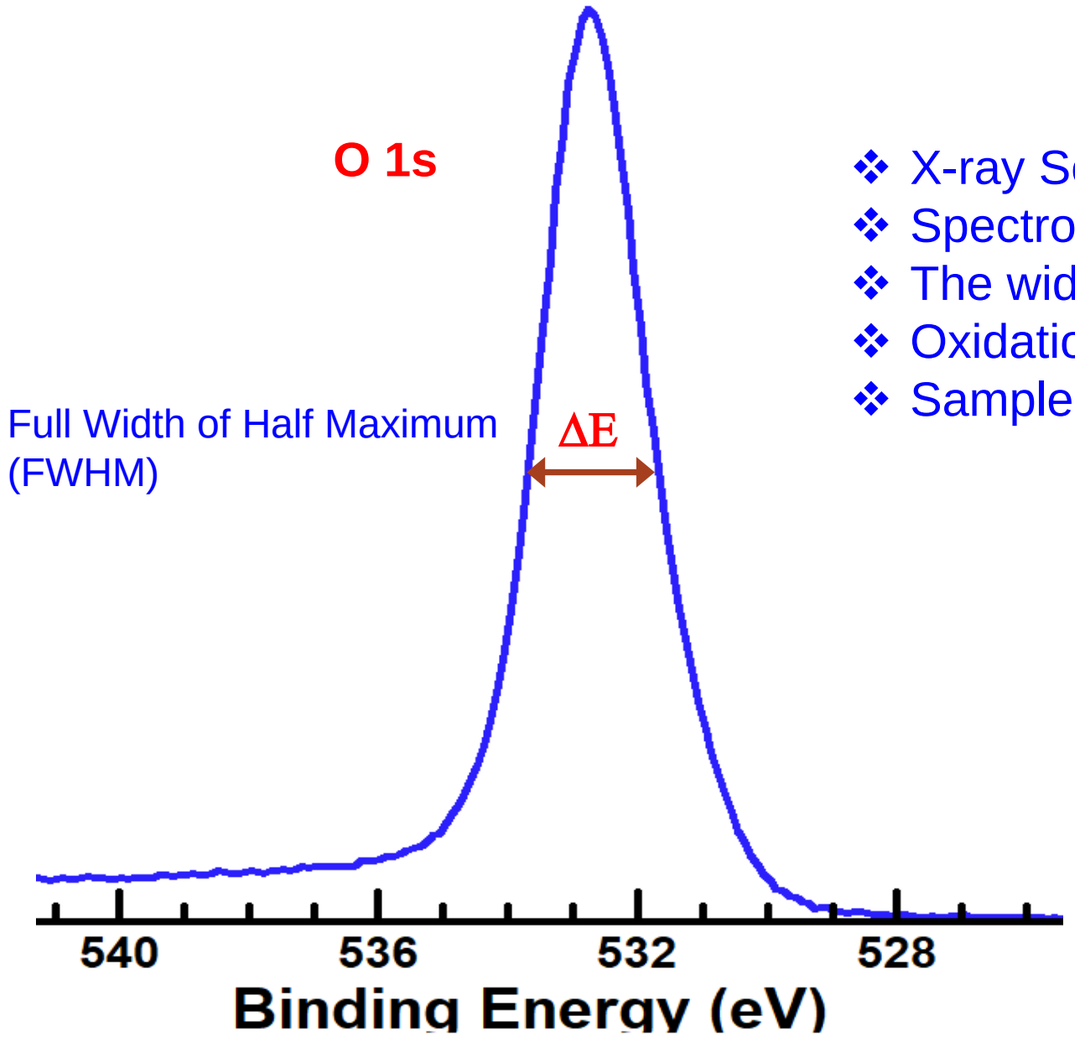

- X-ray Source width
- Spectrometer/electron detection system resolution (Pass energy)
- The width of the photoelectron line
- Oxidation states
- Sample charging

X-Ray Sources

Pacific Northwest NATIONAL LABORATORY

Characteristic X-rays

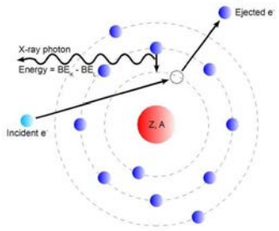

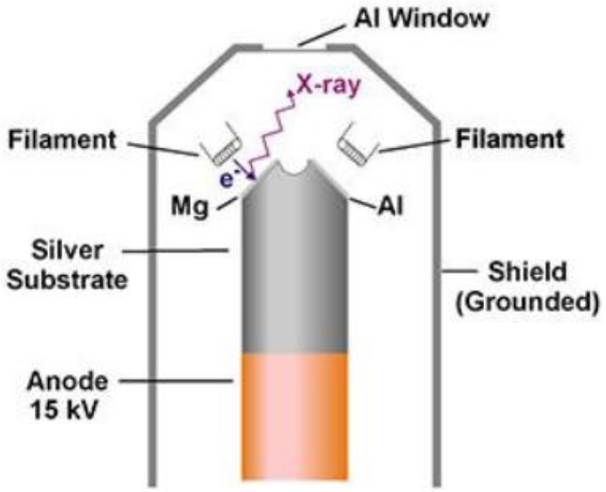

Energy and line widths of available anode materials.

Anode	Radiation	Photon Energy (eV)	Line Width (eV)
Mg	Kα	1253.6	0.7
Al	Kα	1486.6	0.85
Zr	Lα	2042.4	1.6
Ag	Lα	2984.3	2.6
Ti	Kα	4510.9	2.0
Cr	Kα	5417	2.1

Monochromater

Can be reduced to 0.16 eV

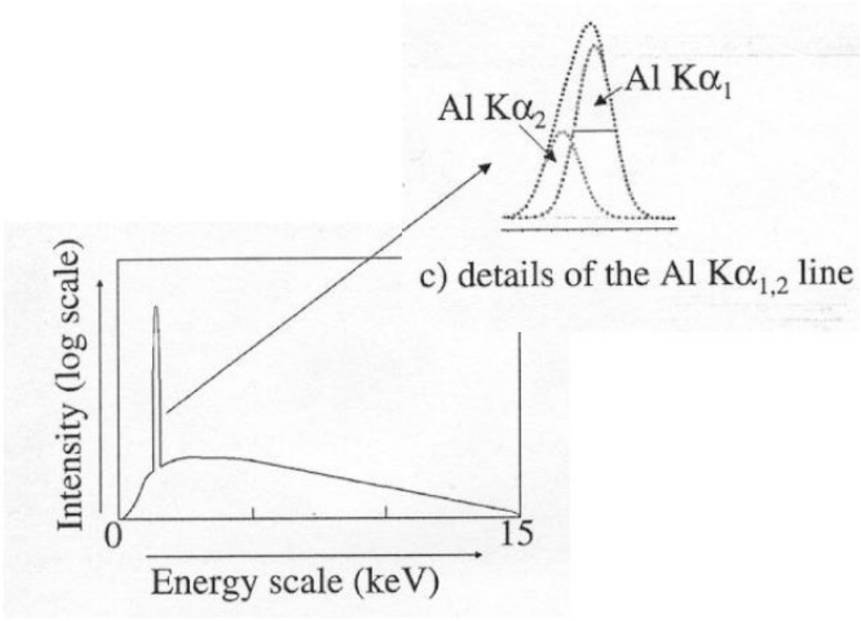

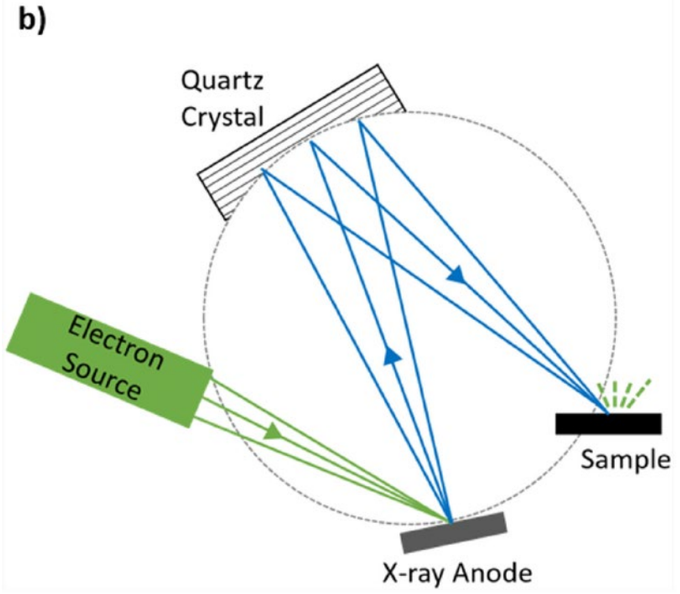

$$2d(\text{Å})\sin(\theta) = n\lambda(\text{Å})$$

Courtesy of thermo scientific XPS

Area of Analysis

1. Small spot X-rays

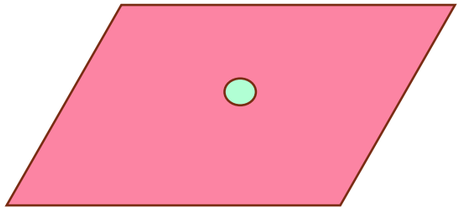

X-ray Beam size can change from 10 μm to 400 μm

2. Large spot X-rays

➡ Electron collection area is defined by the aperture in the column

Slot (300 μm x 700 μm)

- Largest collection area
- High count rates
- Poor Energy resolution

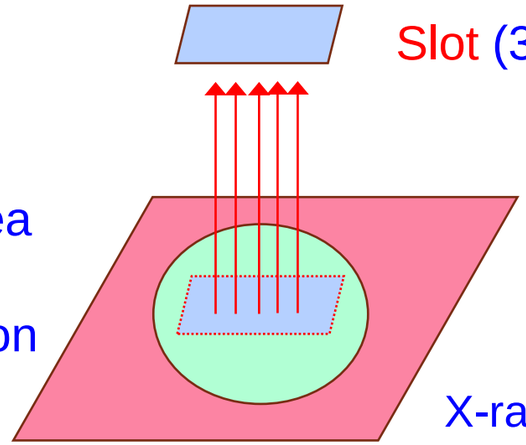

X-ray Beam size ~ 1 mm

Small spot Aperture: 110 μm
: 55 μm
: 27 μm
: 15 μm

- Smallest collection area
- Low count rates
- Good Energy resolution

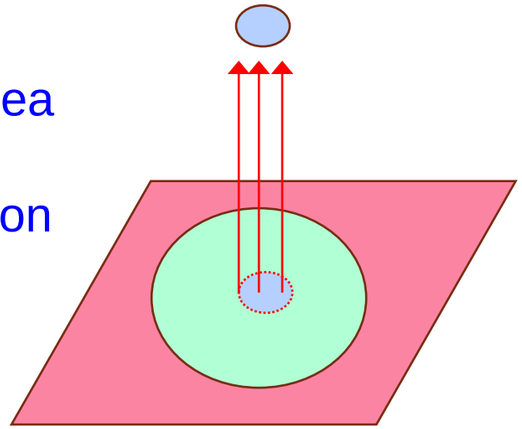

Energy Analyzer: Hemispherical Analyzer

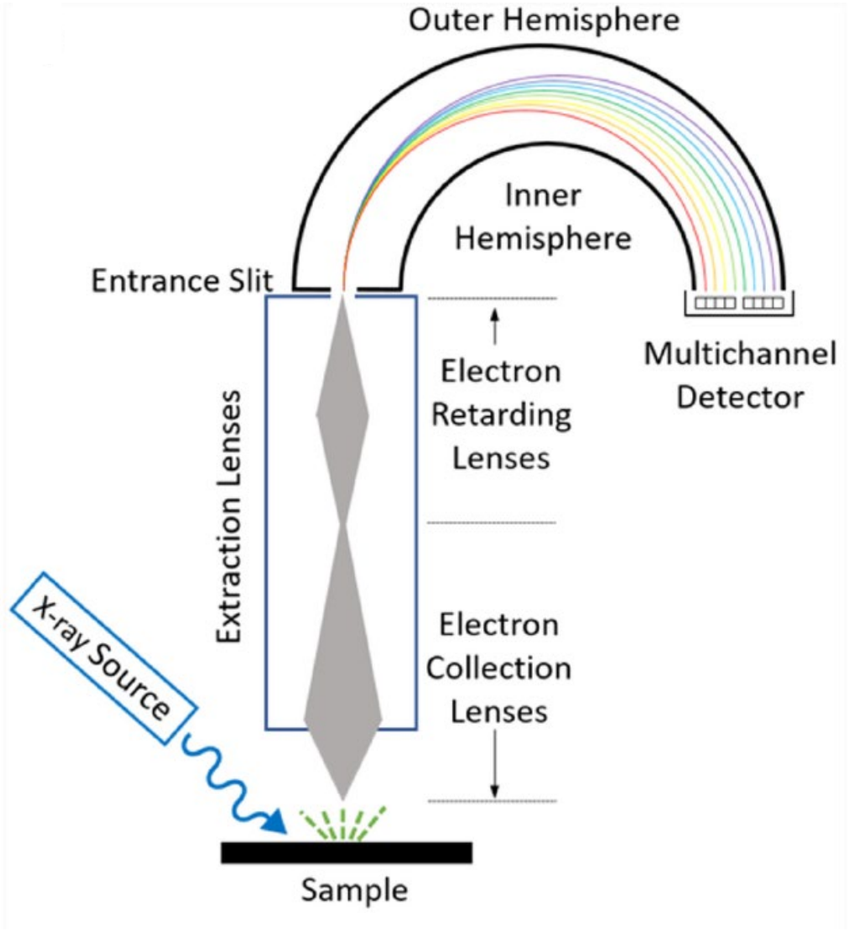

- Only electrons with a specified energy will be able to travel through the analyzer.
- The voltages on the hemispheres can be adjusted to allow electrons of different energies to pass through the analyzer.

J. Vac. Sci. Technol. A 38(6) Nov/Dec 2020; doi: 10.1116/6.0000412 Published under license by AVS.

Energy Analyzer: Pass Energy

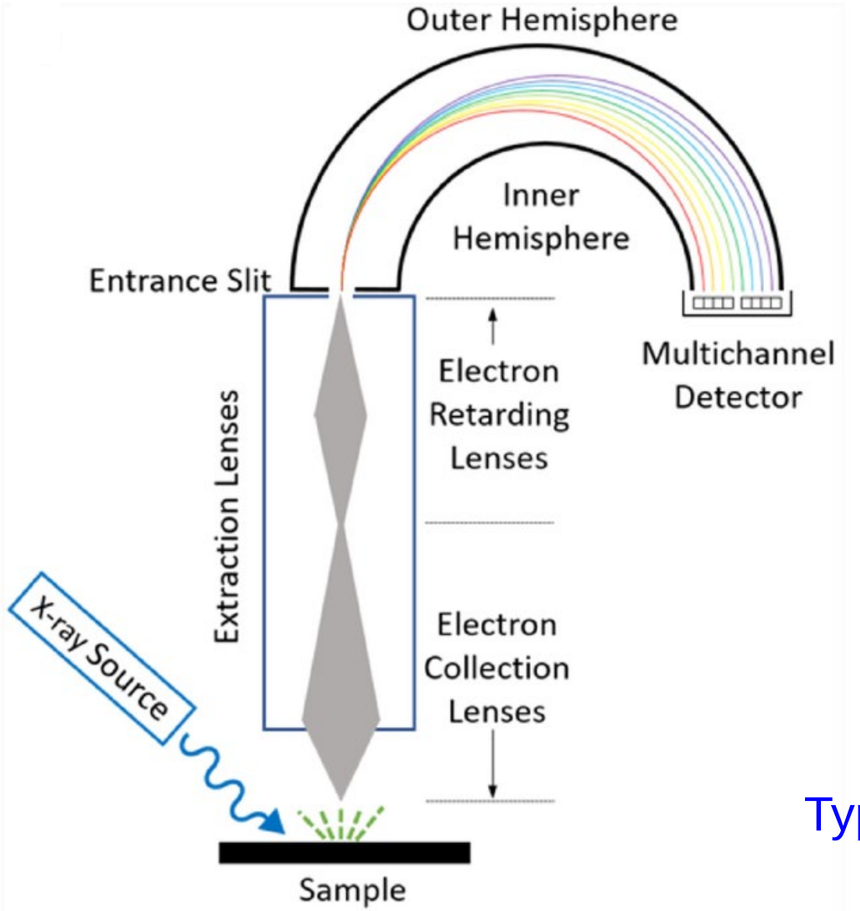

- Energy resolution in XPS is limited by the energy of the electrons being detected, with better energy resolution achieved at lower electron energies.

Pass Energy: **Energy of the electrons entering the analyzer is retarded by user define energy**

- The pass energy affects both electron throughput and resolution.

Large Pass Energy: Lower resolution but higher count rates
Small Pass Energy: Higher resolution but lower count rates

Typical Pass energy for Survey scans = **160 to 200 eV**

Typical Pass Energy for high resolution scans = **20 to 50 eV**

J. Vac. Sci. Technol. A 38(6) Nov/Dec 2020; doi: 10.1116/6.0000412 Published under license by AVS.

Energy Analyzer: Pass Energy

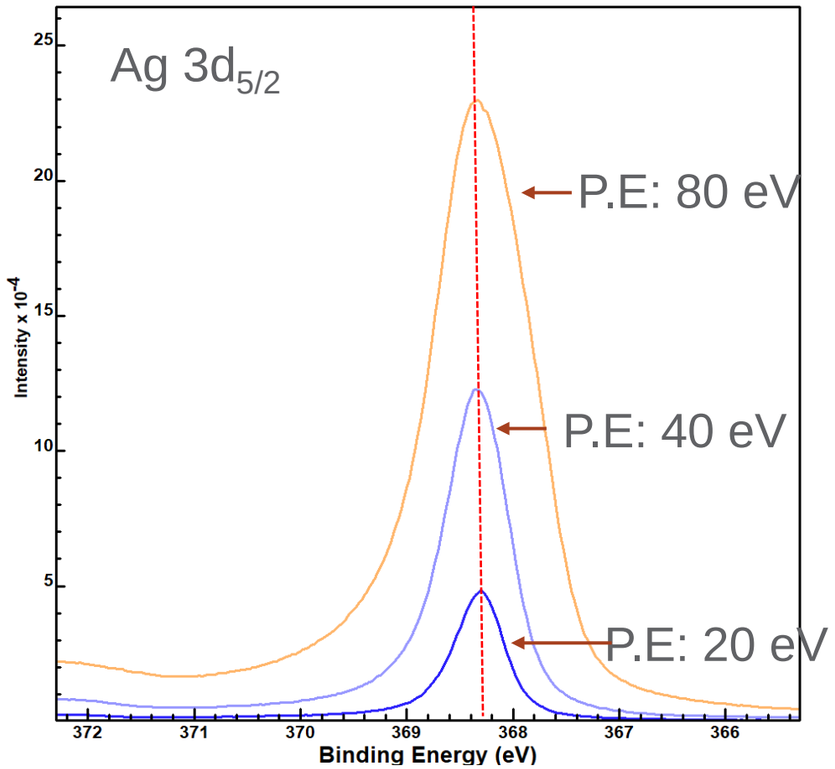

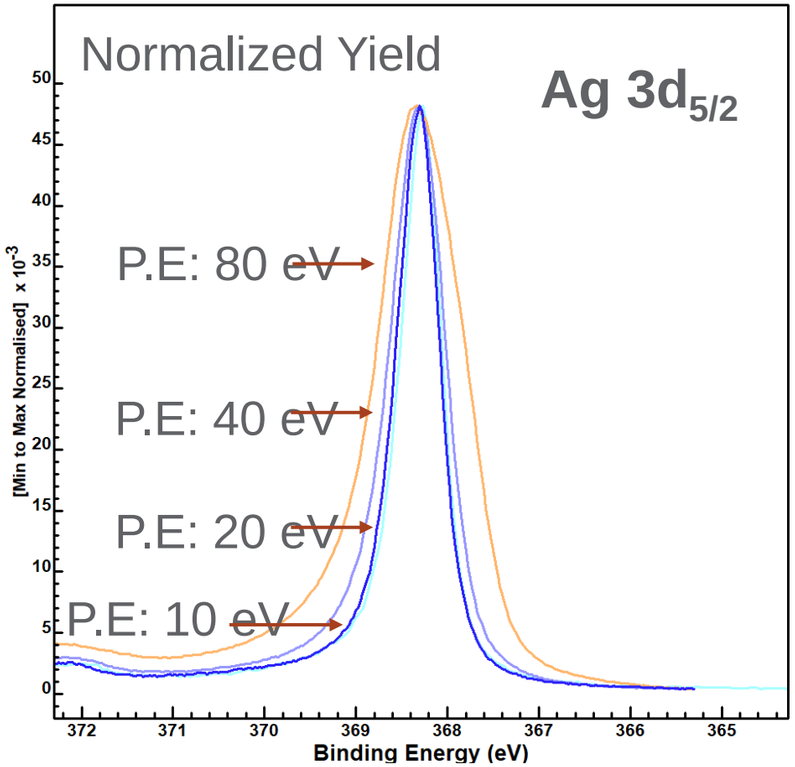

Large Pass Energy: Lower resolution but higher count rates
Small Pass Energy: Higher resolution but lower count rates

J. Vac. Sci. Technol. A 38(6) Nov/Dec 2020; doi: 10.1116/6.0000412 Published under license by AVS.

Energy Analyzer: Electron Multipliers

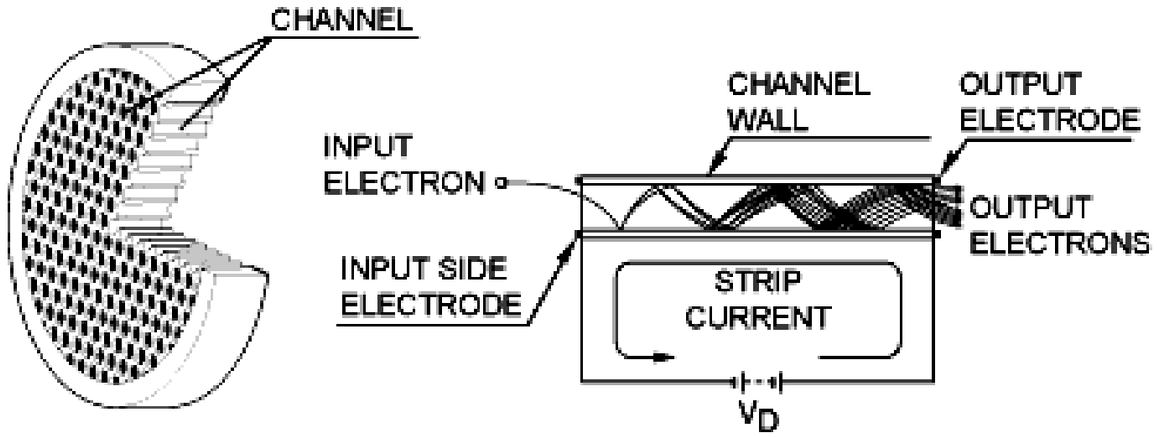

Input ➡ Single electron

Output ➡ ~ 10^6 electrons

Spectroscopy

Low energy resolution wide scan

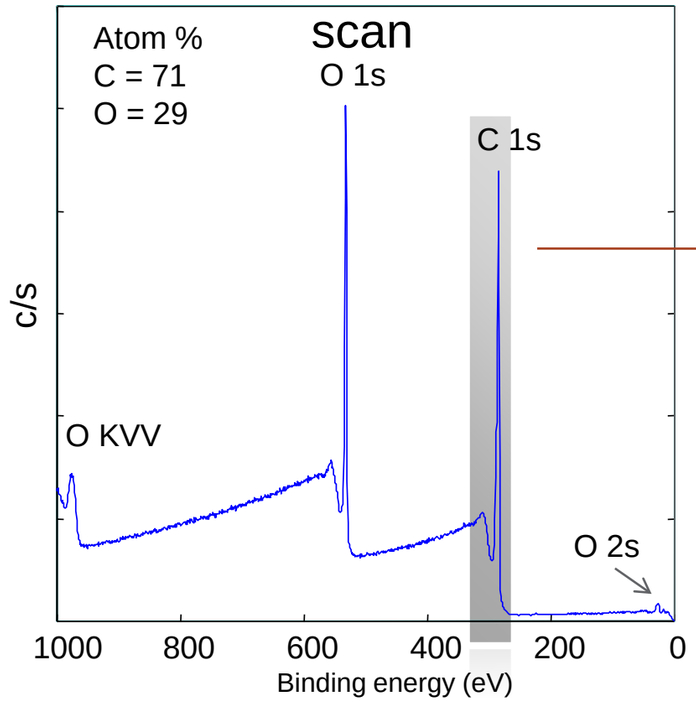

Quantitative elemental information

High energy resolution narrow scan

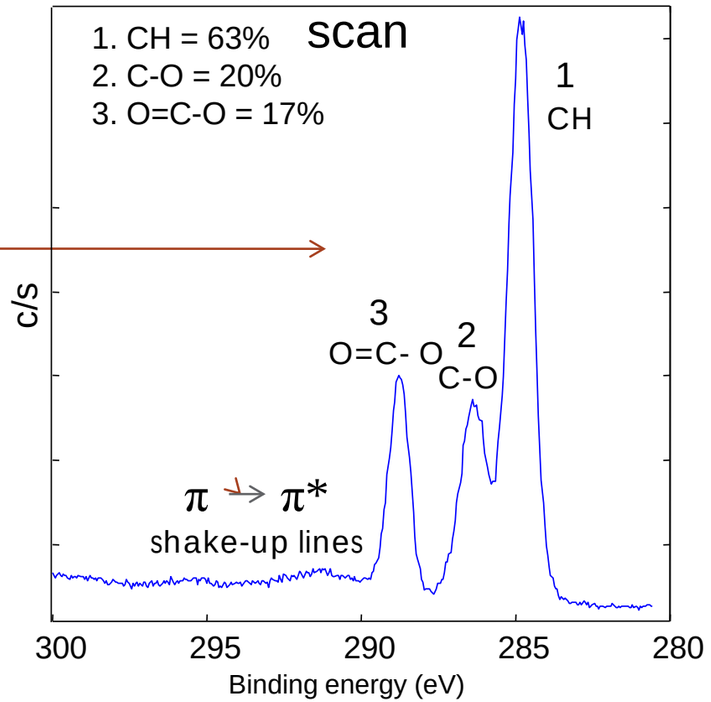

Chemical state information

Mark Engelhard

Imaging XPS

Moving sample stage

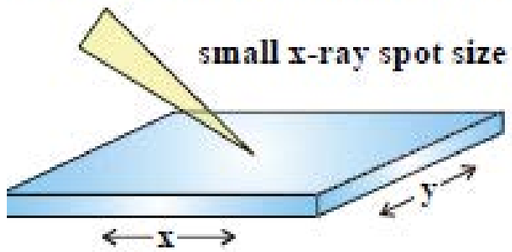

Image: XY position versus Photoelectron Intensity

Resolution: 10 μm

Use of multichannel plate

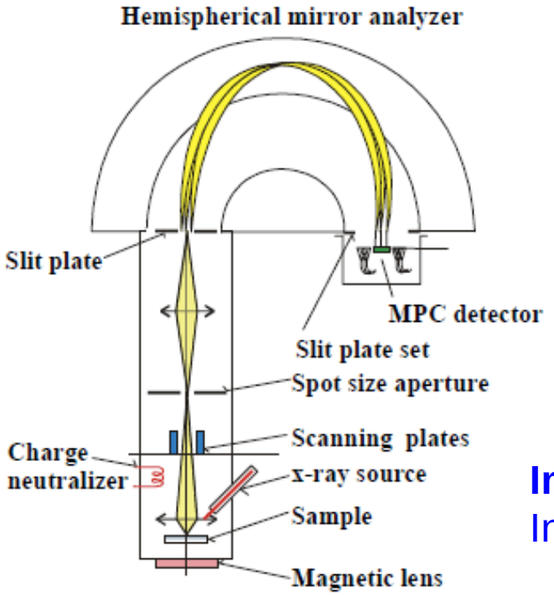

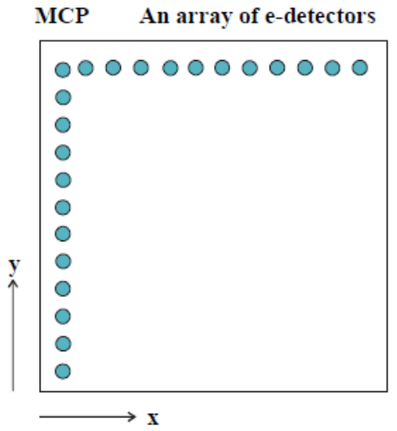

Image: XY position of MCP versus Photoelectron Intensity

Resolution: 3 μm

Imaging XPS

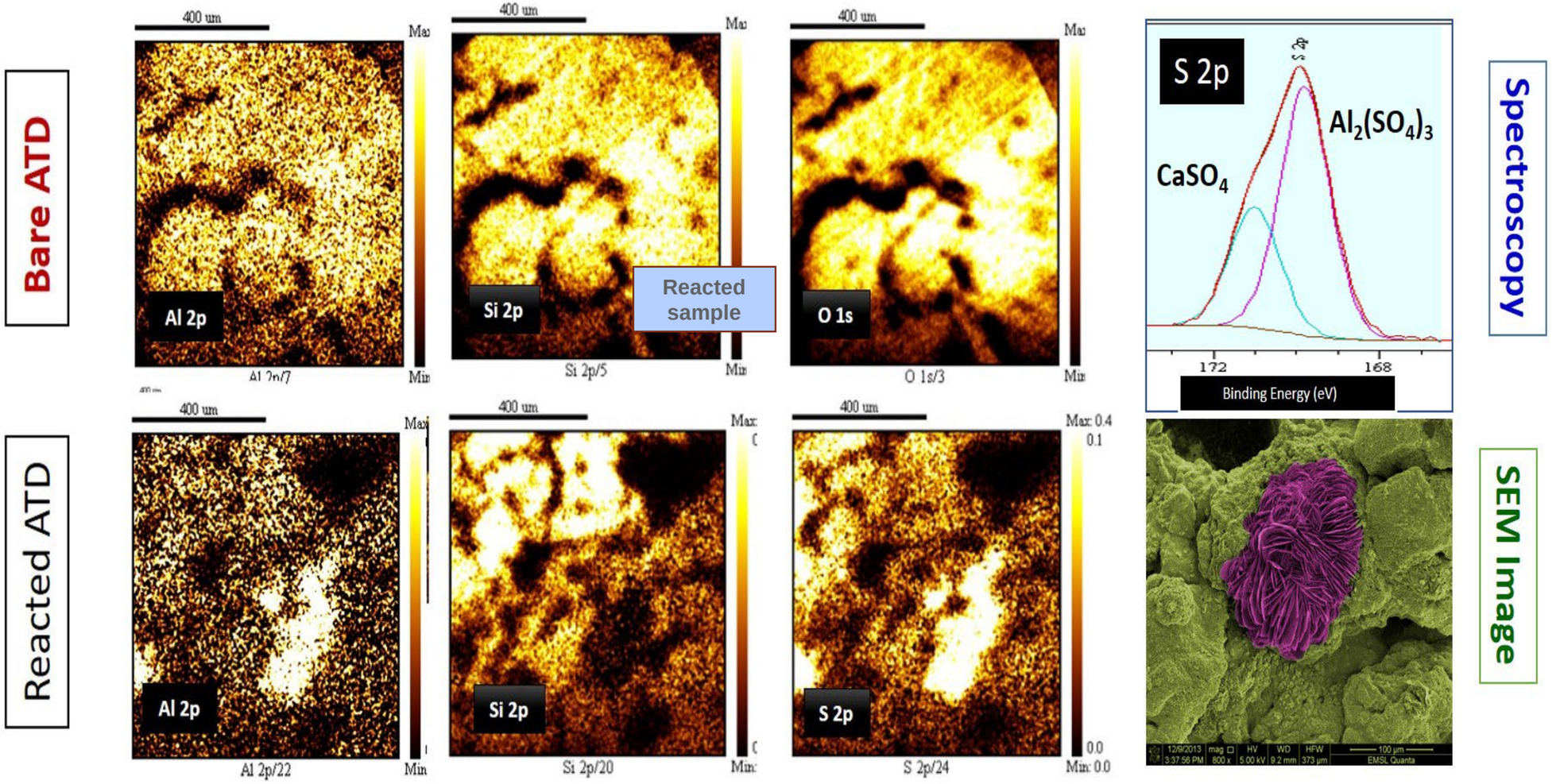

- Al is segregating to certain places
- Sulfur is mainly concentrated where Aluminum content is high
- Al, S rich regions are comparable to “flower” like crystals observed in SEM images

High Energy XPS using Ag source

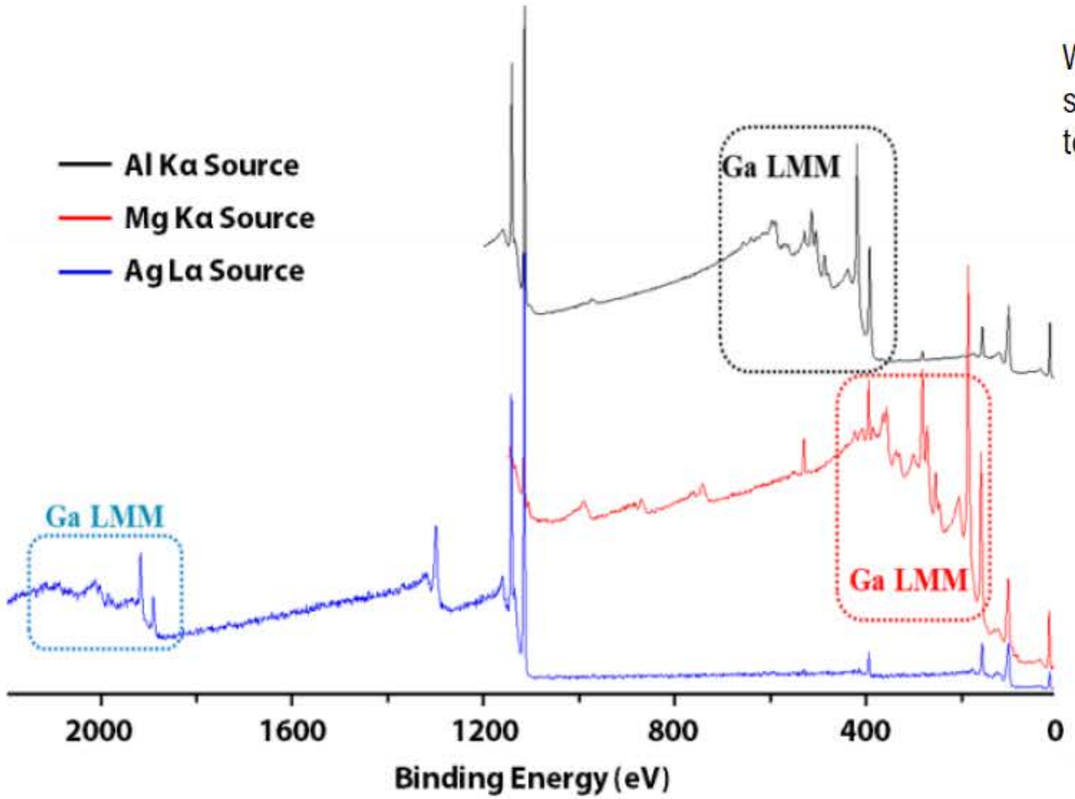

Survey spectra of GaN using monochromatic Al Kα (black)/Ag Lα (blue) and achromatic Mg Kα (red).

When the high energy Ag Lα excitation source is used, the Ga LMM auger series is separated from the N 1s region. This allows the chemical state analysis of nitrogen to be determined as well as accurate sample quantification

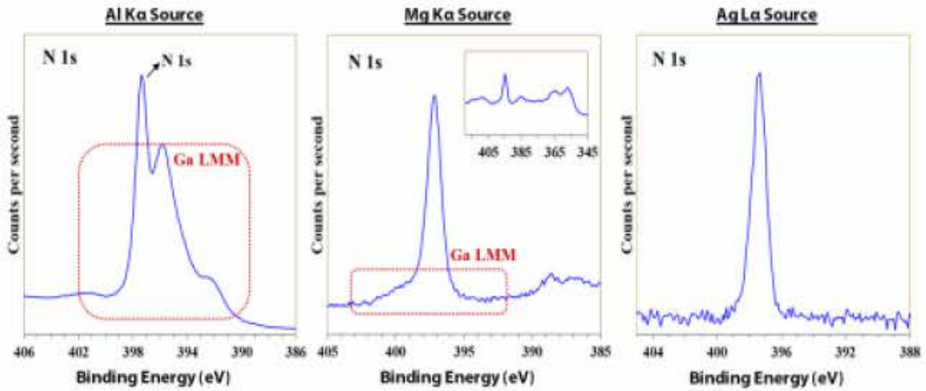

N 1s spectra acquired with monochromatic Al Kα, achromatic Mg Kα and monochromatic Ag Lα X-ray sources.

Auger peaks were shifted hence overlap between core level and Auger peaks were avoided

Courtesy of KRATOS ANALYTICAL A SHIMADZU GROUP COMPANY

XPS spectrometer #1 : Physical Electronics Quantera Scanning X-ray Microprobe

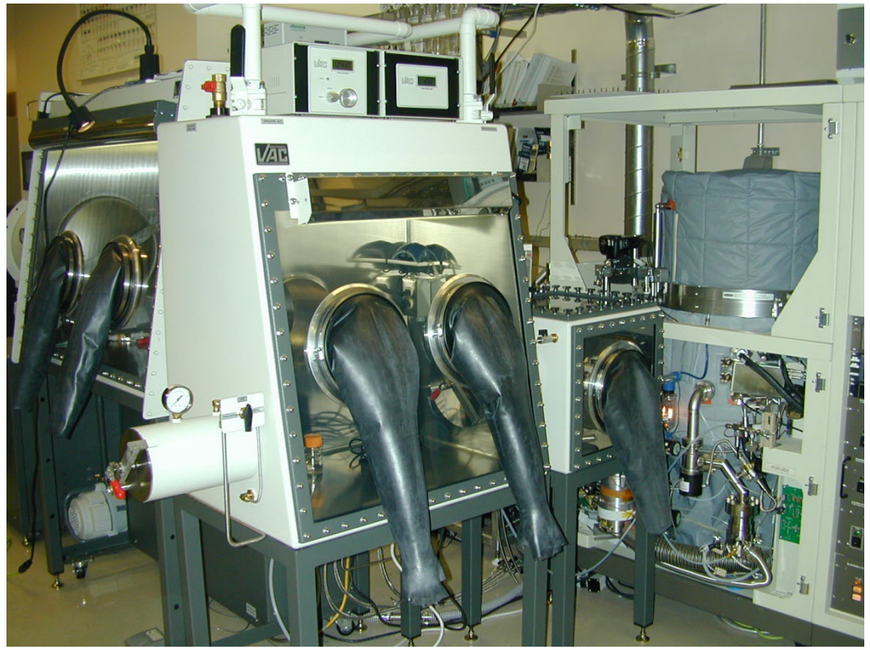

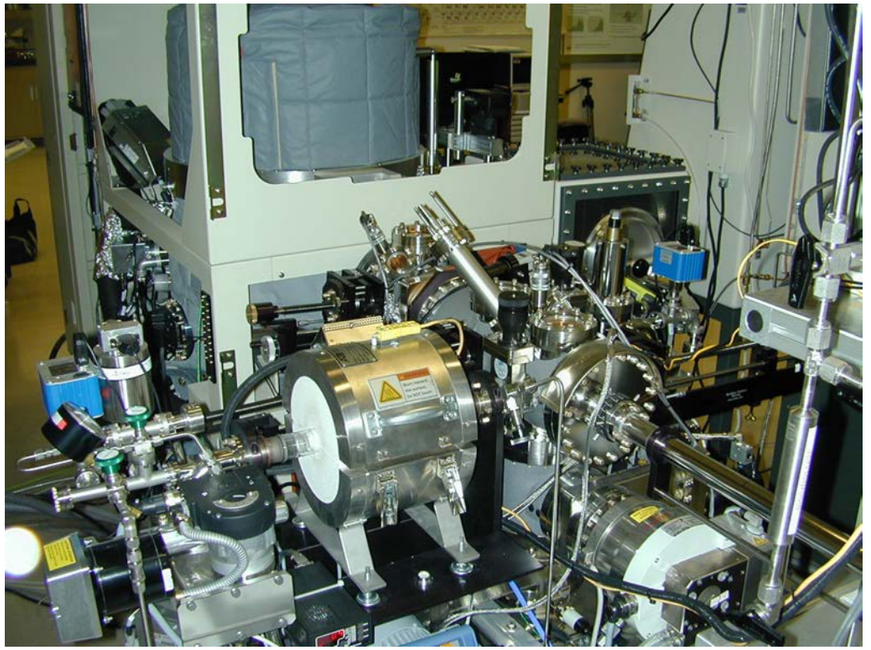

Spectrometer is equipped with inert atmosphere glove box systems for in-situ processing

- Attached recirculated glove box for sample processing
- Custom attached glove boxes for sample mounting and transfer

Two processing side chambers

- High pressure reactor with heat to 1,000ºC
- Low pressure-controlled tube furnace with sample heating up to 1,000ºC
- Gas exposure capabilities include: H_2, O_2, N_2, CO, NO/He, and He
- Controlled liquid vapor exposures
- Pfeiffer OMNI star gas analysis system

XPS spectrometer # 2: Ultra DLD Kratos XPS Multi Model system

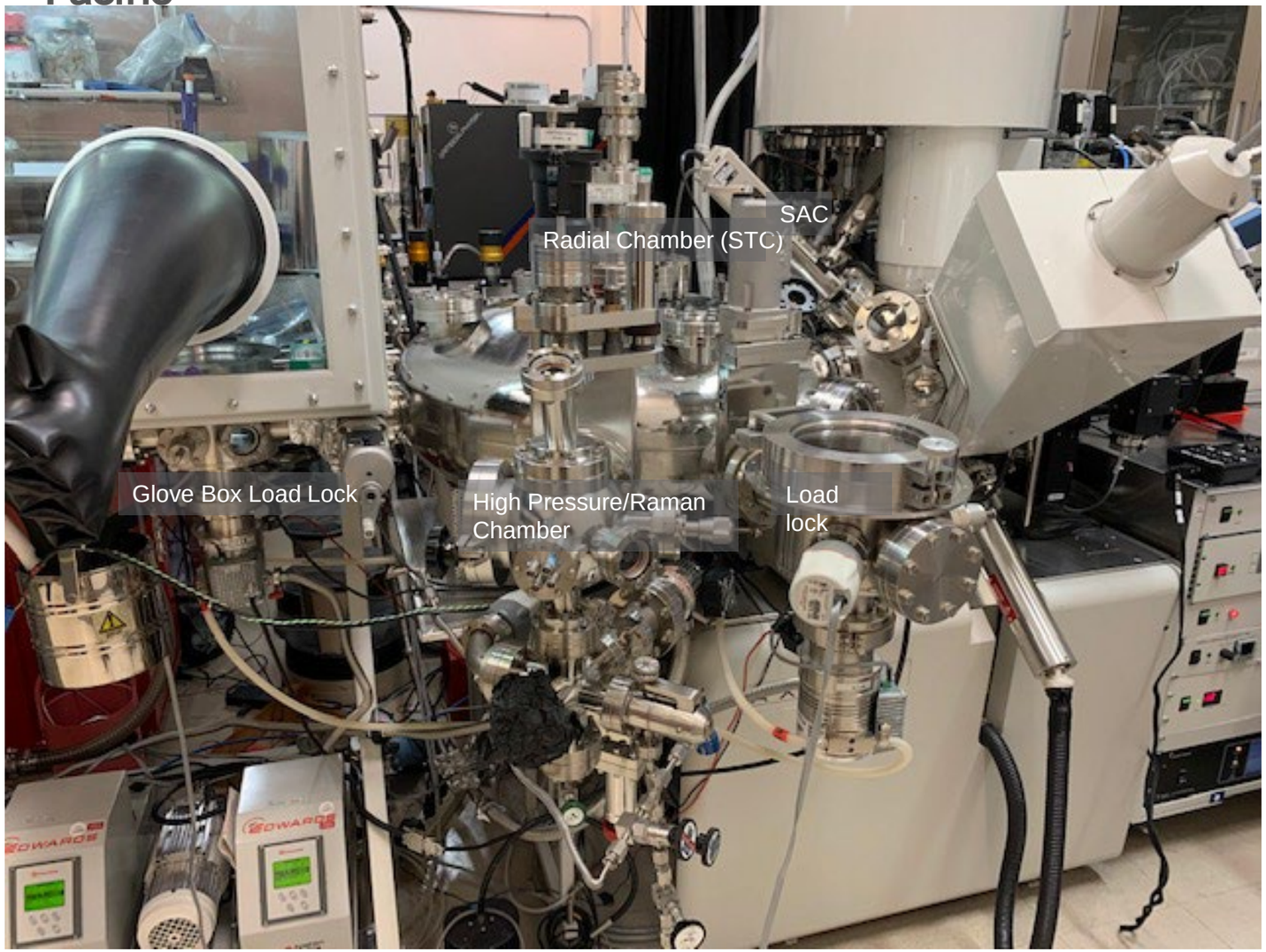

XPS spectrometer # 2: Ultra DLD Kratos XPS Multi Model system

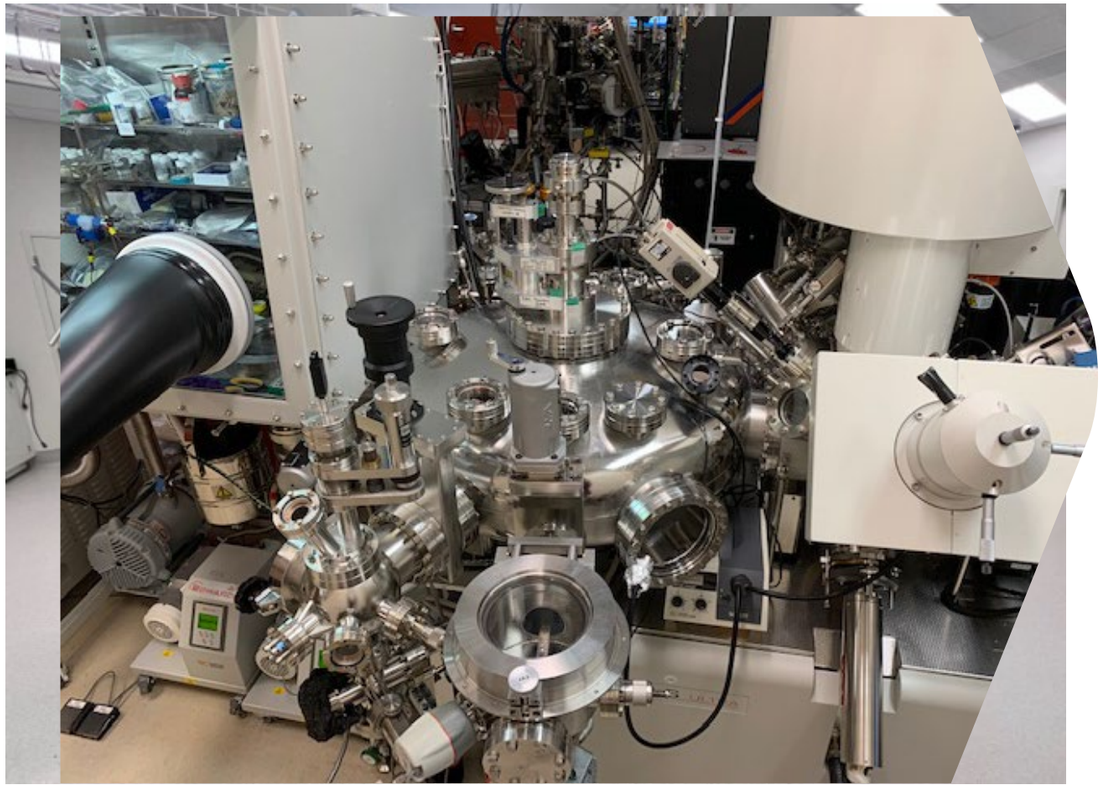

- High-sensitivity XPS system with monochromatic Al Kα and Ag Lα X-rays (for high z elements)
- Dedicated detectors for spectroscopy and parallel imaging with energy resolution of 0.48eV and spatial resolution of ~ 3µm
- Attached inert atmosphere glove box systems for air sensitive samples
- *In situ* Ar ion gun for depth profile measurements
- Samples can be maintained at liquid nitrogen temperature during analysis (volatile samples)
- In-situ Thermal desorption spectroscopy (TDS) & Ultraviolet Photoelectron Spectroscopy (UPS)
- Attached High-pressure and operando Raman Spectroscopy
- Dedicated leak valves for *in situ* gas exposure measurements
- Special transfer load lock for transporting samples easily between XPS and ion soft-landing systems

Pacific Northwest
NATIONAL LABORATORY

Thank you

Pacific Northwest
NATIONAL LABORATORY

X-Ray Photoelectron Spectroscopy (XPS)

Part 4: Quantitative XPS Analysis and Introduction to XPS Peak fitting

July 10, 2023

Vaithiyalingam Shutthanandan

Ajay Karakoti

Theva Thevuthasan

U.S. DEPARTMENT OF ENERGY BATTELLE

PNNL is operated by Battelle for the U.S. Department of Energy

What Information can be Obtained from X-ray Photoelectron Spectroscopy (XPS)?

- Elements identification: can detect **Li to U**
- Quantitative (Compositional analysis)
- Chemical state identification
- Depth analysis (z)
  - Sputter depth profiling (Destructive)
  - Inert gas ions
  - C_{60} ions
  - Ar cluster ions
- Angle dependent depth profiling: Angle resolved XPS (Non-destructive)

Pre-requisites for Accurate Data Analysis and Interpretation

1. Instrument is calibrated
2. During the data collection, charge neutralization is optimized
3. Correct background subtraction has been used
4. Correct peak shape is identified
5. During the data analysis, correct charge correction method is used

Pre-requisites for Accurate Data Analysis and Interpretation

1. Instrument is calibrated

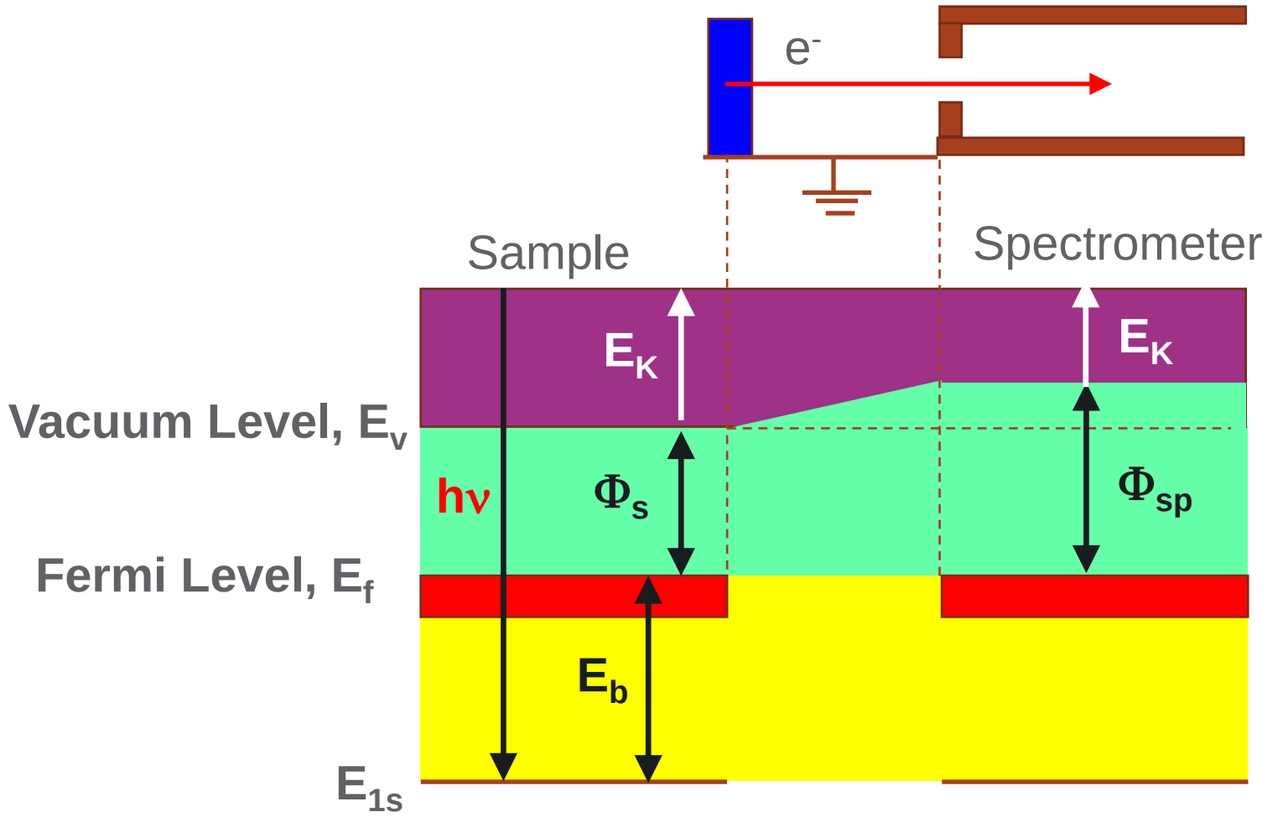

$$E_b = h\nu - E_\kappa - \Phi_{sp}$$

Au $4f_{7/2}$ at 83.96 eV

Ag $3d_{5/2}$ at 368.2 eV

Cu $2p_{3/2}$ at 932.62 eV

Analyzing Insulating Sample

2. During the data collection, **charge neutralization** is optimized

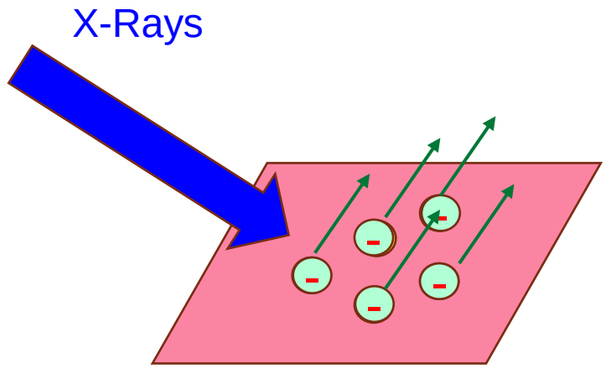

Insulating Sample

(oxides, polymers…….)

Charging → Shift the peak in higher Binding energy side

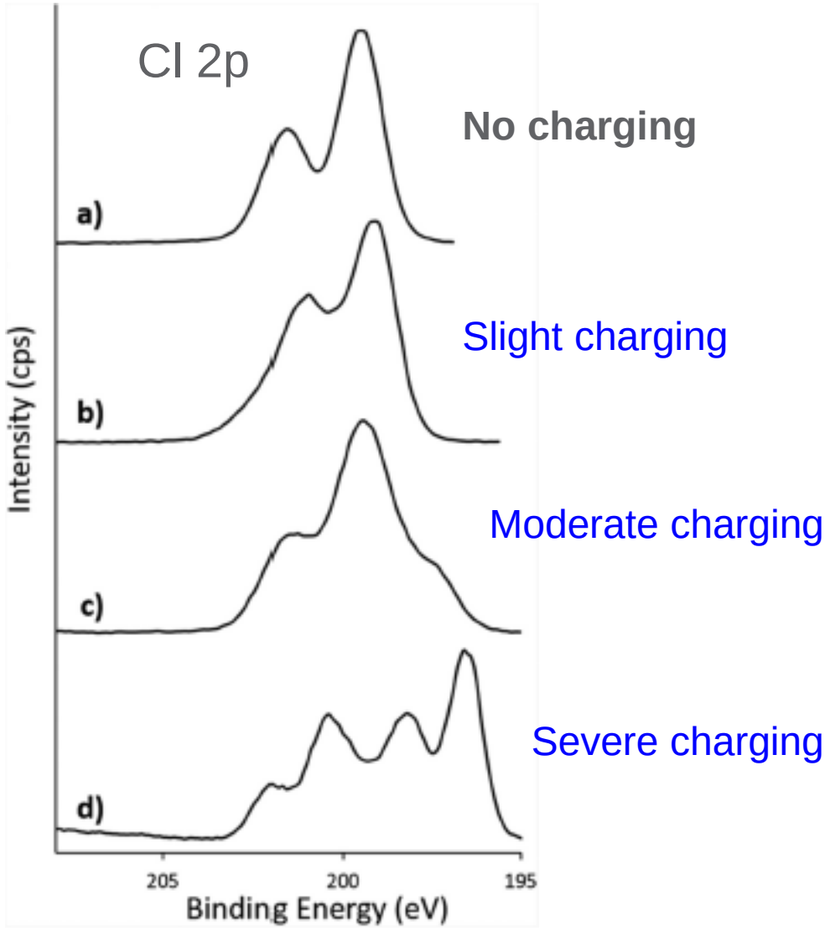

Analyzing Insulating Sample

2. During the data collection, **charge neutralization** is optimized

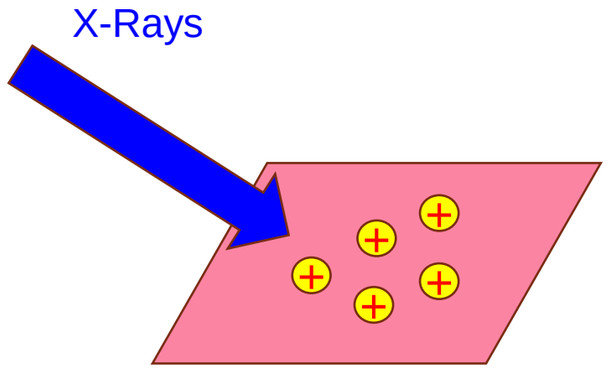

Insulating Sample

(oxides, polymers…….)

Charging → Shift the peak in higher Binding energy side

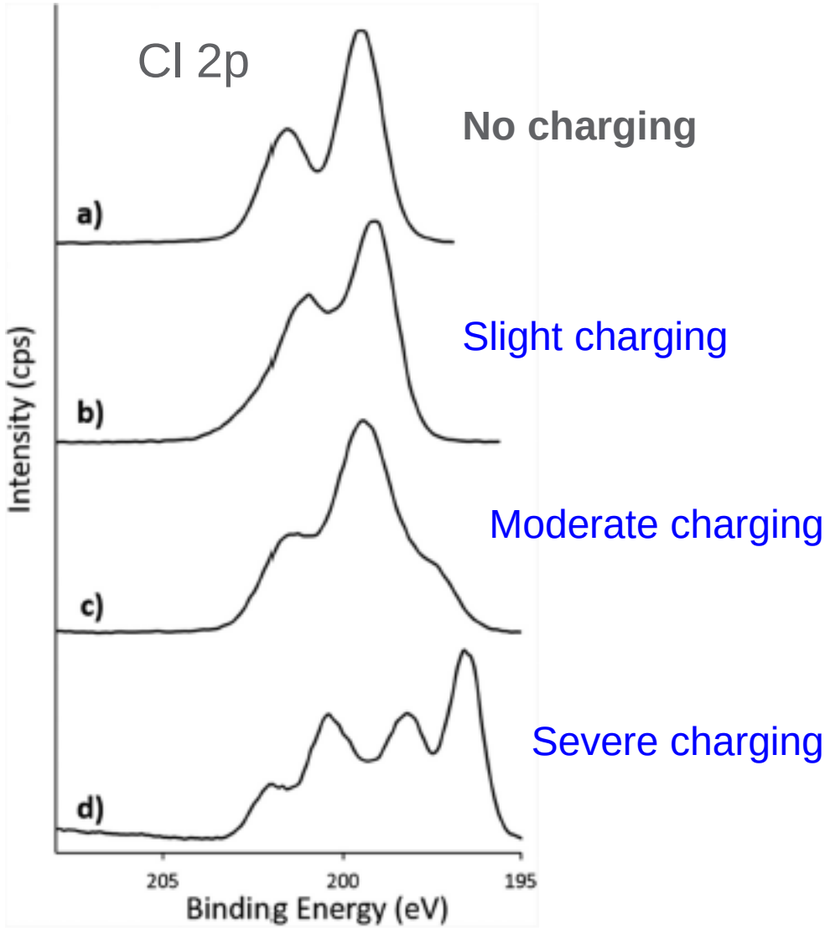

Charge Compensation

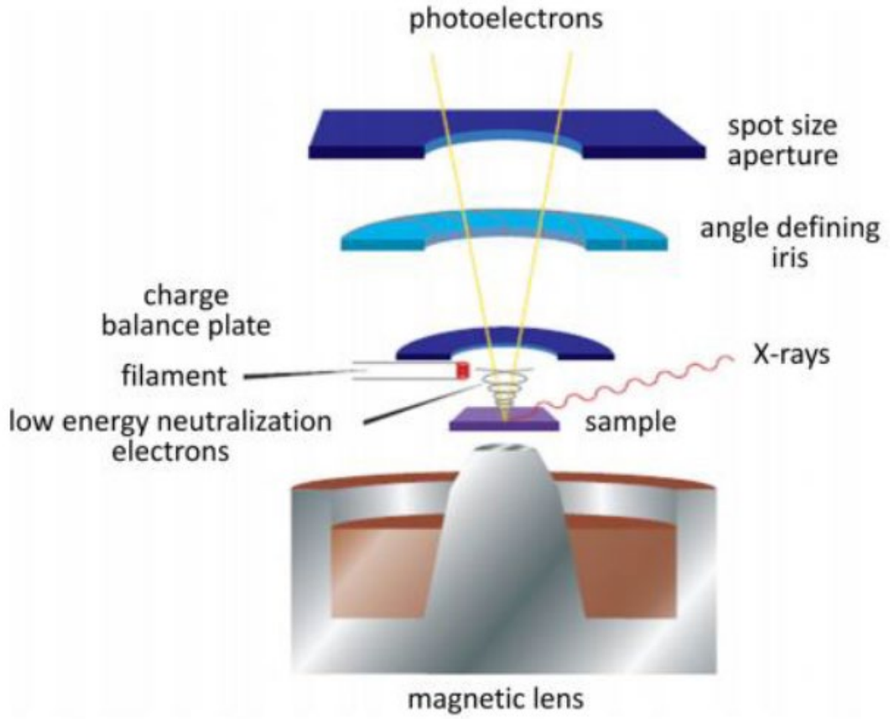

FIG. 4. Schematic diagram showing the charge neutralizer assembly, relative to the magnetic and electrostatic lenses of the Kratos AXIS spectrometer.

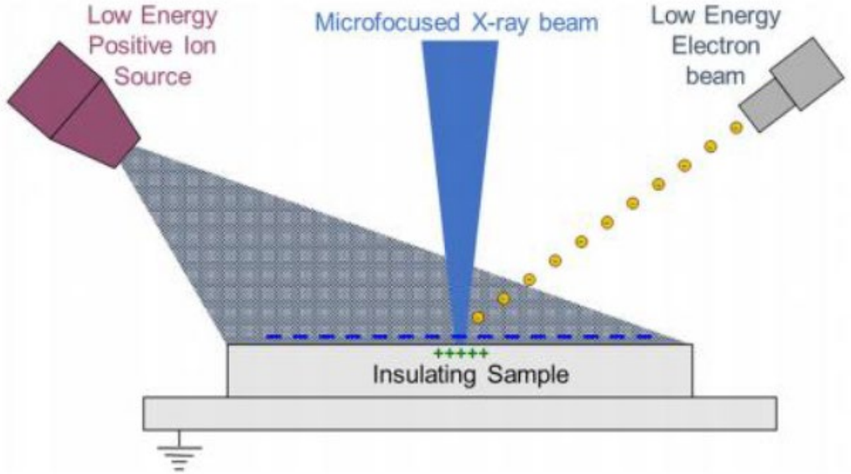

FIG. 5. Schematic drawing of PHI's dual beam charge neutralization method that uses a low-energy electron beam to neutralize the charge created by the x-ray source simultaneously with a low-energy ion beam to eliminate electrostatic charges on the sample surface.

- Even with the proper use of a charge neutralizer, peak shifts are usually observed,
- To correct the energy scale, we need some sort of internal standard with a known energy binding energy

J. Vac. Sci. Technol. A 38(3) May/Jun 2020; doi: 10.1116/6.0000057

Charge Compensation

❖ During the data collection, **charge neutralization** is optimized

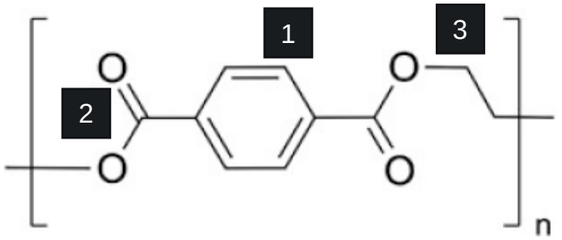

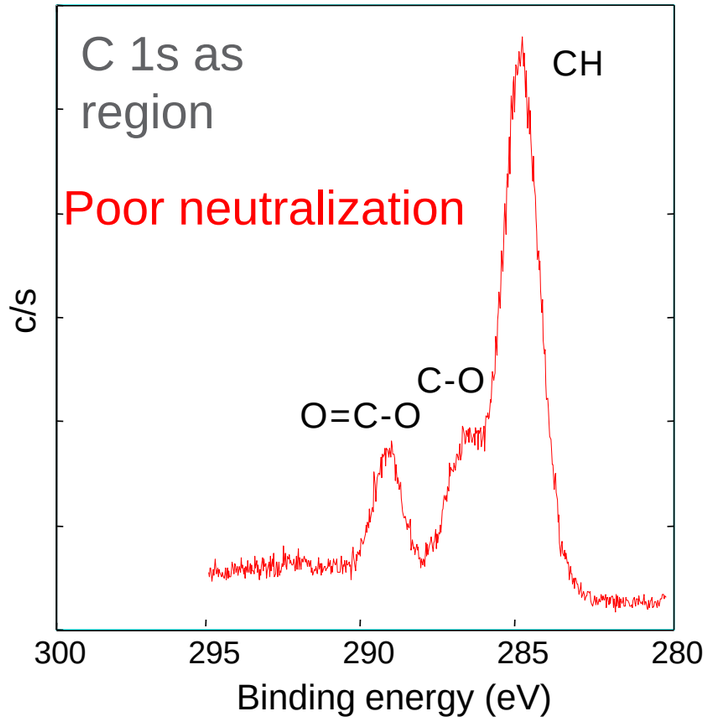

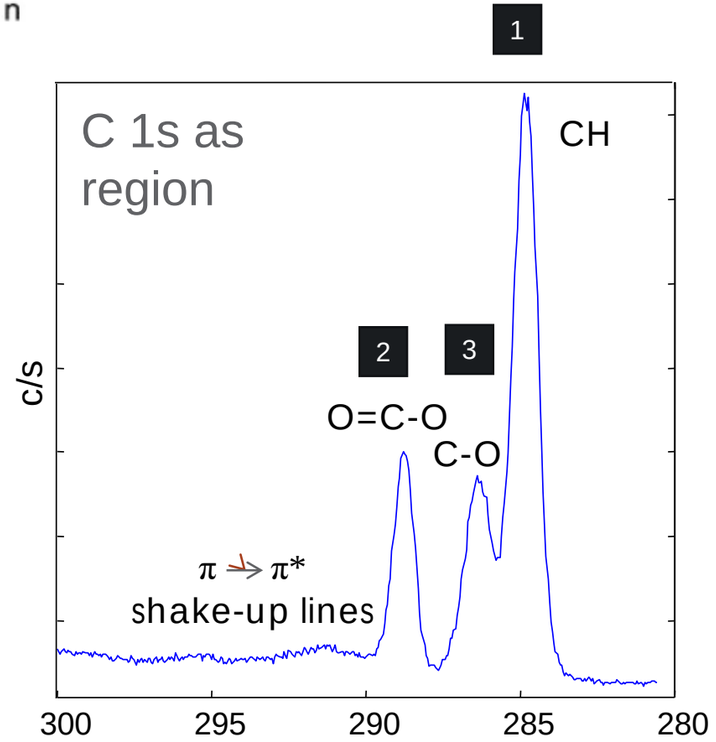

Pre-requisites for Accurate Data Analysis and Interpretation

3. Correct **background subtraction** has been used

Linear

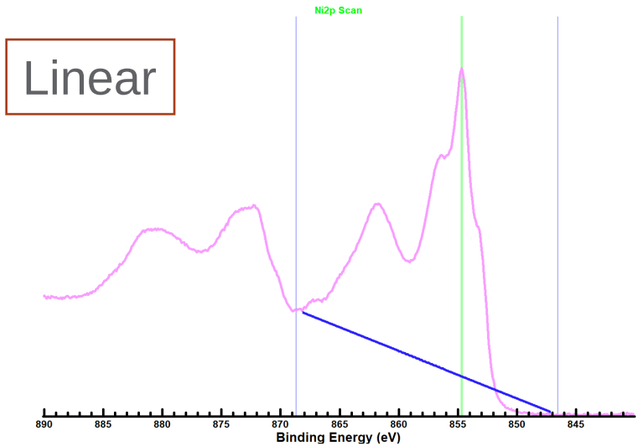

Shirley

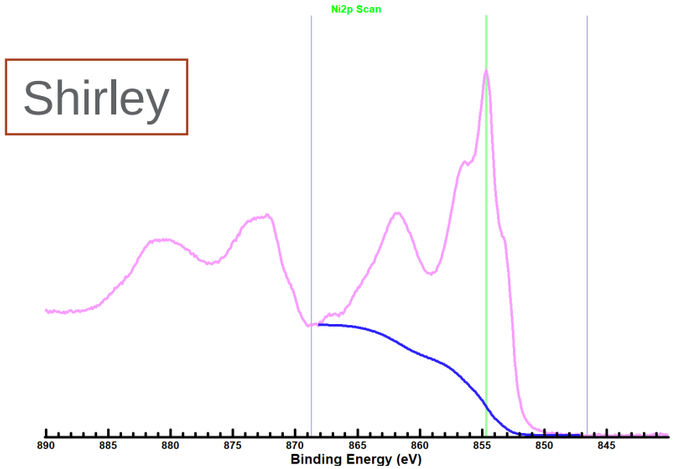

Tougaard

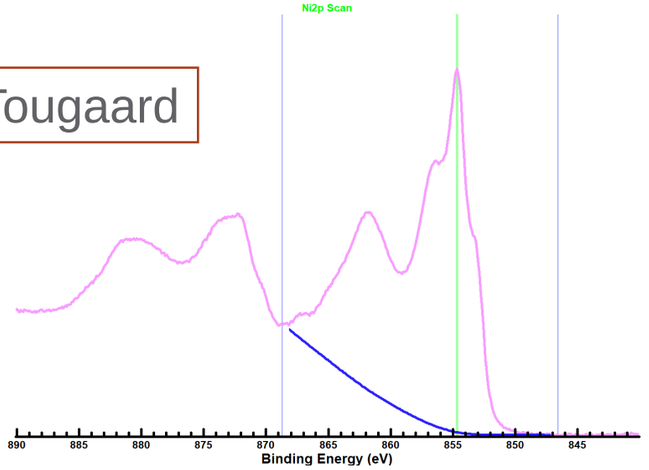

- Each background style give slightly different peak areas

- Commonly used background is “**Shirley**” background

Pre-requisites for Accurate Data Analysis and Interpretation

4. Correct **peak shape** is identified

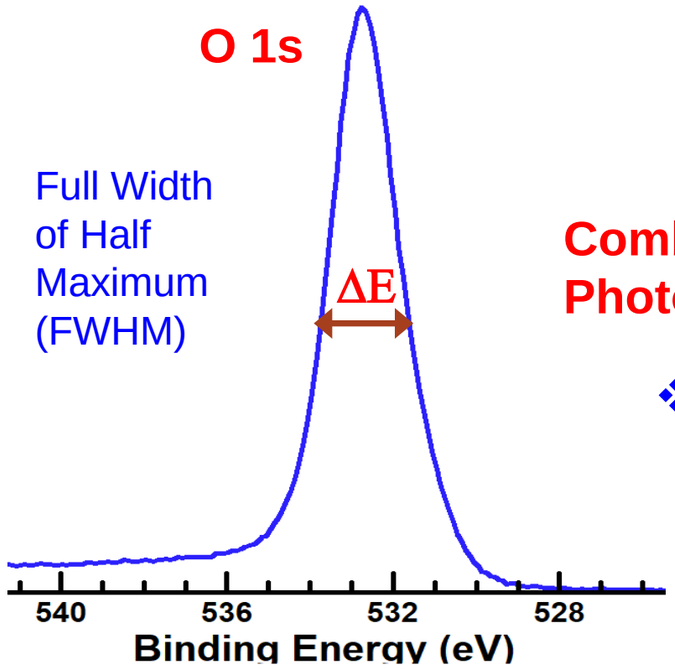

- The photoelectric process (the uncertainty principle) will give a **Lorentzian** energy distribution
- Instrument broadening and other factors (phonon broadening) will give a **Gaussian** peak shape

Combination of these two-peak shapes will give the final peak shape of the Photoelectric peak

- Sample charging also affect the peak shape

GL(p) : Gaussian/Lorentzian product formula where the mixing is determined by **m = p/100**, GL(100) is a pure Lorentzian while GL(0) is pure Gaussian.

LA(α, β, m) = Asymmetric line-shape where α and β define the spread of the tail on either side of the Lorentzian component. The parameter m specifies the width of the Gaussian used to convolute the Lorentzian curve.

Oxides and compound : GL(30)
Metals : Asymmetric function = LA (4.2,9,4)

Pre-requisites for Accurate Data Analysis and Interpretation

5. During the data analysis, correct charge correction method is used

Charge Reference to C 1s at 285 eV

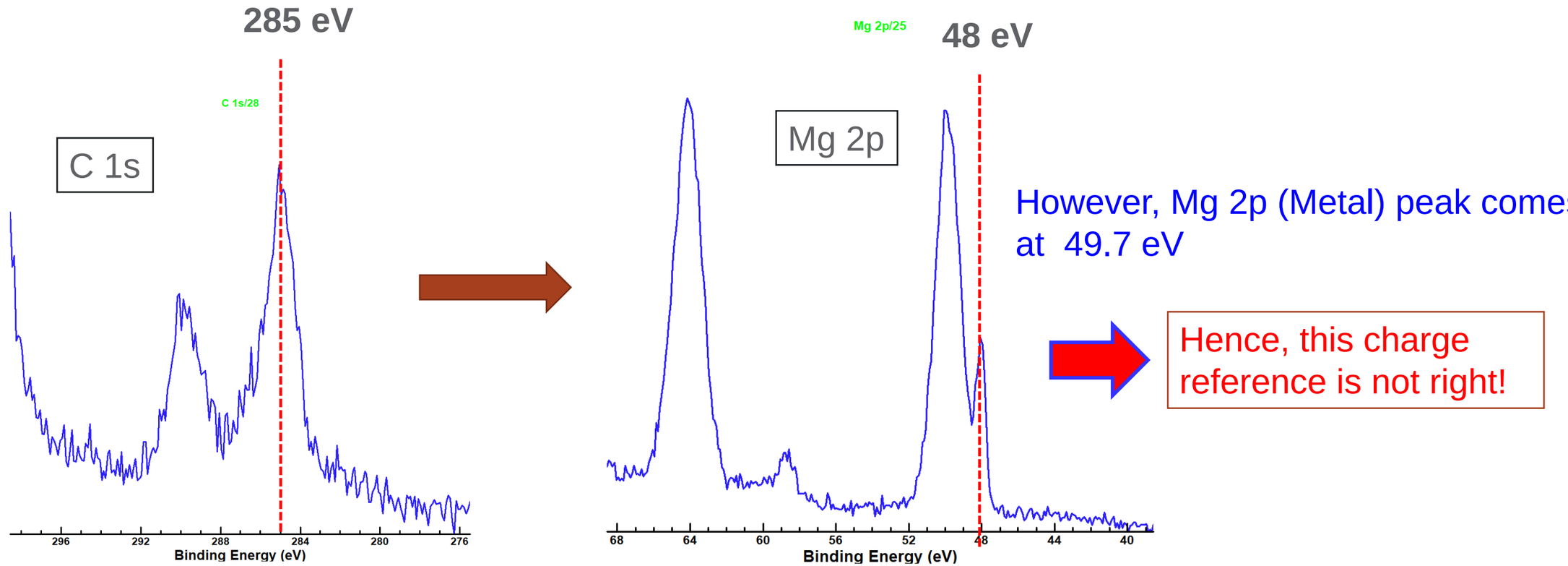

However, Mg 2p (Metal) peak comes at 49.7 eV

Hence, this charge reference is not right!

This charge referencing is not right!

Pre-requisites for Accurate Data Analysis and Interpretation

Charge Reference to Mg 2p at 49.7 eV

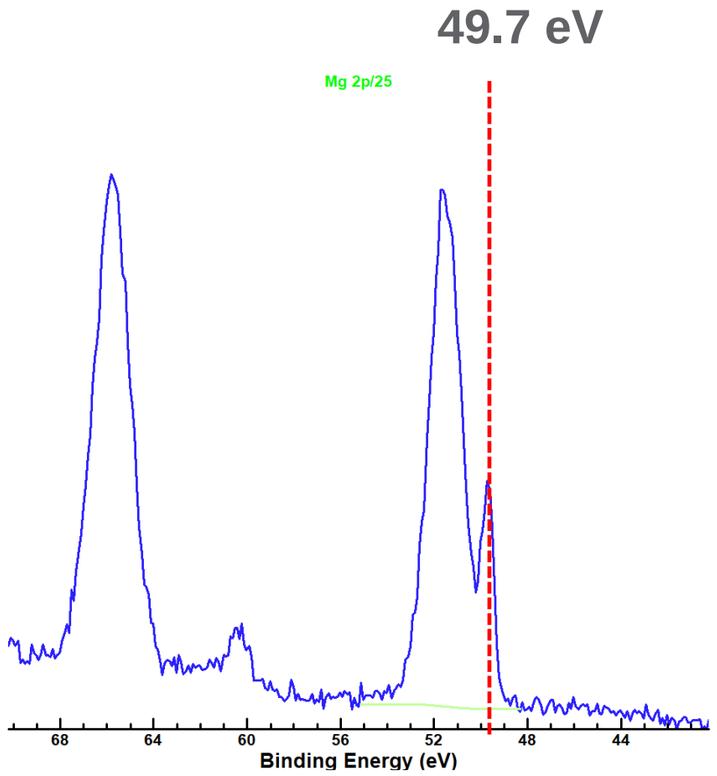

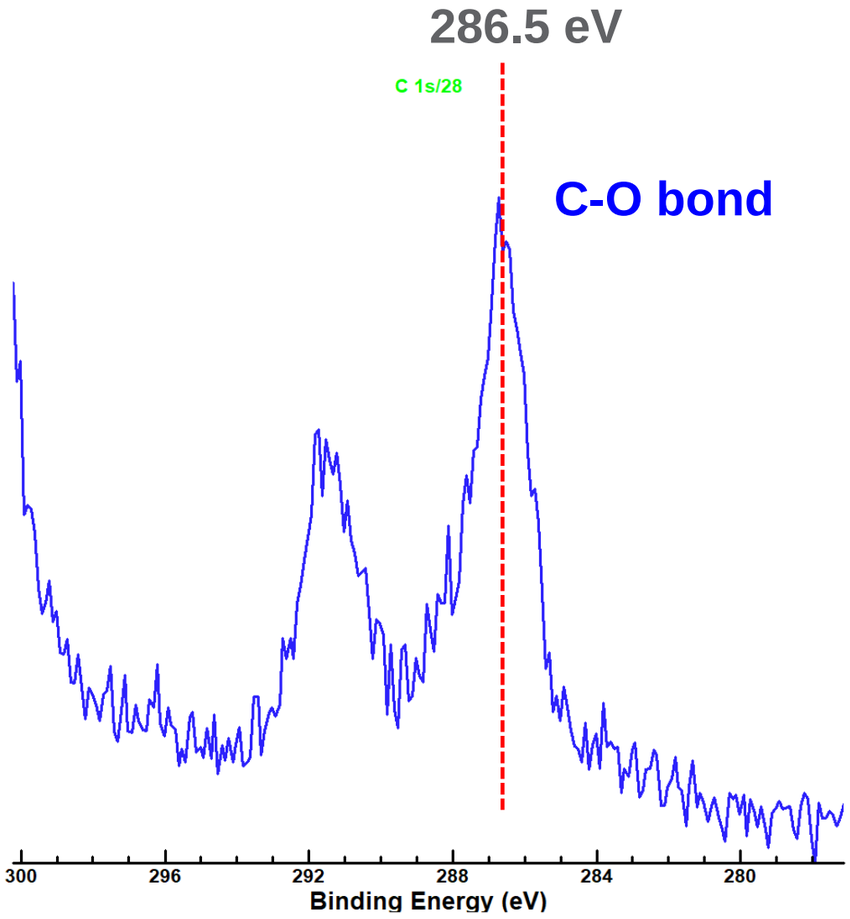

Pacific Northwest
NATIONAL LABORATORY

Introduction to XPS Peak Fitting

CasaXPS

CasaXPS: Processing Software for XPS, AES, SIMS and More

Other software available: (1) **Phi Multipack** form Physical Electronics
(2) **Avantage** from Thermo Fisher
(3) **XPSFit41** (free software)
(4) **Origin**

CasaXPS

1. Elemental Identification using Survey scans
2. Quantification using Survey scans
3. Charge Referencing in High Resolution scans
4. Quantification using High Resolution scans
5. Peak Fitting to get Chemical Speciation
6. Complicated XPS Peak Fittings (Multiplet Fitting)
7. Depth Profile measurements

Quantitative Analysis by XPS

For a homogeneous sample:

Intensity of the XPS peak = $I = N\sigma DJL\,\lambda\,AT$

$$\Rightarrow \quad N = \frac{I}{\sigma DJL\,\lambda\,AT}$$

- N = Concentration, atoms/cm^3
- σ = Photoelectric cross-section, cm^2
- D = Detector efficiency
- J = X-ray flux, photon/cm^2-sec
- L = Orbital symmetry factor
- λ = Inelastic electron mean free path, cm
- A = Analysis area, cm^2
- T = Analyzer transmission efficiency

Let's define **$S = \sigma DJL\,\lambda\,AT$** = **Elemental Sensitivity Factor**

sensitivity factors (S) are usually given by the XPS instrument manufactures

$$N = \frac{I}{S}$$

Relative concentration $C_x = \dfrac{N_x}{\sum N_i} = \dfrac{\frac{I_x}{S_x}}{\sum \frac{I_i}{S_i}}$

C.S. Fadley "Basic Concepts of X-ray Photoelectron Spectroscopy" From "Electron Spectroscopy, Theory, Techniques, and Applications" C.R. Brundle and A.D. Baker, Eds., Pergamon Press, 1978, Volume 11, Chapter 1

Quantification of Elemental Concentration

For sample with unknown composition

Step 1: Acquire survey scan to identify what elements are present

Step 2: Acquire high resolution scans for each elements present

Step 3: Calculate the peak area under each peak (after background subtraction - we will come back to this later)

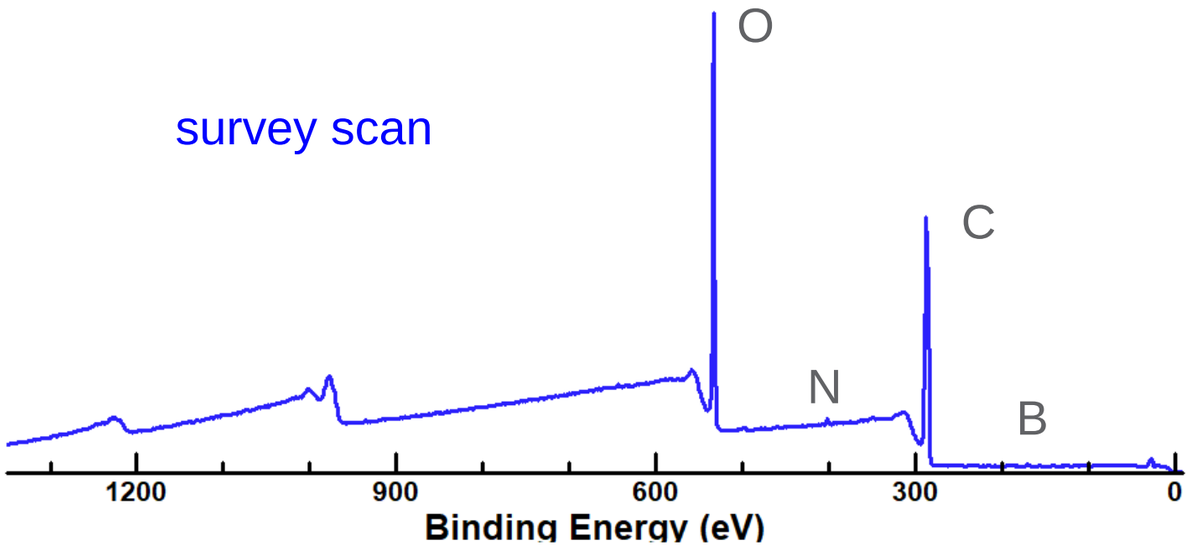

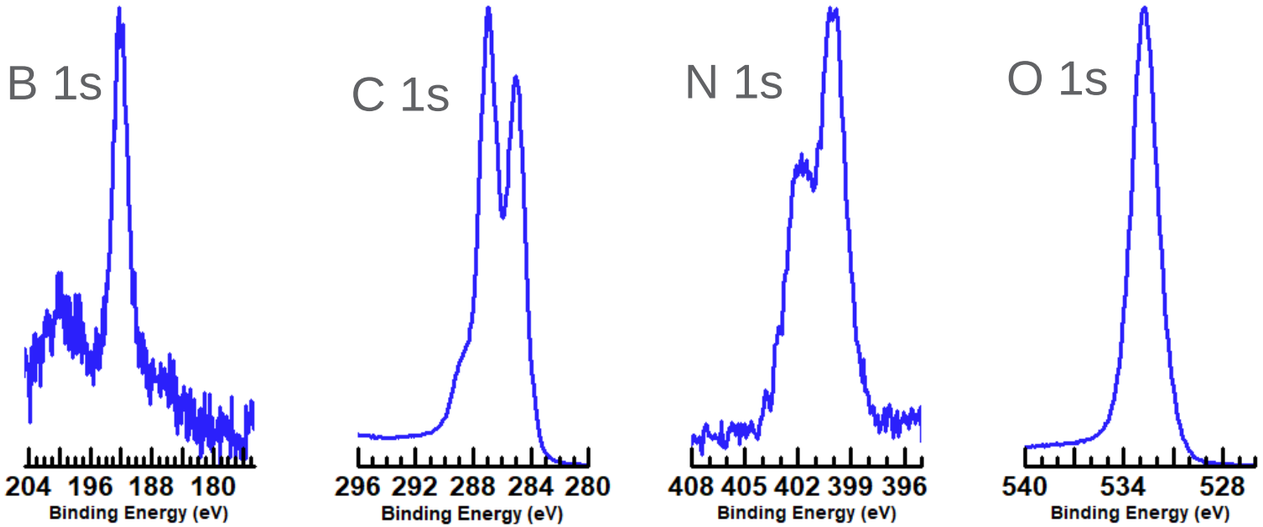

Area= 1516 **Area= 376767** **Area= 8698** **Area= 466020**

Quantification of Elemental Concentration

Step 4: Calculate the concentration using the equations

Relative concentration $C_C = \frac{N_C}{\sum N_i} = \frac{\frac{I_C}{S_C}}{\frac{I_C}{S_C} + \frac{I_O}{S_O} + \frac{I_N}{S_N} + \frac{I_B}{S_B}}$

Element	Sensitivity Factor
C 1s	1
O 1s	2.93
N 1s	1.8
B 1s	0.486

$$C_C = \frac{376767/1}{376767/1 + 466020/2.93 + 8698/1.8 + 1516/0.486}$$

$C_C = 0.695$

$C_C = 69.5$ at %

Similarly, we can calculate other concentrations: C = 69.5 at % ; O = 29 at%, N = 0.9 at %, B = 0.6 at %

CasaXPS

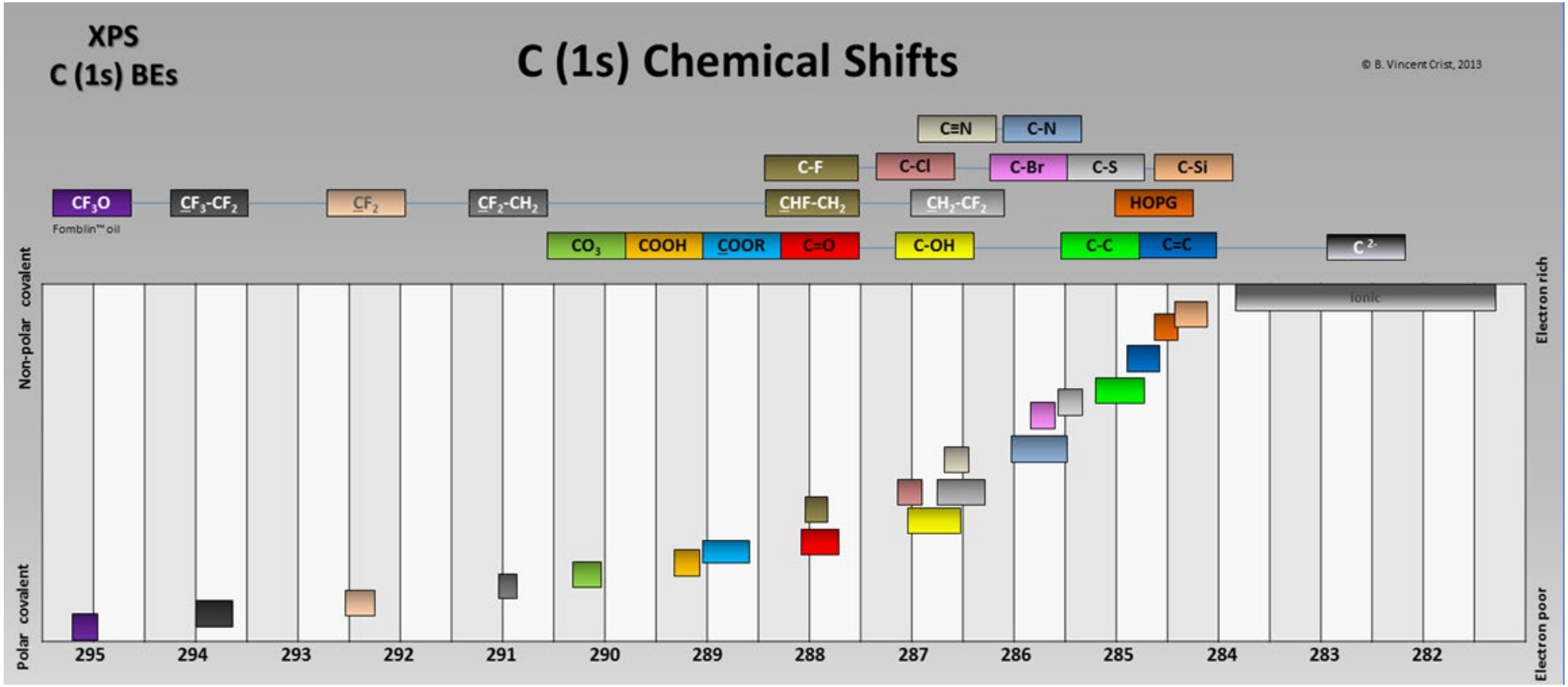
XPS
C (1s) BEs
C (1s) Chemical Shifts
© B. Vincent Crist, 2013
C≡N
C-N
C-F
C-Cl
C-Br
C-S
C-Si
CF3O
CF3-CF2
CF2
CF2-CH2
CHF-CH2
CH2-CF2
HOPG
Fomblin™ oil
CO3
COOH
COOR
C=O
C-OH
C-C
C=C
C 2-
Non-polar covalent
Polar covalent
Ionic
Electron rich
Electron poor
295
294
293
292
291
290
289
288
287
286
285
284
283
282

Fittings of Carbon-based materials

Species	Peak Ident.	Starting Position (eV)	Common Range (eV)	FWHM (eV)	Lineshape	Area Constraint	Notes
C=C	A	284.5		0.4 to 0.8 eV	LA(1.2,2.5,5) #		Peak defined here by pure graphite sample
C-C, C-H	B	A+0.5	A+0.3 to A+0.5	0.9 to 1.3 (up to 1.5)	GL(30) ##		In most relatively pure graphitic based systems not a lot of this peak should be expected
C-OH, C-O-C	C	A+2.0	A+1.8 to A+2.2	B*1	GL(30)		
C=O	D	A+3.5	A+3.3 to A+3.5	B*1	GL(30)		
O-C=O	E	A+4.5	A+4.3 to A+4.8	B*1	GL(30)		
π to π* Sat.	F	A+6.41		2.7	GL(30)	A*0.06963	Position, FWHM and area constraints can change depending on starting material (e.g. graphite vs CNT) - use values from appropriate reference sample

https://www.xpsfitting.com/search/label/carbon

Pacific Northwest
NATIONAL LABORATORY

pure graphite

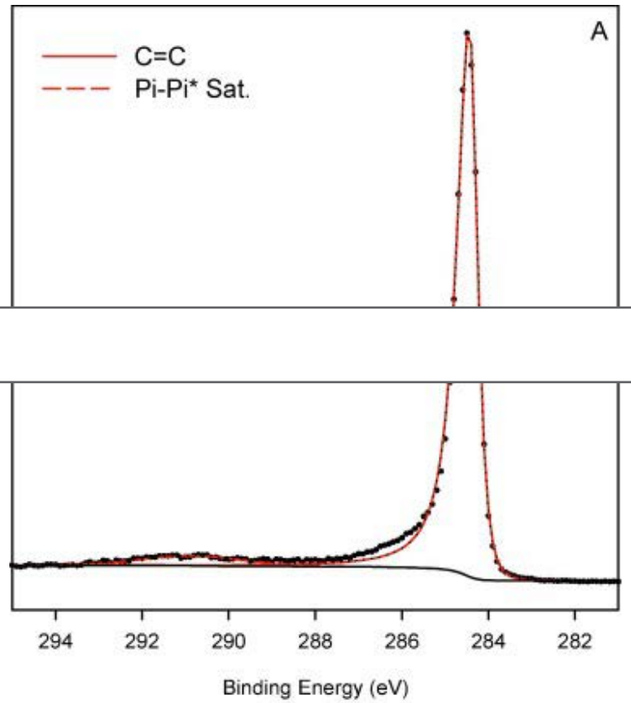

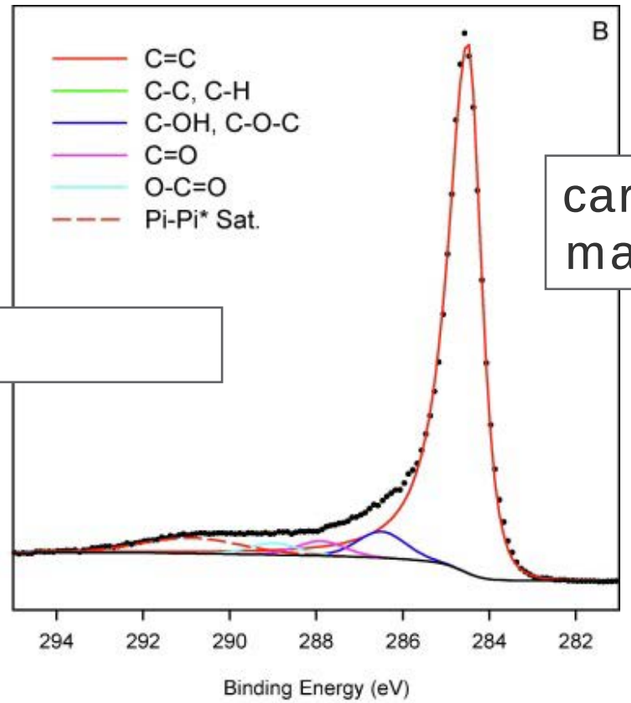

carbon nanotube-based material

oxidized graphene

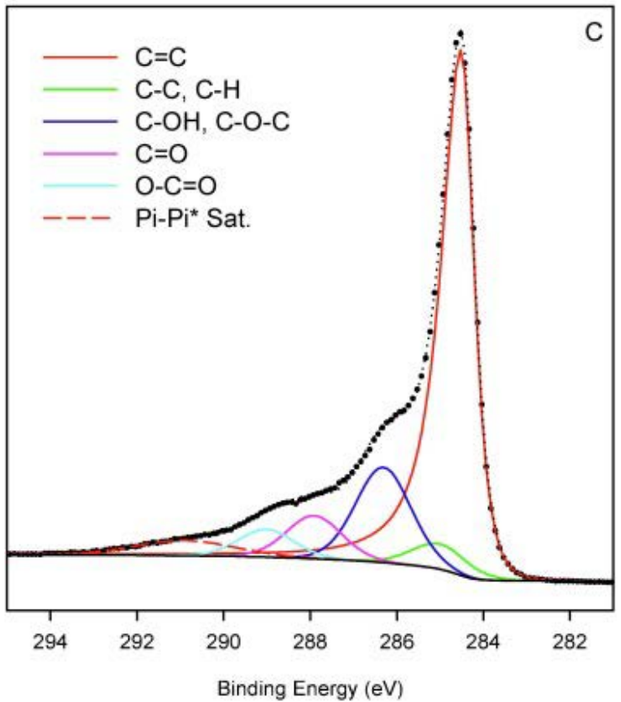

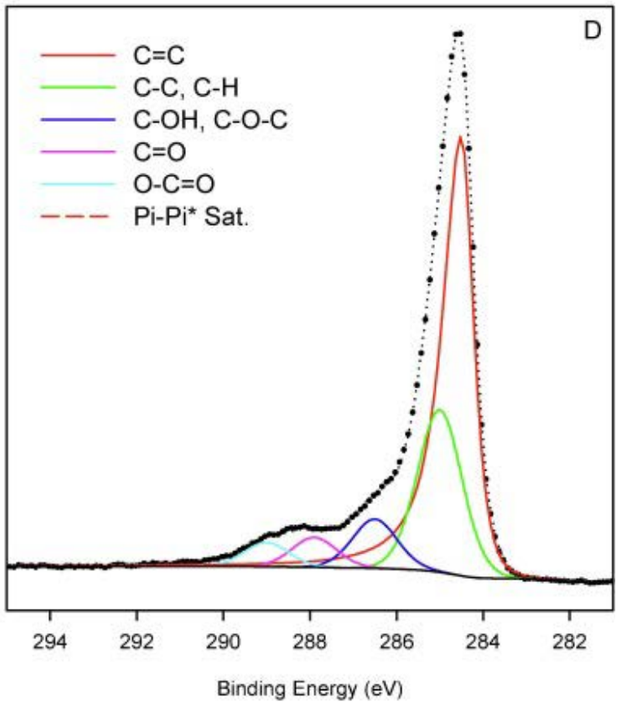

acid modified graphene and organic compound mixture

https://www.xpsfitting.com/search/label/carbon

Complicated XPS Peak Fittings (Multiplet Fitting)

Pacific Northwest NATIONAL LABORATORY

Fe 2+

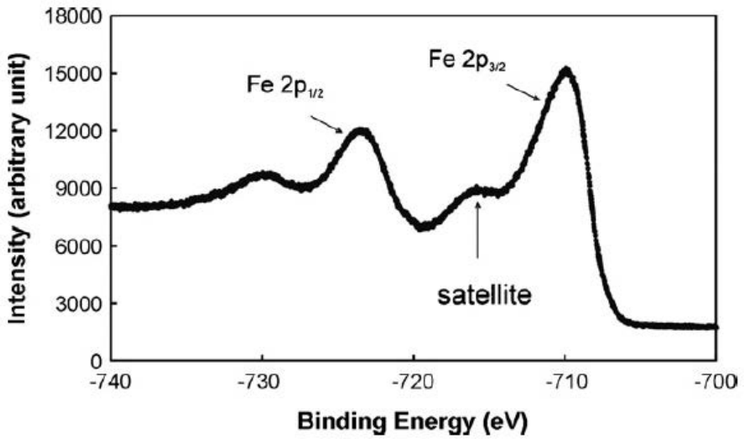

Fig. 7. The XPS spectrum of Fe 2p from the fractured surface of the Fe_2SiO_4 standard sample.

Fe 3+

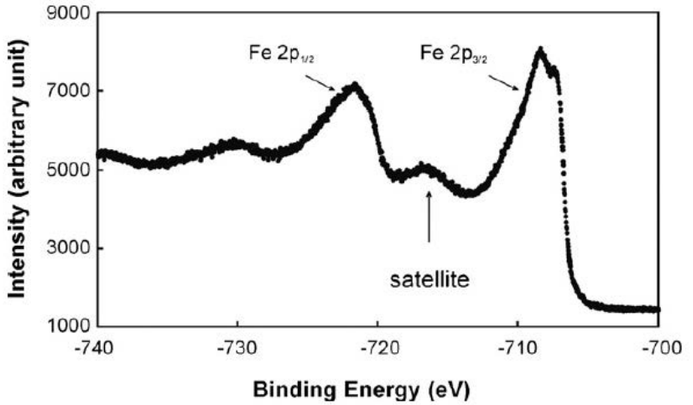

Fig. 5. The XPS spectrum of Fe 2p from the fractured surface of the Fe_2O_3 standard sample.

Fe 2+ and 3+

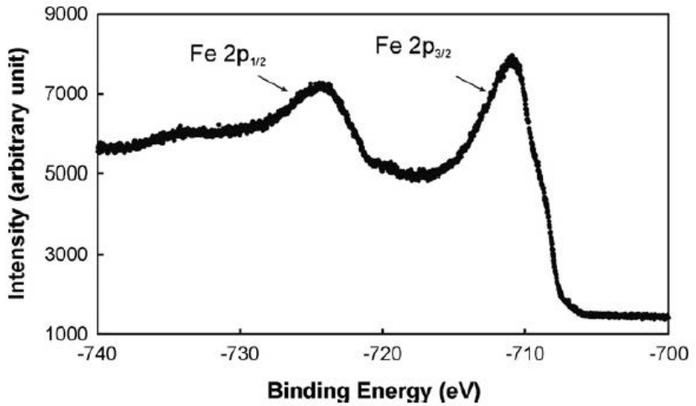

Fig. 9. The XPS spectrum of Fe 2p from the fractured surface of the Fe_3O_4 standard sample.

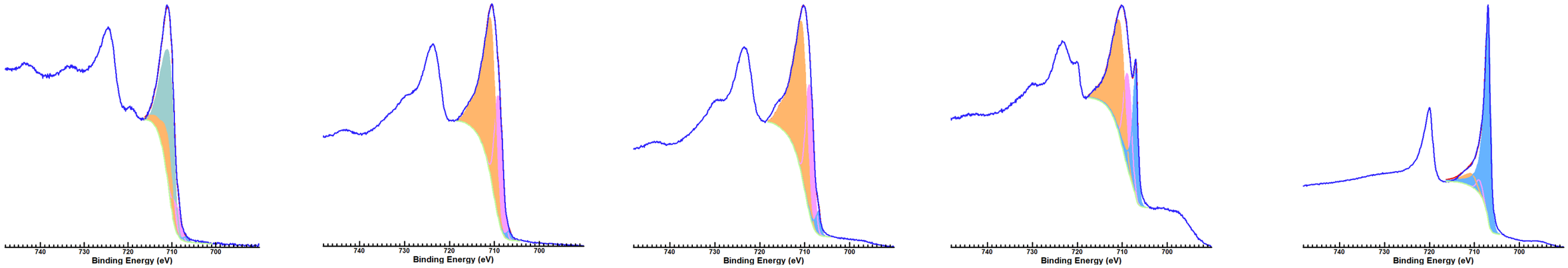

0 Sec | 100 Sec | 290 Sec | 540 Sec | 1040 Sec

Depth (sputter Time)

Compound	Peak 1 (eV)	FWHM, 10 eV Pass Energy	%	Peak 2 (eV)	Δ Peak2 - Peak1 (eV) a)	FWHM, 10 eV Pass Energy	%	Peak 3 (eV)	Δ Peak3 - Peak2 (eV)	FWHM, 10 eV Pass Energy	%	Peak 4 (eV)	Δ Peak4 - Peak3 (eV)	FWHM, 10 eV Pass Energy	%	Peak 5 (eV)	Δ Peak5 - Peak4 (eV)	FWHM, 10 eV Pass Energy	%	Peak 6 (eV)	Δ Peak6 - Peak5 (eV)	FWHM, 10 eV Pass Energy	%	
Fe(0)	706.6	0.88	100.0																					b)
FeO	708.4	1.4	24.2	709.7	1.3	1.6	30.1	710.9	1.2	1.6	14.5	712.1	1.2	2.9	25.6	715.4	3.3	2.5	5.6					
α-Fe2O3	709.8	1.0	26.1	710.7	0.9	1.2	22.0	711.4	0.7	1.2	17.4	712.3	0.9	1.4	11.1	713.3	1.0	2.2	14.8	719.3	6.0	2.9	8.6	
γ-Fe2O3	709.8	1.2	27.4	710.8	1.0	1.3	27.4	711.8	1.0	1.4	20.3	713.0	1.2	1.4	9.1	714.1	1.1	1.7	5.1	719.3	5.2	2.2	10.0	
Ave. Fe2O3	**709.8**	**1.1**	**26.8**	**710.8**	**1.0**	**1.3**	**24.7**	**711.6**	**0.8**	**1.3**	**18.9**	**712.7**	**1.1**	**1.4**	**10.1**	**713.7**	**1.1**	**2.0**	**10.0**	**719.3**	**5.6**	**2.6**	**9.3**	
Std. Dev.	0.0	0.1	0.9	0.1	0.1	0.1	3.8	0.3	0.2	0.1	2.1	0.5	0.2	0.0	1.4	0.6	0.1	0.4	6.9	0.0	0.6	0.5	1.0	
α-FeOOH	710.2	1.3	26.7	711.2	1.0	1.2	25.3	712.1	0.9	1.4	21.0	713.2	1.1	1.4	12.1	714.4	1.2	1.7	7.2	719.8	5.4	3.0	7.7	
γ-FeOOH	710.3	1.4	27.3	711.3	1.0	1.4	27.6	712.3	1.0	1.4	20.1	713.3	1.0	1.4	10.5	714.4	1.1	1.8	5.4	719.5	5.1	2.8	8.9	
Ave. FeOOH	**710.3**	**1.4**	**27.0**	**711.3**	**1.0**	**1.3**	**26.5**	**712.2**	**0.9**	**1.4**	**20.6**	**713.3**	**1.1**	**1.4**	**11.3**	**714.4**	**1.1**	**1.8**	**6.3**	**719.7**	**5.3**	**2.9**	**8.3**	
Std. Dev.	0.1	0.1	0.4	0.1	0.0	0.1	1.6	0.1	0.1	0.0	0.6	0.1	0.1	0.0	1.1	0.0	0.1	0.1	1.3	0.2	0.2	0.1	0.8	
Average Fe(III)	**710.0**	**1.2**	**26.9**	**711.0**	**1.0**	**1.3**	**25.6**	**711.9**	**0.9**	**1.4**	**19.7**	**713.0**	**1.1**	**1.4**	**10.7**	**714.1**	**1.1**	**1.9**	**8.1**	**719.5**	**5.4**	**2.7**	**8.8**	
Std. Dev.	0.3	0.2	0.6	0.3	0.0	0.1	2.6	0.4	0.1	0.1	1.6	0.5	0.1	0.0	1.3	0.5	0.1	0.2	4.5	0.2	0.4	0.4	0.9	
Fe3O4 2+	708.4	1.2	16.6	709.2	0.8	1.2	14.8																	d)
Fe3O4 3+	710.2	1.4	23.7	711.2	1.0	1.4	17.8	712.3	1.1	1.4	12.2	713.4	1.1	1.4	5.7	714.5	1.1	3.3	9.1	c)				d)
FeCr2O4 (Chromite)	709.0	2.0	40.5	710.3	1.2	1.5	12.9	711.2	0.9	1.5	17.8	712.3	1.2	1.5	8.3	713.8	1.4	3.6	20.6					e)
NiFe2O4	709.5	2.0	34.1	710.7	1.3	2.0	33.2	712.2	1.4	2.0	22.3	713.7	1.6	2.0	10.4									
FeCO3 (Siderite)	709.8	1.5	24.3	711.1	1.3	1.5	13.2	712.0	0.9	3.6	41.9	715.6	3.6	3.4	20.0	719.4	3.8	1.5	0.70					

a) Binding energies are significant to 0.1eV but an additional figure is added because energy splittings are much more accurate than the absolute binding energies.
b) Asymmetric peakshape and FWHM defined by standard iron metal sample (LA(1.2,4.8,3))
c) Satellite structure for 3+ though likely present will be buried under Fe 2+ Fe 2p1/2 portion of spectrum
d) Sum of 2+ and 3+ areas is 100
e) Taken with a 20 eV pass energy

M.C. Biesinger, B.P. Payne, A.P. Grosvenor, L.W.M. Lau, A.R. Gerson, R.St.C. Smart, Appl. Surf. Sci. **257** (2011) 2717.

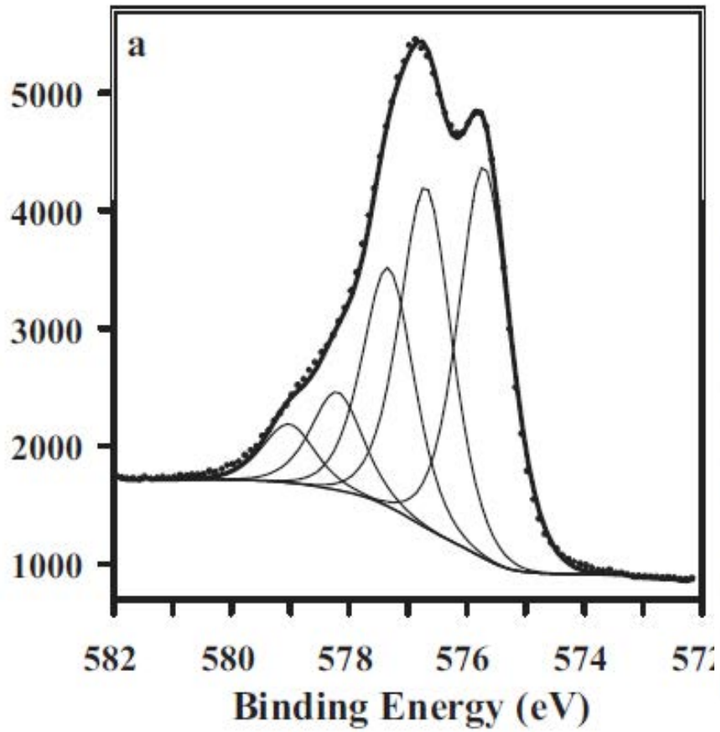

Compound	Peak 1 (eV)	%	Peak 2 (eV)	Δ Peak2 - Peak1 (eV) a)	%	Peak 3 (eV)	Δ Peak3 - Peak2 (eV)	%	Peak 4 (eV)	Δ Peak4 - Peak3 (eV)	%	Peak 5 (eV)	Δ Peak5 - Peak4 (eV)	%	FWHM, 10 eV Pass Energy	FWHM, 20 eV Pass Energy	
Cr(0)	574.2	100													0.80	0.90	b)
Cr(III) Oxide	575.7	36	576.7	1.01	35	577.5	0.78	19	578.5	1.00	8	578.9	0.41	5	0.88	0.94	c)
Cr(III) Hydroxide	577.3	100													2.58	2.60	d)
FeCr2O4 (Chromite)	575.9	41	577.0	1.09	39	577.9	0.88	13	578.9	1.04	7				1.12	1.20	
NiCr2O4	575.2	35	576.2	1.02	34	577.0	0.81	18	578.1	1.05	9	579.2	1.13	4	1.09		
Cr(VI) Mixed Species	579.5	100													1.40	1.50	e)
Cr(VI) Oxide	579.6	100													1.28	1.38	f)

a) Binding energies are significant to 0.1eV but an additional figure is added because energy splittings are much more accurate than the absolute binding energies.
b) Asymmetric peakshape and FWHM defined by standard chromium metal sample (LA(1.3,4,5))
c) FWHM for multiplet splitting single peaks can be estimated by metal FWHM
d) This BE value is for an aged hydroxide, freshly prepared hydroxide has a BE of 577.1 eV.
e) Binding energy from Literature average, broadened FWHM to incorporate a variety of Cr(VI) species
f) Binding energy and FWHM from standard CrO3 sample

M.C. Biesinger, B.P. Payne, A.P. Grosvenor, L.W.M. Lau, A.R. Gerson, R.St.C. Smart, Appl. Surf. Sci. ***257*** *(2011) 2717*.

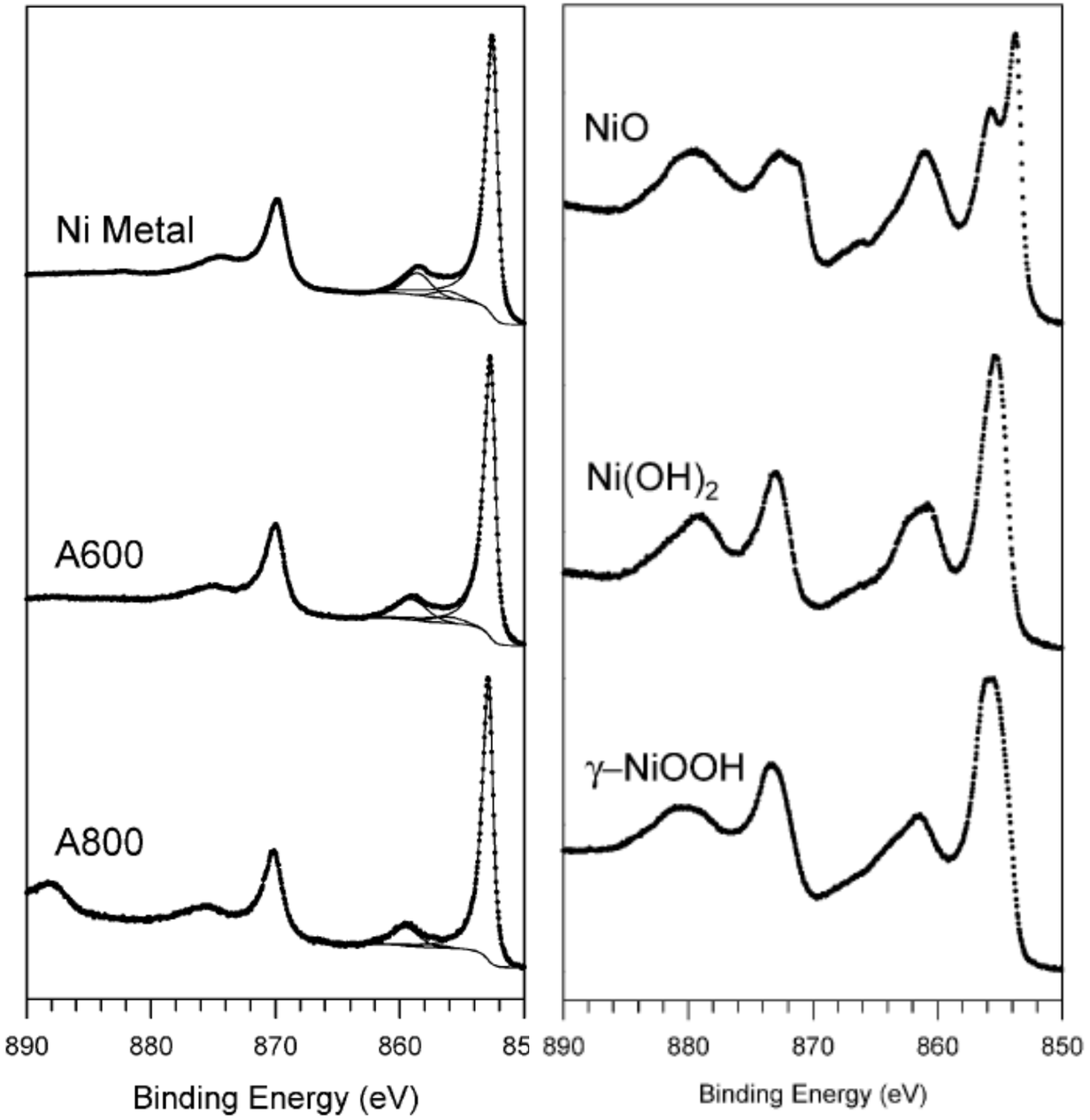

Compound	Peak 1 (eV) a)	%	Peak 1, FWHM, 10 eV Pass Energy	Peak 1, FWHM, 20 eV Pass Energy	Peak 2 (eV)	Δ Peak2 - Peak1 (eV) a)	%	Peak 2, FWHM, 10 eV Pass Energy	Peak 2, FWHM, 20 eV Pass Energy	Peak 3 (eV)	Δ Peak3 - Peak2 (eV)	%	Peak 3, FWHM, 10 eV Pass Energy	Peak 3, FWHM, 20 eV Pass Energy	Peak 4 (eV)	Δ Peak4 - Peak3 (eV)	%	Peak 4, FWHM, 10 eV Pass Energy	Peak 4, FWHM, 20 eV Pass Energy	
Ni Metal from [1]	852.6	79.6	1.00	1.02	856.3	3.65	5.6	2.48	2.48	858.7	2.38	14.8	2.48	2.48						b) d)
Ni Metal - New Line Shape	852.6	81.2	0.94	0.95	856.3	3.65	6.3	2.70	2.70	858.7	2.38	12.5	2.70	2.70						c) d)
NiO	853.7	14.3	0.98	1.02	855.4	1.71	44.2	3.20	3.25	860.9	5.44	34.0	3.85	3.76	864.0	3.10	3.6	1.97	2.04	
Ni(OH)2	854.9	7.4	1.12	1.16	855.7	0.77	45.3	2.25	2.29	857.7	2.02	3.0	1.59	1.59	860.5	2.79	1.4	1.06	1.06	
Gamma NiOOH	854.6	13.8	1.40		855.3	0.70	12.4	1.50		855.7	0.36	9.7	1.40		856.5	0.78	20.7	1.40		
Beta NiOOH (3+ Portion)	854.6	9.2	1.40		855.3	0.70	8.3	1.50		855.7	0.36	6.4	1.40		856.5	0.78	13.8	1.40		e)
Beta NiOOH (2+ Portion)	854.9	2.5	1.12		855.7	0.77	15.1	2.25		857.7	2.02	1.0	1.59		860.5	2.79	0.5	1.06		e)
NiCr2O4	853.8	7.0	1.22	1.30	855.8	1.95	20.5	1.82	1.86	856.5	0.71	24.7	3.91	3.81	861.0	4.50	2.3	1.27	1.33	
NiFe2O4	854.5	17.3	1.35	1.36	856.0	1.52	38.2	3.03	2.98	861.4	5.41	38.5	4.49	4.50	864.7	3.29	2.8	3.04	3.01	

Compound	Peak 5 (eV)	Δ Peak5 - Peak4 (eV)	%	Peak 5, FWHM, 10 eV Pass Energy	Peak 5, FWHM, 20 eV Pass Energy	Peak 6 (eV)	Δ Peak6 - Peak5 (eV)	%	Peak 6, FWHM, 10 eV Pass Energy	Peak 6, FWHM, 20 eV Pass Energy	Peak 7 (eV)	Δ Peak7 - Peak6 (eV)	%	Peak 7, FWHM, 10 eV Pass Energy	Peak 7, FWHM, 20 eV Pass Energy	
Ni Metal from [5]																b) d)
Ni Metal - New Line Shape																c) d)
NiO	866.3	2.38	3.9	2.60	2.44											
Ni(OH)2	861.5	1.00	39.2	4.64	4.65	866.5	4.96	3.7	3.08	3.01						
Gamma NiOOH	857.8	1.33	8.7	1.90		861.0	3.20	23.3	4.00		864.4	3.38	11.4	4.40		
Beta NiOOH (3+ Portion)	857.8	1.33	5.8	1.90		861.0	3.20	15.6	4.00		864.4	3.38	7.6	4.40		e)
Beta NiOOH (2+ Portion)	861.5	1.00	13.1	4.64		866.5	4.96	1.2	3.08							e)
NiCr2O4	861.3	0.26	39.4	4.34	4.31	866.0	4.73	6.1	2.07	2.13						
NiFe2O4	867.0	2.27	3.2	2.61	2.66											

a) Binding energies are significant to 0.1eV but an additional figure is added because energy splittings are much more accurate than the absolute binding energies.
b) Assymetric peakshape for peak 1 defined by standard nickel metal sample, CasaXPS peakshape parameter = A(0.4,0.55,10)GL(30)
c) Assymetric peakshape for peak 1 defined by standard nickel metal sample, CasaXPS peakshape parameter = LA(1.1,2.2,10)
d) Metal peak is corrected to Au 4f7/2 set to 83.95 eV. All other peaks are charge corrected to C 1s (C-C, C-H, adventitious carbon) set to 284.8eV.
e) Beta NiOOH has a ratio of 2:1 Ni(III):Ni(II). Peak percentages for the 3+ and 2 + portions for Beta NiOOH total 100%.

M.C. Biesinger, B.P. Payne, A.P. Grosvenor, L.W.M. Lau, A.R. Gerson, R.St.C. Smart, Appl. Surf. Sci. ***257*** *(2011) 2717.*

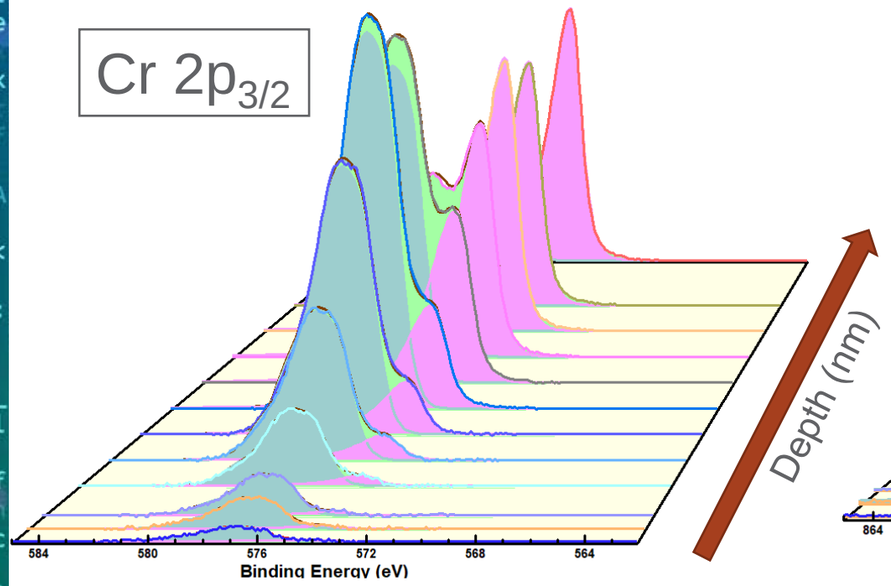
Cr 2p3/2
584
580
576
572
568
564
Binding Energy (eV)

Depth (nm)

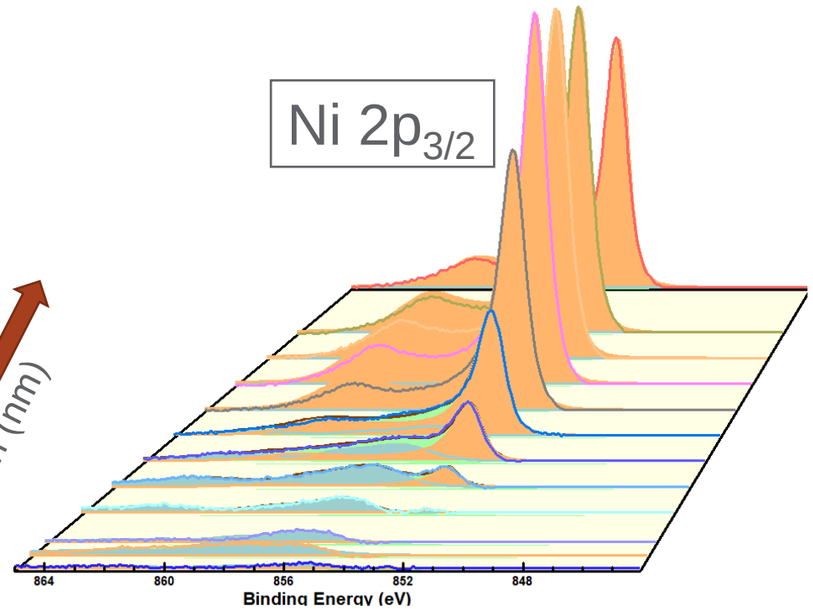
Ni 2p3/2
864
860
856
852
848
Binding Energy (eV)

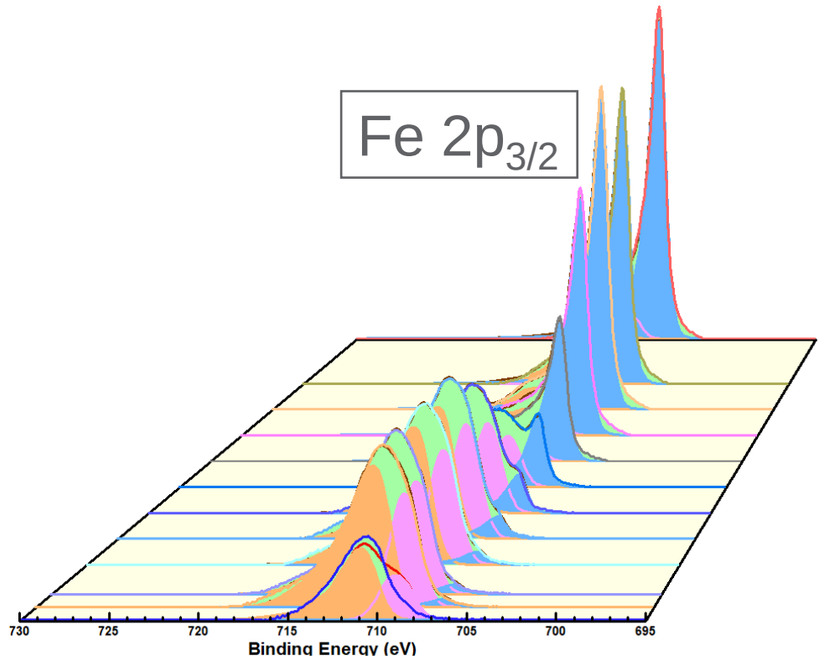
Fe 2p3/2
730
725
720
715
710
705
700
695
Binding Energy (eV)

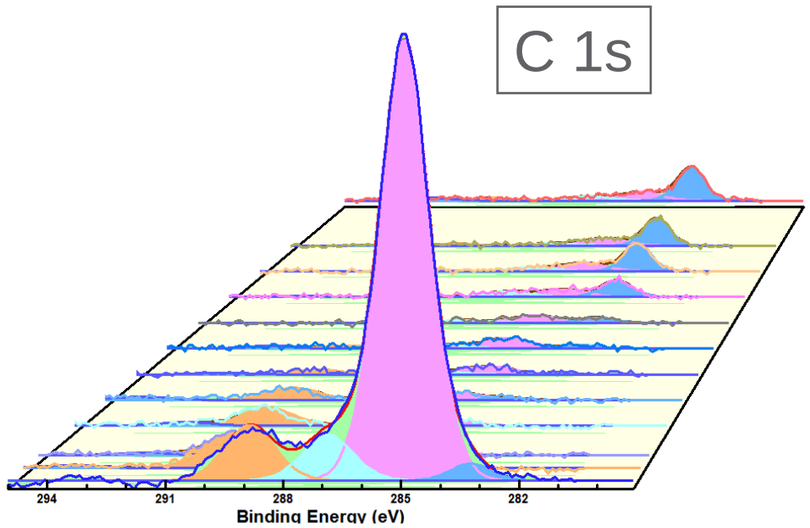
C 1s
294
291
288
285
282
Binding Energy (eV)

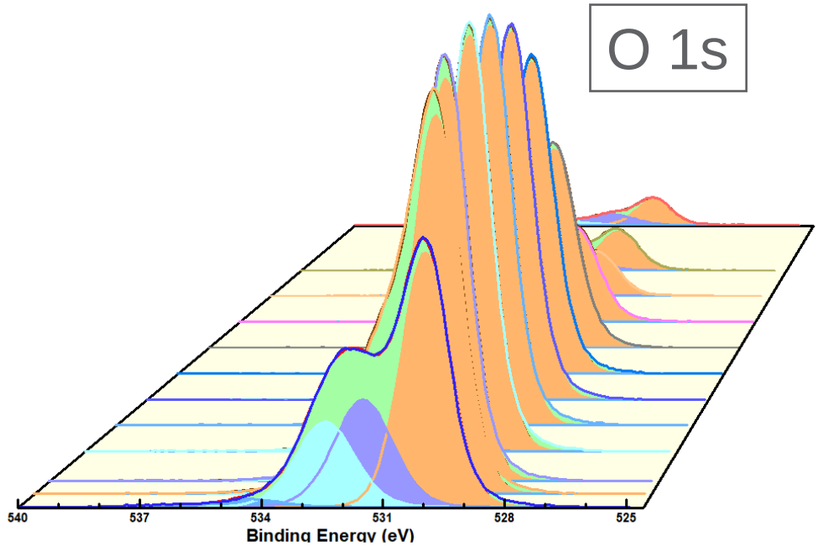
O 1s
540
537
534
531
528
525
Binding Energy (eV)

Pacific Northwest
NATIONAL LABORATORY

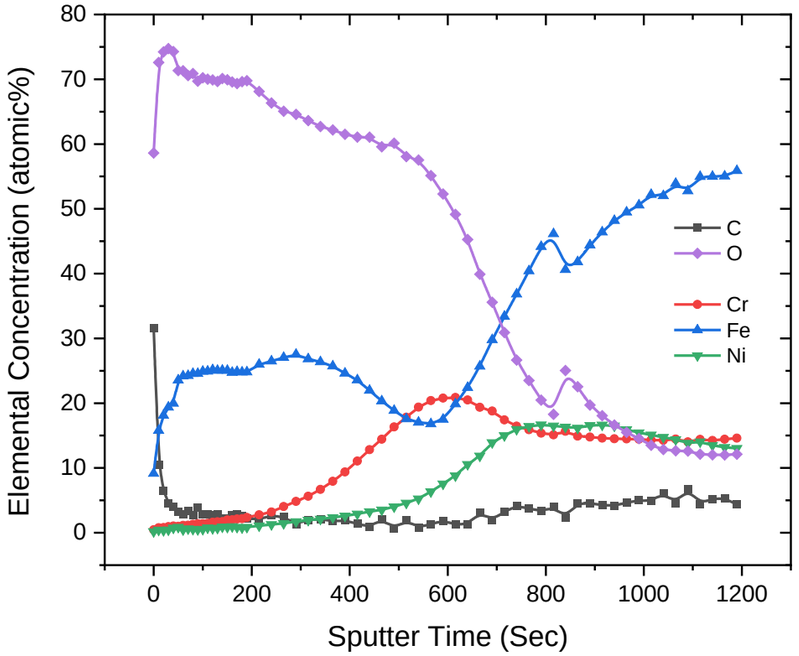

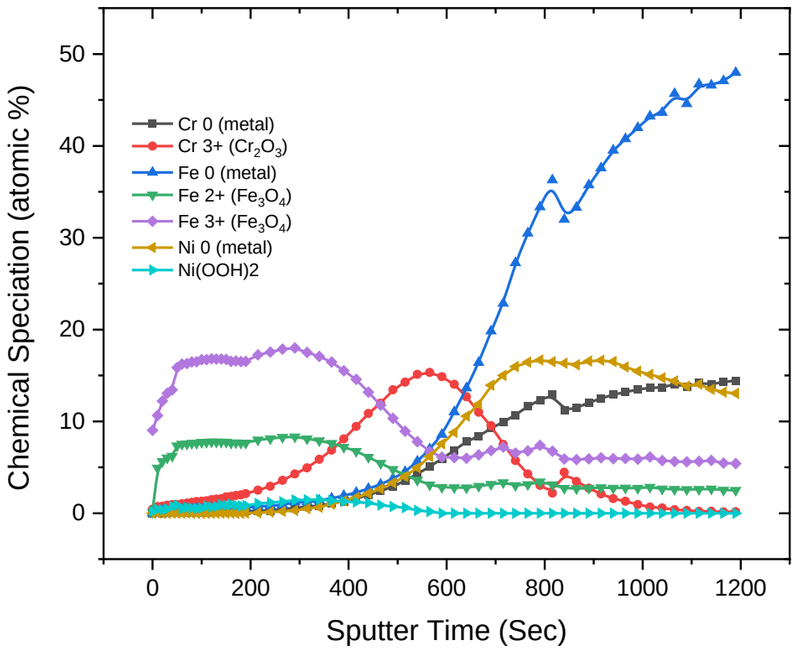

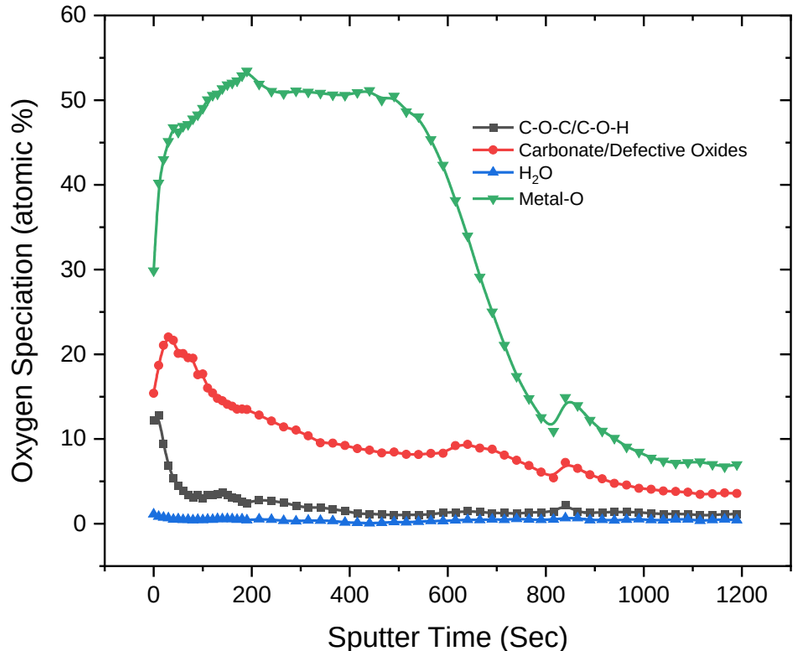

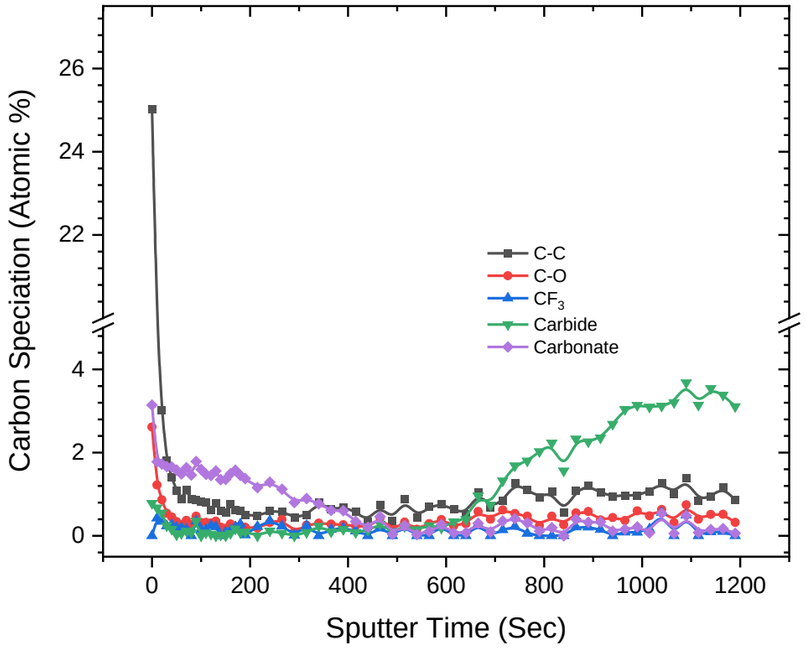

Pacific Northwest
NATIONAL LABORATORY

Pitfalls In XPS Analysis

Pitfall 1: Identifying Noise as XPS Peaks

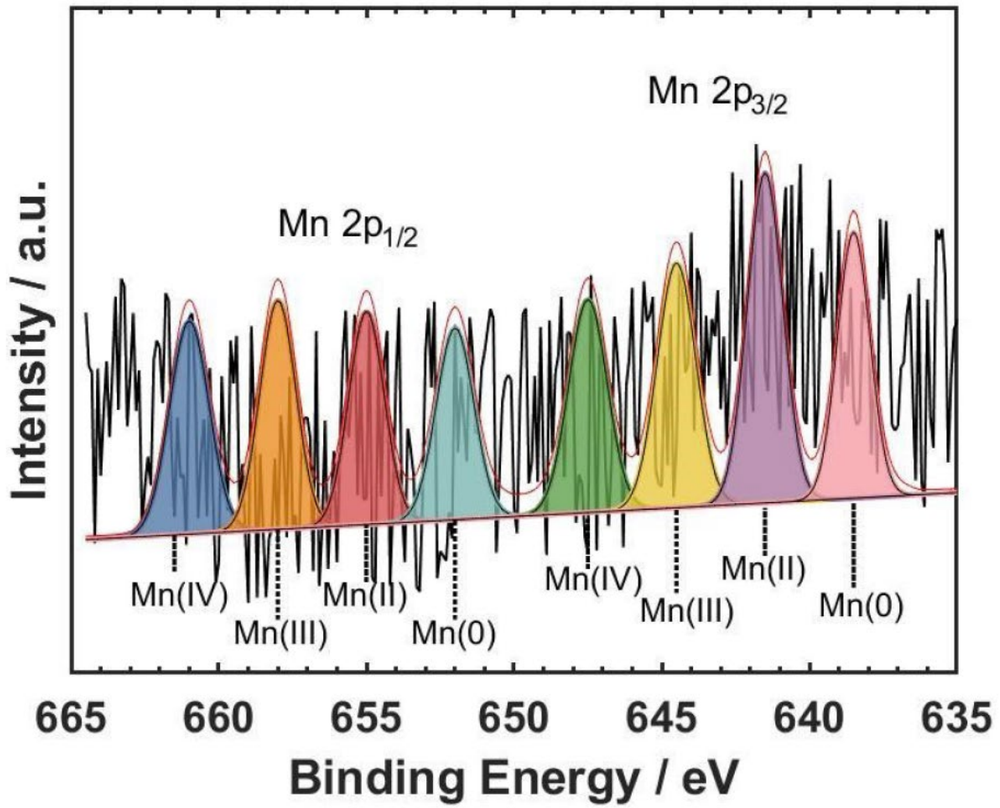

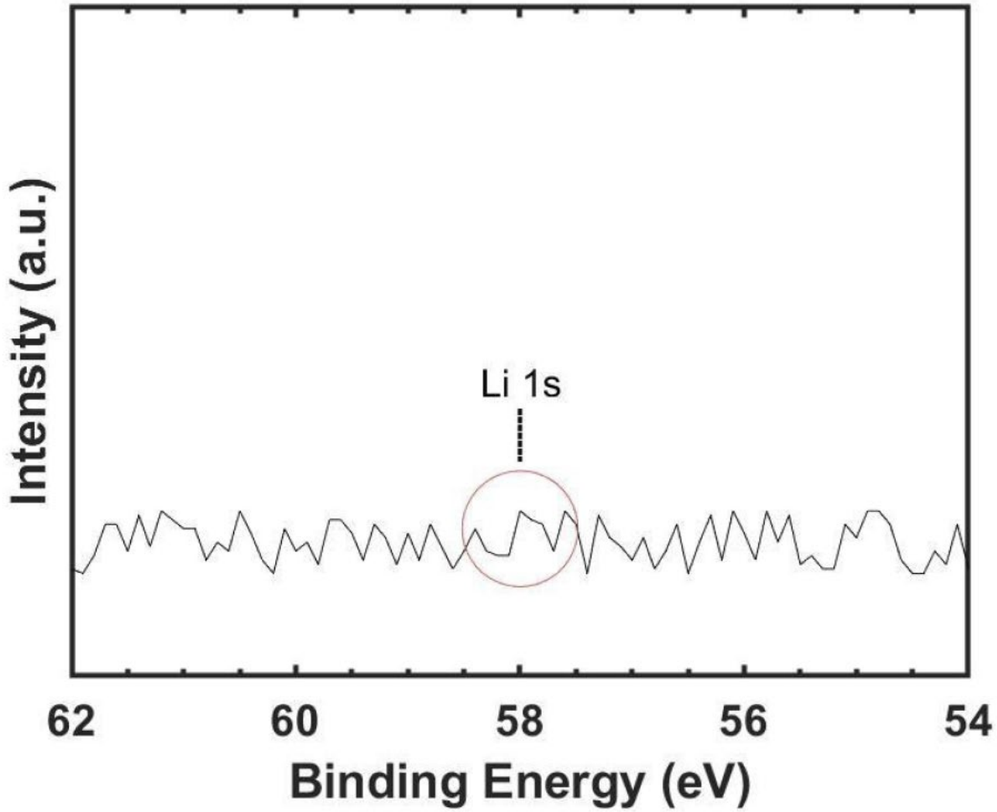

❖ The noise and fluctuations in the baseline of this data are of comparable size

George Hobbs Major Brigham Young University, "Use and Misuse of X-Ray Photoelectron Spectroscopy (XPS):Reproducibility, Gross Errors, Data Reporting, and Peak Fitting", Ph.D Thesis, 2023

Pitfall 2: Not Including the Spin-Orbit Contribution

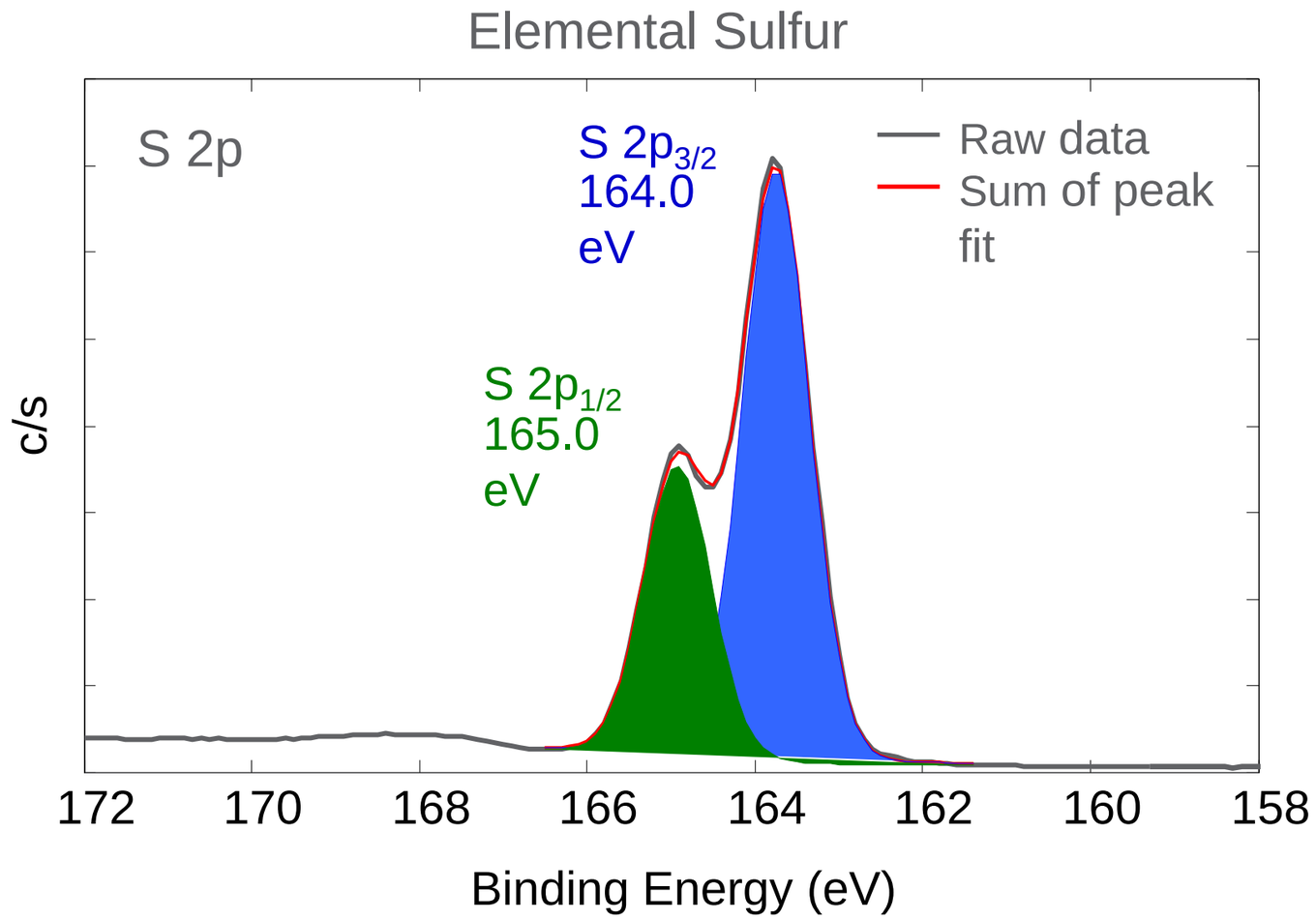

Peak Binding Energies
Gauss Lorentz fit
Gauss = 90%
FWHM = 0.94 eV
Area ratio lock = 0.5
Peak separation lock = 1.18 eV

George Hobbs Major Brigham Young University, "Use and Misuse of X-Ray Photoelectron Spectroscopy (XPS):Reproducibility, Gross Errors, Data Reporting, and Peak Fitting", Ph.D Thesis, 2023

Pitfall 2: Not Including the Spin-Orbit Contribution

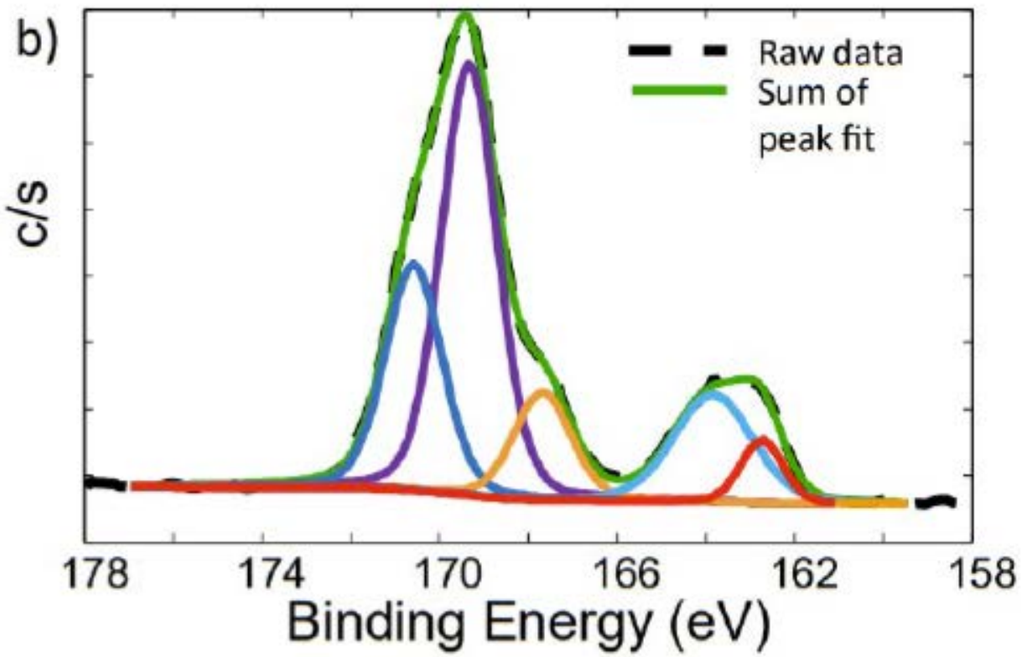

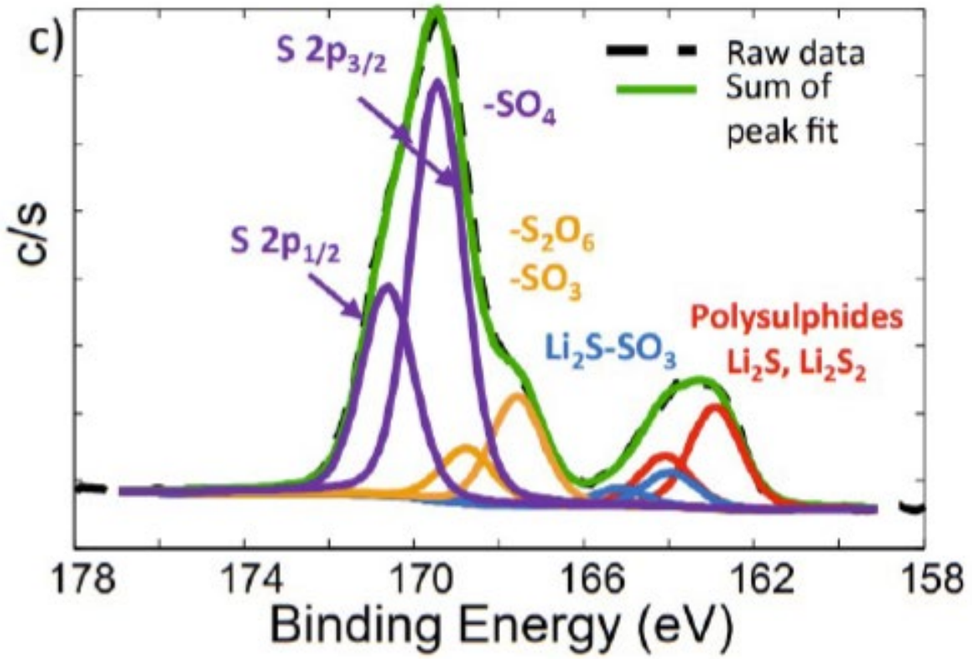

Incorrect fit: Spin-orbit splitting was not included

Correct fit: Spin-orbit splitting was included

George Hobbs Major Brigham Young University, "Use and Misuse of X-Ray Photoelectron Spectroscopy (XPS):Reproducibility, Gross Errors, Data Reporting, and Peak Fitting", Ph.D Thesis, 2023

Pitfall 3: Used Different Peak Widths and Peak Positions for same Sample

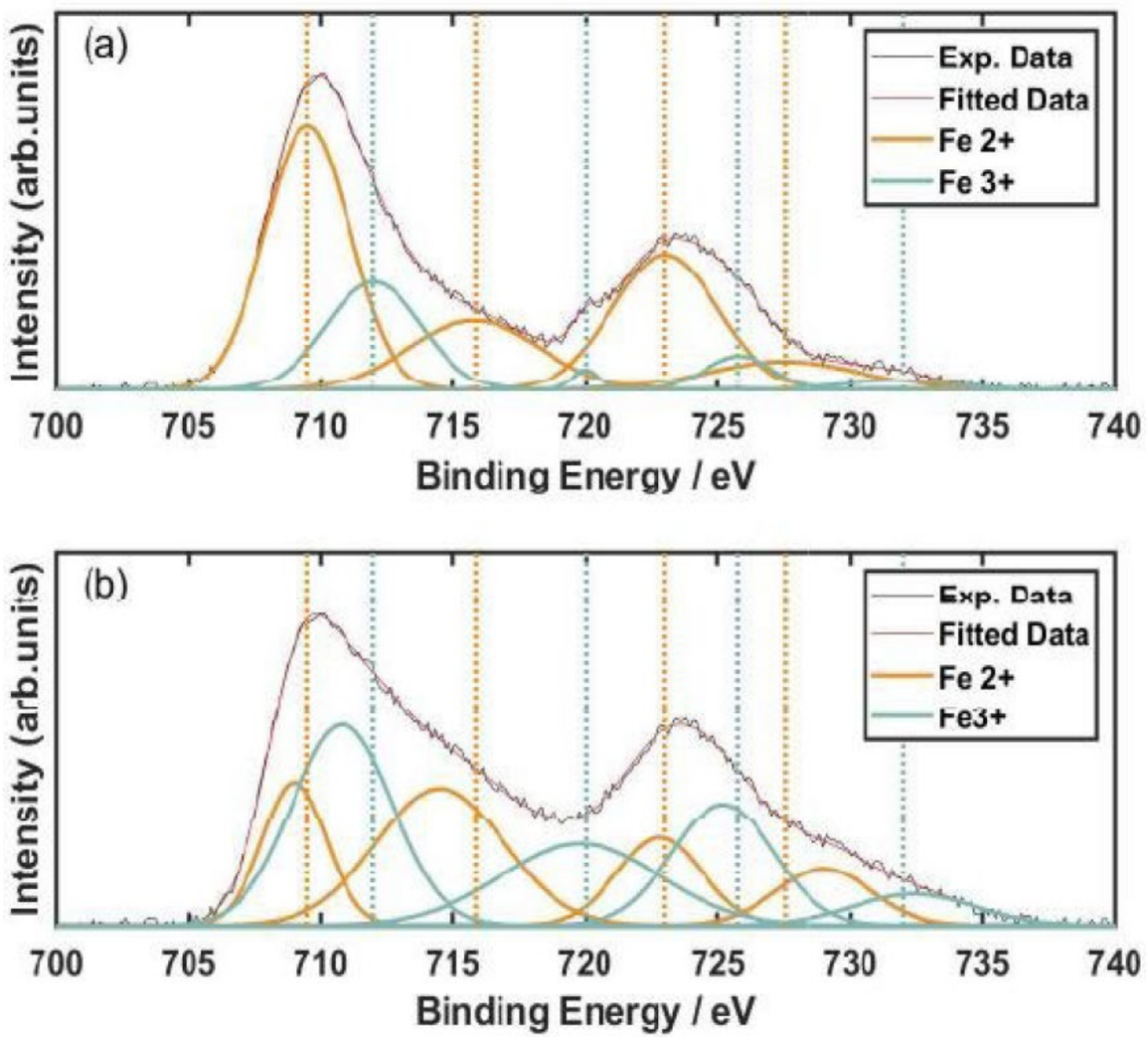

- Same fitting protocol should apply to both fits

George Hobbs Major Brigham Young University, "Use and Misuse of X-Ray Photoelectron Spectroscopy (XPS):Reproducibility, Gross Errors, Data Reporting, and Peak Fitting", Ph.D Thesis, 2023

Pitfall 4: Not Fitting the Entire Region

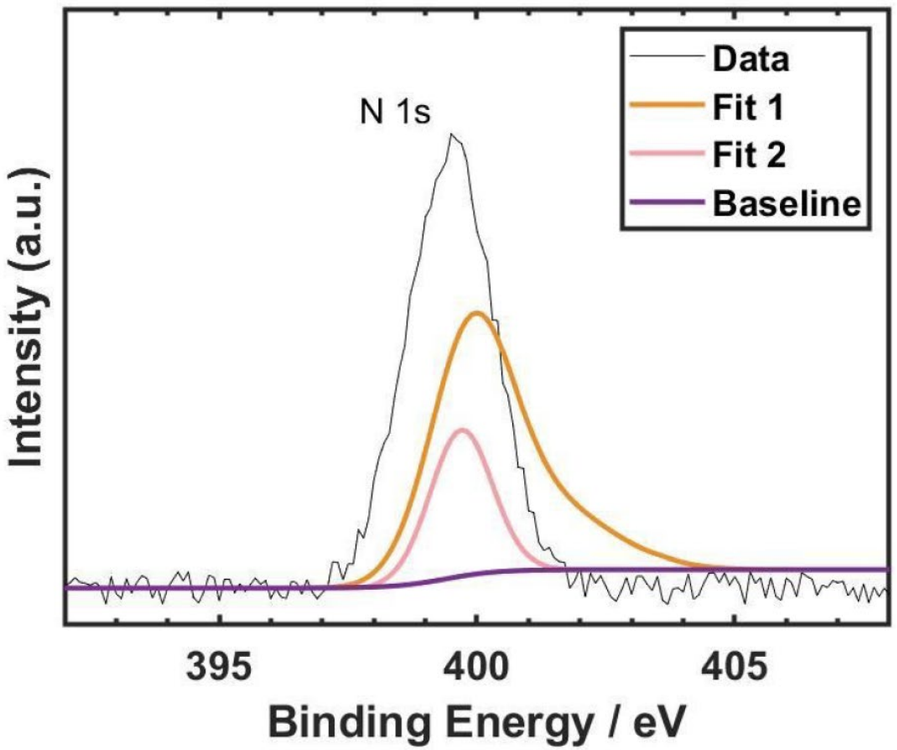

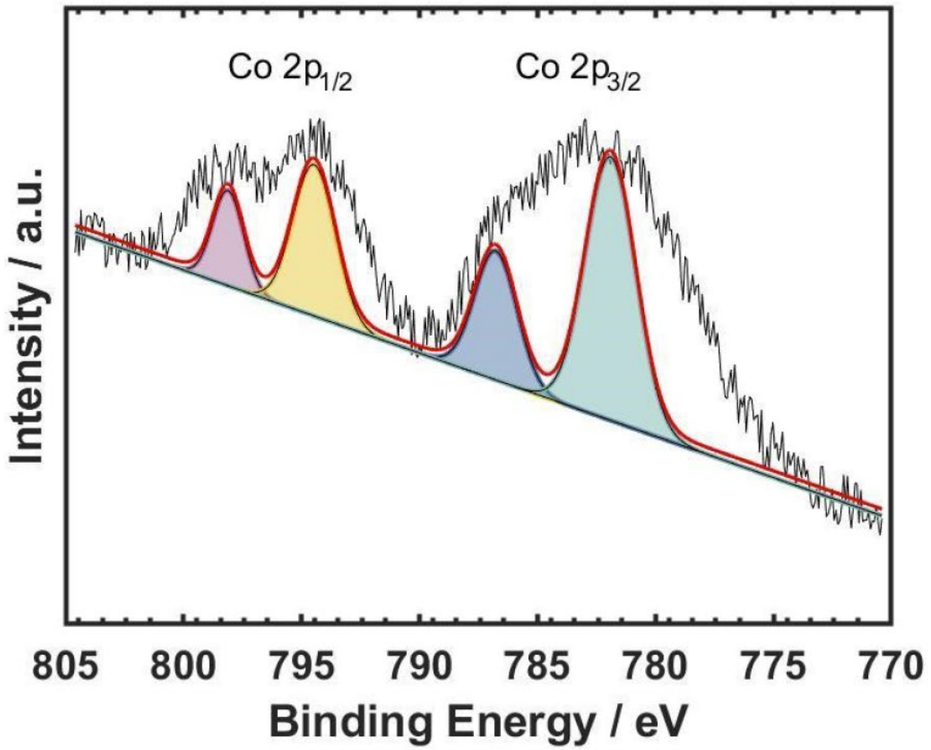

- other chemical components that appear to be present in the material have been ignored

George Hobbs Major Brigham Young University, "Use and Misuse of X-Ray Photoelectron Spectroscopy (XPS):Reproducibility, Gross Errors, Data Reporting, and Peak Fitting", Ph.D Thesis, 2023

Pitfall 5: Interfering Peaks

XPS curve fits of Ru 3d & C1s spectral regions

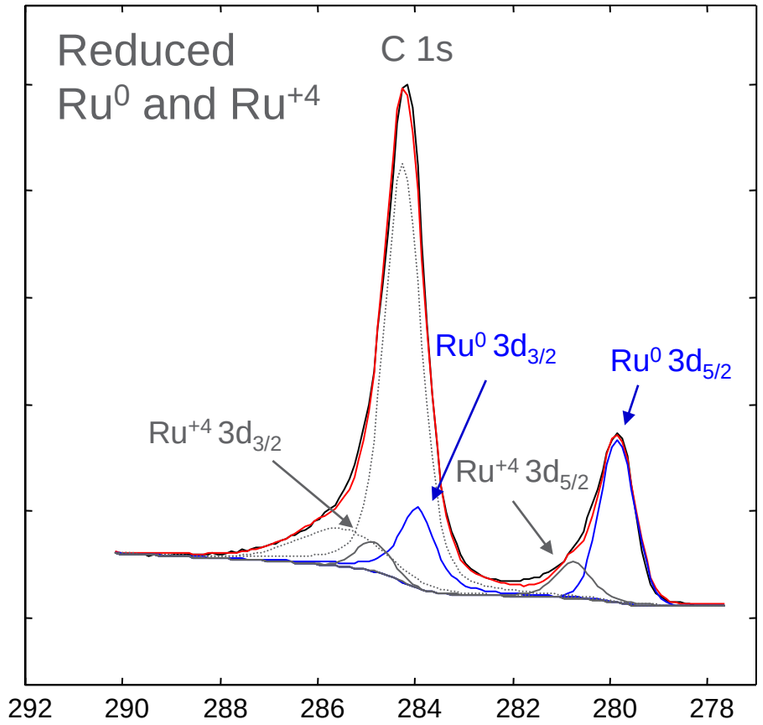

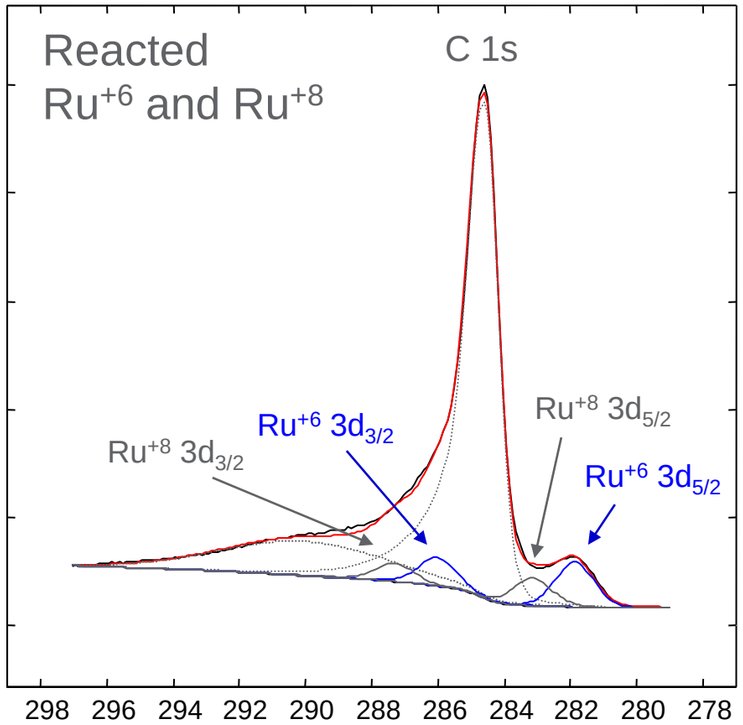

Acknowledgments

- Mark Engelhard, Pacific Northwest National Laboratory
- Ajay Karakoti, Pacific Northwest National Laboratory
- Theva Thevuthasan, Pacific Northwest National Laboratory
- Don Baer, Pacific Northwest National Laboratory

- Kateryna Artyushkova, Physical Electronics

- **Kratos Analytical**
- **Thermo Fisher Scientific**
- **Physical Electronics**

Useful Links

- NIST XPS database https://srdata.nist.gov/xps/main_search_menu.aspx
- **X-ray Photoelectron Spectroscopy (XPS) Reference Pages: http://www.xpsfitting.com/**
- **Thermo: https://xpssimplified.com/**
- **XPS Spectra -Chemical Shift | Binding Energy-: http://techdb.podzone.net/xpsstate-e/**
- CasaXPS manual: **http://www.casaxps.com/ebooks/ebooks.htm**
- CaseXPS: **http://www.casaxps.com/**
- Special Topic Collection: Reproducibility Challenges and Solutions: **https://avs.scitation.org/topic/specialcollections/reprod2020?SeriesKey=jva**

Pacific Northwest
NATIONAL LABORATORY

Thank you